



**HAL**  
open science

# Role of Phospholipase D in Vascular Calcification

Najwa Skafi

► **To cite this version:**

Najwa Skafi. Role of Phospholipase D in Vascular Calcification. Cellular Biology. Université de Lyon; Université Libanaise, 2017. English. NNT : 2017LYSE1339 . tel-01771501

**HAL Id: tel-01771501**

**<https://theses.hal.science/tel-01771501>**

Submitted on 19 Apr 2018

**HAL** is a multi-disciplinary open access archive for the deposit and dissemination of scientific research documents, whether they are published or not. The documents may come from teaching and research institutions in France or abroad, or from public or private research centers.

L'archive ouverte pluridisciplinaire **HAL**, est destinée au dépôt et à la diffusion de documents scientifiques de niveau recherche, publiés ou non, émanant des établissements d'enseignement et de recherche français ou étrangers, des laboratoires publics ou privés.



N°d'ordre NNT : xxx

## THESE de DOCTORAT DE L'UNIVERSITE DE LYON

opérée au sein de

**l'Université Claude Bernard Lyon 1**

**Ecole Doctorale N° accréditation**

**Ecole Doctorale Interdisciplinaire Sciences-Santé**

**Spécialité de doctorat** : Aspects moléculaires et cellulaires de la biologie

Soutenue publiquement le 20/12/2017, par :

**Najwa SKAFI**

---

# Role of Phospholipase D in Vascular Calcification

---

Devant le jury composé de :

CUVILLIER, OLIVIER	Directeur de Recherche INSERM	Intitut de Pharmacologie et Biology Structurale	Rapporteur
KOMATI, Hiba	Professeur	Université d'Ottawa	Rapporteur
VICO, LAURENCE	Directeur de Recherche INSERM	Université Jean Monnet Saint Etienne	Rapporteur
Magne, David	Professeur	Université Lyon 1	Examineur
MEBAREK, Saida	Maître de Conférences	Université Lyon 1	Directrice de thèse
BADRAN, Bassam	Professeur	Université Libanaise	Directeur de thèse
BRIZUELA MADRID, Leyre	Maître de Conférences	Université Lyon 1	Co-directrice de thèse
HUSSEIN, Nader	Professeur	Université Libanaise	Co-directeur de thèse
HADCHITI, Elie	Professeur associé	Université Libanaise	Invité
HAMADE, Eva	Professeur	Université Libanaise	Invitée

# UNIVERSITE CLAUDE BERNARD - LYON 1

## **Président de l'Université**

Président du Conseil Académique

Vice-président du Conseil d'Administration

Vice-président du Conseil Formation et Vie Universitaire

Vice-président de la Commission Recherche

Directrice Générale des Services

**M. le Professeur Frédéric FLEURY**

M. le Professeur Hamda BEN HADID

M. le Professeur Didier REVEL

M. le Professeur Philippe CHEVALIER

M. Fabrice VALLÉE

Mme Dominique MARCHAND

## ***COMPOSANTES SANTE***

Faculté de Médecine Lyon Est – Claude Bernard

Faculté de Médecine et de Maïeutique Lyon Sud – Charles Mérieux

Faculté d'Odontologie

Institut des Sciences Pharmaceutiques et Biologiques

Institut des Sciences et Techniques de la Réadaptation

Département de formation et Centre de Recherche en Biologie Humaine

Directeur : M. le Professeur G.RODE

Directeur : Mme la Professeure C. BURILLON

Directeur : M. le Professeur D. BOURGEOIS

Directeur : Mme la Professeure C. VINCIGUERRA

Directeur : M. X. PERROT

Directeur : Mme la Professeure A-M. SCHOTT

## ***COMPOSANTES ET DEPARTEMENTS DE SCIENCES ET TECHNOLOGIE***

Faculté des Sciences et Technologies

Département Biologie

Département Chimie Biochimie

Département GEP

Département Informatique

Département Mathématiques

Département Mécanique

Département Physique

UFR Sciences et Techniques des Activités Physiques et Sportives

Observatoire des Sciences de l'Univers de Lyon

Polytech Lyon

Ecole Supérieure de Chimie Physique Electronique

Institut Universitaire de Technologie de Lyon 1

Ecole Supérieure du Professorat et de l'Education

Institut de Science Financière et d'Assurances

Directeur : M. F. DE MARCHI

Directeur : M. le Professeur F. THEVENARD

Directeur : Mme C. FELIX

Directeur : M. Hassan HAMMOURI

Directeur : M. le Professeur S. AKKOUCHE

Directeur : M. le Professeur G. TOMANOV

Directeur : M. le Professeur H. BEN HADID

Directeur : M. le Professeur J-C PLENET

Directeur : M. Y.VANPOULLE

Directeur : M. B. GUIDERDONI

Directeur : M. le Professeur E.PERRIN

Directeur : M. G. PIGNAULT

Directeur : M. le Professeur C. VITON

Directeur : M. le Professeur A. MOUGNIOTTE

Directeur : M. N. LEBOISNE

## **Publications**

1. Characterization and assessment of potential microRNAs involved in phosphate-induced aortic calcification (Accepted article)

Journal: Journal of Cellular Physiology

Date of acceptance: 01-Aug-2017

Position: Co-first author

Maya Fakhry, Najwa Skafi, Mohammad Fayyad-Kazan, Firas Kobeissy, Eva Hamade, Saida Mebarek, Aida Habib, Nada Borghol, Asad Zeidan, David Magne, Hussein Fayyad-Kazan and Bassam Badran.

2. Phospholipase D is central to high phosphate-induced vascular calcification (submitted article)

Journal: BBA - Molecular Basis of Disease

Date of submission: 03-Oct-2017

Position: First author

Najwa Skafi, Dina Abdallah, Christophe Soulage, Sophie Reibel, Nicolas Vitale, Eva Hamade, Wissam Faour, Bassam Badran, Nader Hussein, Rene Buchet, Leyre Brizuela and Saida Mebarek.

## **Oral communications**

1. BioBeirut 5 international meeting: Cancer Biology and immunology

Lebanon, 19 and 20 Nov 2015

Mechanisms of vascular calcification

2. Les 18èmes Journées Françaises de Biologie des Tissus Minéralisés

France, 1, 2 and 3 June 2016

Phospholipase D Metabolic Pathway in Vascular Calcification

3. La journée scientifique de l'institut IGBMS

France, 12 July 2016

Role of Phospholipase D in Vascular Calcification

4. 21ème Journée Scientifique de L'EDISS

France, 13 Oct 2016

Action of Phospholipase D during Vascular Calcification

5. Les 19èmes Journées Françaises de Biologie des Tissus Minéralisés

France, 18, 19 and 20 May 2017

Involvement of Phospholipase D pathway in Vascular Calcification

## **Discipline**

Equipe Métabolisme, Enzymes et Mécanismes Moléculaires MEM2  
Institut de Chimie et Biochimie Moléculaires et Supramoléculaires  
UMR CNRS 5246/Université Lyon1  
Bâtiment Raulin, 43 Bd du 11 novembre 1918  
69622 Villeurbanne Cedex, France

Laboratoire de biologie du cancer et d'immunologie moléculaire  
Faculté des sciences I  
Université libanaise  
Hadath, Beyrouth, Liban

## Abstract

Vascular calcification is the accumulation of calcium phosphate crystals in blood vessels via a pathological process that resembles physiological bone or cartilage formation. Calcification in the medial layer is mainly seen in diabetic and chronic kidney disease patients. Its main consequence is the loss of elasticity which is indispensable for the function of large arteries. Accordingly, vascular medial calcification was significantly associated with mortality in hemodialysis patients. Vascular calcification treatments are limited to those that correct its causative health problems, but no efficient, specific and targeted interventions are available. Therefore, a deep understanding of its molecular mechanisms is needed to find novel therapeutic targets. Phospholipase D catalyses the hydrolysis of phospholipids into phosphatidic acid and a head group. It is implicated in different cellular functions and diseases. It was found to be activated by factors involved in osteogenesis and others involved in vascular calcification. Thus, we investigated its role in vascular calcification in 3 models: an *in-vitro* model of murine smooth muscle cell line MOVAS cultured with ascorbic acid and  $\beta$ -glycerophosphate, an *ex-vivo* model of rat aortas cultured in high phosphate medium, and an *in-vivo* model of adenine-induced kidney disease in rats in which vascular calcification is induced by further administration of high phosphorus/calcium diet and active vitamin D injections. Calcification was detected in these models using different approaches including alkaline phosphatase activity, calcium dosage, and/or evaluation of osteo-chondrocytic markers expression. *Pld1* expression was seen upregulated in all the three models, especially during early stages of calcification, and was accompanied with increased phospholipase D activity in the *in-vitro* and *ex-vivo* model. The inhibition of total phospholipase D activity in these two models, or that of phospholipase D1 in case of MOVAS model, abolished calcification. Phospholipase D2-specific inhibition did not induce significant effects. Two pathways by which phospholipase D can be activated were tested, protein kinase C and sphingosine 1-phosphate pathways, but they were found to be involved in calcification but not necessary for phospholipase D activation during this process. Alternatively, the preliminary results showed that PLD may be acting by activation of sphingosine kinase 2 whose activity was found necessary for calcification in the MOVAS model. Further investigations are needed to understand the mechanisms by which phospholipase D is activated and by which it is acting. Phospholipase D could be a novel target for vascular calcification especially that its inhibition in patients did not induce adverse health effects.

**Keywords:** phospholipase D, vascular calcification, alkaline phosphatase, smooth muscle cells, chronic kidney disease, aorta.

# Résumé

## Le rôle de la phospholipase D dans la calcification vasculaire

La calcification vasculaire est l'accumulation de cristaux de calcium dans les vaisseaux sanguins à travers un processus pathologique qui ressemble à la formation de l'os ou du cartilage. Elle apparaît notamment chez les patients diabétiques ou atteints d'une insuffisance rénale chronique. La conséquence principale de la calcification vasculaire est la perte de l'élasticité qui est indispensable pour la fonction des grandes artères, elle est de plus associée à la mortalité des patients hémodialysés. Les traitements contre la calcification vasculaire sont généralement limités à ceux qui corrigent les facteurs causatifs des problèmes de santé mais aucune intervention efficace, spécifique et ciblée n'est disponible. Par conséquent, une compréhension profonde des mécanismes moléculaires impliqués dans la calcification vasculaire est nécessaire dans le but de trouver de nouvelles cibles thérapeutiques. La phospholipase D catalyse l'hydrolyse des phospholipides en acide phosphatidique et une tête polaire, elle est aussi impliquée dans différentes fonctions cellulaires et maladies. Il a été démontré qu'elle peut être activée par des facteurs impliqués dans l'ostéogenèse et par d'autres impliqués dans la calcification vasculaire. Ainsi, nous avons étudié le rôle de la phospholipase D dans la calcification vasculaire dans 3 modèles différents. Le premier est un modèle *in-vitro* de cellules musculaires lisses murines (lignée cellulaire MOVAS), elles sont cultivées en présence d'acide ascorbique et de  $\beta$ -glycérophosphate. Le deuxième est un modèle *ex-vivo* d'explants d'aortes cultivés en présence de fortes concentrations de phosphate et le troisième est un modèle *in-vivo* d'insuffisance rénale chronique produite chez des rats. Dans ce dernier modèle, la calcification vasculaire est induite par un régime riche en phosphore et en calcium et par des injections de vitamine D active. La calcification dans ces trois modèles a été suivie par l'analyse de la minéralisation en dosant les dépôts de calcium, de l'activité phosphatase alcaline, et de l'expression de différents marqueurs ostéochondrocytaires. Une augmentation de l'expression génique de *Pld1* a été observée dans les trois modèles, en particulier au cours des premières étapes de la calcification, et a été accompagnée d'une activité accrue de la phospholipase D dans les modèles *in vitro* et *ex-vivo*. L'inhibition de l'activité phospholipase D dans ces deux modèles ou de la phospholipase D1 dans le modèle MOVAS a bloqué complètement la calcification. Par contre, l'inhibition spécifique de la phospholipase D2 n'a pas montré des effets significatifs. Deux voies par lesquelles la phospholipase D peut être activée ont été testées, la voie de la protéine kinase C et la voie de la sphingosine-1-phosphate. Ces deux voies métaboliques se sont révélées être impliquées dans le processus de calcification mais pas forcément dans l'activation de la

phospholipase D au cours de ce processus. Des résultats préliminaires ont montré que la phospholipase D pourrait agir après activation de la sphingosine kinase 2 dont l'activité s'est avérée nécessaire pour la calcification dans le modèle MOVAS. Des études supplémentaires sont nécessaires pour comprendre par quels mécanismes la phospholipase D est activée et comment elle agit. La phospholipase D pourrait être une nouvelle cible thérapeutique pour le traitement de la calcification vasculaire vu que son inhibition ne semble pas avoir des effets secondaires chez les patients.

**Mots-clés:** phospholipase D, calcification vasculaire, phosphatase alcaline, cellules musculaires lisses, insuffisance rénale chronique, aorte.

# Table of contents

Abstract.....	3
Résumé.....	6
List of figures.....	10
List of Tables.....	11
List of Abbreviations.....	12
Preface.....	16
Chapter I: Introduction.....	18
<b>Part 1: Physiological Mineralization.....</b>	<b>18</b>
1. Bone structure.....	18
2. Bone formation.....	21
3. Bone remodelling.....	32
<b>Part 2: Vascular calcification.....</b>	<b>35</b>
1. Types and consequences.....	35
2. Cellular and molecular mechanisms.....	39
3. Experimental models of vascular calcification.....	54
4. Diagnosis.....	56
5. Treatments.....	57
<b>Part 3: Phospholipase D.....</b>	<b>60</b>
1. Overview on PLD superfamily structure, localization and function.....	61
2. Functions of PLD1 and 2 and their regulation.....	62
3. Roles of PLD in diseases.....	71
4. PLD in bone formation.....	72
5. Possible role of PLD in VC.....	75
Objectives.....	76
Chapter II: Materials and methods.....	78
1. Cell culture.....	78
2. Aortic explant culture.....	78
3. Animal experiments.....	79
4. Alkaline phosphatase (AP) activity assay.....	80
5. Calcium assay.....	80
6. Total RNA extraction, reverse transcription and quantitative real-time polymerase chain reaction (qPCR) analysis.....	81
7. Western blot.....	82
8. PLD activity assay.....	83
9. SK activity assay.....	84

10. S1P dosage assay .....	84
11. Statistical analysis .....	84
<b>Chapter III: Results</b> .....	<b>86</b>
<b>Part 1: MOVAS murine smooth muscle cell vascular calcification model</b> .....	<b>86</b>
1. The role of PLD during calcification in MOVAS cells .....	86
2. The effects of PKC inhibition on calcification in MOVAS cells and on PLD activity..	93
3. The possible link between S1P and PLD during MOVAS calcification.....	95
<b>Part 2: <i>Ex-vivo</i> rat aorta vascular calcification model</b> .....	<b>102</b>
1. Role of PLD during rat aorta calcification .....	102
2. Role of S1P metabolic pathway during rat aorta calcification .....	106
<b>Part 3: Adenine-induced CKD rat model of vascular calcification</b> .....	<b>108</b>
<b>Discussion and conclusion</b> .....	<b>114</b>
<b>Perspectives</b> .....	<b>120</b>
<b>Summaire</b> .....	<b>124</b>
<b>List of References</b> .....	<b>155</b>
<b>Annex</b> .....	<b>180</b>

## List of figures

Figure 1: The structure of an adult long bone.....	20
Figure 2: osteoblastic differentiation during bone formation.....	22
Figure 3: Mechanisms of biomineralization. ....	26
Figure 4: Endochondral ossification during long bone formation. ....	32
Figure 5: the general structure of elastic and muscular arteries.....	36
Figure 6: The Windkessel function of the aorta and large elastic arteries. ....	39
Figure 7: The mechanism of vascular calcification.....	41
Figure 8: Phosphate homeostasis.....	45
Figure 9: Specificities of phospholipases.....	60
Figure 10: The domains in PLD1 and PLD2 proteins. ....	61
Figure 11: PA metabolic pathway. ....	62
Figure 12: The role of PA in membrane dynamics. ....	63
Figure 13: The different types of PKC and their structure. ....	64
Figure 14: S1P metabolic pathway.....	67
Figure 15: S1P specific receptors signalling pathways.....	68
Figure 16: IC <sub>50</sub> of Halopemide, VU0155069 and CAY10594 for inhibiting PLD1 and PLD2 in-vitro and in cells [350]. ....	79
Figure 17: Calcification in MOVAS cells.....	87
Figure 18: PLD expression and activity during calcification in MOVAS cells. ....	90
Figure 19: The effects of different PLD inhibitors on calcification in MOVAS cells.. ....	91
Figure 20: The effects of the timing of PLD inhibition on calcification in MOVAS cells.....	92
Figure 21: The effects of PKC inhibition on calcification in MOVAS cells and on PLD activity.. ....	94
Figure 22: The expression and activities of different S1P metabolic pathway effectors during calcification in MOVAS cells. ....	96
Figure 23: extracellular S1P production and S1P receptors expression during calcification in MOVAS cells. ....	97
Figure 24: The effects of modulation of S1P production and signalling on calcification in MOVAS cells. ....	99
Figure 25: The effect of SK1 inhibitors on SK1 activity.....	98
Figure 26: The crosstalk between PLD and S1P signalling pathways. ....	101
Figure 27: Characterization of the rat aorta <i>ex-vivo</i> model of VC.....	103
Figure 28: PLD expression and activity during Pi-induced rat aorta calcification. ....	104
Figure 29: The effects of PLD inhibition on Pi-induced rat aorta calcification. ....	105
Figure 30: The effect of PLD genetic ablation on calcium accumulation. ....	106
Figure 31: Gene expressions and activities of enzymes of S1P metabolic pathway during rat aorta calcification.....	107
Figure 32: Representation of the rat adenine-induced CKD model.....	108
Figure 33: The establishment of CKD in the rats given high-adenine diet.....	110
Figure 34: VC in aortas of rat adenine-induced CKD model. ....	111
Figure 35: Pld and Sphk2 expression during VC in the aortas of adenine-induced CKD rats..	113

## List of Tables

<b>Table 1: The sequences of the primers used in qPCR with their respective annealing temperatures (Ta).</b> .....	82
<b>Table 2: General characteristics of control and CKD rats.</b> .....	109

## List of Abbreviations

1,25(OH)<sub>2</sub>D: 1, 25-dihydroxyVitD  
25(OH)D: 25-hydroxyVitD  
αSMA: α-smooth muscle actin  
β-GP: β-glycerophosphate  
A: absorbance  
Aβ: amyloid-β peptide  
AA: ascorbic acid  
ABI: ankle-brachial index  
AD: Alzheimer disease  
AngII: angiotensin II  
ANKH: progressive ankylosis protein homolog  
AP: alkaline phosphatase  
APC: Adenomatous polyposis coli protein  
APEX1: DNA-(apurinic or apyrimidinic site) lyase  
ApoE: Apolipoprotein E  
APP: amyloid precursor protein  
AT: AngII receptor  
ATF4: cyclic AMP-dependent transcription factor  
BACE1: β-site amyloid precursor protein cleaving enzyme-1  
BCA: bicinchoninic acid  
BMP: bone morphogenic proteins  
BMPR: bone morphogenic proteins receptor  
BMSCs: bone marrow stromal cells  
BSP II: bone sialoprotein II  
Ca: calcium  
CAC: coronary artery calcification  
CaSR: Calcium sensing receptor  
CBFβ: core binding factor β  
CKD: chronic kidney disease  
COX: cyclooxygenase  
CRP: C-reactive protein  
CT: computed tomography  
CYP11B2: aldosterone synthase  
CYP24A1: 24-hydroxylase  
CYP27B1: 1α-hydroxylase  
DAG: diacylglycerol  
DBP: VitD binding protein  
DC-STAMP: dendritic cell specific transmembrane protein  
DGK: DAG kinase  
DMEM: Dulbecco's modified Eagle's medium  
DMP1: dentin matrix protein 1  
DNA: deoxyribonucleic acid  
EBCT: electron-beam CT

ECL: enhanced chemiluminescence  
ECM: extracellular matrix  
EGFR: epidermal growth factor receptor  
ER: endoplasmic reticulum  
ERK1/2: extracellular signal-regulated kinase 1/2  
ESRD: end-stage renal disease  
FBS: fetal bovine serum  
FFA: free fatty acid  
FGF: fibroblast growth factor  
FGF23: fibroblast growth factor 23  
FGFR: fibroblast growth factor receptor  
fMLP: N-formyl-methionyl-leucyl-phenylalanine  
FRP: N-formyl peptide receptor  
GAP: GTPases activating enzyme  
GAS6: growth arrest-specific 6  
GEF: guanine nucleotide exchange factor  
GFR: glomerular filtration rate  
GPCR: G-protein coupled receptors  
GPI: glycosylphosphatidylinositol  
GRB2: Growth factor receptor-bound protein 2  
GSH-PX: glutathione peroxidase  
HA: hydroxyapatite  
HbA1C: glycated hemoglobin  
HD: hemodialysis  
HDAC: histone deacetylase  
HDL: high-density lipoprotein  
HPP: hypophosphatasia  
HRP: horseradish peroxidase  
hTERT: human telomerase reverse transcriptase  
IGF: insulin-like growth factor  
IHH: Indian hedgehog  
IL-6: interleukin 6  
IVUS: intravascular ultrasound  
KLF4: Kruppel-like factor  
KO: knock-out  
LC3II: light-chain 3-II  
LDLR: Low density lipoprotein receptor  
LEF-1: lymphoid enhancer binding factor 1  
LPA: lysophosphatidic acid  
LPAAT: LPA acyl transferase  
LPP: lipid phosphate phosphatases  
LRP5/6: lipoprotein receptor-related protein 5/6  
LV: left ventricle  
M-CSF: macrophage colony-stimulating factor  
MDA: malondialdehyde

MEF2C: myocyte enhancer factor 2C  
MGP: matrix Gla protein  
MMP: matrix metalloproteinase  
MSC: mesenchymal stem cell  
MSCT: multislice CT  
mTOR: mammalian target of rapamycin  
mTORC1: mTOR complex 1  
MV: matrix vesicle  
N-CAM: neural cell adhesion molecule  
NPT2: sodium-phosphate co-transporter type II  
NICD: Notch intracellular domain  
NFATc1: Nuclear factor of activated T-cells cytoplasmic 1  
NPP1: ectonucleotide pyrophosphatase/phosphodiesterase 1  
NT: non-treated  
OCN: osteocalcin  
OCT: coherence tomography  
OPN: osteopontin  
PA: phosphatidic acid  
PAP: phosphatidic acid phosphatase  
PBS: Phosphate-buffered saline  
PC: phosphatidylcholine  
PDGF: Platelet-derived growth factor  
PE: phosphatidylethanolamine  
PGE2: prostaglandin E2  
PH: pleckstrin homology domain  
PHB2: Prohibitin 2  
PHOSPHO1: PE/PC phosphatase  
Pi: inorganic phosphate  
PI (4, 5) P<sub>2</sub>: phosphatidylinositol (4, 5) diphosphate  
PI3K: phosphatidylinositol-3-kinase  
PIP<sub>3</sub>: phosphatidylinositol triphosphate  
PIPKI: PI4P kinase I  
PKA: protein kinase A  
PKC: protein kinase C  
PLB: phospholipase B  
PLC: phospholipase C  
PLD: phospholipase D  
PMA: phorbol-12-myristate-13-acetate  
pNP: paranitrophenol  
pNPP: p-nitrophenyl phosphate  
PPAR $\gamma$ : peroxisome proliferator-activated receptor  $\gamma$   
PPi: inorganic pyrophosphate  
PS: phosphatidylserine  
PtdButOH: phosphatidylbutanol  
PTHrP: parathyroid hormone-related peptide

PWV: pulse wave velocity  
PX: phox consensus sequence  
qPCR: quantitative polymerase chain reaction  
RANKL: receptor activator of nuclear factor kappa-B ligand  
RER: rough endoplasmic reticulum  
ROS: Reactive oxygen species  
RTK: Tyrosine kinase receptor  
RUNX: runt-related transcription factor  
S1P: sphingosine 1-phosphate  
SEM: standard error of the mean  
SK: sphingosine kinase  
SM: sphingomyelin  
Sm22 $\alpha$ : smooth muscle 22- $\alpha$   
SMAD: mothers against decapentaplegic homologs  
SMase: sphingomyelinase  
SMCs: Smooth Muscle cells  
SOD: superoxide dismutase  
SOS: Son of Sevenless  
SOX9: sex determining region Y-box 9  
SPL: S1P lyase  
SPNS2: Spinster 2  
SPP: S1P phosphatases  
SRY: sex determining region Y  
Ta: annealing temperature  
TCF: T cell factor  
TGF $\beta$ : transforming growth factor- $\beta$   
TLC: thin layer chromatography  
TNAP: tissue non-specific alkaline phosphatase  
TNF $\alpha$ : tumor necrosis factor  $\alpha$   
TRAP: Tartrate-resistant acid phosphatase  
ULK1/2: UNC-51 like kinase-1/2  
VC: vascular calcification  
VDR: VitD receptor  
VDRA: VitD receptor agonist  
VEGF: vascular endothelial growth factor  
VitD: vitamin D  
VSMCs: vascular smooth muscle cells  
WT: wild-type

## Preface

Calcium deposition, mainly as calcium phosphate crystals, is normally restricted to the skeleton and teeth. Physiological mineralization is directed by specialized cells, mainly: osteoblasts in bone, chondrocytes in cartilage and odontoblasts in teeth. These cells are able to provide the required environment for calcium phosphate crystals formation mainly by producing matrix vesicles. These specialized structures contain all the requirements for producing and concentrating phosphate and calcium ions inside their lumen, thus driving the formation of hydroxyapatite crystals. Among the enzymes owned by these vesicles, tissue non-specific alkaline phosphatase has a central role in calcification, and its activity is indicative for the mineralization capacity of cells. Vascular calcification is the pathological accumulation of calcium phosphate crystals in blood vessels. It is seen in the context of different pathologies including chronic kidney disease, diabetes and atherosclerosis. Its consequences depend largely on its location. For example, calcification in the intimal layer of arteries in case of atherosclerosis can affect plaque stability and risk for thrombosis. On the other hand, when it is present in the medial layer, it mainly affects the elasticity of the artery. Its significance depends of the type of arteries that it affects. For example, when present in large arteries, loss of elasticity can cause serious heart failure. Vascular calcification is a process similar to bone or cartilage tissue formation. The most accepted hypothesis suggests the trans-differentiation of smooth muscle cells into osteo-chondrocyte-like cells under the effect of osteo-chondrocyte-specific transcription factors. These cells then gain the ability to express bone/cartilage-specific proteins and may produce matrix vesicles-like structures. The mentioned processes take place under the effect of different stimuli which depends on the underlying disease, including: hyperphosphatemia (in chronic kidney disease), hyperglycemia (in diabetes), oxidative stress and inflammation (in case of atherosclerosis). The complete mechanism that leads to the onset of vascular calcification is not yet understood, which may explain the lack of effective targeted therapies. Phospholipase D is an enzyme that mainly hydrolyses phosphatidylcholine producing choline and phosphatidic acid. Due to the wide functions of phosphatidic acid and its derivatives, phospholipase D was found to be involved in many cellular functions and diseases. Phospholipase D was seen to be activated by different factors involved in bone homeostasis and osteoblast differentiation. Moreover, different factors, which are known for their role in cardiovascular diseases, were able to activate it. Thus, Phospholipase D may be a novel player in the pathogenesis of vascular calcification. Our work focused on investigating the role of PLD in vascular calcification in context of chronic kidney disease and hyperphosphatemia in 3 different models: *in-vitro*

smooth muscle cell line (MOVAS), *ex-vivo* rat aortas, and an *in-vivo* adenine-induced chronic kidney disease rat model. Different factors that may regulate PLD activity, like protein kinase C and the bioactive lipid sphingosine 1-phosphate, were also examined.

# Chapter I: Introduction

## Part 1: Physiological Mineralization

Physiological mineralization, also called biomineralization, is normally restricted to bone, cartilage and teeth. The function of the skeleton is not limited to locomotion and protection of soft tissues and vital organs, it acts also as a reservoir for calcium, phosphate, growth factors and cytokines that are released according to body demands. Moreover, it harbours the bone marrow which is the main source of blood cells [1]. Mineralization is a lifelong process that starts during bone formation in prenatal and early postnatal life and continues during bone growth, remodelling and repair until death.

### 1. Bone structure

The human skeleton is made up of 213 bones classified mainly into four groups according to their shape: long bones, short bones, flat bones and irregular bones. Among these, long bones have a common well known structure [2]. They are mainly made up of a long tube of cortical bone, named diaphysis, and two rounded epiphysis at each side. Between the diaphysis and the epiphysis, there is a zone called metaphysis. The epiphysis and metaphysis are made of an outer cortical bone holding within it a network of trabecular bone with bone marrow spaces. At joints, the long bone epiphysis is covered with articular cartilage. At all the other sites, the long bones are covered by a periosteum; a layer made up of fibrous connective tissue and linked to the bone tightly by thick collagenous fibres called Sharpeys' fibres. The inner side of the bone is also covered by a membrane called endosteum (Figure 1). Similarly, bones of the other groups (short, flat and irregular) are normally made up of an outer hard cortical bone with trabecular bone from the inside [2].

#### 1.1 Bone and cartilage cells

Bones are made up of a tightly organized extracellular matrix (ECM) with resident (osteocytes and bone lining cells), mineralizing (osteoblasts) and bone resorbing cells (osteoclasts). Cartilages have a different ECM with only one type of cells (chondrocytes).

##### 1.1.1 Osteoblasts

Osteoblasts are responsible for the formation of all skeletal bones. They are derived from mesenchymal stem cells (MSCs) (detailed in Part 1. 2. A). The mature form is a large cuboidal mononucleated cell with large nucleus, golgi apparatus and endoplasmic reticulum (ER) [1,2]. These cells are usually present on the bone surfaces, and constitute only about 4-6% of bone cells. They synthesize bone matrix, the osteoid, by secreting collagen I and other

matrix proteins, like osteocalcin (OCN), osteopontin (OPN), osteonectin and bone sialoprotein II (BSP II), and they mineralize this matrix with apatite crystals mainly via the action of tissue non-specific alkaline phosphatase (TNAP), which is also produced by them. When osteoblasts become encased within their own bone matrix, they differentiate into osteocytes. Alternatively, they can differentiate into bone-lining cells or undergo apoptosis [1].

### .1.2 Osteocytes

Osteocytes are the most abundant bone cells (90-95%). They are derived from osteoblasts that were enclosed in ECM. During this transition, the nucleus enlarges and the number of rough ER (RER) and golgi apparatus decreases as they begin to lose the expression of TNAP, OCN, BSP II and collagen I, and gain the ability to express dentin matrix protein 1 (DMP1) which controls phosphatemia and sclerostin, a Wnt signalling inhibitor. They are post-mitotic long-living cells with a lifespan of about 25 years. Osteocytes found in trabecular bone are rounded, however those found in cortical bone are elongated, and each is present inside a space called lacuna. Each osteocyte has up to 50 cytoplasmic extensions. These structures emerge before the cells are totally encased in ECM, and they occupy narrow spaces called canaliculi [1]. The dendrite-like extensions of different cells are connected to each other by means of gap junctions made up of connexins. These junctions allow osteocytes to communicate metabolically and electrically, enabling them to act as mechanosensors. They control bone resorption and formation by regulating the functions of osteoblasts and osteoclasts in order to adapt for body needs and mechanical forces. Also, they have roles in supporting bone metabolism. Osteocytes usually undergo apoptosis with age or in response to estrogen deficiency or glucocorticoid treatment [3].

### .1.3 Bone lining cells

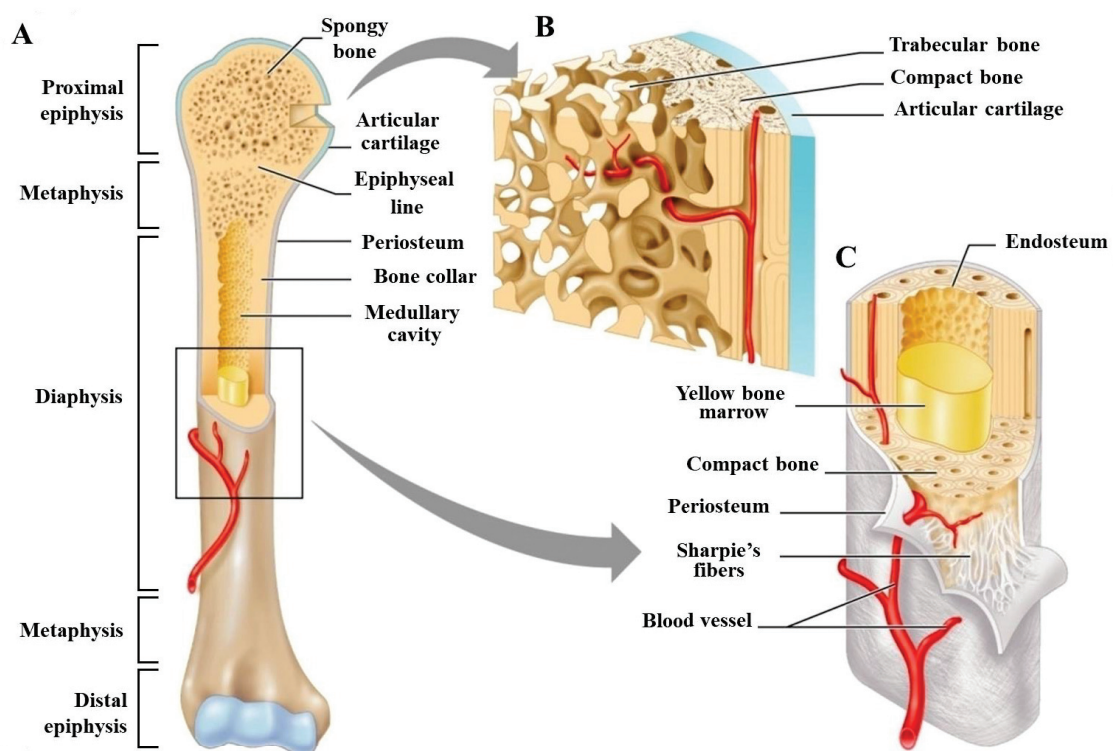
Bone lining cells are derived from mature osteoblasts. They are quiescent and flattened cells covering the bone surface, with cytoplasmic processes containing gap junctions so that they can communicate with adjacent bone lining cells or osteocytes. They protect bone against resorption, when it should not occur, by preventing the contact between bone and osteoclasts. On the contrary, they help in the osteoclastic differentiation when resorption must occur. Also, they retain the ability to re-differentiate back to osteoblasts [1].

#### .1.4 Osteoclasts

Osteoclasts are unique for their bone resorbing activity, which is needed in bone modelling and remodelling during all the life. They are multinucleated cells derived from monocytes or macrophages of hematopoietic origin [2].

#### .1.5 Chondrocytes

Chondrocytes are the sole cell type present in cartilage. They are responsible of its ECM formation and mineralization. They are derived from MSCs, and they have important role during the initial steps of bone formation and growth. In adults, it resides in cartilage tissues like the articular cartilage. In these sites, each chondrocyte is responsible of renewing the matrix around it [4].



Copyright © 2006 Pearson Education, Inc., publishing as Benjamin Cummings.

**Figure 1: The structure of an adult long bone.** A typical long bone is made up of a long cylindrical diaphysis with metaphysis and rounded epiphysis at each side (A). At the metaphysis and the epiphysis the bone is made up mostly of trabecular bone with an outer thin layer of compact bone covered by the articular cartilage in case of the epiphysis (B). At the diaphysis, the bone consists of compact bone covered by periosteum from the outer side and by endosteum from the inner side (C). [5]

## .2 Bone extracellular matrix

Bone ECM is made up of 25% organic matrix (the osteoid), 65% inorganic matrix and 10% water (by weight) [6]. 90 % of the organic matrix consists of collagenous proteins, mainly collagen type I produced by osteoblasts. The rest of organic matrix consists of non-collagenous proteins such as: OCN, OPN, osteonectin, fibronectin, bone morphogenic proteins (BMPs), growth factors and BSP II. Also, some small leucine-rich proteoglycans are present including: biglycan, decorin and lumican [1]. The inorganic matrix is made mainly of calcium-phosphate crystals in the form of hydroxyapatite (HA) ( $\text{Ca}_{10}(\text{PO}_4)_6(\text{OH})_2$ ). Along with collagen, these crystals give bone its characteristic stiffness and resistance. Other mineral ions are also present, including: potassium, sodium, bicarbonate, citrate, magnesium, carbonate, zinc, barium, strontium and fluorites [1].

## 2. Bone formation

Bone formation occurs mainly according to one of two processes; Intramembranous bone formation which occurs in flat bones, like the craniofacial bones and clavicle, or endochondral bone formation which occurs in the rest of the bones [3,7].

### 2.1 Intramembranous bone formation

Intramembranous bone formation is the process of ossification which occurs directly in condensed mesenchyme without a transitional step of cartilage. MSCs of ectoderm origin migrate to the site of bone formation and condense around a network of capillaries. Cells in the center of the aggregate begin to differentiate into preosteoblasts [3].

#### 2.1.1 Osteoblastic differentiation

Preosteoblasts differentiate into mature OBs by passing through 3 different stages; stage 1 osteoblasts express fibronectin, collagen 1, transforming growth factor- $\beta$  (TGF $\beta$ ) receptor 1 and OPN, and they continue to proliferate. Stage 2 osteoblasts stop proliferating and start the maturation with more secretion of collagen 1 and TNAP. At stage 3, the osteoblasts are mature and cuboidal. They secrete OCN to the extracellular matrix and promote the formation and deposition of hydroxyapatite crystals (figure 2) [8].

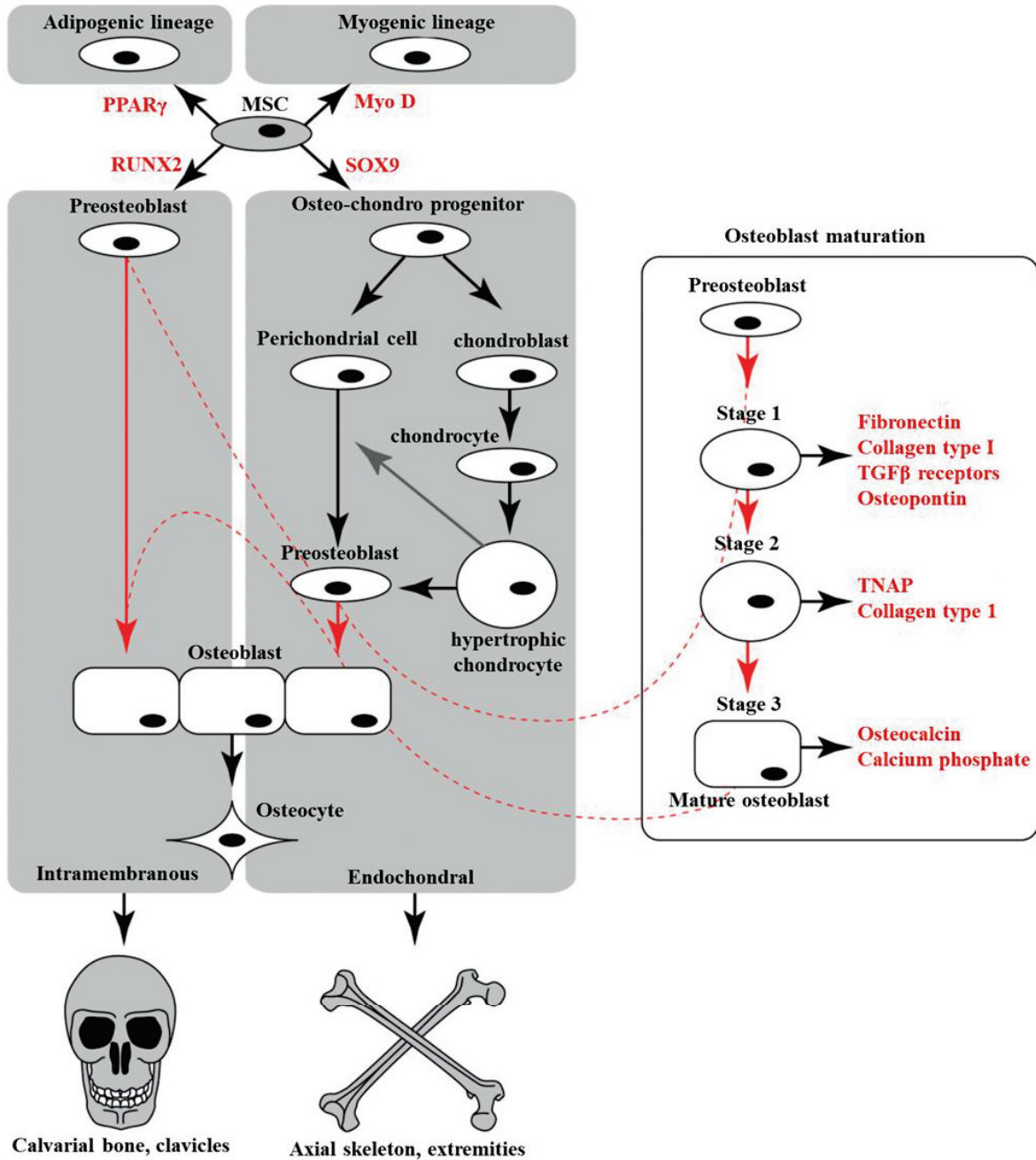


**Figure 2: osteoblastic differentiation during bone formation.** MSCs can give rise to 4 cell lineages under the effect of different transcription factors: adipogenic lineage under the effect of PPAR $\gamma$ , myogenic lineage under the effect of MyoD, osteo-chondro progenitors under the effect SOX9 or preosteoblasts under the effect of RUNX2. Osteo-chondro progenitors can also give rise to preosteoblasts passing through a stage of perichondrial cells. Preosteoblasts differentiate into mature osteoblasts passing through 3 stages: in stage 1, cells secrete fibronectin, osteopontin, collagen type I and express TGF $\beta$  receptors. In stage 2, cells secrete collagen type I and TNAP. Mature osteoblasts at stage 3 express osteocalcin and favours the formation of calcium phosphate crystals. Hypertrophic chondrocytes can also trans-differentiate into preosteoblasts. Osteoblasts are responsible for mineralization in both intramembranous and endochondral ossifications. Mature osteoblasts can differentiate into osteocytes [8].

- Role of RUNX2

The primary commitment is driven by expression of runt-related transcription factor (RUNX2), the master transcription factor of osteoblast lineage [8]. It belongs to a family of transcription factors (RUNX1, 2 and 3) that can bind to a consensus sequence (TGP<sub>y</sub>GGP<sub>y</sub>P<sub>y</sub>) on target genes as a heterodimer with their transcriptional cofactor, core binding factor  $\beta$  (CBF $\beta$ ) [9]. Its expression in MSCs begins during condensation, continues in preosteoblasts and through different steps in maturation and decreases in late stages of osteoblast maturation [10]. It is absolutely needed for osteoblast commitment and bone formation, as *Runx2* KO mice were devoid of bone and they die at birth due to defects in breathing. Osteoblastic differentiation in these mice was blocked at initial stages with low expression of early (OPN) and late (OCN) osteoblast markers [11,12]. RUNX2 can activate the expression of different genes important in osteoblastic differentiation and function, such as: *Spp1* (gene coding for OPN), *colla1* (gene of collagen type 1), *Ibsp* (gene coding for BSP II), *Bglap* (the gene of OCN), and it was shown to directly bind to the promoters of these genes [13]. Its expression was sufficient to induce osteoblastic differentiation in non-osteoblastic cell types like, C3H10T1/2 (pluripotent fibroblasts) and mouse skin fibroblasts [13]. However, it was shown to block the late stages of osteoblast maturation. Transgenic mice overexpressing RUNX2 specifically in committed osteoblasts, under the control of *Colla1* promoter, had severe osteopenia with fragile skeleton prone to fractures. At 3 months of age, the bones of these mice were mainly consisting of immature woven bone, instead of lamellar bone seen in their wild-type (WT) counterparts. The number of osteoblasts was higher by 2 times, however there were more immature osteoblasts (expressing *Spp1*) and less mature osteoblasts (expression *Bglap*) compared to WT mice [14]. Accordingly, the expression of dominant negative RUNX2, under the control of *Colla1* promoter, led to an increase in the rate of trabecular bone formation and mineralization compared to WT. These findings indicate that RUNX2 is indispensable for initial osteoblast commitment, but it inhibits progression to final mature osteoblasts [15].

- Roles of other transcription factors

During the differentiation steps of osteoblasts and their maturation, RUNX2 is not the only transcription factor involved. Osterix is a zinc-finger transcription factor whose expression can be induced by RUNX2 via direct binding to its promoter [16]. It is critical for osteoblastic differentiation. *Sp7* (gene coding for Osterix) KO mice were devoid of bone and osteoblast differentiation was blocked at very early stages. *Runx2* was expressed normally,

however *coll1a1* level was very low with complete absence of *Ibsp*, *Spp1*, *Bglap* [17]. Cyclic AMP-dependent transcription factor (ATF4) is another transcription factor involved in osteoblastic differentiation, as *Atf4* KO mice have decreased bone mass [18]. It is expressed downstream RUNX2 and, then ATF4 binds to it in order to induce OCN expression. Thus, it is especially needed for late steps of osteoblastic differentiation [19].

- Roles of paracrine and endocrine factors

On the other hand, osteoblastic differentiation is also controlled by paracrine and endocrine factors. Wnt family members are important inducers for osteoblastic commitment and differentiation. They are paracrine glycoproteins that can bind to frizzled on cell surface, and recruit Low-density lipoprotein receptor-related protein 5/6 (LRP5/6) coreceptor (canonical Wnt signalling). They transmit a signal intracellularly to disrupt the interaction of  $\beta$ -catenin with Axin and Adenomatous polyposis coli protein (APC), which normally target it for degradation. Thus,  $\beta$ -catenin will be free to translocate to nucleus, bind to co-factors like T cell factor (TCF) and lymphoid enhancer binding factor 1 (LEF-1) and activate the expression of genes including *Runx2* [20] [9].  $\beta$ -catenin is crucial for osteoblastic differentiation and bone formation, because its inactivation led to the loss of bone in both endochondral and intramembranous ossification and to the ectopic formation of cartilage [21]. Wnt10b is one of the osteogenic Wnt members that act by  $\beta$ -catenin pathway. Other Wnt members that act independently of  $\beta$ -catenin (non-canonical Wnt signalling) can also have important roles in osteoblastic differentiation like Wnt5a and Wnt4 [9]. BMPs are also important in bone formation especially postnatally. These are endocrine factors belonging to TGF $\beta$  superfamily. They act by binding to receptors with serine/threonine kinase activity. Upon binding, they activate R-SMADs that can go to the nucleus in association with SMAD4 and modulate gene expression. Many BMPs are potent osteogenic factors, that act upstream RUNX2, inducing its expression and the expression of Osterix. Interestingly, BMP-2 and BMP-7 were approved for clinical use in some types of bone fractures [9,22].

### 2.1.2 Bone mineralization

- Role of TNAP

TNAP is a crucial enzyme for mineralization, since it hydrolyses the most potent mineralization inhibitor, pyrophosphate (PPi), to produce inorganic phosphate (Pi), a mineralization promoter. Alkaline phosphatase (AP) has four genes in humans, coding for the placental, germ-cell, intestinal and TNAP. TNAP is coded by human *ALPL* gene and is expressed in liver, bone, kidney, central nervous system, fibroblasts and endothelial cells.

TNAP expressed in diverse tissues differs by its glycosylation [23]. It is an ectoenzyme, attached to the outer surface of cells, by a glycosylphosphatidylinositol (GPI) anchor connected to its C-terminus. In the skeleton, it is expressed on the surface of osteoblasts and hypertrophic chondrocytes, and it is enriched on membranes of specialized vesicles secreted by these cells, called matrix vesicles (MVs) [24]. In humans, deactivating mutations in *ALPL* gene which causes a decrease in AP serum activity leads to hypophosphatasia (HPP). HPP is an inherited disease manifested mainly by hypomineralization of the skeleton. Its severity varies widely according to the age of its onset. Its symptoms may start in embryonic life, leading to death of the fetus, in newborns, in children and in adults. In the latter, sometimes it is manifested by dental problems only [25]. There are more than 300 causative mutations in the *ALPL* gene identified till now [23]. *Alpl* KO mice showed many features similar to HPP. They were born with normal phenotype, and then after few days they began to appear smaller than WT ones. Then, they progressively developed bone deformations manifested by hypomineralization and frequent fractures. Most of them died before puberty, mostly due to vitamin B<sub>6</sub>-dependent seizures [25,26]. Primary OBs from these mice differentiate normally as concluded from normal gene expression of bone markers, like *Spp1*, *Bglap*, *Col1a1*, *Runx2* and *Smads* (gene for Mothers against decapentaplegic homologs SMADs). After incubation with ascorbic acid (AA) and  $\beta$ -glycerophosphate ( $\beta$ -GP), *Alpl* KO osteoblasts were able to form nodules similar to WT ones. However, they were not able to mineralize these nodules. Addition of recombinant TNAP to the culture restores nodule mineralization. Thus, TNAP may not be important in osteoblastic differentiation, but it is indispensable for mineralization by OBs [27].

- Role of matrix vesicles

Mineralization occurs mainly in 2 steps. First, apatite crystals are formed inside MVs (intravesicular) and then they are elongated through the ECM (extravesicular) [24]. MVs are specialized, small (100- 300 nm), membrane-bound structures [28], produced by osteoblasts, hypertrophic chondrocytes and odontoblasts. They are the initial site at which apatite crystals are formed [24]. Calcium import from extracellular space into MVs lumen is facilitated by Calcium (Ca) channels in their membrane which may be formed by annexins. Also, they contain Ca-binding lipid and proteins, such as phosphatidylserine (PS) and calbindin D<sub>9k</sub>, respectively. In this way, MVs can concentrate Ca in their lumen. Also, MVs can concentrate Pi. For example, Phosphoethanolamine (PE) and phosphatidylcholine (PC) can provide Pi when being hydrolysed by the PE/PC phosphatase (PHOSPHO1), an enzyme abundantly present inside MVs. Furthermore, Pi is imported from extracellular space by means of type

III Na/Pi transporters present in their membrane. When a certain concentration of Pi and Ca is achieved inside MVs, they form apatite crystals. In the second step of mineralization, these crystals start to exit from MVs and become elongated between collagen fibrils. In this step, the main determinant of apatite crystals formation is the Pi/PPi ratio. PPi in the extracellular space is produced mainly by the action of ectonucleotide pyrophosphatase/phosphodiesterase 1 (NPP1) through hydrolysis of ATP. NPP1 is present on MVs and on cells. Also, intracellular PPi can be exported out of cells by the action of progressive ankylosis protein homolog (ANKH), present on cellular membranes. TNAP is the main PPi hydrolysing enzyme. It hydrolyses PPi into Pi, thus elevating the Pi/PPi ratio and allowing mineralization (Figure 3) [24,28,29]. Interestingly, MVs were formed and mineralized normally in *Alpl* KO mice and HPP patients, however the extravesicular mineralization was inhibited. This recapitulates the specific role of TNAP in PPi hydrolysis and extravesicular mineralization [30,31].

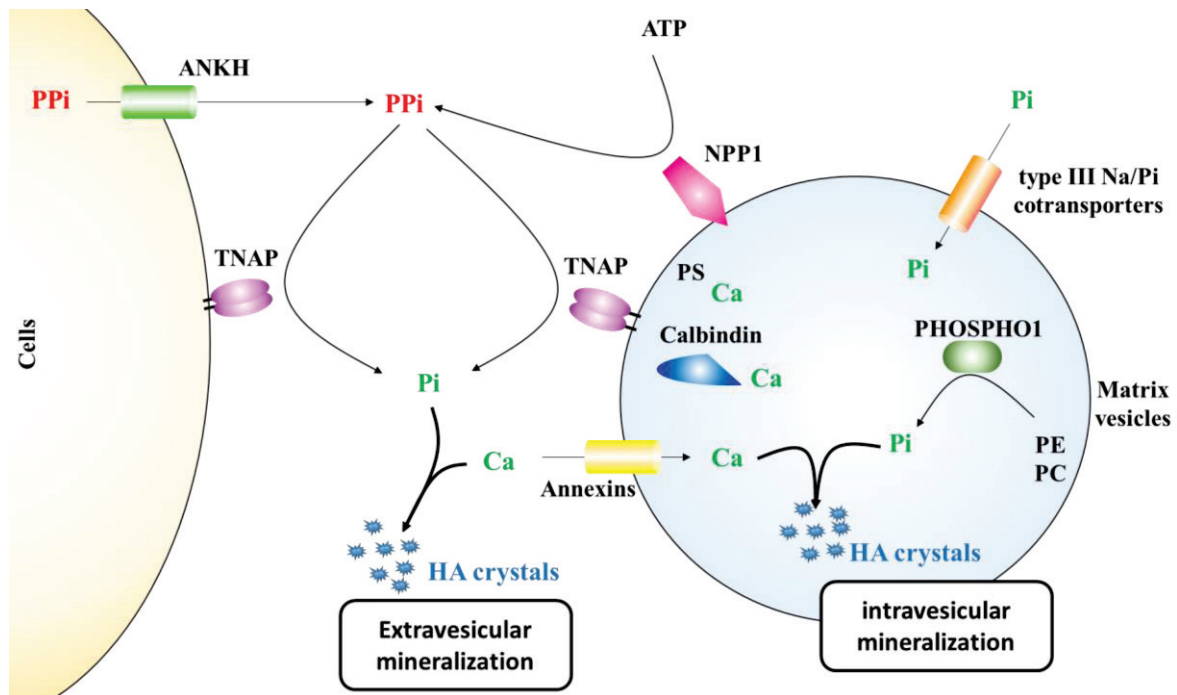


**Figure 3: Mechanisms of biomineralization.** Biomineralization occurs in bone or cartilage matrix by deposition of HA crystals via two steps. The first step is the intravesicular mineralization, in which HA crystals are deposited inside MVs, after the achievement of high Pi and Ca concentrations. In MVs, Pi is imported from extracellular space by type III Na/Pi transporters, and it is produced in MVs lumen via the hydrolysis of PE and PC by PHOSPHO1. Ca is imported from the ECM by annexins and it is concentrated inside MVs due to binding to PS and Calbindin. Extravesicular mineralization follow the initial step by elongation of HA crystals already formed inside MVs. It is achieved by decreasing PPi and the increasing Pi concentrations by the action of TNAP. PPi is generated by NPP1 via hydrolysis of ATP in the extracellular space or it is exported from cells by ANKH.

### 2.1.3 The final steps of bone formation

When the ECM is properly mineralized, mature osteoblasts that are surrounded by it will differentiate into osteocytes, and cells that are on bone surface either undergo apoptosis or differentiate into bone lining cells [8]. The trabecular bone is first formed and then it is thickened gradually and become filled with hematopoietic cells. The outer membrane of the bone, the periosteum, is formed by condensation of surrounding mesenchyme [3].

Bones are first produced as woven bone during embryogenesis and growth, when osteoblasts are acting rapidly to produce osteoid and mineralize it [6]. This type of bone is also formed during fracture healing and in some pathological cases like: osteitis fibrose cystica, hyperthyroidism, Paget's disease or bone metastasis of some types of cancer especially prostate cancer [2,3,32]. Within woven bone, the collagen fibrils are narrow (diameter= 10-20 nm) and they are laid down in disorganized manner. Moreover, the HA crystals are not associated with collagen (extrafibrillar) but with proteoglycans [6]. Woven bone is weak, and in normal cases it is replaced with lamellar bone (secondary bone) during bone remodelling [2]. Within secondary bone, the collagen fibrils are large in diameter (78 nm), and they are laid down in alternating parallel orientation to form sheets (lamellae). Lamellae are arranged in concentric layers around blood vessels forming osteons [6]. Osteons are cylindrical in cortical bone where they are packed densely and semilunar in trabecular bone where they are arranged in networks [2]. HA crystals in this type of bone is present within collagen (intrafibrillar) or on the surface of collagen (interfibrillar) [6]. Lamellar bone is much stronger than woven bone, and it is present in all bones of healthy adults [3].

## 2.2 Endochondral bone formation

Endochondral bone formation occurs in most bones of the skeleton, except the sites indicated for intramembranous ossification. It involves bone formation from a previously built cartilage model. This part will focus on the formation of long bones (Figure 4).

### 2.2.1 Overview

Even in this type of bone formation, mesenchymal condensation is the first step. Arriving to a certain cell density is needed for subsequent chondrogenesis. At this stage, cells in the center of the aggregate begin to differentiate into chondrocytes with downregulation of collagen I. Cells that are at the boundary form the perichondrium, retain the expression of collagen I and maintain the ability to differentiate either into osteoblasts or chondrocytes. Chondrocytes

begin to secrete collagen type II, IX and XI, matrix gla protein and aggrecan, building a rod of hyaline cartilage [4,33]. Then, this cartilage model grows in length (interstitial growth) due to proliferation of chondrocytes to reach the proper size, and in thickness (appositional growth) due to the addition of matrix by chondrocytes on the periphery of the cartilage model [3]. Also, more chondrocytes can still differentiate from the perichondrial cells. Chondrocytes in the middle of the diaphysis exit cell cycle and begin their maturation. When the chondrocytes become hypertrophic, they start secreting collagen type X, Matrix metalloproteinase 13 (MMP13) and TNAP which induces mineralization in the hypertrophic cartilage. TNAP is mainly secreted on membranes of MVs, similar to those produced by osteoblast (described earlier in this subpart). These events are accompanied by vascular invasion of the hypertrophic cartilage which is facilitated by degradation of the extracellular matrix via MMP13. Also, hypertrophic chondrocytes secrete receptor activator of nuclear factor kappa-B ligand (RANKL) aiding in the formation of chondroclasts (a form of cartilage resorbing cells), which secrete MMP9 helping in ECM degradation. Blood vessels bring with them osteoprogenitors which differentiate into osteoblast and form the primary ossification center, producing trabecular bone. Hypertrophic chondrocytes then undergo apoptosis, whereas few of them may differentiate into osteoblasts and contribute to the trabecular bone formation [33,34]. Perichondrial cells in the inner layer of the perichondrium differentiate into osteoblasts and secrete bone matrix making the bone collar [4].

### 2.2.2 MSC condensation

Early in fetal life, mesenchymal cells aggregate and condense in the form of a rod. The condensation is not driven by increased MSCs proliferation but by active aggregation of cells. It is accompanied by overexpression of neural cell adhesion molecule (N-CAM), N-cadherin, syndecan, and versican. N-CAM and N-cadherin are cell-cell adhesion molecules that function to couple cells tight together. Aggregated MSCs produce ECM rich in collagen I, hyaluronan, tenascin and fibronectin. MSCs have different embryonic origins in diverse skeleton sites. They are derived from the neural crest in case of bones of craniofacial region, like the middle ear bone, from the paraxial mesoderm in case of bones of the axial skeleton and from the lateral plate mesoderm in case of appendicular skeleton [8,33]. BMPs are important regulators during MSCs condensation, as the inhibition of BMP signalling inhibited chondrocyte progenitor condensation *in-vitro* and *in-vivo* [35,36].

### 2.2.2 Chondrogenic differentiation

- Role of SOX9

SRY (sex determining region Y)-box 9 (SOX9) is a crucial chondrogenic transcription factor and the earliest marker of chondrogenesis. It drives the initial commitment of MSCs into chondrocyte lineage, which can give either chondrocytes or perichondrial cells [4,8]. It is expressed in MSCs during the condensation step and in chondrocytes during stages that precede hypertrophy [37]. Its expression is regulated by BMP signalling, and it is indispensable for the formation of endochondral skeleton, as its genetic deletion in MSCs in mice led to a complete loss of limbs [38,39]. It can induce the expression of early chondrogenic proteins like collagen II and aggrecan, and it can have a role in subsequent steps, where it works in combination with SOX5 and SOX6 [38]. However, it was shown to inhibit premature hypertrophy by preservation of the proliferative state, but once chondrocytes are hypertrophic, it help them to express collagen X and be functional [4,40].

- Role of endocrine and paracrine factors

BMP signalling is not only important for MSCs condensation, but also for chondrogenesis. It was shown to play a role after the expression of collagen II as the specific *col2a1*-dependent deletion of its receptors (BMPRI and BMPRII) led to severe defects or a complete loss of the endochondral skeletal elements [41]. Deletion of SMAD1 and SMAD3 using the same system gave similar results [42]. On the contrary, Wnt signalling inhibits chondrogenesis as the overexpression of a stable form of  $\beta$ -catenin in limb mesenchyme inhibited the formation of cartilage [43]. Notch signalling can also inhibit chondrogenesis and MSCs condensation. It is a membrane bound receptor. Upon binding to its ligand on adjacent cells, it undergoes sequential cleavages leading to the generation of a fragment called Notch intracellular domain (NICD) which can go the nucleus and regulate gene expression [33]. Overexpression of an active NICD in limb mesenchyme inhibited chondrocyte differentiation and cartilage formation [44].

- Regulation of chondrocyte maturation in the embryonic growth plate

In late embryogenesis, long bones are made up of trabecular bone in the middle of the diaphysis with an embryonic growth plate at each side. From epiphysis to the middle of diaphysis, the embryonic growth plate is made up of different layers: a proliferative zone of rounded chondrocytes, another layer of proliferative columnar cells, a prehypertrophic zone, a hypertrophic zone and a layer of terminally hypertrophic chondrocytes just near the trabecular bone. This specific arrangement of chondrocytes is controlled by different factors. Proliferative chondrocytes are maintained by factors that induce proliferation and inhibit

hypertrophy. Among these, parathyroid hormone-related peptide (PTHrP) inhibits premature hypertrophy by activating Sox9. It is secreted by cells of the periarticular perichondrium and received by proliferative and maturing chondrocytes before the hypertrophic stages [4,33]. The limbs of *Pthrp* KO mice were short with other skeletal defects due to errors in chondrocyte proliferation and premature hypertrophy [45]. Moreover, the proliferation and the transition from round to columnar chondrocytes is stimulated by Indian hedgehog (IHH). In the embryonic growth plate, IHH is secreted by prehypertrophic and early hypertrophic cells and received by proliferative chondrocytes and the overlaying perichondrial cells. IHH also stimulate the production of PTHrP [4,33]. Wnt5a and Wnt5b are expressed in cells passing from proliferative to the hypertrophic stages. A specific level of these factors is needed for this transition, because any change in their level such as overexpression or downregulation delayed hypertrophy [31]. Also, hypertrophy is tightly regulated by different nuclear factors. Among these, SOX9 is an important regulator of hypertrophy; as mentioned earlier, it inhibits premature hypertrophy when it must not occur, but it stimulates the function of hypertrophic chondrocytes [40]. RUNX2 can act as a pro-hypertrophic transcription factor. Its expression begins during early stages of mesenchyme condensation, continues only in perichondrial cells, and it is re-expressed in prehypertrophic and early hypertrophic cells [33]. Myocyte enhancer factor 2C (MEF2C) is another pro-hypertrophic transcription factor expressed in these cells, and it can induce the expression of RUNX2. The deletion or inactivation of either RUNX2 or MEF2C led to loss of hypertrophy [33,46,47]. In contrast, histone deacetylase 4 (HDAC4) inhibits premature hypertrophy in different ways. It can inhibit MEF2C or RUNX2 activity. The genetic deletion of this factor led to increased hypertrophy [33,48].

### 2.2.3 Osteoblastic differentiation

The subsequent differentiation of osteoblasts in endochondral ossification is also regulated by different factors. Also in this type of bone formation, osteoblasts are first formed as preosteoblasts and then they differentiate in 3 steps similar to those described for intramembranous ossification to become mature. However, some of the controlling signals are different. For example, IHH is not needed for osteoblastic differentiation in intramembranous ossification, but it is crucial in the endochondral type. This is evidenced by the complete loss of osteoblasts in the endochondral skeleton upon *Ihh* genetic deletion in mice and the normal formation of osteoblast in the intramembranous elements [49]. IHH can activate the expression of RUNX2 and Osterix by suppression of Gli3, a suppressor of RUNX2 expression. As mentioned above, it is secreted by prehypertrophic and hypertrophic

chondrocytes and can act on perichondrial cells to induce osteoblastic differentiation [33]. The canonical-Wnt signalling is important in both types of bone formation, and it is needed for all steps of osteoblastic differentiation. Also, BMP2 and 4 are equally important in both ossification types. In endochondral ossification, different FGFs are secreted by perichondrial cells. They act in different ways due to the presence of different receptors (FGFR1, 2 and 3). In general, they have roles in control of early osteoblastic differentiation, preosteoblast proliferation and mature osteoblast mineralizing activities. RUNX2 and Osterix are equally important in endochondral and intramembranous osteoblastic differentiation [33].

#### 2.2.4 Final steps of long bone formation

Later, approximately in the time of birth, a secondary ossification center is formed in each end of the bone at the epiphysis. The process is much similar to that of the primary ossification center, and it results in the formation of the trabecular bone of the epiphysis. The trabecular bone in diaphysis will be then broken down by osteoclasts to create the medullary cavity. A small zone of cartilage between both the primary and secondary ossification centers remains after birth until the age of 21, approximately, and it is named the epiphyseal plate. It contains approximately the same cell arrangement as the embryonic growth plate but it occupies less space. After birth, these chondrocytes continue to proliferate, become hypertrophic and they are then replaced by osteoblasts and bone. This lead to an increase in bone length (longitudinal growth). When the chondrocytes in this site are depleted, the longitudinal growth is arrested. The line between primary and secondary ossification centers is called the epiphyseal line. There is also an appositional bone growth (or radial growth), in which bones increase in diameter. In this type of growth, osteoblasts in the periosteum (which is derived from the perichondrium) begin to secrete bone matrix against the bone collar, and osteoclasts degrade bone from the cavity's side, until a specific thickness is achieved [3].

In order to maintain bone strength, bone matrix is continuously degraded and formed again during the whole life in a process named bone remodelling.

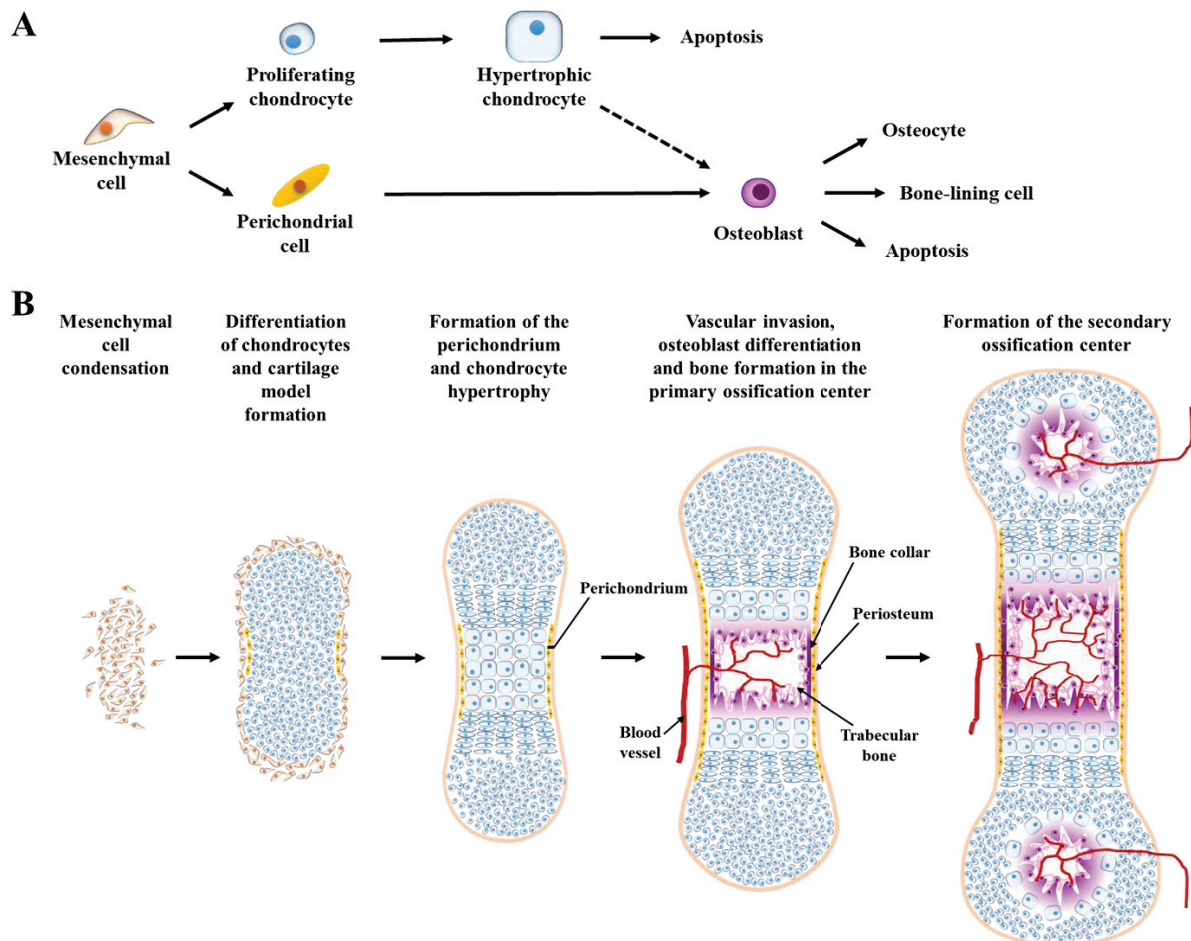


**Figure 4: Endochondral ossification during long bone formation.** Endochondral bone formation begins by mesenchymal cell condensation. Then, cells in the center of the aggregate differentiate into chondrocytes which will build the cartilage model, while cells at the periphery form the perichondrium, containing perichondrial cells. Chondrocytes at the middle of the rod begin to be hypertrophic and mineralize the cartilage in their vicinity. Later, blood vessels invade the hypertrophic cartilage bringing with them osteoblast precursors that differentiate into osteoblasts and form the trabecular bone at the primary ossification center. Perichondrial cells at the inner phase of the perichondrium differentiate into osteoblasts that form the bone collar. Then, a secondary ossification center appears at each epiphysis, resembling the process that occurs in the primary center. Hypertrophic chondrocytes undergo apoptosis, but few of them can trans-differentiate into osteoblasts. Mature osteoblasts undergo apoptosis or they can further differentiate into osteocytes or bone lining cells. (the idea of the figure was adopted from [4])

### 3. Bone remodelling

The process of bone remodelling starts before birth and continues until death [2]. During this process, old bone is replaced with new mechanically stronger one. It is also important in maintaining mineral homeostasis (especially that of Pi and Ca) and in bone reshaping in response to mechanical stress. Thus, it preserves the quality of bone and reshape it to meet the organism's needs. Mainly, it is characterized by 3 phases: the initiation, the reversal and the bone formation phase [1,3]. In the initiation phase, macrophage/monocyte osteoclast precursors are recruited to the site of bone remodelling. The layer of bone-lining cells that

normally cover bone surfaces is lifted so that osteoclast precursors can attach to bone ECM. The mononuclear macrophages fuse to form multinucleated osteoclasts [2]. This step needs at least 2 factors: macrophage colony-stimulating factor (M-CSF) and RANKL. M-CSF is a paracrine factor secreted by mesenchymal cells and osteoblasts. It stimulates proliferation and inhibits apoptosis of osteoclast precursors. RANKL is a membrane-bound ligand expressed on osteoblasts. It binds to RANK, its receptor, on osteoclast progenitors and stimulates the expression of the osteoclastogenic factor: Nuclear factor of activated T-cells cytoplasmic 1 (NFATc1). NFATc1 interacts with other transcription factors to induce the expression of dendritic cell specific transmembrane protein (DC-STAMP), an important factor for osteoclast precursor fusion, and Tartrate-resistant acid phosphatase (TRAP) and cathepsin K, which both mediate osteoclast activity [1]. Osteoclasts attach to bone matrix via integrins that bind bone matrix components. For example,  $\beta 1$  integrin on osteoclasts binds to collagen, fibronectin and laminin in bone matrix. Also,  $\alpha v \beta 3$  integrin on osteoclasts binds OPN and BSP11 in bone matrix [2]. Then osteoclasts resorb bone matrix by secreting hydrogen ions, via the action of  $H^+$ -ATPase proton pump and chloride channels, in order to lower the pH to 4.5 thus dissolving deposited calcium. Cathepsin K, MMP9, and TRAP, produced by osteoclasts, act together to break down the organic matrix. This will leave a cavity in bone: saucer-shaped Howship's lacunae in trabecular bone and cylindrical harversian canals in cortical bone [2]. The following phase is the reversal phase in which the osteoclasts detach leaving the place for osteoblast progenitors which are recruited to the site of bone resorption. Then, these cells differentiate into mature osteoblasts and effectuate new bone matrix formation and mineralization in the last phase. Osteoblasts and osteoclasts communicate directly and indirectly in different manners. Preosteoblast recruitment and maturation is induced by factors released from the resorbed bone matrix like: TGF- $\beta$ , insulin-like growth factors (IGFs), BMPs, Platelet-derived growth factor (PDGF) and fibroblast growth factor (FGF). Osteoclasts by themselves can secrete factors to induce osteoblastic differentiation like Wnt10b, BMP6 and sphingosine 1-phosphate (S1P). Osteoclasts may also help in osteoblastic differentiation by direct binding to osteoblast progenitors. For example, Ephrin B2 on osteoclasts can bind to Ephrin B4 on osteoblast progenitors enhancing osteoblastic differentiation and inhibiting osteoclastogenesis [1]. After bone formation, 50 to 70% of the osteoblasts undergo apoptosis and the rest differentiate into osteocytes or bone lining cells that cover the newly formed bone surface while keeping connections with nearby osteocytes by cytoplasmic extensions. The main regulators of bone remodelling are osteocytes. When they undergo apoptosis, they release chemotactic molecules for osteoclast progenitors recruitment [1]. The viable osteocytes near the apoptotic ones secrete RANKL to enhance

osteoclast differentiation. Moreover, they act as mechanosensors; upon mechanical loading they secrete factors to induce bone formation, like IGF-1 and PGE<sub>2</sub>, and upon mechanical unloading they produce factors to inhibit osteoblast activity like sclerostin and DKK-1, and stimulate local osteoclastogenesis [1]. The osteoclasts and osteoblasts working in the same site are tightly coupled and they are considered as bone remodelling unit. The life span of this unit is between 2 and 8 months [2,3]. The balance between bone resorption and bone formation decide whether the bone mass will decrease, increase or remain the same. Normally in humans, in the first 30 years the balance is positive with an increase in bone mass. Later, the bone mass is kept at an adequate size until the age of 50, approximately. After this, the balance becomes negative and the bone mass decreases [3].

Understanding the molecular mechanisms of differentiation of osteoblasts and chondrocytes and formation of bone and cartilage is important to understand the mechanisms of vascular calcification which was found to be a similar process with involvement of both cell and tissue types [50,51], as will be detailed in the next part.

## **Part 2: Vascular calcification**

### **1. Types and consequences**

Calcification is the term used for ectopic accumulation of calcium crystals in extraskeletal tissues. In the cardiovascular system, it occurs mostly in blood vessels and in heart valves. In arteries, calcification can be found in any layer. Blood vessels are mainly made up of 3 layers: tunica intima, tunica media and tunica adventitia (figure 5). The intima is the innermost layer of the vessel which is in direct contact with blood. It is mainly made up of a layer of endothelial cells situated on a basement membrane with some pericytes [52] (Figure 5). Calcification in this layer is associated with atherosclerosis. It may affect plaque stability depending on its pattern. While microcalcifications, characterized by spots or granules of calcification, destabilize the plaque and favour its rupture, macrocalcifications, characterized by diffuse and continuous calcification, stabilize it and prevent its rupture [53].

The medial layer of blood vessels is mainly made up of fenestrated sheets of elastin with smooth muscle cells (SMCs) situated between them. This layer is highly organized in larger arteries especially the elastic ones near the heart, such as the aorta, but the elastin fibers are discontinuous in the muscular arteries and present within a large layer of SMCs (Figure 5). Most of the arteries in the body are of the muscular type [52,54]. Calcification in this layer was described for the first time in 1903 by Johan George Mönckeberg who called it at that time: calcific sclerosis [55]. Now, it can be alternatively referred to as Mönckeberg arteriosclerosis. It is mostly seen in patients with diabetes and chronic kidney disease (CKD) [51,56].

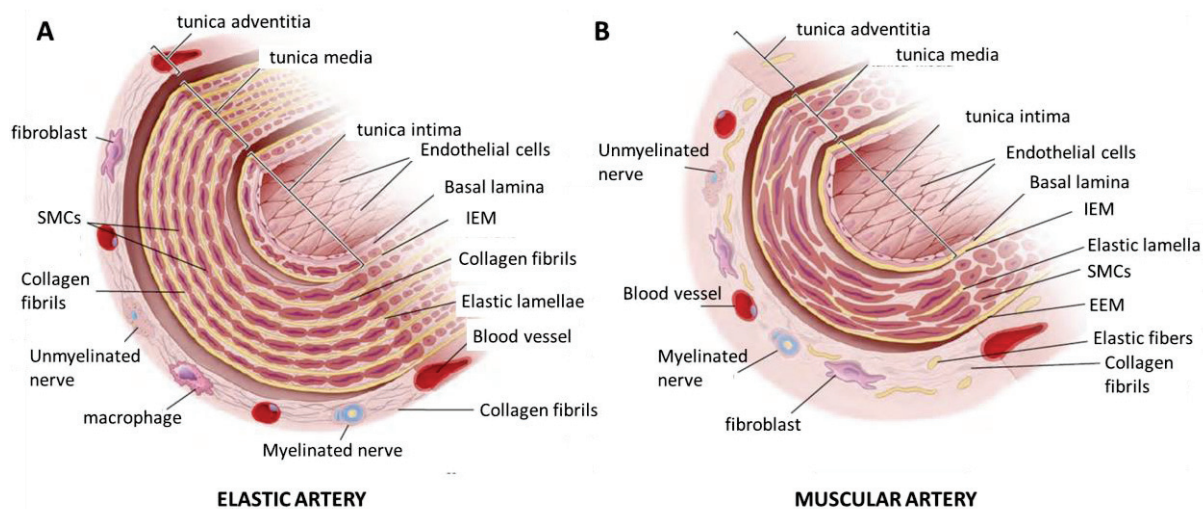


**Figure 5: the general structure of elastic and muscular arteries.** Arteries are made up of 3 layers: tunica intima, tunica media and tunica adventitia. Tunica intima is made up of endothelial endothelial cells situated on a basal lamina. An internal elastic membrane separates tunica intima from tunica media. The latter is made up mainly of SMCs and elastic lamella, with some collagen fibrils. The elastic lamellae are highly organized and contineous in elastic arteries in contrary to what is seen in muscular arteries. Tunica adventitia is the outermost layer of arteries, and it is usually made up of fibroblasts, collagen fibrils and blood vessels, and nerves in large arteries. Abbreviations: IEM: internal elastic membrane, EEM: external elastic membrane. [57]

Kidney disease is any damage in a kidney that affects its function. It is divided into 5 stages according to the severity of damage as measured by the ability of kidneys to filtrate blood measured as glomerular filtration rate (GFR). Stage 1 and stage 2 kidney disease is characterized by no change and mild decrease in GFR, respectively, with proteinuria. Kidney disease is considered chronic starting from stage 3 when GFR fall below  $60 \text{ ml/ min/ } 1.73 \text{ m}^2$  for at least 3 month. After this, the progressive loss of kidney function leads to stage 4 ( $15 \text{ ml/ min/ } 1.73 \text{ m}^2 < \text{GFR} < 29 \text{ ml/ min/ } 1.73 \text{ m}^2$ ) and stage 5 CKD. Stage 5 CKD is identified by  $\text{GFR} < 15 \text{ ml/ min/ } 1.73 \text{ m}^2$  or complete loss of kidney function, and it is defined as end-stage renal disease (ESRD) in which dialysis is the only solution for blood filtration [58].

In CKD, usually both forms of VC are found, intimal and medial, but the presence of intimal form may be due to increased age and other risk factors, because in young CKD patients, vascular calcification (VC) is restricted to the medial layer. Medial calcification was thought to occur only in ESRD, however it can begin in as early as kidney disease stage 2 [51,56].

While intimal calcification affects the diameter of blood vessels, medial calcification interferes with another important function of arteries. Normally, the arterial system has 2 functions; not only it is responsible for conducting blood and distributing it to body organs and tissues (conduit function), but also it allows the maintenance of continuous blood flow and helps in dampening pressure oscillations induced by the heart cyclic activity (dampening

or Windkessel function) (Figure 6). Large elastic arteries, but not small ones, are especially important in the second function. Among these, the aorta is the principle player. Normally, the aorta has high elasticity owing to the huge amount of elastin present in its wall, especially in its proximal part. In systole, when the left ventricle (LV) ejects blood into the aorta, the change in pressure (pulse pressure) cause the aortic wall to distend in order to accommodate part of the ejected blood. Usually, only about 50% of the ejected blood is forwarded directly to the peripheral circulation, while the rest is stored in the aorta and large arteries that expand using some of the kinetic energy provided by the ejected blood. This energy is stored in the aortic wall as potential energy. Then in diastole, the aorta recoils back ejecting the blood into the peripheral circulation and into the coronary artery, which depends mainly on diastolic blood supply [59,60]. Thus, a continuous blood flow and sufficient myocardium perfusion are maintained regardless of the heart intermittent function. This improves left ventricular relaxation and minimizes heart work.

There is another factor that also helps in maintaining good diastolic function: the pulse wave. This wave is initiated at the aortic wall as an increase in pressure when blood is ejected from the LV, and it traverses the arterial tree in a speed that exceeds that of blood to allow its displacement easily. It becomes reflected at more distal sites due to different factors like branching, narrowing or increasing resistance of arteries. In a healthy arterial system, the reflected wave strikes back at the ascending aorta in early diastole boosting diastolic pressure [59,60]. This occurs perfectly when the aortic elasticity is optimal. However, these functions are affected in different conditions that decrease elasticity [61,62].

Medial calcification mainly increases the stiffness of arteries [61,62]. In case of CKD, most of the calcifications are present in large arteries such as the aortic arch and the abdominal aorta [63]. A stiffened aorta cannot expand adequately. In this case, most of the systolic blood will be passed directly to the circulation, leaving very little amount to be forwarded during diastole. This will lead to reduced coronary artery flow and a nearly discontinuous peripheral blood flow (diastolic dysfunction). Also, the pulse wave velocity (PWV), the speed at which the pulse wave travels through arteries, increases in stiffer arteries, and the reflected wave will hit the proximal aorta during systole, elevating the systolic pressure and further decreasing the diastolic pressure. To compensate for these defects, the LV has to increase the pressure at which it ejects blood leading to LV afterload and hypertrophy [64,65]. Also, the heart has to work faster in order to maximize blood supply for periphery circulation leading to heart failure especially that it is under partial coronary ischemia due to diastolic dysfunction [65].

These theoretical complications were proven in a large number of epidemiological studies. In patients of CKD, cardiovascular events are the leading cause of death with high incidence of LV hypertrophy (75%) and congestive heart disease (40%) [66,67]. The presence and extent of calcification, especially the medial form, were shown to be strong predictors of all-cause and cardiovascular mortality in hemodialysis (HD) patients [62,68]. In HD patients also the extent of calcification was associated with aortic stiffness and LV afterload, independently of age and blood pressure [62,69]. On the other hand, there was a specific increase in aortic stiffness in these patients but not in the femoral or brachial arteries, arteries of legs and hands, respectively, as detected by measuring PWV. Also, there was a correlation between aortic PWV and left ventricular mass, showing the specific association between aortic stiffness and LV hypertrophy [64]. In accordance with this, the stiffness of the aorta, but not that of the peripheral arteries, was shown to be a strong predictor of CV mortality in CKD patients [70]. Also in a rat model of CKD, thoracic medial calcification was also correlated with aortic stiffness [71]. Thus, the effect of medial calcification on aortic stiffness may be the principle cause of CV mortality in CKD patients.

Lately, VC was also detected in the adventitial layer of blood vessels [72]. This layer is the outermost one made up of connective tissue situated outside the external elastic lamina. It is rich in collagen, produced by myofibroblasts, that prevent rupturing of the vessel at high pressure [54] (Figure 5).

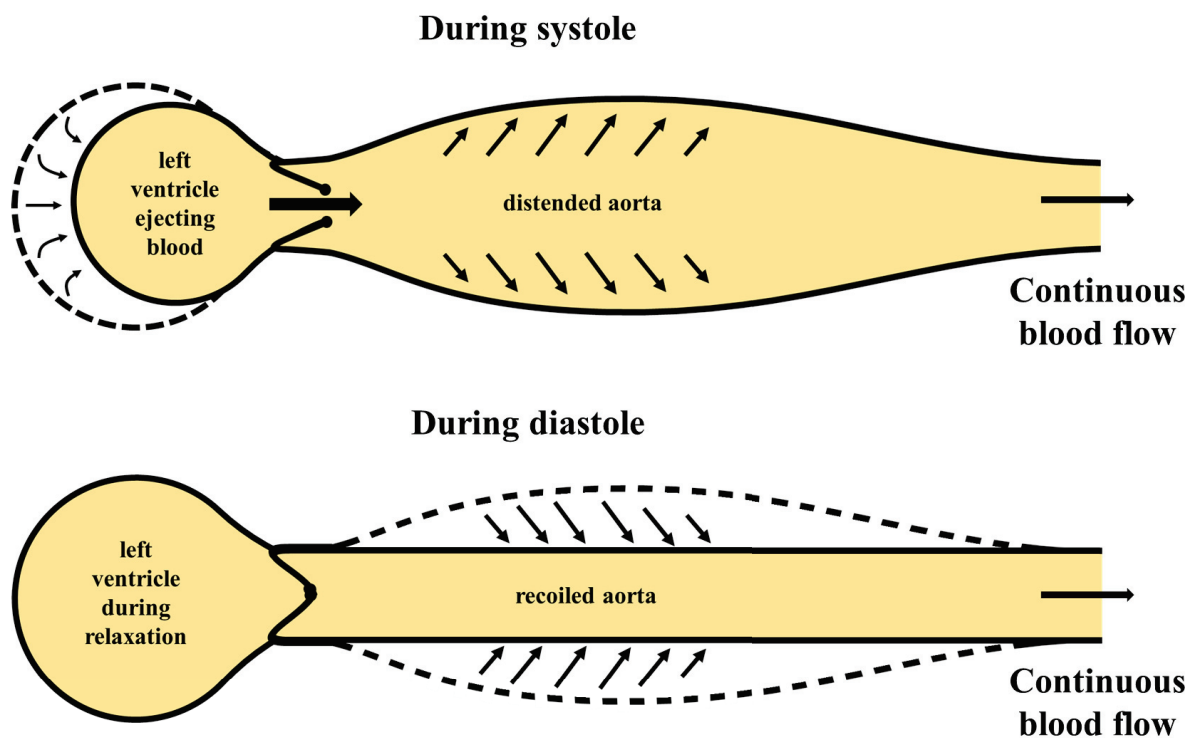


**Figure 6: The Windkessel function of the aorta and large elastic arteries.** During systole, the left ventricle contracts and ejects blood into the aorta. About half of ejected blood is passed directly to the peripheral circulation, whereas the rest is stored in the aorta and large elastic arteries that distend to accommodate the large blood volume. During diastole, the aortic valve close and the aorta recoils again pushing the stored blood to peripheral circulation, and thus providing a continuous blood flow.

## 2. Cellular and molecular mechanisms

Ca is present physiologically in concentrations enough to drive passive precipitation of different Ca salts. However, mechanisms that inhibit this precipitation evolved. In locations of physiological biomineralization, like bones, cartilage and teeth, cellular and molecular pathways cooperate to create an environment permissive for mineral deposition via local inactivation of these inhibitory mechanisms. Calcium-phosphate crystals are initially formed in the same way they do in inorganic supersaturated mixtures. However, cellular-related factors do organize and limit the rate of their deposition, to localize them correctly, mainly to collagen fibers [65]. VC was thought to involve passive precipitation of Ca and Pi when their concentrations increase beyond physiological levels. However, it was proved to engage multiple cellular and molecular events, similar to those seen in normal bone formation [67]. Although medial and intimal calcifications implicate different factors and mechanisms, they both encompass a key step of trans-differentiation of SMCs into bone or cartilage forming cells, osteoblasts or chondrocytes, which is the most accepted hypothesis for the origin for calcifying vascular cells. VSMCs are mesenchymal-derived cells which are, under stress,

capable of trans-differentiating into osteoblasts, chondrocytes or adipocytes [51]. Recently, it was suggested that circulating osteoprogenitor cells derived from bone marrow can home to injured vessels and induce calcification. The basis of this hypothesis is the finding that bone-marrow derived cells can migrate to injured vessel and differentiate to VSMCs, and there was association between the level of OCN-positive circulating mononuclear cells and VC in mouse models and human studies [73–75]. However, this hypothesis do not have any further experimental evidences. The resultant osteo-chondrocyte-like cells can then direct mineral deposition in the same way as in bone and cartilage. In intimal calcification, VSMCs can migrate from vessels media and be responsible for calcification [51,76].

VSMCs trans-differentiate under different types of stresses to osteo-chondrocyte-like cells. They lose the expression of SMC-specific proteins, such as  $\alpha$ SMA and SM22 $\alpha$ , and their contractile properties and gain a proliferative synthetic phenotype. Under the effect of osteo-chondrocyte transcription factors such as RUNX2, Osterix, MSX2 and SOX9, they gain the ability to produce and secrete bone or cartilage-specific ECM proteins, like OPN, BSP1, osteonectin, collagen I/II and OCN, and mineralization-competent MVs [50,51,55,56]. The phenotypic switch of VSMCs was evidenced *in-vivo* in animals and humans [77]. Wide repertoire of different factors can induce such phenotypic switch depending on the context of the underlying disease. In CKD, hyperphosphatemia and probably inflammation are considered the main direct factors, however in atherosclerosis the main direct factors could be inflammation and oxidative stress. In diabetes, hyperglycemia can also directly induce osteo-chondrogenic differentiation of SMCs [50]. Calcification is also accompanied by some degree of SMC and macrophage apoptosis, which is thought to contribute to ectopic calcification. Moreover, elastin degradation is a characteristic of medial calcification, but also act as a mediator for it, and it contributes much to stiffness observed in case of arteriosclerosis. Furthermore, calcification is enhanced by a systemic or local decrease in different mineralization inhibitors [55,56] (Figure 7).

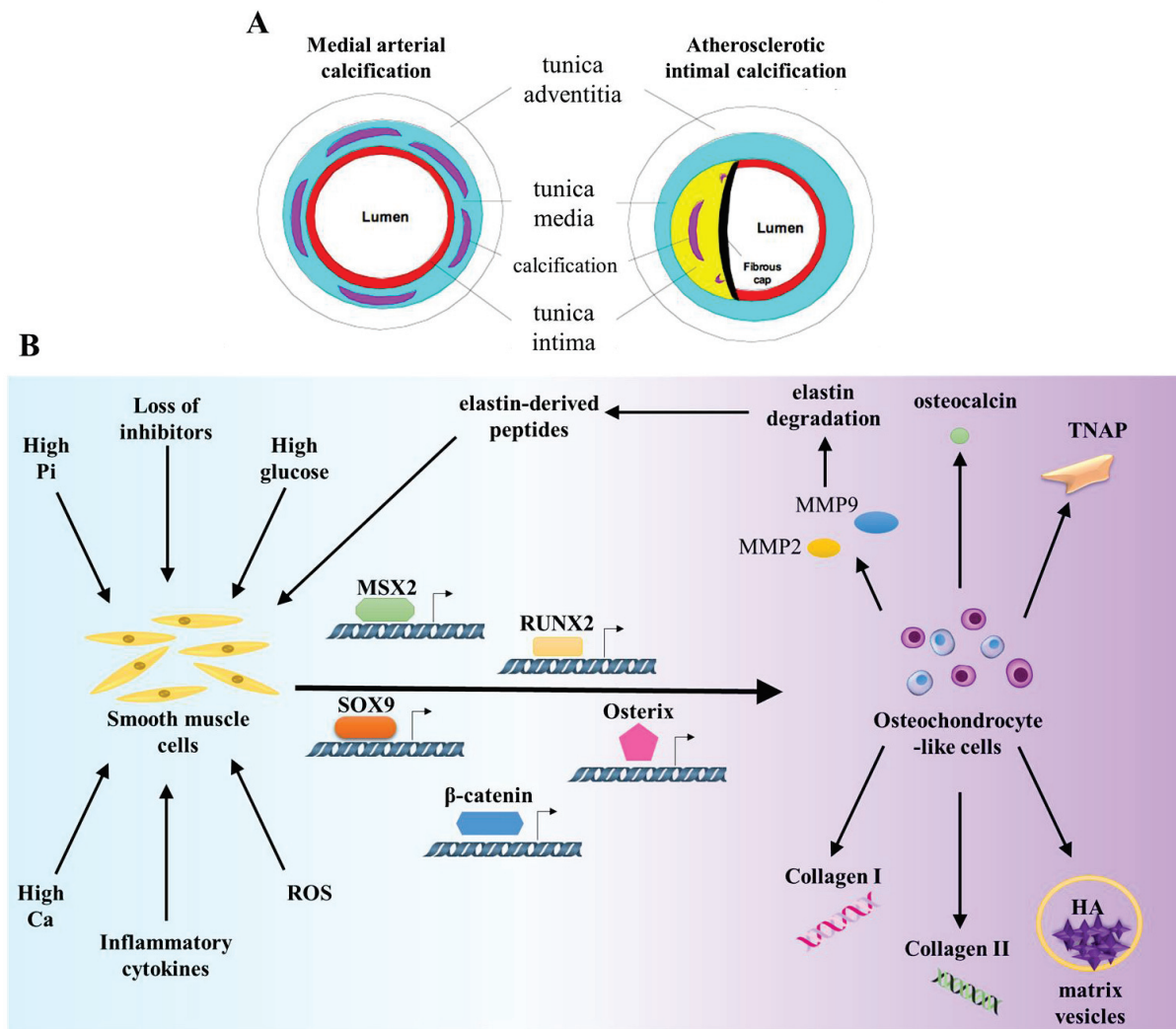


**Figure 7: The mechanism of vascular calcification.** A: VC is mainly seen in the medial or in the intimal layer of blood vessels [78]. B: The most accepted hypothesis for VC is the trans-differentiation of SMCs into osteo-chondrocyte-like cells. This occurs in response to a wide spectrum of stimuli, like: high Pi, high Ca, high glucose, reactive oxygen species (ROS) and inflammatory cytokines. Also, the loss of calcification inhibitors can induce calcification. These stimuli can induce the expression and activity of different osteo-chondrogenic transcription factors including: RUNX2, SOX9, Osterix, MSX2 and/or  $\beta$ -catenin. Under the effect of these transcription factors, the trans-differentiated cells gain the ability to produce bone- or cartilage-specific proteins, including OCN, TNAP, collagen type I or/and II. Also, they produce MMPs that induce elastin degradation. Degraded elastin can also activate the phenotypic switch of SMCs. Moreover, the cells gain the ability to produce mineralization-competent matrix vesicles which act as nidus for primary HA deposition.

## 2.1 Role of vitamin D

### 2.1.1 VitD metabolism

VitD is a steroidal prohormone that can be synthesized in the skin as VitD3 from 7-dehydrocholesterol in a reaction that requires ultraviolet light. Alternatively, it can be obtained by dietary intake as VitD2 (ergocalciferol) or D3 (cholecalciferol). Both types are carried to the liver where they are converted to 25-hydroxyVitD (25(OH)D). Then, this form is

transported through blood by binding to VitD binding protein (DBP), to be received at the level of kidney. In the kidney, it is taken up by the proximal tubular cells by a receptor called megalin after being filtered into the glomerulus. In these cells, under the action of  $1\alpha$ -hydroxylase (CYP27B1) enzyme, it becomes converted to 1,25-dihydroxyVitD ( $1,25(\text{OH})_2\text{D}$ ), which is also called calcitriol and it is the main active form of VitD. Also in the kidney,  $25(\text{OH})\text{D}$  and  $1,25(\text{OH})_2\text{D}$  can be inactivated via conversion to  $24,25(\text{OH})_2\text{D}$  and  $1,24,25(\text{OH})_3\text{D}$ , respectively, by 24-hydroxylase (CYP24A1) (Figure 8). Hydroxylation at the 24 position inactivates VitD. The activity and expression of VitD hydroxylases in the kidney are regulated mainly by parathyroid hormone (PTH) and fibroblast growth factor 23 (FGF23). PTH increases the activity of renal CYP27B1 leading to increase in active VitD production [55,79]. On the other hand, FGF23 inhibits renal CYP27B1 expression and increase CYP24A1 expression leading to inhibition of calcitriol formation and its degradation [80]. Calcitriol and other VitD receptor (VDR) agonists (VDRA) can bind directly to intracellular VDR and activate it [79,81]. Active VitD acts on intestine to increase Pi and Ca absorption. Also, it activates osteoclastogenesis in bone, thus mobilizing large amounts of Pi and Ca to the circulation [82].

### 2.1.2 Dysregulation of VitD metabolism in CKD

With declining renal function, many patients develop VitD deficiency due to different factors including the decrease in renal mass which lead to loss of CYP27B1 and the decrease in GFR leading to reduced delivery of  $25(\text{OH})\text{D}$  to the renal CYP27B1. Also, in the context of proteinuria, reduced megalin leads to decreased reabsorption of  $25(\text{OH})\text{D}$ -DBP [79,81,83,84]. These are accompanied with dysregulation of hormones that regulate the activities and expression of renal hydroxylases, like FGF23 which was seen to be increased in CKD [79,81]. In the other way round, VitD controls negatively the production of PTH. Thus, VitD deficiency in the context of CKD is the main cause of secondary hyperthyroidism seen in this disease. However, the effect of PTH on kidney cells is reduced due to accumulation of uremic toxins because of diminished GFR. Thus, VitD deficiency is the result of increased FGF23 and decreased responsiveness to PTH at the kidney level [79,82]. VitD deficiency was shown to be associated with increased risk of death in CKD patients [85,86]. Thus, interventions to correct its level and subsequently attenuate hyperparathyroidism are used. VDR agonists were given to CKD and ESRD patients and showed a decrease in all-cause and cardiovascular mortality, especially in patients with secondary hyperparathyroidism [86,87]. VitD help in attenuating kidney injury in mechanisms different than regulating mineral

levels. These roles include its inhibition of fibrosis, inflammation, apoptosis and different pathways involved in kidney injury like the renin-angiotensin-aldosterone system [81].

### 2.1.3 VitD and vascular calcification

The role of VitD in VC is controversial, with discrepancies between different doses and different models used. There are different reasons for these discrepancies; VDR is expressed in VSMCs, thus VDRA, along with their systematic effect, can act directly on these cells. Also, the dose of VDRA and the presence of other risk factors may affect enormously the results. Moreover, different VDR analogues may have different effects on VC [88].

In two studies in ESRD patients, VitD deficiency was not associated with increased risk of VC unless in a subgroup of obese patients [89,90]. However, these studies were depending on the level of 25(OH)D. In another study, measuring the level of 1,25(OH)<sub>2</sub>D, both low and high levels were found to be associated with increased VC. In this study, the level of 1,25(OH)<sub>2</sub>D did not correlate with that of 25(OH)D, which may explain the inconsistencies between these studies [91]. Low doses of VDRA, administered to HD patients with secondary hyperparathyroidism such as cinacalcet, a VDRA, induced a decrease in aortic and cardiac valve calcification [92]. Also, the administration of calcifediol, another VDRA, but not calcitriol led to a decrease in PWV after 6 months of treatment in CKD patients [93]. Moreover, the comparison of calcitriol effect to the effect of another VDRA, paricalcitol, showed a significant decrease in mortality rate of HD patients in case of paricalcitol compared to calcitriol [94]. Thus, epidemiological studies in CKD patients revealed the importance of VitD level regulation at adequate doses, and capitalized the different mechanisms involved in the action of diverse VDRA. *In-vivo*, calcitriol induced VC and increased PWV in different studies utilizing rats in which CKD is induced by nephrectomy or high-adenine diet [95–97]. However, in a study in CKD mice, low dosages of calcitriol, which were enough to decrease PTH, protected against VC, but higher dosages increases the burden of aortic calcification [98]. On the other hand, the usage of paricalcitol in CKD rats didn't cause any VC, even when it is used in a dosage that cause similar increase in serum Pi and Ca as seen with calcitriol [96,97]. Thus, the protective effect of paricalcitol is not dependent on serum Pi and Ca, but it may have direct protective roles on VSMCs. The direct effects of VDRA on VSMCs was investigated *in-vitro*. In these models, calcitriol was shown to increase calcification at doses > or = 10 nM, however the use of paricalcitol at any dose did not cause any calcification but even attenuated the calcification induced by high Pi [97,99]. The dose importance is manifested by a protective action of calcitriol in concentrations between 0.5 and 5 nM on human VSMCs calcification caused by high Ca, but

a concentration of 10 nM was ineffective. The protective effect of calcitriol was attributed to the increase in expression of Ca sensing receptors (CaSR) which is inversely associated with VC [100]. Calcitriol was even protective against high Pi-induced calcification in human VSMCs even when used in 100 nM concentration, thus adding more discrepancies between different studies [101]. Finally, a delicate investigation of calcitriol systematic and direct roles was done by Iomashvili et al. [102]. In this study, calcitriol induced aortic calcification in uremic but not in normal mice. Also, *Vdr*<sup>-/-</sup> aortic segments were transplanted in *Vdr*<sup>+/+</sup> mice and then they were rendered uremic. In these mice, calcitriol induced same level of calcification in native aorta and in the allograft, indicating that the calcification inductive role of calcitriol is due to systematic rather than direct effects [102]. Thus, interpreting the exact role of VitD in calcification is hard due to systematic and local effects that may differ in their results and that also depends largely on the dose used.

## 2.2 Role of high phosphate

### 2.2.1 Phosphate homeostasis

Phosphate homeostasis is regulated mainly at 3 sites: intestine, kidneys and bones by 3 main factors: VitD, PTH and FGF23. As explained in the previous part, VitD increases serum Pi by increasing its intestinal absorption and its mobilization from bone. PTH is a phosphaturic hormone that normally acts at the kidney level to induce Pi excretion. However, it also increases the synthesis of VitD, which can increase the absorption of Pi. Thus, Pi dietary intake can affect largely the role of PTH and VitD [82]. FGF23 is another phosphaturic factor. FGF23 is synthesized and released from bone by osteocytes and osteoblasts, and it binds to its receptor in kidneys to decrease Pi reabsorption at the level of proximal tubules by decreasing the expression of sodium-phosphate co-transporter type II (NPT2A and NPT2C), thus increasing Pi excretion. Also, as mentioned earlier, FGF23 acts on the kidney to decrease the production of calcitriol, leading to further decrease in serum Pi. To act, FGF23 needs an obligate co-receptor, called klotho. [51,80,82,103]. Mice KO for either klotho or FGF23 had similar phenotypes with higher serum Pi along with an increase in vascular medial calcifications [104,105] (Figure 8).

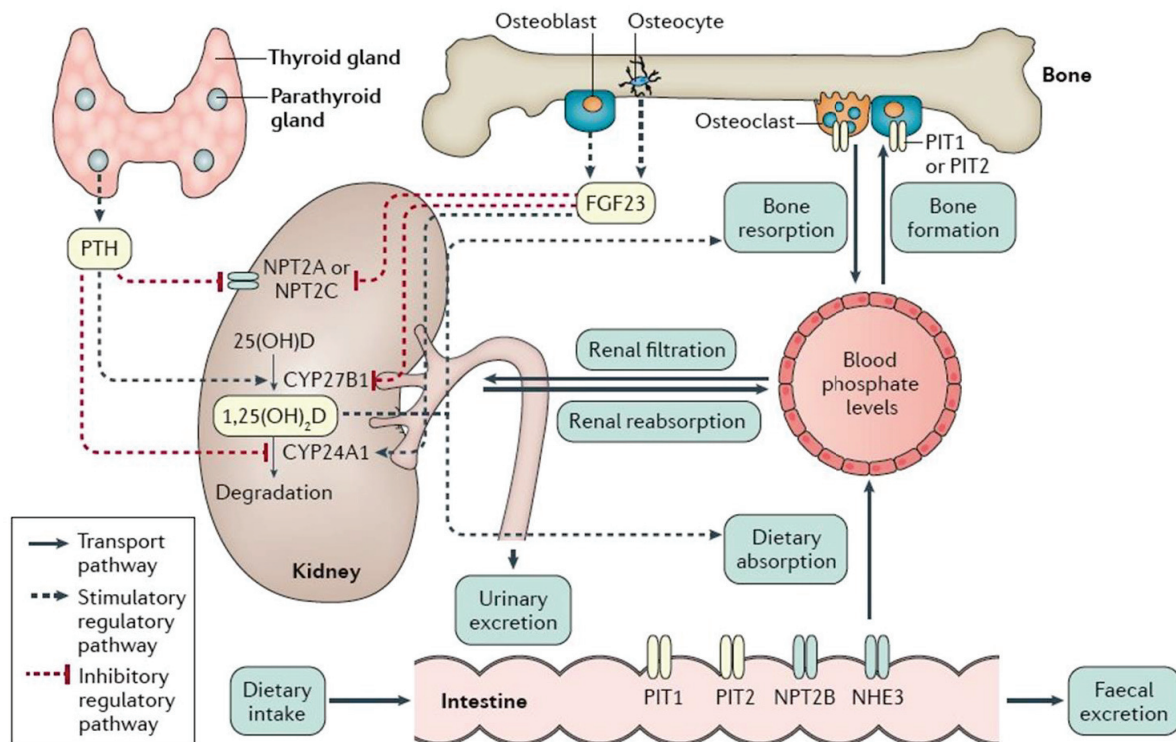


**Figure 8: Phosphate homeostasis.** The blood Pi level is maintained due to the action of 3 factors mainly on bone, kidney and intestine. FGF23, produced by osteoblasts and osteocytes, induces phosphate excretion in urine by inhibiting its reabsorption via decreasing the expression of its transporters: NPT2A and NPT2C. Also, at the level of kidney, it inhibits the production of 1,25(OH)<sub>2</sub>D by inhibiting the action of CYP27B1, and it induces its inactivation by activating CYP24A1. On the other hand, PTH produced by the parathyroid gland, also induces phosphate renal excretion via inhibiting NPT2A and NPT2C. Also, it increases the production of 1,25(OH)<sub>2</sub>D by activating CYP27B1 and inhibiting CYP24A1. 1,25(OH)<sub>2</sub>D act at the level of intestine to increase phosphate absorption and at the level of bone to induce bone resorption and phosphate mobilization into blood [154].

### 2.2.2 Dysregulation of phosphate homeostasis in CKD

In CKD, Pi homeostasis is perturbed due to different factors. Due to decreased kidney mass and function, less Pi is excreted in urine. However, during the first 3 stages of kidney disease, serum Pi remains approximately within normal range despite the declining kidney function. This can be explained by the early increase in FGF23 serum level in response to early minor changes in serum Pi. The increase in FGF23 helps in keeping serum Pi constant and in decreasing calcitriol level. Also, VitD deficiency leads to a feedback at the level of parathyroid gland, leading to secondary hyperparathyroidism. High PTH can also increase Pi excretion in the first stages of CKD. However, with more deterioration in kidney function and mass in CKD stages 4 and 5, resistance to high FGF23 develops due to decrease in Klotho expression. Also, the effect of PTH will decrease especially due to accumulation of uremic toxins. These events will lead to uncontrollable hyperphosphatemia [80,106]. Moreover,

VDRA given to attenuate secondary hyperparathyroidism, especially calcitriol, can further increase serum Pi in CKD patients [88].

### 2.2.3 High phosphate and VC

The normal level of serum Pi is between 3 and 4.5 mg/dL. In individuals with normal kidney function, this level can also reach 6.2 mg/dL. In CKD patients, serum Pi level remains in the normal range until stage 4 and increase further in stage 5 CKD (ESRD) patients [103]. In a study on HD patients, about 10% had serum Pi > 9 mg/dL, and about 30% had serum Pi > 7 mg/dL [104]. In this group, serum Pi > 5 mg/dL was associated with increased risk of death and cardiovascular morbidity [105]. Also, in pre-dialysis CKD patients, mildly elevated serum Pi within the normal range was associated with death independently of cardiovascular risk factors and CKD stage [106,107]. Higher Pi serum level in people with normal kidney function was shown to be associated with cardiovascular disease morbidity and mortality [108,109]. Moreover, high Pi levels within normal range in healthy adults was shown to be associated with increased risk of coronary artery calcification, left ventricular hypertrophy and heart failure [110–112]. Also in CKD patients, high Pi was associated with increased PWV along with vascular and valvular calcification [113,114]. Phosphate binders are now used to treat hyperphosphatemia in CKD patients.

- Induction of VC by high phosphate

CKD mice fed on normal-phosphorus diet didn't develop VC, however a high-phosphorus diet caused vascular medial calcification without atherosclerosis formation. SMCs in these mice showed trans-differentiation into osteo-chondrocytic phenotype with decrease in SM22 $\alpha$  expression and upregulation of RUNX2 and OPN. The level of calcification was associated with increased serum Pi [107,108]. Also, CKD rats fed on high-phosphorus diet developed significant aortic calcification, which was attenuated by the usage of sevelamer, a phosphate binder that effectively decreases serum Pi [109]. Also *in-vitro*, high Pi medium was routinely used to induce calcification in VSMCs. High Pi also induces their trans-differentiation into osteo-chondroblastic cells with increased expression of *Runx2* and *Bglap*, increased AP activity and decreased SM22 $\alpha$  expression [110,111]. Alternative to Pi,  $\beta$ -GP was also used as an organic donor for Pi to induce calcification in cultured VSMCs. Along with calcification, it was also able to induce osteo-chondrogenic phenotype switch with increased expression of *Runx2*, *Spp1*, *Colla1* and *Alpl* [112,113]. Moreover, Pi was used as a stimulator of calcification in organ cultures of mice or rat aortas. *Runx2* expression was seen to be increased in some of these studies but not in all [110,114–116].

- Molecular mechanisms of Pi-induced calcification

Pi is a major constituent of HA, the principle mineral found in bone and blood vessels in case of VC. An increase in extracellular Pi can favour the formation of hydroxyapatite, especially when PPI level is rendered low by higher expression and activity of TNAP. In this case, the increase in Pi/PPI ratio, like in case of bone mineralization, can lead to mineral deposition. However, the role of Pi in VC is not restricted to this; Pi can play an active role in driving VSMC osteo-chondrogenic differentiation. The active role of Pi is in part dependent on its take up by VSMC. VSMCs express type III sodium-dependent Pi transporters: PiT1 and PiT2, with PiT1 being the major form [106,117]. Pi-induced calcification and phenotypic changes in VSMCs was inhibited by downregulation of *Pit1* and inhibiting Pi internalization. Its overexpression in these cells restores Pi transport, Pi-induced calcification and phenotypic change [117]. To confirm this, Crouthamel et al. generated a mouse model with VSMS-specific deletion of *PiT-1*, as *PiT1*-KO mice die before birth [77,118]. In these mice, CKD induction and high-phosphorus diet led to aortic calcification to the same extent as in WT animals. However, PiT2 was overexpressed in KO mice. Thus, VSMCs were isolated from these mice, and they were able to take up Pi and calcify when cultured in high Pi conditions. But, when PiT2 was downregulated, Pi-induced calcification was inhibited. Thus, the Pi transporter PiT1 has a critical role in Pi-induced calcification, and PiT2 can compensate for its loss [118]. The role of PiT1 was thought to be only due to its ability to import Pi, however an elegant study done by Chavkin et al. had shown that PiT1 helps in Pi-induced calcification both dependently and independently on Pi import. In this study, they overexpressed Pi transport-deficient or WT PiT1 in PiT1-deficient VSMCs. The Pi-transport-deficient PiT1 was also able to induce VSMCs trans-differentiation but not optimal calcium deposition in response to Pi [119]. The mechanisms by which Pi induces SMCs trans-differentiation is still not fully elucidated. However, many studies identified possible mechanisms including extracellular signal-regulated kinase 1/2 (ERK1/2) activation, Wnt/ $\beta$ -catenin signalling activation, aldosterone synthase (CYP11B2) expression, microtubules modulation, Kruppel-like factor (KLF4) expression, DNA methylation and reactive oxygen species (ROS) production. High-Pi induced phosphorylation of ERK1/2 prior to downregulation of SMC markers [119,120]. The blockage of ERK1/2 activation by MEK inhibitor, U0126, inhibited Pi-induced trans-differentiation of SMC [120]. In response to high Pi, PiT1 deficient VSMCs didn't show increase in ERK1/2 phosphorylation, however the overexpression of transport-deficient PiT1 was able to restore Pi-induced ERK1/2 activation. Thus, Pi-transport independent function of PiT1 accounts for Pi-induced activation of ERK1/2, which is important for trans-differentiation of SMCs [119]. Pi also induces the activation of  $\beta$ -catenin

and its nuclear translocation. The blockage of Wnt/ $\beta$ -catenin signalling inhibited Pi-induced *Runx2* expression in VSMC and it was found that *Runx2* is a direct target for activated  $\beta$ -catenin in these cells [121]. A recent study showed that Pi can induce the expression of CYP11B2 by promoting the nuclear export of its expression repressor (DNA-(apurinic or apyrimidinic site) lyase, APEX1). Interestingly, downregulation of CYP11B2 decreased calcification and phenotypic changes of SMCs induced by Pi [122]. Also, microtubule dynamics were shown to be involved in Pi-induced VSMC calcification. Pi was shown to decrease the expression and phosphorylation of PKC $\alpha$  and PKC $\delta$  that upon downregulation led to disassembly of microtubules and actin, respectively. In another study, depolymerisation of microtubules led to increase in Pi-induced calcification, while their stabilization led to inhibition of calcification, osteo-chondrogenic transformation and matrix vesicles release [123,124]. Thus, Pi may induce microtubule depolymerisation to favour calcification and MV release. Moreover, Pi induced the expression of the transcription factor KLF4 whose downregulation led to inhibition of Pi-induced increase in osteogenic markers and decrease SMC-specific factors. Interestingly, KLF4 was found also to be upregulated in the aortas of adenine-induced uremic rats [125]. Moreover, the decrease in SM22 $\alpha$  expression was shown to be due to its promoter methylation in response to high Pi, and the methylation inhibitor procaine was able to inhibit SM22 $\alpha$  downregulation and SMC calcification in response to Pi [110]. Furthermore,  $\beta$ -GP led to increase in production of ROS in cultured SMCs along with osteogenic differentiation and calcification. The inhibition of mitochondrial ROS production reduced calcification significantly. Thus, oxidative stress may contribute to Pi effects on SMCs [126].

- Pi effects on apoptosis and senescence

Also, Pi was shown to induce senescence and apoptosis. Sirtuin 1 was able to inhibit premature senescence in VSMC. Pi induced senescence by decreasing sirtuin 1 expression. The activation of sirtuin 1 inhibited Pi-induced senescence-associated calcification in SMCs. Thus, Pi may induce calcification in some way by inducing senescence, especially that high passage cells with replicative senescence were more sensitive to Pi-induced calcification [127]. In some *in-vitro* models of SMCs, Pi was shown to induce apoptosis. It was proposed that this is achieved by a downregulation in growth arrest-specific 6 (GAS6) and its receptor AXL that are considered survival mediators. The importance of Gas6 downregulation was validated by adding recombinant Gas 6 to VSMCs which inhibits apoptosis and calcification. Also, it was shown that statins can decrease both apoptosis and calcification induced by Pi in VSMCs [128]. Thus, Pi can enhance calcification by inducing senescence or apoptosis.

### 2.3 Role of calcium

Normally, Ca serum level is kept within narrow range (9- 10.5 mg/dL) due to the action of different factors at 3 main tissues like Pi: bone, intestine and kidney. Mainly, calcitriol acts at the intestine to increase its absorption and at bone to increase its mobilisation. Thus, calcitriol serves to increase serum Ca. PTH mainly acts at the level of kidney to increase calcitriol synthesis and stimulate Ca reabsorption, thus also increasing its serum concentration. FGF23 also induce Ca reabsorption at kidney level. Extracellular Ca is sensed by the widely expressed CaSR. Upon a small increase in Ca, CaSR is directly activated to induce different signals according to tissue type. In the parathyroid gland, CaSR send signals to inhibit PTH synthesis and production when it is activated by high Ca. Thus, the decrease in PTH and consequently calcitriol must lead to a decrease in serum Ca back to its normal level. In CKD, Ca homeostasis is perturbed leading to hypocalcemia due to resistance to PTH and FGF23, as described earlier, and VitD deficiency. However, dialysis and supplementation with active VDRA and calcium-based phosphate binder can lead to sporadic hypercalcemia [56,129,130]. High extracellular calcium in vessels of CKD patients is not only due to high serum Ca but also due to local increase of Ca released from apoptotic SMC. It can signal through CaSR, however CaSR was shown to be downregulated in calcifying VSMCs and calcified arteries from CKD patients. Intracellular Ca become elevated due to import from extracellular space via Ca channels or due to lysosomal degradation of small calcium nanocrystals [129].

In vessels, high Ca contributes to VC in different ways. The usage of Ca channels blockers was associated with lower rate of calcification progression and mortality, and was able to block VC in high VitD-treated rats, cultured VSMCs and *ex-vivo* aortas [129,131–134]. However, not all types of Ca channels blockers were able to induce this effect, only verapamil had effect on *in-vitro* calcification, which may be due to other effects independent of its action on Ca channels [131]. Ca can induce apoptosis causing a further increase in local Ca and the release of apoptotic bodies, which can potentially act as nidus for HA crystal deposition. Also, it was shown to increase the production of mineralization competent matrix vesicles containing preformed HA crystals especially with the loss of calcification inhibitors seen in CKD patients [56,129,130,135]. Importantly, high Ca was also shown to enhance Pi-induced calcification of *ex-vivo* rat aorta in a concentration dependent manner by increasing Pit1 expression. High Ca alone was able to induce calcification in some studies but not in all [136,137]. Thus, Ca may be an important contributor to Pi-induced calcification, but more research is needed to know the exact mechanism by which it acts.

## 2.4 Role of apoptosis

Apoptosis is evident in arteries from dialysis patients [138]. *In vitro*, cultured VSMCs were shown to undergo some degree of apoptosis under the effect of calcification stimulation conditions, like high Pi, high Ca, high glucose or in the presence of calcium-phosphate nanocrystals that can be phagocytosed and degraded in the lysosome to generate high intracellular Ca level [115,135,139–142]. Inhibition of apoptosis by caspase inhibitors led to a decrease in Pi-induced calcification in VSMCs [115,140]. Pi induces apoptosis partly by downregulating the anti-apoptotic molecule, Gas6 [140]. VSMCs apoptosis can contribute to calcification in different ways; apoptotic cells release high amount of Ca thus further increasing local Ca load. Also, VSMC loss lead to decrease in the production of Matrix Gla Protein (MGP), an important calcification inhibitor. Moreover, apoptotic bodies released by dying cells can act as nidus for calcification, as HA crystals were found in vesicles released from dying cells in dialysis arteries [138]. Normally, inside the cells, the high phosphate ions and calcium ions are kept in different compartments, cytosol and sarcoplasmic reticulum, respectively. However, during apoptosis they are released together inside apoptotic bodies, which may lead to precipitation of HA crystals [51,56,143].

## 2.5 Role of inflammation

Inflammation is linked to VC associated with atherosclerosis, diabetes and CKD. In atherosclerosis, stimulation of macrophages by cholesterol and fatty acids leads to secretion of inflammatory cytokines. In diabetes, high glucose can lead directly to an increase in vascular inflammation and secretion of inflammatory cytokines, such as tumor necrosis factor  $\alpha$  (TNF $\alpha$ ) and interleukin 6 (IL-6), by VSMCs [143]. In CKD, inflammation is always present and its markers, serum IL-6 and C-reactive protein (CRP), were seen to be associated with mortality. Increased inflammation in CKD has different causes including, increased production of cytokines and decreased clearance of inflammatory mediators, retention of uremic toxins and development of metabolic acidosis. Also, the process of dialysis by itself can induce acute inflammation [144]. Moreover, high Pi can act directly on VSMCs to increase inflammatory cytokines production, like TNF $\alpha$ , which was proved to be elevated *in-vitro* and *in-vivo* in uremic rats fed on high-phosphorus diet [145]. High serum IL-6 was associated with coronary artery and aortic calcification [146,147]. Also in HD patients, serum CRP was associated with the onset of coronary artery calcification [148]. More specifically,

aortic inflammation was shown to be associated with increased calcification and stiffness [149]. In fact, inflammatory cytokines can have direct effects on VSMCs and can induce phenotypic switch. For example, TNF $\alpha$  can induce osteo-chondrogenic phenotypic switch of cultured VSMCs upregulating the expression of *RUNX2*, *SP7*, *ALPL*, *MSX2* and *BSP1*. It also induces AP activity and matrix calcification by these cells [150,151]. Moreover, TNF $\alpha$  and also IL-1 $\beta$  were able to increase production of BMP2 and decrease the expression of *Mgp* in VSMCs [152]. Thus, inflammation seen in CKD, diabetes and atherosclerosis may play a direct and important role in arterial calcification.

## 2.6 Role of oxidative stress

Oxidative stress occurs when there is imbalance between ROS production and antioxidant defence mechanisms, resulting in accumulation of ROS, which have high reactivity and can cause damage to lipids, proteins and DNA. The progression of CKD is accompanied by an increase in systemic oxidative stress manifested by an increase in serum level of malondialdehyde (MDA) and 15-(F)2t-isoprostane, markers of oxidative stress, and a decrease in serum level of the antioxidant markers, superoxide dismutase (SOD) and glutathione peroxidase (GSH-PX) [153,154]. Arterial medial calcification in uremic rats, in which kidney disease was induced by high-adenine diet, was accompanied by an increase in aortic and systemic oxidative stress. The use of the anti-oxidants, tempol or quercetin, decreased oxidative stress, arterial calcification and osteogenic trans-differentiation of VSMCs into osteochondrocyte-like cells [155,156]. Also, *in-vitro*, Pi-induced calcification in VSMCs was accompanied with increase in ROS. Quercetin was able to inhibit ROS accumulation and Pi-induced apoptosis and calcification [156]. ROS can act directly on VSMCs to induce a phenotypic switch. Hydrogen peroxide, a common ROS, induced calcification in cultured SMCs with an increase in expression of *Runx2*, *Alpl*, *Bglap* and *Colla1*, and a decrease in *Sm22 $\alpha$*  and  *$\alpha$ Sma* expression [157].

## 2.7 Role of elastin degradation

Elastin is the main constituent of large arteries which give them their elastic properties. Elastin degradation is a major process in medial calcification contributing directly to arterial stiffness. VSMCs undergoing phenotypic switch upregulate the expression of MMPs, especially MMP2 and MMP9, which were also seen to be upregulated and activated in

arterial biopsies of CKD or diabetic-CKD patients, and they were associated with increase in arterial stiffness. MMP2 and MMP9 are the main players in elastin degradation [56,158–160]. Degraded elastin do not just represent a consequence of arteriosclerosis, but it can also actively promote calcification, by two main mechanisms; degraded elastin have high affinity to Ca facilitating the deposition of HA crystals along the elastic lamella. Also, elastin derived peptides can bind to elastin-laminin receptors on VSMCs and actively alter the expression of different genes resulting in an osteo-chondrogenic phenotype. This is proved in studies using elastin peptides on isolated SMCs, which showed that these peptides are able to increase the expression of osteo-chondrocytic markers, including *Apl*, *Bglap* and *Runx2*, and AP activity [161,162]. *In-vivo*, the inhibition of MMPs in uremic rats given high VitD and phosphorus diet was able to inhibit medial calcification and phenotypic switch of SMCs [158]. Moreover, elastin degradation leads to the release of elastin-associated glycoproteins, like TGF- $\beta$ , that can also affect VSMCs phenotype [161,162].

## 2.8 Loss of inhibitors

Ectopic calcification is not induced by a simple increase in serum Ca and Pi, because calcification inhibitors are present in sufficient amount to inhibit HA crystals formation.

### 2.8.1 PPI

PPI is one of the most potent inhibitors. It is generated via ATP hydrolysis by NPP1 [56,163] (Figure 3). Circulating PPI contributes more for calcification inhibition than local PPI produced in vessels, and it is sufficient for preventing calcification. This is highlighted by a study in which WT aortas were transplanted into *Enpp1* KO mice and showed calcification, whereas *Enpp1* KO aortas transplanted into WT mice didn't develop calcification [164]. In humans, the mutation that cause deficiency in NPP1 cause idiopathic infantile arterial calcification characterized by extensive calcifications of large and medium arteries, and it leads to death in the first 6 months of life due to heart failure. When SMCs start to acquire osteo-chondrocyte-like phenotype, they gradually express TNAP which can hydrolyse PPI into Pi, raising Pi/PPI ratio and creating an environment permissive for calcification. Also, during HD, PPI is removed leading to a decrease in its circulating level [56].

### 2.8.2 Fetuin A

Fetuin A is another important systematic inhibitor. It is a glycoprotein secreted by the liver. It works by binding free Ca and HA crystals to inhibit their further growth. Fetuin A deficient mice have increased risk of wide spread soft tissue calcifications [165,166]. Fetuin A was also taken up by cultured VSMCs and was able to inhibit calcification *in-vitro*, induced by

high Pi and Ca, in a dose dependent manner. This indicates that it possess a direct effect on VSMCs. The effect of Fetuin A is not only mediated by its inhibition of HA crystals formation, but also by inhibition of VSMCs apoptosis [167]. Fetuin A is a negative acute phase protein, thus in dialysis patients its level decreases due to increased inflammation [56].

### 2.8.3 MGP

MGP is another important inhibitor of calcification produced by different cells including VSMCs. Phosphorylation and  $\gamma$ -carboxylation are obligatory for MGP secretion and function.  $\gamma$ -carboxylation requires vitamin K as a cofactor. It inhibits calcification by direct binding to Ca and calcium-phosphate crystals [56,168]. *Mgp*-KO mice develop arterial calcification as soon as 2 weeks after birth [169]. In CKD, its expression is reduced due to VSMCs apoptosis, and high Pi can weaken its binding to Ca. Moreover, warfarin, which is given to CKD patients, inhibits the action of vitamin K, thus inhibiting the carboxylation and function of MGP. Thus, in CKD, the percentage of non-functional uncarboxylated MGP rises [56]. *In-vitro*, warfarin usage enhanced calcification and MGP was uncarboxylated, while vitamin K treatment inhibited calcification [168]. Moreover, *in-vivo* treatment of rats with warfarin also led to extensive arterial calcification [170,171].

Normally, vesicles generated by SMCs are loaded with MGP and fetuin-A, thus they cannot form HA crystals. The presence of MV-like structures was detected *in-vivo* in calcifications of tunica intima and media in human, rabbit and chicken aortas and *in-vitro* in calcifying VSMCs [172–174]. Human VSMCs cultured *in-vitro* in osteogenic conditions, high Ca and Pi medium, were able to produce mineralization-competent matrix vesicles containing preformed calcium-phosphate crystals. In non-osteogenic condition these cells also produced MVs-like structures but they were loaded with fetuin-A and MGP, and they were unable to calcify [135,174,175]. Due to loss and non-functionality of fetuin A and MGP, matrix vesicles produced in vessels of CKD patients are mineralization competent [56].

## 2.9 Role of hyperglycemia

High glucose seen in case of diabetes is considered a risk factor for VC. Elevated fasting plasma glucose was seen to be correlated with coronary artery calcification (CAC) [176,177]. Also, glycated hemoglobin (HbA1C), which is an indicator of glucose status, and insulin resistance were also shown to be associated with CAC [178,179]. In fact, glucose can have direct effects on VSMCs inducing oxidative stress, inflammatory cytokines production and VSMCs phenotypic transition [143,179]. *In-vitro*, high glucose induced a phenotypic switch in VSMCs inducing the expression of *RUNX2*, *BGLAP*, *ALPL*, *COL2* and *SOX9* with an

increase in AP activity and calcification capacity [180,181]. The mechanism of this phenotypic switch may involve production of inflammatory factors, like IL-1 $\beta$  and TNF $\alpha$  [181,182].

### 3. Experimental models of vascular calcification

#### 3.1 *In-vitro* models

Vascular smooth muscle cells (VSMCs) were identified as the major cell type involved in both intimal and medial calcifications and the type of cells undergoing trans-differentiation into osteo-chondrocyte-like cells forming bone or cartilage-like structures inside the wall of blood vessels. Since then, *in-vitro* cultures of isolated primary VSMCs were the gold standard for studying the mechanistic features of VC. Because VC is a multifactorial disease associated with different systemic diseases, *in-vitro* studies of single-cell culture allows the identification of direct effects of many systemic inducers such as: hyperphosphatemia, hyperglycemia, inflammation and oxidative stress. Also, it facilitates the investigation of their mechanism of action. In this regard, VSMCs were isolated from the arteries, especially the aorta, of different organisms including bovine, rat, mouse and more importantly human origins [122,180,183,184]. They were cultured with different calcification-inducing conditions including: high Pi, high Ca, high glucose, and in the presence of calcification inducers like inflammatory cytokines or hydrogen peroxide [110,135,151,157,180]. Under these conditions, VSMCs were able to downregulate SMC-specific genes like smooth muscle 22- $\alpha$  (*Sm22 $\alpha$* ) and  $\alpha$ -smooth muscle actin ( *$\alpha$ SMA*) and upregulate the expression of osteo-chondrocyte markers like *Runx2*, *Sp7*, *Msx2*, *Sox9*, *Bglap*, *Spp1*, *Colla1* and *Col2*. Also, they exhibit increased AP activity and form nodules that gradually calcify. Also, some cell-lines can be used instead of primary VSMCs because of the relative ease of their usage instead of implying procedures of VSMCs isolation. MOVAS is a murine SMC line that showed calcifications and phenotypic switch upon culturing with AA and  $\beta$ -GP, an organic phosphate donor [185]. A7r5 is a rat aortic smooth muscle cell line that can calcify upon culturing in high-Pi conditions [186].

The disadvantage of these models is mainly the absence of extracellular matrix which can have tremendous effects of VC progression.

### 3.2 Organ culture models

Whole vessels, like whole aortas, or vessel rings are now used as an *ex-vivo* model to identify direct mechanisms of calcification inducers without skipping the role of extracellular matrix. When all layers of the blood vessel are kept, this model can help to identify the histological type of calcification caused by a specific factor, and it preserves the role of signalling between different cells. Also, when desired, the adventitial and intimal layers can be removed to examine the effect of a factor especially on SMCs from the medial layer [116].

### 3.3 *In-vivo* models

*In-vivo* models provide more realistic representation of the complex nature of diseases associated with VC. These models include animals with CKD, diabetes or atherosclerosis. Moreover, VC was induced by KO of calcification inhibitors or the administration of calcification inducers.

- CKD animal models

In mice, a phenotype resembling CKD can be induced by a 2 steps surgery: electrocauterization of the surface of one kidney followed by nephrectomy of the second kidney. In this model, VC do not develop spontaneously, unless the mice used were already predisposed to VC. These mice include ones with metabolic disorder due to KO of Low density lipoprotein receptor (*Ldlr*<sup>-/-</sup>) or ones with atherosclerosis in which apolipoprotein E (*ApoE*<sup>-/-</sup>) is KO. When CKD is induced in these mice, they develop extensive calcification [187].

In rats, CKD was used to be achieved by 5/6 nephrectomy, which also consists of 2 steps: a decrease of the first kidney mass by 2/3 and a total kidney nephrectomy of the second one after 1 week. CKD in this model is not sufficient to induce calcification; a high-phosphorus diet and/or the administration of calcitriol (active vitamin D, VitD) is required to induce VC [187]. In 1982, a new model of CKD was developed, in which rats are given high adenine diet. When dietary adenine is high, it is hydroxylated producing 2,8-hydroxyadenine, which have low-solubility, so it precipitates in the kidney tubules leading to kidney dysfunction with symptoms resembling those seen in CKD. The administration of high adenine diet for 4 weeks was enough to develop VC which was evident in the medial layer of the aorta. Administration of high phosphorus diet, calcitriol or both can augment VC. This model has an advantage over the first two models because it do not require any surgery and it is characterized by high survival rate [187].

- Calcification inhibitors KO mice

Extraskelatal mineralization is repressed by a series of molecules that inhibit calcium phosphate crystals deposition. Mice that are KO for these inhibitors develop VC spontaneously, including matrix Gla protein (*Mgp*) KO and *osteoprotegrin* KO mice [188,189]. Also, KO of the calcification inhibitor fetuin-A led to ectopic calcification when the mice were put on high-mineral or VitD diet [166].

- Other models

Giving rats warfarin, a vitamin K antagonist, leads to a rapid and extensive medial vascular and valvular calcification [170]. *Ldlr*<sup>-/-</sup> mice fed on high-fat diet develop diabetic phenotype associated with aortic medial calcification [190].

#### 4. Diagnosis

VC can be detected by various types of imaging systems. Conventional radiography can detect calcified vessels as continuous ‘tram-tracks’ in case of medial calcifications or as patchy and irregular lesions in case of atherosclerosis. It is an available inexpensive technique that can detect the presence of calcifications, but cannot quantify it. This makes it hard to be used for following its progression along time or in response to a treatment [191,192]. However, Adragao invented a simple scoring system, depending on the presence of VC in the iliac, femoral, digital and radial arteries (1 point for each artery, 2 points if the calcification was detected bilaterally), resulting in a simple scale from 0 to 8 [192]. Another semi-quantitative scoring system, is the Kauppila score that deals with calcification in the abdominal aorta in lateral x-ray [191]. Like radiography, ultrasonography is an inexpensive technique that can also detect calcifications and differentiate between intimal and medial forms. Medial VC can be seen as string of beads in B-mode type, or as flow patterns in colour flow duplex type [193]. Also, it can detect the change in diameter of arteries during systole and diastole to give idea about their elasticity. Because stiffness may be linked to medial VC, it can predict the presence of such lesions [191]. However, ultrasound is limited for detection of superficial arteries (like the carotid and femoral arteries) because the ultrasound wave has a limited penetration ability [191,192]. On the other hand, computed tomography (CT) is a more developed imaging system that can accurately detect and quantify VCs. Two types of CT can be used: electron-beam CT (EBCT) and multislice CT (MSCT). These techniques are expensive and involve the exposure to radiation, but they are very precise in quantifying VC and following its progression. However, they cannot differentiate between intimal and medial

calcifications. VC is quantified using CT according to different scoring systems. Among these, Agaston score is a product of area of calcification by the peak density, thus giving idea about the size and calcium content of the lesion. Volume score is another scoring system that counts all pixels in the lesion giving idea about the size only. Echocardiography can detect only cardiac valve calcifications [192]. Also, endovascular interventions can be used including intravascular ultrasound (IVUS) and optical coherence tomography (OCT). OCT has higher resolution, however it cannot give an idea about the whole medial layer due to its limited penetration [191,193].

Listed above are the direct ways by which VC can be identified; however, medial VC can be predicted indirectly due to its effects on vessel properties and elasticity. The ankle-brachial index (ABI) is a ratio of systolic ankle pressure over the systolic arm pressure. When  $ABI > 1.3$ , it can predict the presence of medial VC [191]. Also, a high PWV can predict medial calcification as mentioned above. It is a measurement of the distance travelled by the pulse wave over the time it took. Thus, the pulse wave is detected at two different sites in the arterial tree, and the calculated PWV can give idea about the state of the arteries between these 2 sites. The elasticity of the aorta is the most clinically relevant measurement, thus the carotid-femoral PWV is the most familiar one, because it gives idea about the state of the aorta. But, PWV can be also taken for any other artery like the brachial or femoral arteries [191].

## **5. Treatments**

Due to the late knowledge about the clinical consequences of VC, current treatments are somehow limited to those that correct VC risk factors. Many studies are now searching for novel VC targets, however the similarity between VC and bone formation makes it more complicated to target it systematically without posing detrimental effects on bone and teeth.

5.1 Treatments that involve the control of disturbances associated with VC include:

### **5.1.1 Control of hyperphosphatemia**

CKD patients are advised to limit their dietary phosphate intake, but with ensuring sufficient protein amount. The form of phosphate also matters; inorganic phosphate found in food additives and in fast food is more efficiently absorbed than organic phosphate. Thus, CKD patients are advised also to control the quality of their food. Moreover, Pi is cleared during dialysis, thus increasing dialysis session frequency and length could help to decrease hyperphosphatemia. Other dialysis factors can also alter Pi clearance, like blood and dialysate flow rate and dialyzer membrane surface area. Furthermore, to effectively lower serum Pi

level, different types of phosphate binders were given to CKD patients. The currently available phosphate binders include Ca or magnesium salts, sevelamer and lanthanum carbonate. All of them were shown to lower Pi serum level effectively, however calcium-free phosphate binders were more effective in delaying VC progression. This is likely due to an increase in serum Ca after giving calcium-based phosphate binders, which is also a risk factor for VC [55]. For example, sevelamer was shown to slow down the progression of VC in CKD compared to calcium-based phosphate binders [194], however in other studies it was ineffective [195,196]. Also, it was not able to attenuate LV hypertrophy or arterial stiffness as measured by LV mass and PWV, respectively, in stage 3 CKD patients [197].

### 5.1.2 Treating secondary hyperparathyroidism

Calcimimetics are given to CKD patients with secondary hyperparathyroidism to lower their serum PTH. These molecules increase the sensitivity of CaSR to Ca, thus activating it and inhibiting PTH production by the parathyroid gland. Knowing that CaSR is also expressed on VSMCs, calcimimetics can have direct effects on these cells, and they were shown to increase the production of MGP by VSMCs *in-vitro* [55,198]. Also *in-vivo* and clinically, they were shown to slow down the progression of VC [199–201]. Given the fact that VitD can have negative effect on PTH production, also VDRA were given to treat hyperparathyroidism in CKD patients. However, VDRA usage is sometimes accompanied by increase in serum Ca and Pi and can induce adynamic bone disease, which can lead to enhancement of VC. New VDRA, like paricalcitol, were shown to decrease PTH production with lower effect on Ca and Pi level [55].

### 5.1.3 Minimizing inflammation

In HD patients, systemic inflammation is mainly due to the dialysis procedure. Thus, some adjustments must be considered during dialysis to lower inflammation. These may include the usage of more biocompatible material and ultrapure dialysate. Also, malnutrition is a risk factor for inflammation, thus it is important to ensure adequate nutrition even with diets that restricts high phosphate intake [202].

5.2 New treatments that could be beneficial for delaying the progress of VC are now being developed, including:

#### 5.2.1 Bisphosphonates

PPi have short half-life [55]. Instead, bisphosphonates are synthetic analogues of PPi that are used for osteoporosis treatment. They can inhibit osteoclast activity and also can inhibit

calcium-phosphate crystal deposition both in blood vessels and bone [191,202]. In HD patients and in *in-vivo* CKD animals, they were able to delay the progression of VC [203,204]. However, in some human studies of predialysis CKD patients and in women with osteoporosis, bisphosphonates had no effect on VC [205,206]. Bisphosphonates are normally cleared by kidney, thus when kidney function deteriorates, they can accumulate in bone causing adynamic bone disease. Thus, it is not totally safe to use bisphosphonates except in severe cases of VC [202].

### 5.2.2 Denosumab

Denosumab is an osteoprotegerin mimicker that can inhibit RANKL and inhibit osteoclast differentiation. Its usage in animals showed that it can inhibit VC [207]. However, in a human study on postmenopausal women with osteoporosis, denosumab was not able to delay the progression of VC [208]. Also, due to its anti-resorptive activity, it should be used with caution when patients have a low-bone turnover disease and it can lead to severe hypocalcemia [202].

### 5.2.3 Vitamin K

The percentage of uncarboxylated MGP was found to be elevated in CKD patients. HD patients also have severe vitamin K deficiency. Thus, vitamin K supplementation could be a good intervention to restore the inhibitory function of MGP on VC [55,202].

### 5.2.4 Sodium thiosulfate

Sodium thiosulfate is used in clinical practice as an antidote for cyanide poisoning. It interacts with deposited calcium in vessels and form a highly soluble salt, calcium thiosulfate. It is well tolerated and it was shown to treat calciphylaxis, which is characterized by calcifications in arterioles [202]. Thus, it could be effective in treating VC.

VC is one of the major contributors to cardiovascular mortality especially due to its effects on cardiovascular dynamics, and up till now, there is no specific, effective and approved treatment for it. Understanding the molecular mechanisms behind this complex disease is indispensable for designing new treatments or preventive strategies.

### Part 3: Phospholipase D

Phospholipids are major and crucial components of biological membranes. Ideally, they are made up of a glycerol backbone with fatty acid chains linked to the first 2 carbons of glycerol and a phosphate possibly with a head group, like choline, ethanolamine, serine or inositol, linked to the third carbon. However, they are not only structural components, but they can actively participate in cell signalling, especially after being modified by different types of enzymes including kinases and hydrolases. Enzymes that hydrolyse phospholipids are called phospholipases. There are different groups of phospholipases that can hydrolyse different bonds in phospholipids and give rise to different lipid products. The resultant products can act as anchor for proteins or can activate different effectors and act as secondary messengers. Among phospholipases, phospholipases As, PLA<sub>1</sub> and PLA<sub>2</sub>, have deacylase activity and they are responsible to the hydrolysis of acyl chains at positions *sn*-1 and *sn*-2, respectively, thus producing lysophosphatidic acid (LPA) and free fatty acids. Phospholipase B (PLB) is also a deacylase responsible for hydrolysis of acyl chains in LPA. Phospholipase C (PLC) and phospholipase D (PLD) are phosphodiesterases that hydrolyse the proximal and distal phosphodiester bonds, respectively, leading to production of diacylglycerol (DAG) and phosphorylated head group in case of PLC or phosphatidic acid (PA) and head group in case of PLD (Figure 9) [209,210].

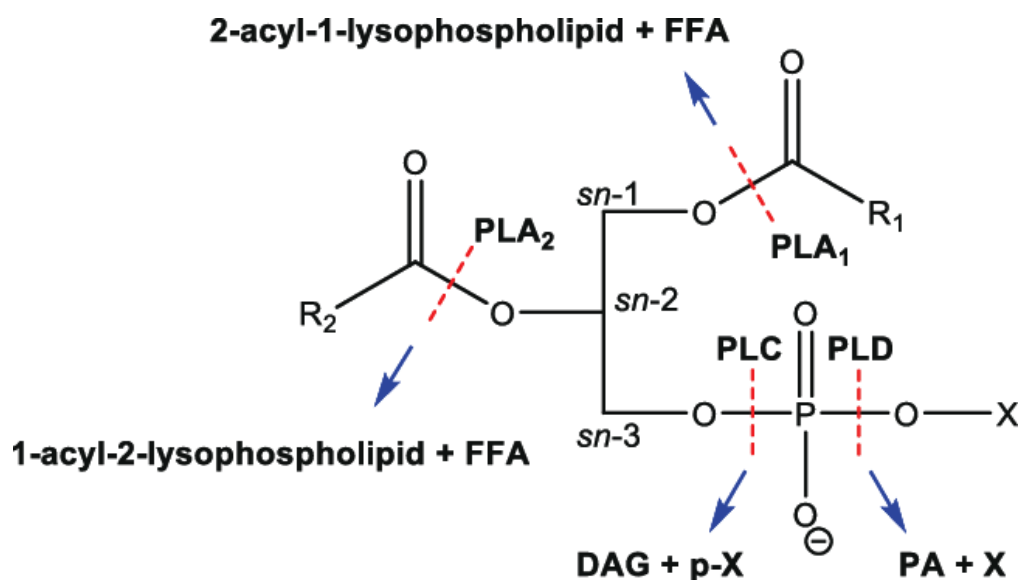


**Figure 9: Specificities of phospholipases.** Phospholipids can be hydrolysed by different enzymes with different specificities. PLA<sub>1</sub> and PLA<sub>2</sub>, can hydrolyse the acyl ester bond giving rise to free fatty acids (FFA) and LPA. PLC hydrolyses the phosphodiester bond at the glycerol side generating DAG and phosphorylated head group (p-X). PLD hydrolyses the phosphodiester bond at the side of head group, giving rise to a free head group (X) and PA. [211]

## 1. Overview on PLD superfamily structure, localization and function

PLD superfamily consists of 6 members: PLD1 to 6, among which, only PLD1 and PLD2 are responsible for the phosphodiesterase activity on phospholipids. PLD1 and PLD2 share 50 % similarity in the protein sequence, and they share most of their domains, except for an inactivating loop present only in PLD1 that makes its basal activity remarkably lower than that of PLD2. Catalytic lipase activity is driven by a dimerized catalytic site consisting of two highly conserved HKD motifs, each contains a specific sequence of amino acids: His-x-Lys-x-x-x-Asp. Thus, each one of PLD1 and PLD2 have 2 HKD motifs. The rest of the common domains are mainly involved in interaction with lipids and other proteins and thus aid in intracellular localization and activation, and they are: phox consensus sequence (PX), pleckstrin homology domain (PH) and phosphatidylinositol (4, 5) diphosphate (PI (4, 5) P<sub>2</sub>) binding motif (Figure 10).

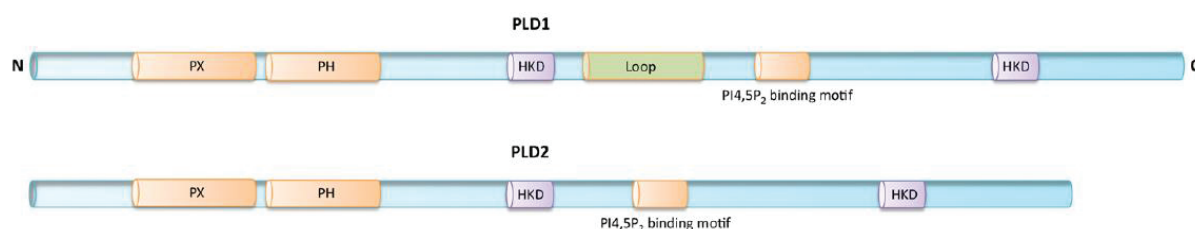


**Figure 10: The domains in PLD1 and PLD2 proteins.** PLD1 and PLD2 possess nearly the same arrangement of protein domains which consist of 2 copies of the catalytic motif: HKD, which corresponds to a conserved amino acid sequence: His-x-Lys-x-x-x-Asp, and a series of regulatory domains: PX, PH and PI (4, 5) P<sub>2</sub> binding motif. Unlike PLD2, PLD1 has an additional loop sequence that negatively regulate its activity [212].

PLD3 and PLD4 also have 2 HKD motifs, but they are otherwise not similar to PLD1 and PLD2. Despite the presence of the catalytic motif, no enzymatic activity was detected for these proteins. PLD3 and PLD4 are ER transmembrane proteins, with the bulk of the protein including HKD motifs is projected to ER lumen. Only a short N-terminal sequence is projected to cytoplasm. Polymorphisms in *PLD3* gene is linked to Alzheimer disease. The deficiency in PLD4 in humans was linked to autoimmune diseases. PLD5 have a sequence that resembles the HKD motif, however neither catalytic activity nor any function was assessed for this protein. Lately, polymorphism in *PLD5* gene was linked to autism. PLD6, also called mitoPLD, is a mitochondrial protein present in its outer membrane. The bulk of this protein is projected to the cytoplasm and it contains only 1 HKD motif. PLD6 needs to dimerize to form a functional catalytic site that is able to hydrolyse cardiolipin thus producing PA. In this concern, it has roles in mitochondrial fission and fusion. Also, it can act as endonuclease, and it has important roles in the formation of piwiRNA during

spermatogenesis. In this report, the focus will be only on PLD1 and PLD2, which may be collectively referred to as PLD [212,213].

## 2. Functions of PLD1 and 2 and their regulation

PLD1 and 2 mainly act as phospholipases that can hydrolyse membrane phospholipids, mainly PC which is the most abundant phospholipid in cellular membranes. This hydrolysis leads to the production of PA which is involved in different cellular functions. PA can bind proteins to recruit them to cellular membranes where they are needed to transduce signals. Also, this interaction may be able to actually activate different proteins. Thus, PA acts as secondary messenger in different cellular signalling pathways. Also, PA can be hydrolysed to other lipid second messengers like DAG and LPA, which also can regulate different signalling pathways (Figure 11).

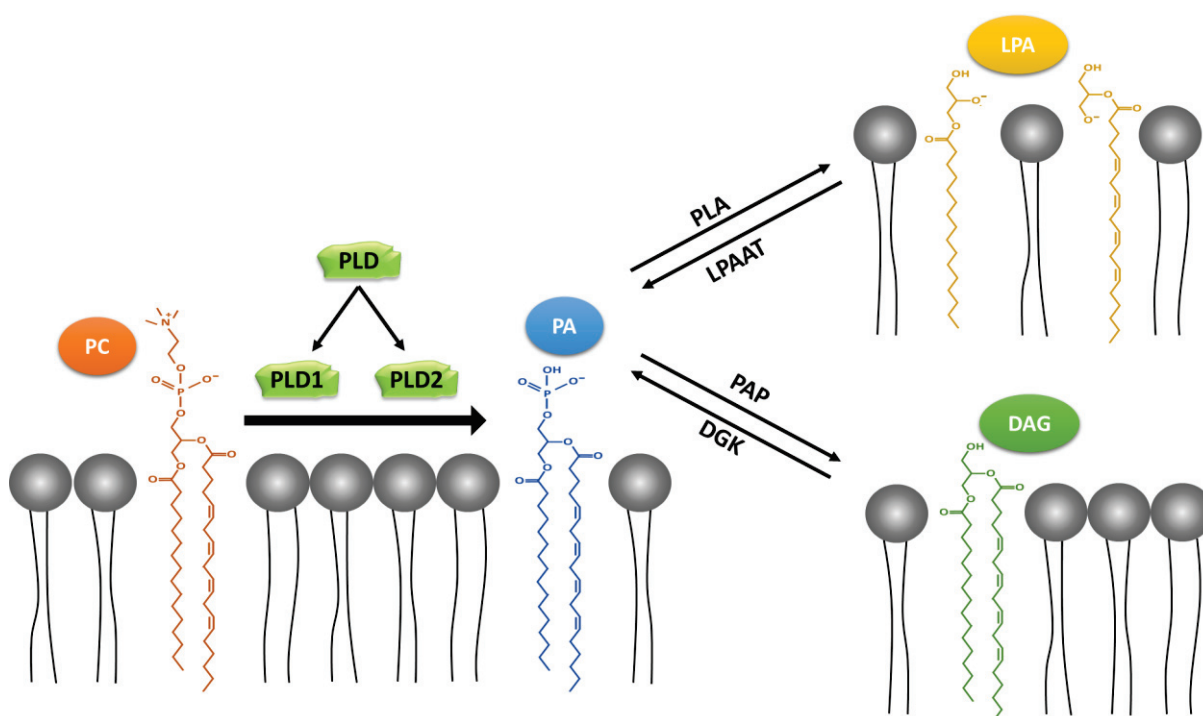


**Figure 11: PA metabolic pathway.** PA is produced by hydrolysis of phospholipids, mainly PC, by either PLD1 or PLD2. PA can be dephosphorylated by a phosphatidic acid phosphatase (PAP) generating DAG. DAG can also be phosphorylated by DAG kinase (DGK) to give back PA. Also, one of the acyl chains in PA can be hydrolysed by a PLA producing LPA. LPA can also be converted back to PA by addition of an acyl chain by the action of a LPA acyl transferase (LPAAT).

Also, having a small negatively charged head helps PA to adopt a shape of a cone promoting a negative membrane curvature when its level rise, facilitating vesicle formation and fusion [213] (Figure 12). On the other hand, functions of PLD1 and 2 is not limited to its lipase activity, but they also have lipase-independent activities. PLD can be involved in different

signalling pathways through direct protein-protein interactions. Moreover, PLD2, but not PLD1, has an additional guanine nucleotide exchange factor (GEF) activity, so it can activate G proteins [214]. The signalling pathways in which PLD participate and its regulators will be discussed in the following subparts.

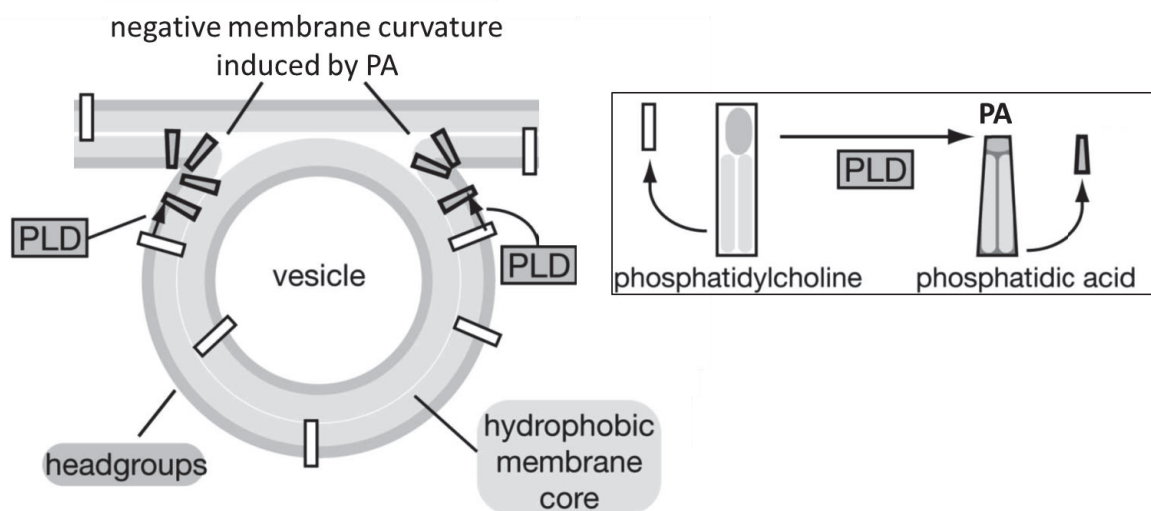


**Figure 12: The role of PA in membrane dynamics.** PA generated in the membrane by the action of PLD can induce a negative curvature in the membranes where it is abundant due to its cone-like shape. This process can facilitate vesicles fusion (edited from [215]).

## 2.1 Regulation by Protein kinase C (PKC)

PKC is now a known PLD activator. It is a family of serine/threonine kinases that consists mainly of 3 groups: the classical or conventional isoforms, PKC $\alpha$ ,  $\beta$ I,  $\beta$ II and  $\gamma$ , the novel PKCs, PKC $\delta$ ,  $\epsilon$ ,  $\theta$ ,  $\eta$  and  $\mu$ , and the atypical PKCs, PKC $\zeta$  and  $\lambda$ . They can act on different or similar substrates, however their activities are regulated in different manners. Conventional PKCs are Ca-dependent and they are activated by DAG and phorbol esters. However, novel PKCs are Ca-independent but they can be also stimulated by DAG and phorbol esters. On the contrary, atypical PKCs do not need Ca and they are not activated by DAG or phorbol esters but rather by acidic phospholipids including PA, PS and polyphosphoinositides [216] (Figure 13).

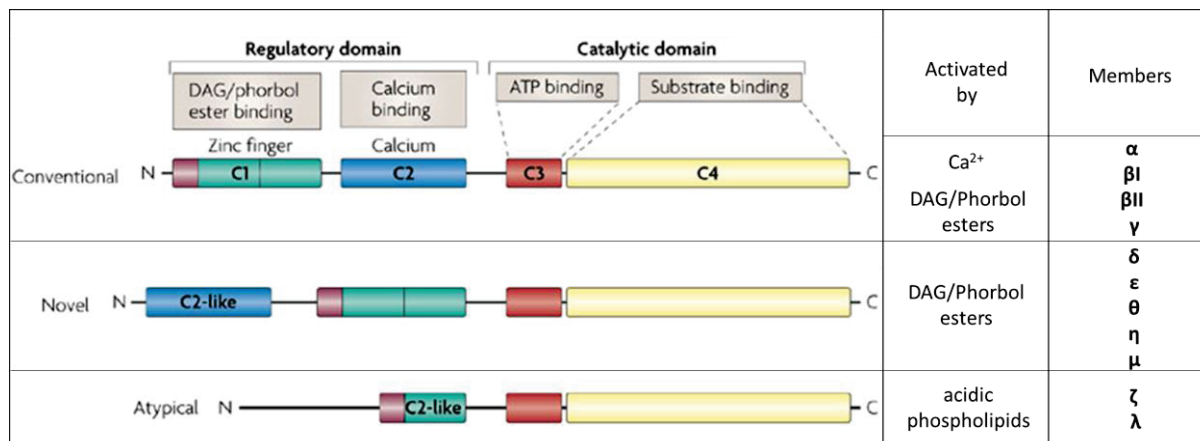


**Figure 13: The different types of PKC and their structure.** All PKC isoforms have a conserved catalytic domain made up of an ATP binding domain (C3) and a substrate binding domain (C4). However, they differ by their regulatory domains, according to which they are divided into 3 groups. Conventional PKCs, PKC $\alpha$ ,  $\beta$ I,  $\beta$ II and  $\gamma$ , have a DAG/phorbol ester binding domain and a calcium binding domain, so they can be activated by both. Novel PKCs, PKC $\delta$ ,  $\epsilon$ ,  $\theta$ ,  $\eta$  and  $\mu$ , have an intact DAG/phorbol ester binding domain, but not a functional Calcium binding domain. Atypical PKCs, PKC $\zeta$  and  $\lambda$ , are not responsive to calcium or DAG/phorbol esters, but they can be activated by acidic phospholipids. [217]

The idea behind PLD activation by PKC arose in early studies which detected an increase in PC hydrolysis in response to phorbol esters. Later it was shown that this process involves PKC [216]. *In-vitro*, PKC $\alpha$  was shown to bind and activate PLD1 in a process that requires phorbol esters (like phorbol-12-myristate-13-acetate, PMA) but not ATP [218,219]. Also PKC $\beta$ II, but not PKC $\gamma$ ,  $\delta$ ,  $\epsilon$  or  $\zeta$ , was able to activate PLD1 *in-vitro*. In this study, activation by PKC $\alpha$  and  $\beta$  did not require ATP, giving evidence that PLD is being activated by direct binding rather than phosphorylation [220]. In accordance with this, the inhibition of PKC $\alpha$  kinase activity by dephosphorylation did not affect its ability to stimulate PLD. Moreover, a regulatory domain of PKC $\alpha$  was enough to activate PLD [221]. However, PLD1 was seen also to be phosphorylated by PKC $\alpha$  and  $\beta$ , but this occurs after PLD activation, and increased phosphorylation was associated with decreased activity [220,222]. Moreover, a mutation in one amino acid (Phe 663) in PKC $\alpha$  which was associated with inhibition of PLD binding also inhibited PLD activation [222]. Also in cells, PKC was shown to be upstream of activated PLD in response to PMA or PDGF, and PKC $\alpha$  and  $\beta$  were both shown to associate with PLD1 [219,223,224].

Not only PLD1, but also PLD2 can be responsive to activation by PKCs. In COS-7 cells, upon treatment with PMA, PLD2 was shown to be activated in a PKC-dependent manner and was shown to associate with PKC $\alpha$  at basal conditions, with an increase in this association after stimulation. PLD2 can be phosphorylated by PKC, however as seen with PLD1, the activation preceded phosphorylation, and activation was also detected at a concentration of PMA that did not induce phosphorylation. Phosphorylation was associated with a decrease in

activity, and kinase-deficient PKC $\alpha$  was more efficient than WT PKC $\alpha$  in activating PLD2 [225]. Thus, conventional PKCs, especially PKC $\alpha$ , are able to activate PLD1 and PLD2 by direct binding rather than by phosphorylation. In models other than PMA induced PLD activation, other PKC isoforms may be implicated. For example, in a study on COS-7 cells where PLD was activated by integrins, PKC $\delta$  was colocalized with PLD2 at lamellipodia and was identified as the principle isoform involved in PLD activation in this model, as dominant negative PKC $\delta$ , but not dominant negative PLC $\alpha$  or  $\epsilon$ , was able to inhibit integrin-induced PLD activation [226]. Also, in a model where PLD2 was activated in response to S1P treatment of human pulmonary artery endothelial cells, the primary PKC responsible for PLD activation was PKC $\epsilon$ . Thus, in different models using different types of cells or different stimuli, PLD1 or PLD2 could be activated by different types of PKCs. Also, recently PKCs was identified to be activated downstream PLD. For example, PKC $\gamma$  was activated downstream PLD1 after stimulation of retinal microvascular endothelial cells by vascular endothelial growth factor (VEGF), and PKC $\zeta$  was activated downstream PLD2 when pulmonary artery endothelial cells were stimulated by S1P, a bioactive lipid [227,228]. Moreover, PKC $\epsilon$  was activated downstream PLD1 in LPS-treated retinal pigment epithelial cells [229].

## 2.2 Regulation by small GTPases

Small GTPases are a superfamily of low molecular weight proteins that are activated upon binding to GTP under the action of a GEF that exchange GDP to GTP on these proteins. GTP-bounded form can bind to different effectors. The hydrolysis of GTP back to GDP via the intrinsic GTPase activity requires a GTPases activating enzyme (GAP) and leads to small GTPases inactivation. They are mainly divided into 5 families: Ras, Rho, Ran, Rab and Arf [230].

PLD1 and PLD2 activities are regulated differentially by different small GTPases belonging to different families. Members of the Arf family can activate both enzymes but to different extents. Among these, Arf1 was shown to bind and strongly activate PLD1 both when isolated and in cells [231–234]. Arf1 was also able to activate PLD2 but to a much lower extent (10x lower) both in cells and *in-vitro* [231,232]. However, Arf6 activated PLD2, but not PLD1 in HeLa cells, but in another study also PLD1 was responsive to it [232,235,236]. Arf4 was involved in PLD2 activation, but not PLD1, in response to EGF [237]. Members of the Rho family of GTPases are also involved in PLD activity regulation. Rac1 was shown to activate both PLD1 and PLD2 in HeLa cells [232], and it was involved in PLD1 activation

during processes of exocytosis [238]. Also in this family, RhoA and cdc42 were able to activate PLD1 by direct interactions [239–242]. In contrast, Rac2 inhibited PLD2 activity by direct binding [243,244]. Furthermore, RalA, a member of the Ras superfamily of GTPases, was able to directly bind and activate PLD2 during endocytosis and phagocytosis processes, and PLD1 during exocytosis, phagocytosis and *in-vitro* [234,236,245,246]. Aside from being known for its lipase activity, it was lately discovered that PLD2, but not PLD1, possesses a GEF activity. In this concern, PLD2 was shown to bind and activate different small GTPases including Rac2 and RhoA [243,247,248]. The GEF activity of PLD2 was identified within the PX/PH domains [243,247,249].

### 2.3 Sphingosine 1-phosphate (S1P)

Sphingolipids are a large group of membrane lipids that upon modifications or hydrolysis give rise to important signalling and effector molecules. S1P is one of the most important signalling molecules among sphingolipids. The hydrolysis of the variable acyl chain from ceramides by ceramidases gives rise to sphingosine. Sphingosine can be phosphorylated by one of 2 kinases: sphingosine kinase 1 (SK1) or SK2, resulting in S1P. S1P can be degraded in one of two pathways; the first one is reversible in which S1P is dephosphorylated back to sphingosine under the action of S1P phosphatases (SPP1 and SPP2) or some less specific lipid phosphate phosphatases (LPPs). Alternatively, S1P can be degraded irreversibly by S1P lyase (SPL) into ethanolamine phosphate and trans-2-hexadecenal (Figure 14) [250–253].

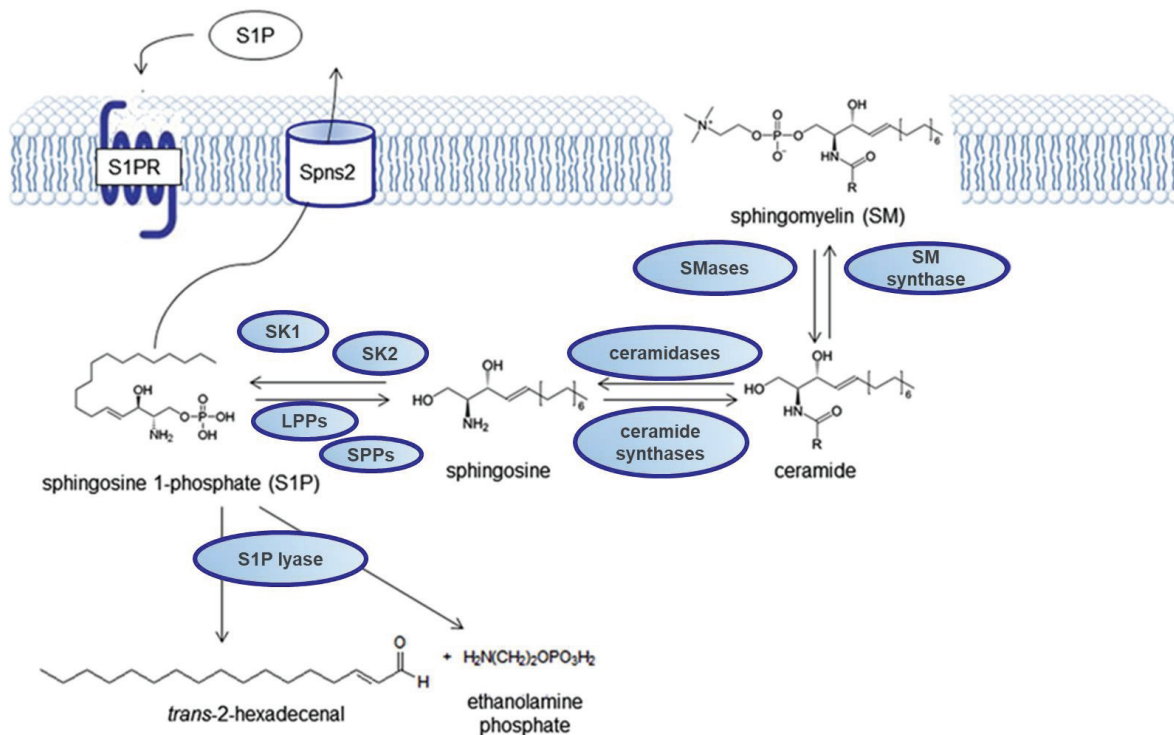


**Figure 14: S1P metabolic pathway.** Ceramides are formed from sphingomyelin (SM) by the action of sphingomyelinases (SMases). In its turn, ceramide can give rise to sphingosine by the action of ceramidases that cleaves its variable side chain. S1P is formed via phosphorylation of sphingosine by the action of SK1 or SK2. S1P can be dephosphorylated again by SPPs or other non-specific LPPs. Also, it can be degraded irreversibly by S1P lyase producing trans-2-hexadecenal and ethanolamine phosphate [254].

The general role of S1P is opposite to that of ceramides. Ceramides and sphingosine have been linked to apoptosis and cell cycle arrest whereas S1P is a pro-survival and pro-proliferative molecule. This gave the notion of a sphingolipid rheostat that can determine the fate of cells [255]. However, now the situation is more complicated, especially that ceramides with different side chains can have opposite effects on cell survival and proliferation, and that S1P can be provided by adjacent cells in a paracrine fashion and thus can affect a cell without being produced by it [250].

In fact, S1P can be released from cells by transporters including ATP-dependent ABC transporter or by its own transporter, Spinster 2 (SPNS2), depending on cell type. S1P is soluble in both aqueous and hydrophobic conditions. Thus, it can shuttle easily between membranes. In fact, about 70% of S1P resides in membranes whereas the rest are soluble. S1P is also seen in the circulation, bounded to some carriers like albumin or high-density lipoprotein (HDL), where it is produced mainly by erythrocytes, platelets and vascular endothelial cells. Extracellular S1P can act in an autocrine or paracrine way by binding to one of 5 G-protein coupled receptors (GPCR): S1P<sub>1-5</sub>. Released S1P is thought to be produced by SK1 which translocate to the membrane upon activation and produce S1P in close proximity

to the cellular membrane, where it can be easily released by its transporters. S1P receptors are coupled to different types of G-proteins and they are expressed differentially on different cell types. These differences make it impossible to easily predict the action of extracellular S1P on specific cells, where S1P may mediate cell survival, proliferation, motility or metabolic regulation (Figure 15) [250–253].

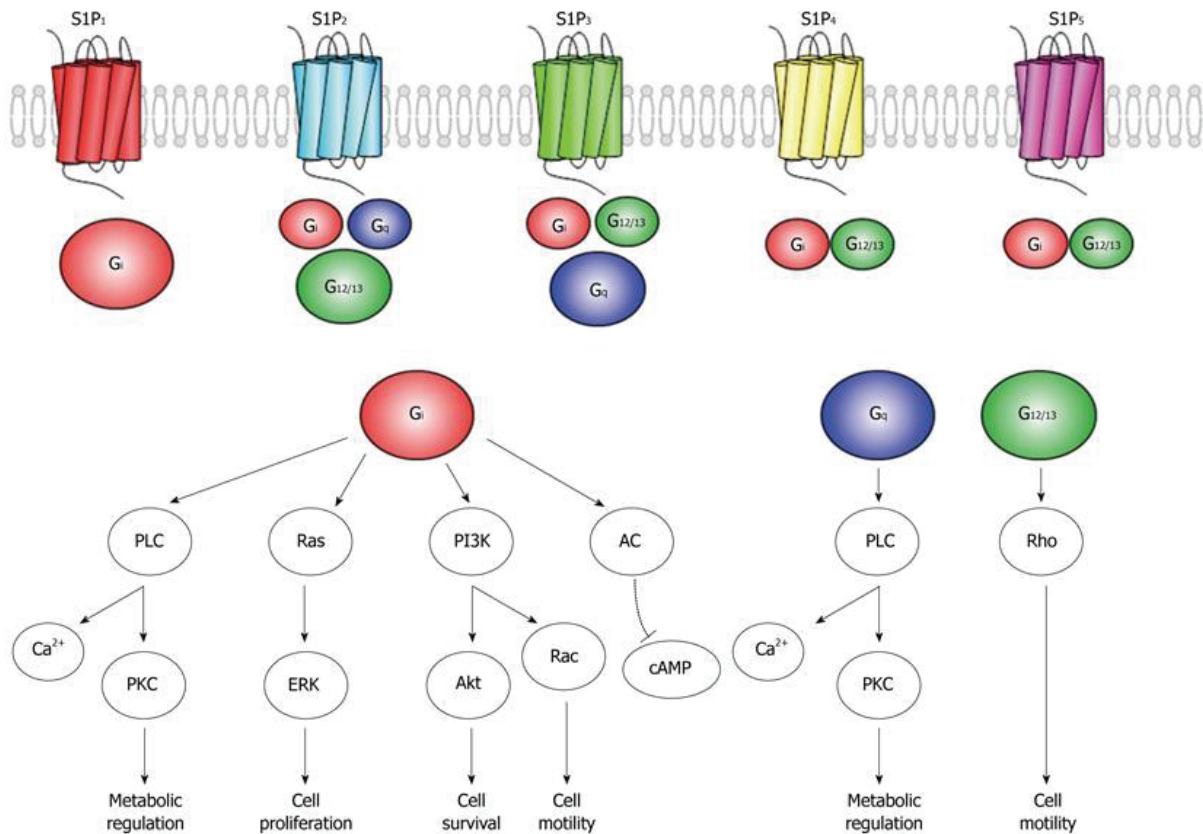


**Figure 15: S1P specific receptors signalling pathways.** Extracellular S1P can affect cell signalling by binding to one of 5 GPCRs: S1P<sub>1-5</sub>. These receptors are coupled to different G-proteins depending on the type and state of cells. Mainly, S1P<sub>1</sub> signals via G<sub>i</sub>, while S1P<sub>2</sub> and S1P<sub>3</sub> can signal via G<sub>i</sub>, G<sub>q</sub> or G<sub>12/13</sub>, and S1P<sub>4</sub> and S1P<sub>5</sub> can signal via either G<sub>i</sub> or G<sub>12/13</sub>. These G proteins then activate different signalling pathways with the final outcome of cell proliferation, survival, motility and metabolic regulation. AC: adenylate cyclase, PI3K: phosphatidylinositol-3-kinase [256].

S1P can additionally act intracellularly. Intracellular S1P can be produced by SK1 or SK2 in cytoplasm and by SK2 in nucleus or mitochondria where SK2 resides [250]. Different intracellular targets for S1P were identified lately; intracellular S1P can bind and activate  $\beta$ -site amyloid precursor protein (APP) cleaving enzyme-1 (BACE1) leading to increase in amyloid- $\beta$  peptide (A $\beta$ ) production which is involved in the pathogenesis of Alzheimer disease (AD) [257]. Cytoplasmic S1P also binds to the transcription factor peroxisome proliferator-activated receptor  $\gamma$  (PPAR $\gamma$ ) and activates the transcription of its target genes [258]. Mitochondrial S1P, produced by SK2, was shown to bind Prohibitin 2 (PHB2), a mitochondrial protein that regulates its assembly and function [259]. Moreover, nuclear S1P

can bind to human telomerase reverse transcriptase (hTERT) and prevent its ubiquitination and degradation [260]. Also, it inhibits the action of HDAC1/2 and enhances the expression of the genes regulated by them [261].

S1P is a known activator of PLD; it was able to activate it in different cell types via distinct signalling pathways. PLD activation in response to S1P implicated pertussis toxin-sensitive Gi-coupled receptors in skeletal muscle C2C12 cells [262], human airway epithelial cells CFNPE9o(-) [263–265], human bronchial epithelial cells Beas-2B [266], human pulmonary artery endothelial cells HPAECs [228] and adrenal gland cells responsible for aldosterone secretion [267]. Also, it involved activation by PKC in many cell types, including: PKC $\alpha$  and PKC $\delta$  in C2C12 and adrenal glomerulosa cells [262,267,268], PKC $\epsilon$  in NIH 3T3 cells and HPAECs [228,269], and PKC $\delta$  in CFNPE9o(-) and in human lung adenocarcinoma cells A549 [265,270]. Activation of PKCs was accompanied by their recruitment to cell membrane upon stimulation by S1P [262,265,269], and it seems that PKC translocation, at least in some models, is downstream of Gi-coupled receptors because it was inhibited by pertussis toxin [265]. Other effectors are also involved in signal transduction between S1P and PLD. These include RhoA in C2C12 and Beas-2B [266,268] and Src tyrosine kinase in CFNPE9o(-) which was seen to be acting upstream of PKC translocation [265]. Thus, S1P is inducing PLD activation via different pathways dependent on the cellular system utilized, but generally, in many cells, it involves binding to Gi-coupled receptors and subsequent recruitment and activation of different PKC isoforms or activation of Rho GTPases, which are both important in subsequent PLD activation. However, this mechanism is not a general one, because for example in some cell types PLD activation by S1P was not dependent on Gi-coupled receptors [271]. In the other way round, SK1 was shown to bind directly to and be activated by PA. Also, PLD activation led to a colocalization with SK1 at the perinuclear and plasma membrane regions, without any direct interactions. These data suggest that also SK1 can be activated by PA produced by PLD [272]. Thus, activation of PLD may also induce S1P production.

S1P is an important factor in bone homeostasis as it has important roles in osteoblasts and osteoclasts progenitors' recruitment and differentiation. Also, it is considered an important coupling effector between these two cell types [251,273,274]. S1P was lately shown to have an osteogenic potential in different studies. It was able to induce osteogenic differentiation of C3H10T1/2 which are multipotent stem cells. In these cells, S1P inhibited adipogenic

differentiation by decreasing the expression of the adipogenic differentiation factor, C/EBP $\beta$ , in a Gi-dependent mechanism. Also, the osteogenic effect on these cells was mediated by Wnt signalling, as an increase in Wnt5a and LRP5/6 was observed and the use of Wnt5a-neutralizing antibody reduced S1P-induced osteoblastic differentiation [275,276]. In osteoblast-like cells, MC3T3-E1 and Saos-2 cells, S1P was able to enhance osteoblastic differentiation and mineralization. In these cells also, S1P was able to induce nuclear translocation of  $\beta$ -catenin and enhance its activity [277]. In MC3T3-E1 cells, both S1P<sub>1</sub> and S1P<sub>2</sub> were important in S1P-induced osteoblastic differentiation [278]. Moreover, S1P was seen to be secreted by differentiating primary murine osteoblasts and chondrocytes, along with an increase in SK1 and SK2 expression and activity and an increase in SPNS2 expression. The inhibition of sphingosine kinases led to decrease in the mineralizing capacity and differentiation of both cell types. These data indicate that S1P has important role in differentiation of both osteoblasts and chondrocytes, which may depend on its intracellular and/or extracellular action [279]. Involvement of S1P in osteoblastic and chondrocytic differentiation may give clues for probable involvement of S1P in the trans-differentiation of SMCs in the case of VC.

#### 2.4 Regulation by surface receptors

GPCRs can activate PLDs upon binding to their ligands. The activation in most cases is indirect, as the case of S1P receptors discussed in the previous subpart. As an example, activated G $\alpha_q$  can activate PLC $\beta$  leading to DAG production and increase in Ca<sup>2+</sup>, which both can activate PKCs. PKCs can then activate PLD [280,281]. Moreover, GPCR can activate PLD by activating small GTPases such as RhoA, which is activated by G $\alpha_{12/13}$  [280,282]. G $\alpha_s$ -coupled GPCRs can also induce PLD activation in a mechanism that involve protein kinase A (PKA), Src and Ras [281]. Pertussis-sensitive G $i/o$  can also activate PLD, as it is the case with S1P receptors, and in this case the liberated G $\beta\gamma$  subunits could be responsible for PLD activation [281]. In fact, G $\beta\gamma$  can activate PLC thus activating PLD indirectly, however it can also directly inhibit PLD activity *in-vitro* [280,283]. Moreover, it was shown that PLD<sub>2</sub>, but not PLD<sub>1</sub>, can directly bind to GPCRs [280,284].

Tyrosine kinase receptors (RTKs) can also activate both isoforms of PLD via different signalling pathways that depend on the receptor and cell types. These pathways may implicate the activation of PLC $\gamma$  and the subsequent PKC and PLD activation. Moreover, Ras GTPase can be activated by RTKs after the binding of the adaptor protein Growth factor

receptor-bound protein 2 (GRB2) and the subsequent binding of its GEF: Son of Sevenless (SOS). Ras can then activate RalA leading to PLD1 activation. Ras can activate also phosphatidylinositol-3-kinase (PI3K) thus producing phosphatidylinositol triphosphate (PIP<sub>3</sub>) which can recruit and activate PLD1. Moreover, PLD2 can bind to the SH3 domain of GRB2, and this interaction was seen to be necessary in PLD2 activation by tyrosine kinase receptors. PLD activation in response to these receptors may also involve members of the Arf and Rho GTPases [281].

### **3. Roles of PLD in diseases**

#### **3.1 PLD and cancer**

PLD expression and activity were found to be upregulated in a variety of human cancers [214,285]. Due to its wide integration in different cell signalling pathways, PLD was shown to be implicated in various steps of cancer progression including cell survival, proliferation, invasion, angiogenesis and metastasis. For example, PLD functions as an effector downstream different growth factors that utilize tyrosine kinase receptors [285]. PLD2 was seen to be associated to epidermal growth factor receptor (EGFR), through binding to the SH3 domain of the adaptor protein GRB2. There, it can produce PA and facilitate the recruitment of Sos and activation of Ras [286]. Ras is an oncogene, whose oncogenic ability in fibroblasts was abolished upon PLD1 inactivation [287]. Thus, PLD can act as an activator and as an effector in Ras signalling. Also, PLD2 was found to be essential for the activation of nuclear Erk which is crucial for the proliferative effects of EGF in breast cancer cells HCC1806 [288]. PLD1 was also found to be an indispensable downstream effector of a new oncogene FAM83B [289]. Moreover, for invasiveness, cancer cells need to degrade cell matrix by MMPs. PLD upregulates that expression and activity of MMP2 and MMP9, thus can facilitate invasion of cancer cells [290,291]. PLD is not involved in tumour progression only by having roles within cancer cells, but also it affects other cells that may play a role in tumour progression and metastasis. Angiogenesis is important for tumour growth, but endothelial cells devoid of PLD1 were unable to respond to the angiogenic VEGF and form microvessels. These observations may be involved in the reduction in tumour growth seen in *Pld1* KO mice [292,293]. Moreover, interaction between platelets and tumour cells was seen to be important for seeding to metastatic sites. However, platelets devoid of PLD activity, either by genetic deletion of *Pld1* or by using PLD inhibitors, were unable to bind efficiently tumour cells, and they may be responsible for the decrease in metastatic ability of tumour

cells in *Pld1* KO mice [292]. The above pathways are just examples, but the role played by PLD in cancer is much broader.

### 3.2 PLD and Alzheimer disease

PLD also play roles in AD. PLD activity was seen to be elevated in the brains of AD patients compared to healthy individuals [294]. The main contributing event in the pathogenesis of this disease is the accumulation of A $\beta$  (amyloid  $\beta$ ) which are secreted from neural cells and can induce neural dysfunction and death leading to memory deficits. A $\beta$  peptides are generated by sequential cleavages of the APP by  $\beta$ - and  $\gamma$ -secretase. Presenilins are the main catalytic component of the  $\gamma$ -secretase complex [295,296]. Both PLD1 and PLD2 were found to be involved in AD pathogenesis. In fact, PLD1 was found to be involved in regulating the intracellular trafficking of APP and  $\gamma$ -secretase complex assembly by direct binding to presenilin 1 [285,296]. Whereas, PLD2 can be activated by A $\beta$  peptides in neurons and is involved in its cytotoxic effects, because the ablation of PLD2 eliminated the memory deficit induced by A $\beta$  accumulation in a mouse model of AD [213,285,297]. Thus, PLD1 and PLD2 have non-overlapping roles in the pathogenesis of AD.

### 3.3 PLD and infectious diseases

Both PLD isoforms were shown to have roles in infectious diseases. Briefly, PLD2 inhibition was able to inhibit cellular infection by different strains of influenza *in-vitro* and in mouse models. This effect was attributed to delayed endocytosis giving time for the host cell-response to act, thus reducing the burden of infection [285]. On the other hand, PLD1 inhibition was able to reduce HIV infection, and this was attributed to its role in cellular metabolism. PLD1 normally induces Erk phosphorylation and the subsequent Myc induction that is involved in altering cellular metabolism to meet the requirements of actively dividing activated T cells [285].

PLD role in diseases may not be restricted to the examples listed in this part. Due to the variety of functions played by PA and its derivatives, PLD may participate in wide spectrum of diseases, which may potentially include cardiovascular diseases, as will be detailed in the next subpart.

## 4. PLD in bone formation

PLD activity was detected in osteoblasts and chondrocytes, in which it was found to be induced by different factors involved in bone homeostasis. Among these, PTH activated PLD in the osteoblast-like cell line UMR-106 in a mechanism involving G $\alpha_{12}$ , G $\alpha_{13}$  and RhoA and Arf GTPases [298–300]. PTH was able to enhance osteoblastic differentiation of the

osteoblast-like cell, MC3T3-E1, by a mechanism involving the Wnt/ $\beta$ -catenin pathway [301]. It can also induce osteoblastic differentiation in human skin-derived precursor cell, and it is used to treat osteoporosis due to its anabolic function on bone *in-vivo* [302]. Importantly, Wnt3a enhanced PLD1 expression and activity in a mechanism involving  $\beta$ -catenin. In its turn, PA produced by PLD1 can enhance the transcriptional activity of  $\beta$ -catenin [303]. PLD1 was also shown to have positive effects on  $\beta$ -catenin expression by regulating the expression of microRNA-4496 in colon cancer-initiating cells [304]. Thus, PLD1 can enhance both the expression and the activity of  $\beta$ -catenin, and can be activated by Wnt/ $\beta$ -catenin signalling. Wnt3a prompted calcification and osteo-chondrogenic trans-differentiation in VSMCs, with an increase in RUNX2 and OCN expression. Moreover, inhibition of Wnt/ $\beta$ -catenin signalling reduced Pi-induced OCN expression [121]. Collectively, these studies may propose a role of PLD in osteoblastic differentiation from precursor cells or from VSMCs.

On the other hand, PA produced via PLD can be processed to give rise to prostaglandin E2 (PGE2) in UMR-106 osteoblastic cell line, MC3T3-E1 cells and primary osteoblasts isolated from rat calvaria in response to phorbol esters or endothelin 1. This process involve the dephosphorylation of PA by PAP into DAG, and the hydrolysis of DAG by DAG lipase producing arachidonic acid, which is converted to PGE2 by cyclooxygenases (COX) [305,306]. In the other way round, PGE2 was also able to activate PLD in MC3T3-E1 cells [307]. PGE2 was shown to have anabolic action on bone formation in young, growing and aging rats [308]. It was also shown to increase osteoblastic differentiation and mineralization in murine calvarial primary osteoblasts, murine and rat bone marrow stromal cells (BMSCs) [309–312]. PGE2 acts by binding to one of its 4 receptors EP1, 2, 3 and 4. Among these, EP2 and EP4 were considered to the responsible receptors for the osteogenic functions of PGE2 identified through the use of selective receptor agonists and antagonists and KO models [309–312]. Later, it was shown that the effect of PGE2 is dose-dependent; it enhanced Wnt signalling and RUNX2 expression when given to MC3T3-E1 cells in low concentration, however it inhibited this signalling at higher concentrations. This effect can be due to differential expression of its receptors, because when it is used at low concentrations, EP4 (which induces cAMP production) was upregulated, whereas at higher concentrations, EP3 (which inhibits cAMP production) was upregulated [313]. Recently, EP1 was shown to have anti-osteogenic potential, so that when its deletion in mouse MSCs favours rapid osteogenic differentiation [314]. Moreover, in human BMSCs, PGE2 at low concentration elevated the expression of *ALPL* and *RUNX2*, however it inhibits calcium deposition [315]. In this system, it seems that PGE2 have different roles during initial osteoblastic differentiation and activity.

In summary, these data indicate that PGE2 has an effect on osteoblastic differentiation, and the bidirectional link between PGE2 and PLD, may also provide additional hint for PLD involvement in osteogenesis.

In fact, PLD was actively involved in some models of osteoblastic differentiation. N-formyl-methionyl-leucyl-phenylalanine (fMLP) induced osteoblastic differentiation in human MSCs by acting through its receptor, N-formyl peptide receptor (FRP). These effects were accompanied by an increase in PLD activity. PLD1 downregulation by siRNA inhibited the fMLP-induced increase in AP activity and inhibition of PLD by FIPI, which can inhibit both isoforms, abolished fMLP-induced calcium accumulation. Thus, PLD is an important factor in osteoblastic differentiation in response to fMLP [316]. Moreover, PLD was important in osteoblastic differentiation in response to surface roughness of titanium. In response to increased roughness of titanium surfaces sandblasted with aluminium oxide, the osteoblast like cells MG63 exhibited increased osteogenic differentiation manifested by elevated OCN production and AP activity. These events were accompanied by increase in PLD expression and activity, and they were enhanced by PLD activation and attenuated by PLD inhibition [317]. These results were confirmed in a similar study in which PLD was activated in MG63 cells by increased surface roughness and energy, along with an enhanced osteoblastic differentiation manifested by enhanced AP activity and OCN and osteoprotegerin expression. The usage of ethanol to block PA production by PLD, inhibited these events. Also, the use of siRNA against both PLD1 and PLD2 inhibited osteoblastic differentiation in response to surface roughness and energy [318]. Thus, PLD could be important in osteoblastic differentiation in response to different stimulants.

In accordance with this conclusion, our group studied the role of PLD during osteoblastic differentiation of Saos-2 osteoblastic cell line and primary mouse calvarial osteoblasts. In response to culture with AA and  $\beta$ -GP, these cells differentiate with increased AP activity and mineralization. PLD activity and PLD1 expression increased during differentiation, and the inhibition of PLD1 by a specific inhibitor or a pan-PLD inhibitor diminished AP activity and calcium deposition in both cell types (article under revision, Abdallah, Skafi et al.). Thus, PLD can be important for osteoblastic differentiation and could be equally important during SMCs trans-differentiation.

PLD activity and expression was also detected in chondrocytes, with the resting zone cells having higher PLD activity than growth zone chondrocytes. In resting zone cells, PLD can be activated by  $24,25(\text{OH})_2\text{D}_3$  which plays a role in chondrocytes proliferation and

differentiation [319–321]. However, PLD activity was not increased by 24,25(OH)<sub>2</sub>D<sub>3</sub> or 1 $\alpha$ ,25(OH)<sub>2</sub>D<sub>3</sub> in growth zone cells [321]. Thus, PLD may also have a role in chondrocytic differentiation during specific stages.

## 5. Possible role of PLD in VC

The role of PLD in VC is not yet studied, however it was seen also to be activated by factors that can be involved directly in VC. PLD was activated by hydrogen peroxide in VSMCs. The migration of these cells which was induced by oxidative stress was inhibited by 1-butanol, but not 3-butanol, indicating that PLD is an important effector of oxidative stress signalling in VSMCs [322]. Also, hydrogen peroxide can activate PLD in other cell types, like pheochromocytoma PC12 cells [323]. As detailed earlier, oxidative stress is a cause for VC, and hydrogen peroxide can directly induce osteogenic trans-differentiation of SMCs [157]. Moreover, Angiotensin II (AngII), a peptide that can increase blood pressure, can also induce osteogenic trans-differentiation when applied to VSMCs in a pathway that involve binding to AngII receptor type 1 (AT1) and inhibition of MGP production by VSMCs [324,325]. One study argued an inhibitory action of AngII on VSMCs calcification [326], however the stimulatory role was also proved *in-vivo*; in rabbits given atherogenic diet to induce VC, AT1 blocker was able to attenuate calcification which was associated with an increase in BMP2 and OCN, and a decrease in  $\alpha$ -SMA expression, thus proving again a role for AngII in VSMC trans-differentiation and calcification [327]. AngII was also able to activate PLD in VSMCs in a pathway that involved AT1, G $\alpha$ <sub>12</sub>, G $\beta$  $\gamma$  and RhoA [328–330]. PLD is likely involved in AngII-induced migration of VSMCs [331]. Furthermore, oxidized LDLs, which are known for their atherogenic action, were lately shown to induce osteogenic differentiation and calcification by a direct action on VSMCs [183,332,333]. Oxidized LDLs were also shown to activate PLD in VSMCs and macrophages [334,335]. Therefore, given the strong link between PLD and these calcification inducers, PLD could be actively involved in VC.

## Objectives

Vascular calcification is a widespread disease especially among patients with chronic kidney disease, diabetes and atherosclerosis. Its consequences may include effects on atherosclerotic plaque stability, arterial stiffness, left ventricular hypertrophy, diastolic dysfunctions and heart failure. A disease with such adverse health effects must be given great attention in terms of understanding its molecular mechanisms and finding efficient preventive or curing strategies. Up till now the available treatments are limited to those that target pathologies which lead to vascular calcification such as treatments for hyperphosphatemia, hyperglycemia or hypertension. However, there is lack in treatments that can target mainly vascular calcification onset or progression in an efficient way. This may be due to lack in sufficient understanding of its molecular mechanisms. Now it is known as an active process that resembles bone or cartilage formation in many aspects. Also, it is accepted that smooth muscle cells in the vascular tissue play a central role in this process after trans-differentiating into osteo-chondrocyte-like cells. However, the molecular mechanisms linking the causative agents to trans-differentiation are still not fully understood. Also, the fact the vascular calcification resembles physiological mineralization adds another level of complexity, as it requires finding a treatment that can target vascular calcification without affecting biomineralization in the skeleton. Therefore, we aimed to further understand the molecular mechanisms behind vascular calcification seen in case of chronic kidney disease. Phospholipase D is an enzyme involved in different cellular processes and many diseases. The genetic deletion of phospholipase D in mice and the clinical use of its inhibitor in patients did not cause any obvious health problems. Moreover, phospholipase D was activated by different factors involved in bone homeostasis and others involved in vascular calcification. Thus, we examined its role in this disease. In the context of chronic kidney disease, there are many disturbances contributing to vascular calcification, yet hyperphosphatemia has the most important and direct effects in this process. Thus, our chosen models included murine smooth muscle cell line (MOVAS) and aortic explants cultured in high-phosphate conditions ( $\beta$ -glycerophosphate was the organic donor of phosphate in case of MOVAS). The third model was an adenine-induced chronic kidney disease rat model in which vascular calcification is prompted by high phosphorus and calcium diet + calcitriol injections. In all models, calcification was confirmed by different approaches including measuring alkaline phosphatase activity, Calcium deposition, and expression of osteo-chondrocytic markers, *Runx2* and *Bglap*. We intended to study the expression and activity of phospholipase D1 and D2 during the calcification process. When

possible, we inhibited this activity to understand its role in calcification. Also, we tried to understand the pathways by which phospholipase D is activated and by which it is acting to induce calcification by assessing the protein kinase C and sphingosine 1-phosphate signalling pathways.

## Chapter II: Materials and methods

### 1. Cell culture

The murine VSMC line MOVAS (ATCC<sup>®</sup> CRL-2797<sup>™</sup>) was cultured in high glucose (4.5 g/L) Dulbecco's modified Eagle's medium (DMEM) containing 10% (v/v) fetal bovine serum (FBS), 10 U/mL penicillin and 100 µg/mL streptomycin (all from Sigma Aldrich, Lyon, FR). This medium is identified as **control medium**. To stimulate calcification, cells were cultured in the same medium with 50 µg/mL of AA and 10 mM β-GP (**stimulation medium**). Culture time is chosen according to the aim. To study the calcification and the expression of different genes and proteins and their activities during the calcification process, cells were cultured during 28 days in stimulation medium and were collected each 7 days for analysis. **Non-treated (NT) cells** in these experiments were cultured in control medium for 7 days. To study the effects of different treatments on calcification, cells were cultured for 21 days in stimulation medium, and analysis was done only at the end of this period. NT cells in these experiments were cultured for 21 days in control medium. To study the effects of different treatments on PLD or SK activities, cells were cultured during 14 days in stimulation medium. NT cells were cultured for 14 days in control medium. The treatments used include: Halopemide, a pan-inhibitor for PLD1 and PLD2 (used at 1 and 2 µM), a PLD1 specific inhibitor VU0155069 (used at 600 and 800 nM), a PLD2 specific inhibitor CAY10594 (used at 200 and 300 nM) (all PLD inhibitors were obtained from Cayman chemical (Montluçon, FR)), a PKC inhibitor bisindolylmaleimide X hydrochloride, which was obtained from Enzo Life (Villeurbanne, FR) (used at 1 and 5 µM), a pan-SK inhibitor SKi (used at 5 µM), a SK1 inhibitor PF-543 (used at 100 nM), a SK2 inhibitor K145 (used at 5 µM), and a S1P<sub>1</sub> antagonist FTY720 (used at 2.5 µM). SK inhibitors and antagonists were purchased from Merck Millipore, (Fontenay Sous Bois, FR). Cultures were maintained in a humidified atmosphere consisting of 95% air and 5% CO<sub>2</sub> at 37 °C.

### 2. Aortic explant culture

Whole aortas were isolated from male Sprague Dawley rats (Janvier-Labs, Le Genest-Saint-Isle, FR). They were cleaned with sterile Phosphate-buffered saline (PBS). The adventitia layer was removed by gentle scraping and the intima is supposed to be removed by flushing in 37°C warmed PBS leaving the medial layer for the *ex-vivo* culture. Then, aortas were cultured in high glucose (4.5 g/L) DMEM containing 10% (v/v) FBS, 10 U/mL penicillin and 100 µg/mL streptomycin (all from Sigma Aldrich, Lyon, FR) for 6 days (**control medium**).

Calcification was stimulated by Pi at 6 mM during 6 days (**stimulation medium** for aorta). Halopemide at 10  $\mu\text{M}$  was used to inhibit PLD activity in these conditions. Aortas were also isolated from KO PLD1 and KO PLD2 mice using a similar protocol [336,337].

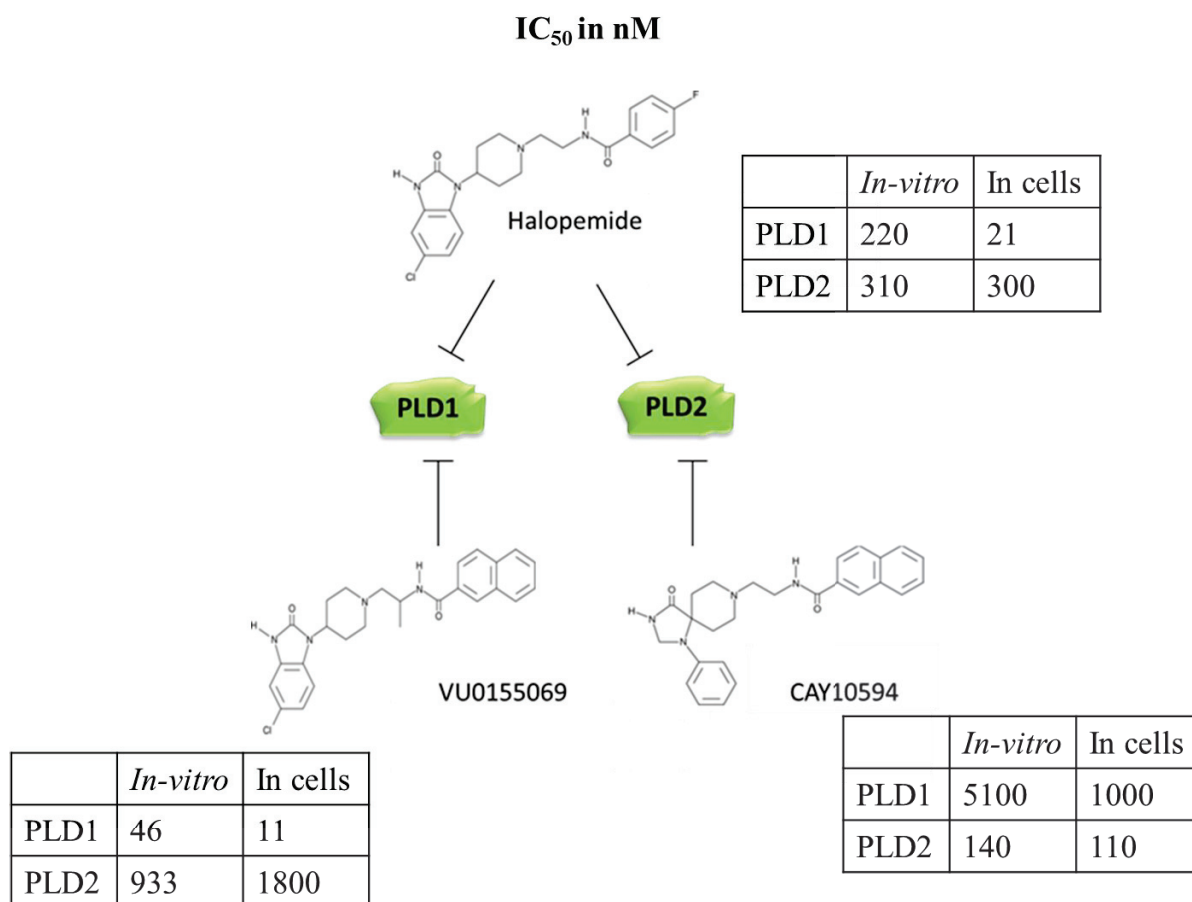


**Figure 16: IC<sub>50</sub> of Halopemide, VU0155069 and CAY10594 for inhibiting PLD1 and PLD2 *in-vitro* and in cells. [338]**

### 3. Animal experiments

All experiments were performed under the authorization n°69-266-0501 and were in agreement with the guidelines laid down by the French Ministry of Agriculture (n° 2013-118) and the European Union Council Directive for the protection of animals used for scientific purposes of September 22<sup>nd</sup>, 2010 (2010/63UE). The protocol was approved by the local ethical committee (Comité Ethique de l'INSA-Lyon - CETIL, CRNEEA n°102) under the reference APAFIS#4601-2016032110173355. Male Sprague Dawley (150-175 g) rats were purchased from Janvier-Labs and housed in an air-conditioned room with a controlled environment of  $21 \pm 0.5^\circ\text{C}$  and 60-70 % humidity, under a 12h light/dark cycle (light on from 7 am to 7 pm) with free access to food and water. CKD was induced in rats by providing an adenine rich-diet. Rats were randomized to either a CKD or a control group. The animals assigned to the CKD group were fed rat chow-containing 0.75% (w/w) adenine on A04 basis

(SAFE, Augy, FR) for 4 weeks. The control animals were fed regular rat chow (A04, 13.4 kJ/g) throughout the observation period (A04, Safe, Augy, FR).

To induce VC, the animals were further fed for 5 or 7 weeks with a custom diet containing 0.9% (w/w) calcium and 0.9% (w/w) phosphorus on A04 basis (P/Ca diet). They were injected three-times weekly with 80 ng/kg of calcitriol (Rocaltrol, Roche, FR) diluted in propylene glycol. The control animals were fed with the standard diet (A04, Safe, Augy, FR) containing 0.71% (w/w) calcium and 0.55% (w/w) phosphorus.

Animals were sacrificed after 5 or 7 weeks of P/Ca diet. Rats were deeply anesthetized with sodium pentobarbital (200 mg/kg ip). Blood (~10 ml) was collected through cardiac puncture in heparinized syringe, centrifuged 5 minutes at 2000 g to separate plasma, snap-frozen in liquid nitrogen and stored at -80°C until analysis. The plasma concentration of urea was determined using UREA-kit S180 (Sobioda, Montbonnot, FR). Animal care and kidney function analysis were performed by Mr. Alexandre Debain and Mr. Christophe Soulage, respectively. Whole aortas were isolated from all rats, and tiny parts from different regions of each aorta were pooled and used for calcium dosage assay. The rest of each aorta was used for RNA extraction and subsequent qPCR analysis.

#### **4. Alkaline phosphatase (AP) activity assay**

For determination of AP activity [339], cells were harvested in 0.2% (v/v) Nonidet P-40 (Sigma Aldrich, Lyon, FR) and disrupted by sonication. For aortas, tissues were smashed using liquid nitrogen and then added to 0.2% Nonidet P-40 and disrupted by sonication. The homogenate was centrifuged at 1500 g for 5 min. In the supernatant, AP activity was determined using p-nitrophenyl phosphate (pNPP) (Sigma Aldrich, Lyon, FR) as substrate at pH=10.4. The absorbance was measured at 405 nm. In the same lysates, the protein content was determined by bicinchoninic acid [340] (BCA, Sigma-Aldrich, Lyon, FR). Results were expressed as nmol of paranitrophenol (pNP) produced/min/mg protein and were normalized relative to their respective controls.

#### **5. Calcium assay**

For aortic explants and MOVAS cells, deposited calcium was extracted from the extracellular matrix using HCl 0.6 M overnight at room temperature. The calcium content of HCl supernatants was dosed by a colorimetric assay using o-cresolphthaline complexone method

(Sigma-Aldrich, Lyon, FR) [341]. The absorbance was measured at 570 nm. Calcium deposition was normalized to the weight of aortas or to the amount of proteins in cells. For the cells, proteins were harvested in NaOH 0.1 M / SDS 0.1 % and centrifuged at 700 g, 5 min at 4°C. In the supernatant, the protein content was determined by BCA assay.

## **6. Total RNA extraction, reverse transcription and quantitative real-time polymerase chain reaction (qPCR) analysis**

RNA was extracted from cells using the NucleoSpin RNA isolation kit by Macherey-Nagel (Villeurbanne, FR) according to the manufacturer's instructions. For aortas, tissues were smashed in liquid nitrogen and transferred to tubes containing TRI Reagent (Sigma Aldrich, Lyon, FR), and then RNA was extracted according to the manufacturer's instructions. Total RNA was quantified by a spectrophotometer at 260 nm, and its purity was determined by the ratios A260/A280 and A260/A230 (A: Absorbance). 1 µg of the resulting RNA was used for reverse transcription, using Superscript II reverse transcriptase (Invitrogen, Villebon-sur-Yvette, FR) and random hexamers (Invitrogen) in a 20-µl final volume. The reaction was done at 42°C for 30 min and stopped by incubation at 99°C for 5 min. 1 µl of cDNA template was used in subsequent qPCRs. qPCR was done using a Light Cycler system (Roche Diagnostics, Meylan, FR). The reactions were performed in a 20-µl final volume with 0.3 µM primers, 2 mM MgCl<sub>2</sub> and 2 µL of Light Cycler Fast Start DNA Master SYBR Green I mix (Roche, Lyon, FR). The protocol started by an activation step (95°C) for 10 min followed by 40 cycles consisting of a denaturation step (95°C) for 10 s, an annealing step (Ta) for 10 s and an elongation step (72°C) for 25 s. primer sequences and the annealing temperature (Ta) for each gene are listed in table 1. Relative quantification was done according to Livak's method using *Gapdh* as a reference gene.

Gene name	Species	Forward primer (5'-3')	Reverse primer (5'-3')	Ta (°C)
<i>Pld1</i>	Rat	CAACTCGGACAGCAT TAGCA	TCCCATGCCAAAACCT AGTC	62
<i>Pld2</i>	Rat	CCCTTTCTGGCCATCT ATGA	ATCCGCTGGTGTATCT TTCG	62
<i>Runx2</i>	Rat	GCCGGGAATGATGAG AACTA	TTGGGGAGGATTTGTG AAGA	60
<i>Bglap</i>	Rat	GTGCAGACCTAGCAG ACACCA	GTAGCGCCGGAGTCT ATTCA	60
<i>Sphk1</i>	Rat	GTCTGATGCACGAGG TGGT	CTCGTGCCCAGCATAG TAGT	58
<i>Sphk2</i>	Rat	TCTGGGGACCAGGAA ATCAC	CCCAGCTTCAGAGATC ATGG	60
<i>Spgl1</i>	Rat	GGCTTGTGGAGACGC AGTAG	GGGCTCGTATTTGGTG CAG	60
<i>Pld1</i>	Mouse	AAGTGCAGTTGCTCCG ATCT	TTCTCTGGGCGATAGC ATCT	56
<i>Pld2</i>	Mouse	GGGCACCGAAAGATA CACCA	CTCAGAACCTCCTCGG GGTA	56
<i>Gapdh</i>	Mouse	GGCATTGCTCTCAATG ACAA	TGTGAGGGAGATGCT CAGTG	62
<i>Sphk1</i>	Mouse	ACAGTGGGCACCTTCT TTC	CTTCTGCACCAGTGTA GAGGC	60
<i>Sphk2</i>	Mouse	TAGATGGGGAGTTAG TGGAGTATG	TGCTTTTAGGCTCGTT CAGG	60
<i>Spgl1</i>	Mouse	AACTCTGCCTGCTCAG GGTA	CTCCTGAGGCTTTCCC TTCT	60
<i>S1pr1</i>	Mouse	CACCGGCCCATGTACT ATTT	GA CTGCCCTTGGAGAT GTTC	60
<i>S1pr2</i>	Mouse	AGTGACAAAAGCTGC CGAATG	GCACGTAGTGCTTAGC ATAGAGAGG	62
<i>S1pr3</i>	Mouse	ATGTACTTTTTTCATCG GCAACTTG	ACGTCTTCTGCCGGA CATA	62

**Table 1: The sequences of the primers used in qPCR with their respective annealing temperatures (Ta).**

## 7. Western blot

Cells were homogenized in 20 mM Tris / HCl pH 7.6 buffer containing 100 mM NaCl, 1% Triton X-100, and 1% of a protease inhibitor cocktail (Sigma Aldrich, Lyon FR). Cell lysates were mixed with Laemmli buffer (BioRad, Californie, US), boiled for precisely 1 min, and separated on 8% SDS polyacrylamide gel containing 4 M urea. The western blots were probed with anti-PLD1- and anti-PLD2-specific polyclonal antibodies kindly provided by Dr S. Bourgoin (Laval University, CA), used at dilutions of 1/10000 and 1/5000, respectively.

Immunoblots were revealed with the enhanced chemiluminescence (ECL) detection system (GE Healthcare, Limonest, FR) and X-ray film autoradiography. Membranes were incubated with an anti- $\beta$ -actin monoclonal antibody (clone AC-74) from Sigma Aldrich for normalization. Bands were then quantified by Image J software (<https://imagej.nih.gov/ij/>).

## 8. PLD activity assay

For cells:

PLD activity was determined by measuring the production of  $^{14}\text{C}$ -phosphatidylbutanol, which is the product of its transphosphatidyltransferase activity. Briefly, cells were incubated for 16 h with 0.5 mCi  $^{14}\text{C}$ -palmitate/L (Perkin Elmer, Villebon Sur Yvette, FR) to label phosphatidylcholine. The radioactive medium was then removed, and cells were washed 3 times with DMEM containing 0.2% BSA. 1-butanol, at a final concentration of 0.8%, was added, and the cells were incubated further for 30 min, the optimal time to recover the maximal formation of phosphatidylbutanol (PtdButOH). Lipids were then extracted as described by Bligh and Dyer [342], except that 2 M KCl in 0.2 M HCl were added to the extraction mixture instead of water for the separation of the aqueous and organic phases. Chloroform phases were then evaporated overnight and resuspended in 50  $\mu\text{l}$  of chloroform. Lipids were separated by thin layer chromatography (TLC) using Silica Gel 60 plates. The TLC plates were migrated using the superior phase of the mixture: ethylacetate/isooctane/acetic acid/water (55/25/10/50). The positions of lipids were identified after staining with iodine vapour by comparison with authentic standards. The silica gel containing radioactive lipids were quantified by liquid scintillation counting after scraping the spots off the plates.

For aortas:

Amplex Red PLD Kit (Molecular Probes, Eugene, OR, US) was used to measure the rate of choline production from PC hydrolysis by PLD, according to the manufacturer's instructions with slight modifications [343]. Tissues were smashed in liquid nitrogen and added to Tris 50 mM buffer pH=8.0. They were then lysed by 3 freeze/thaw cycles. Samples were incubated with 0.5 mM PC (Avanti Polar Lipids, Alabaster, AL, US) and 2 mM levamisol for 30 min at 37 °C. Then, 100  $\mu\text{L}$  aliquots were collected. Extracts were mixed with 100  $\mu\text{L}$  reaction buffer containing 100  $\mu\text{M}$  Amplex Red reagent, 2 U/mL horseradish peroxidase (HRP) (Molecular Probes, Eugene, OR, US), 0.2 U/mL choline oxidase from *Alcaligenes* sp. (MP

Biomedicals, Ilkirch-Graffenstaden, FR). 2 mM of levamisol (Sigma Aldrich, Lyon, FR) was added to the reaction buffer to prevent dephosphorylation of phosphocholine produced by PLC. PLD activity was estimated by measuring the fluorescence of resorufin after 30 min incubation at 37°C using a micro-titre plate reader (NanoQuant Infinite M200, Tecan, Salzburg, AU) at 590 nm after sample excitation at 530 nm. A standard curve was done using choline. PLD activity was normalized to the total protein amount (BCA, Sigma-Aldrich, Lyon, FR).

### **9. SK activity assay**

SK activities were measured by their ability to phosphorylate sphingosine and was calculated as picomoles of S1P formed/ min/ mg of total proteins. For determining SK1 activity, the reaction mixture consisted of 50 mM sphingosine (Enzo Life Sciences, Villeurbanne, FR), 0.25% Triton X-100 (which can inhibit the activity of SK2), [ $\gamma$ -<sup>32</sup>P]-ATP (5 mCi/L, 10 mM) (Perkin-Elmer, Courtaboeuf, FR) and 10 mM MgCl<sub>2</sub>. For SK2, the same mixture was used without Triton X-100 but with 0.1 fatty acid-free bovine serum albumin and KCl 1M (which can inhibit the activity of SK1). The produced labelled S1P was separated by thin layer chromatography on silica gel 60 plates (Dutscher, Brumath, FR) migrated in 1-butanol/ethanol/glacial acetic acid/water (8:2:1:1 by volume). The placement of S1P on the plates was visualized by autoradiography, and the silica gel containing radioactive lipids were quantitated by liquid scintillation counting after scraping the spots off the plates. All the work that needed dealing with <sup>32</sup>P was done by Leyre Brizuela Madrid.

### **10. S1P dosage assay**

MOVAS cells from which the secreted S1P has to be dosed was kept with serum free high glucose (4.5 g/L) Dulbecco's modified Eagle's medium (DMEM) containing 10 U/mL penicillin and 100 µg/mL streptomycin, for 24 hours in order to collect secreted S1P. Then, the amount of S1P in the conditioned media was determined using a competitive SPHINGOSINE 1 PHOSPHATE ELISA kit from Tebu-bio (Le Perray En Yvelines, France) according to the manufacturer's instructions. The amount of S1P was normalized to total secreted proteins after protein dosage in the conditioned media.

### **11. Statistical analysis**

Statistical analysis were done for measurements when at least three independent experiments were performed. Groups were compared using two-sided unpaired t-test. 2-way ANOVA was used to compare the renal status and other rat data in order to compare different groups at the

same time. Results were expressed as mean  $\pm$  standard error of the mean (SEM). Results were considered significant when  $p < 0.05$ .

## **Chapter III: Results**

### **Part 1: PLD in MOVAS murine smooth muscle cell line vascular calcification model**

#### **1. The role of PLD during calcification in MOVAS cells**

##### 1.1 Characterization of MOVAS model

Calcification was induced in MOVAS cells by culturing them with 10 mM  $\beta$ -GP and 50  $\mu$ g/ml AA during 28 days. AA was given to cells in order to enhance collagen I production. It is a required cofactor for the activity of prolyl and lysyl hydroxylases which hydroxylase proline and lysine residues, respectively, in collagen. These modifications are important for structural stability of collagen I. Moreover, in SMCs, AA was shown to be involved in both procollagen synthesis and maturation after being actively taken up by the cells [344–346]. The produced collagen I can act as a matrix for later Ca deposition, and therefore it enhances mineralization.  $\beta$ -GP is considered a donor of phosphate. It provides Pi upon being hydrolysed by phosphatases like TNAP [347]. When MOVAS cells upregulate TNAP,  $\beta$ -GP will be gradually hydrolysed producing high amount of Pi. Thus, the amount of Pi in the culture medium may depends of the increase in the TNAP activity of the cells. AP activity, a measurement of the total APs activities including that of TNAP, was increased in time dependent manner starting from day 14 (Figure 17A). Thus, the cells were gaining the capacity to calcify the matrix. On day 21, the calcification was evident as seen by a significant increase in the amount of calcium deposited on the cellular matrix detected by o-cresolphthaline complexone after being mobilized by HCl. The deposited calcium continued to increase at day 28 (Figure 17B).

The gene expression of the two osteo-chondrocytic markers, *Runx2* and *Bglap*, were evaluated by qPCR, but no significant change was detected at the time points tested (data not shown). RUNX2 is an osteoblastic transcription factor that induce the initial commitment of osteoblastic cells. Thus, its expression may be elevated only transiently so that it can be detected by checking time points between those tested, because 7 days is relatively a long interval so that a transient overexpression can be missed. On the other hand, the mechanism by which MOVAS is gaining a calcifying capacity may include an upregulation of other markers like the chondrocytic transcription factor, *Sox9*, which was shown to be increased in these cells upon culturing in high-glucose medium during the trans-differentiation into chondrocytes [181]. Also, in case of chondrocytic trans-differentiation, *Runx2* is expression

during stages of hypertrophy. Moreover, OCN (whose gene is *Bglap*), is a late marker in osteoblasts and expressed only by hypertrophic or post hypertrophic chondrocytes [348]. Thus, in our culture it is possible that we did not reach these stages especially that the amount of deposited calcium was still increasing until the end of the experiment. Unfortunately, MOVAS cells cannot be maintained in good condition when plated for more than 28 days. The characterization of the molecular pathways, including transcription factors involved, is needed, but till now we can tell that MOVAS provides a good model of calcification comprising different steps, including an increase in AP activity, initiation of calcification and deposition of calcium.

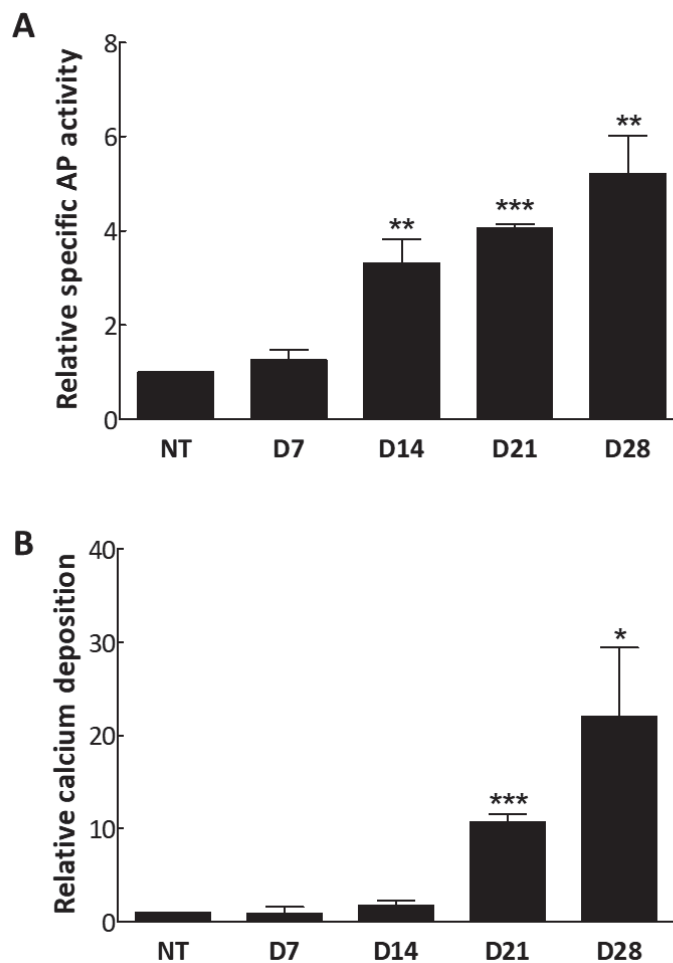


**Figure 17: Calcification in MOVAS cells.** MOVAS cells were incubated with 10 mM  $\beta$ -GP and 50  $\mu$ g/ml AA during 28 days (D28). (A) Relative specific AP activity was calculated by a colorimetric assay using pNPP as substrate and was normalized to total protein content. (B) Relative Ca deposition was quantified using o-cresolphthaline complexone in a colorimetric assay and was also normalized to total protein content. All results are represented as mean  $\pm$  SEM relative to non-treated cells (NT), which was incubated with control medium for 7 days. At least 3 independent experiments were performed for each assay and statistical significance was estimated by student t test. \* Indicated  $p < 0.05$ , \*\* indicated  $p < 0.01$  and \*\*\* indicated  $p < 0.001$  with respect to NT cells.

## 1.2 Expression and activity of PLD during transdifferentiation of MOVAS

In order to predict a role for PLD in vascular calcification, we have first followed the changes in its expression during the different steps of calcification seen in MOVAS cells. The gene expression of *Pld1* increased only slightly (by 17%) but significantly at day 7 after culture in calcification medium. After day 7, its expression decreased to levels less than that of the control at day 28. The gene expression of *Pld2* was stable during the initial stages of MOVAS calcification, but then decreased gradually and significantly starting from day 21 (Figure 18A).

The small increase in *Pld1* gene expression was manifested by a greater elevation in its protein level, which started at day 7 and reached its maximum at day 14 (2 fold with respect to control). After this point, it decreases again to the normal level along with the decrease in gene expression. The protein expression of PLD2 did not show any change during the whole experimental time (Figure 18B and C).

PLD1 and PLD2 are unique for their ability to catalyse a transphosphatidylation reaction between PC and primary alcohols. This was taken as an advantage to measure the activity of PLD by following the formation of PtdButOH after the addition of 1-butanol to living cells. The total PLD activity in MOVAS was assessed using this procedure. It increased significantly starting from day 7, reached a maximum at day 14 and decreased again after this point to reach its basal level at day 28 (Figure 18D). Unfortunately, there is no experiment that can measure specifically PLD1 or PLD2 activity. The contribution of each isoform to the total PLD activity can be predicted from their protein expression, but this is not always true, because PLD, and especially PLD1, has a low basal activity and needs to be activated by different cellular pathways. Thus, the increase in PLD1 expression do not always indicate an increase in its activity.

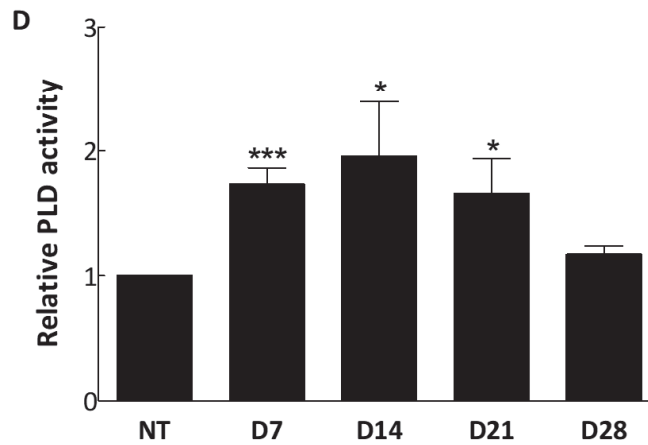
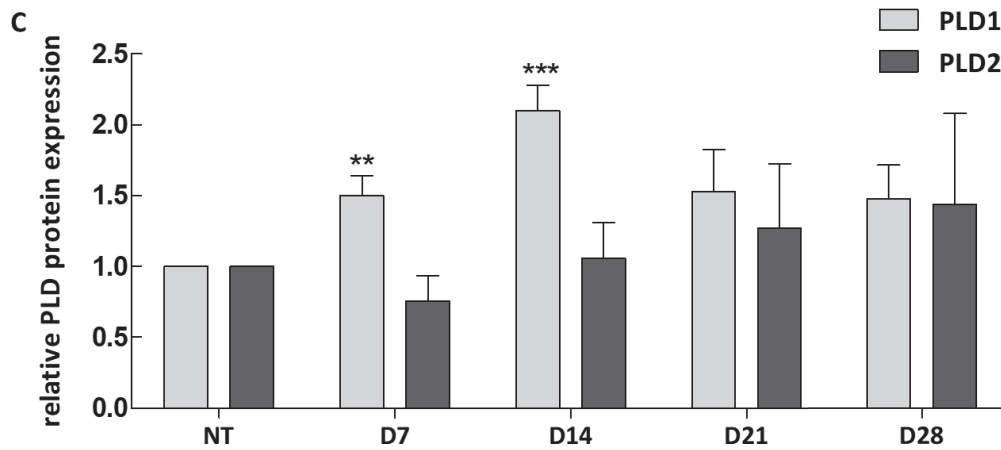
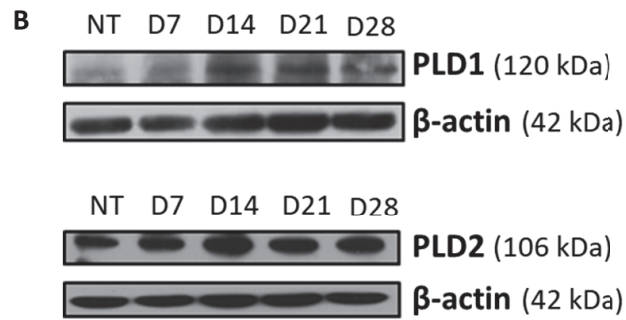
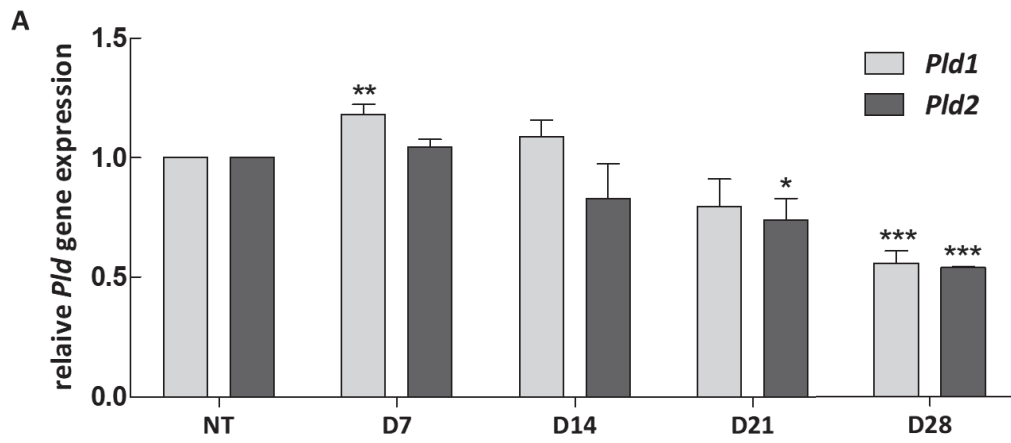


**Figure 18: PLD expression and activity during calcification in MOVAS cells.** MOVAS cells were incubated with 10 mM  $\beta$ -GP and 50  $\mu$ g/ml AA during 28 days (D28). (A) Pld1 and Pld2 gene expression was relatively quantified by qPCR according to Livak's method and using Gapdh as a reference gene. (D) Protein expression of PLD1 (120 kDa) and PLD2 (106 kDa) was examined by western blot with  $\beta$ -actin (42 kDa) being used as a loading control. (E) PLD1 and PLD2 bands obtained by western blot were quantified by image J and normalized to the expression of  $\beta$ -actin. (F) PLD activity in MOVAS cells was measured as the amount of PtdButOH produced normalized to total lipids. All results are represented as mean  $\pm$  SEM relative to non-treated cells (NT), which was incubated with control medium for 7 days. At least 3 independent experiments were performed for each assay and statistical significance was estimated by student t test. \* Indicated  $p < 0.05$ , \*\* indicated  $p < 0.01$  and \*\*\* indicated  $p < 0.001$  with respect to NT cells.

### 1.3 Effect of PLD inhibitors on calcification MOVAS cell

To check if PLD has an active role during calcification or the increase seen in its activity is only a consequence of calcification, we inhibited PLD activity and checked its effect of AP activity and calcium deposition after 21 days of culture. This time was chosen because both AP activity and calcium accumulation were significantly elevated and PLD activity was still high. Moreover, MOVAS cells look healthier at day 21 than day 28 because the long culture time and confluency can impose stress on the cells. The inhibition of PLD for 3 weeks by the pan-PLD inhibitor, Halopemide, abolished the Pi-induced increase in AP activity and Ca deposition at the two tested concentrations: 1 and 2  $\mu$ M (Figure 19A and B).

To check the contribution of each isoform, molecules that inhibit specifically PLD1 or PLD2 were used. The PLD1-specific inhibitor, VU0155069, which was used at 600 nM and 800 nM, was able to inhibit both AP activity and Ca deposition at both concentrations tested (Figure 19A and B). The specific inhibition of PLD2 by CAY10594, 200 nM or 300 nM, did not induce any significant effect on calcification (Figure 19A and B). The effects of VU0155069 were slightly less important than those of Halopemide. This may have several explanations; the first possibility is that PLD1 is the only isoform involved and Halopemide may be more potent in inhibiting PLD1 than VU0155069 in our model. In MOVAS, Halopemide inhibited PLD activity by about 80%, whereas VU0155069 inhibited it by 60%. However, this difference may be due to the action of Halopemide on PLD2. Thus, it is not easy to test this possibility when we can't measure the activity of each enzyme separately. On the other hand, the greater effect of Halopemide may be due to its action on PLD2, which may play a minor role in calcification especially as a compensatory mechanism for the loss of PLD1 activity in case of VU0155069. In all cases, we found that PLD is important for vascular calcification in the MOVAS model, and PLD1 is the main isoform acting during this process. Inhibiting both isoforms may have greater opportunity in blocking calcification because it eliminates the possibility of compensation by PLD2.

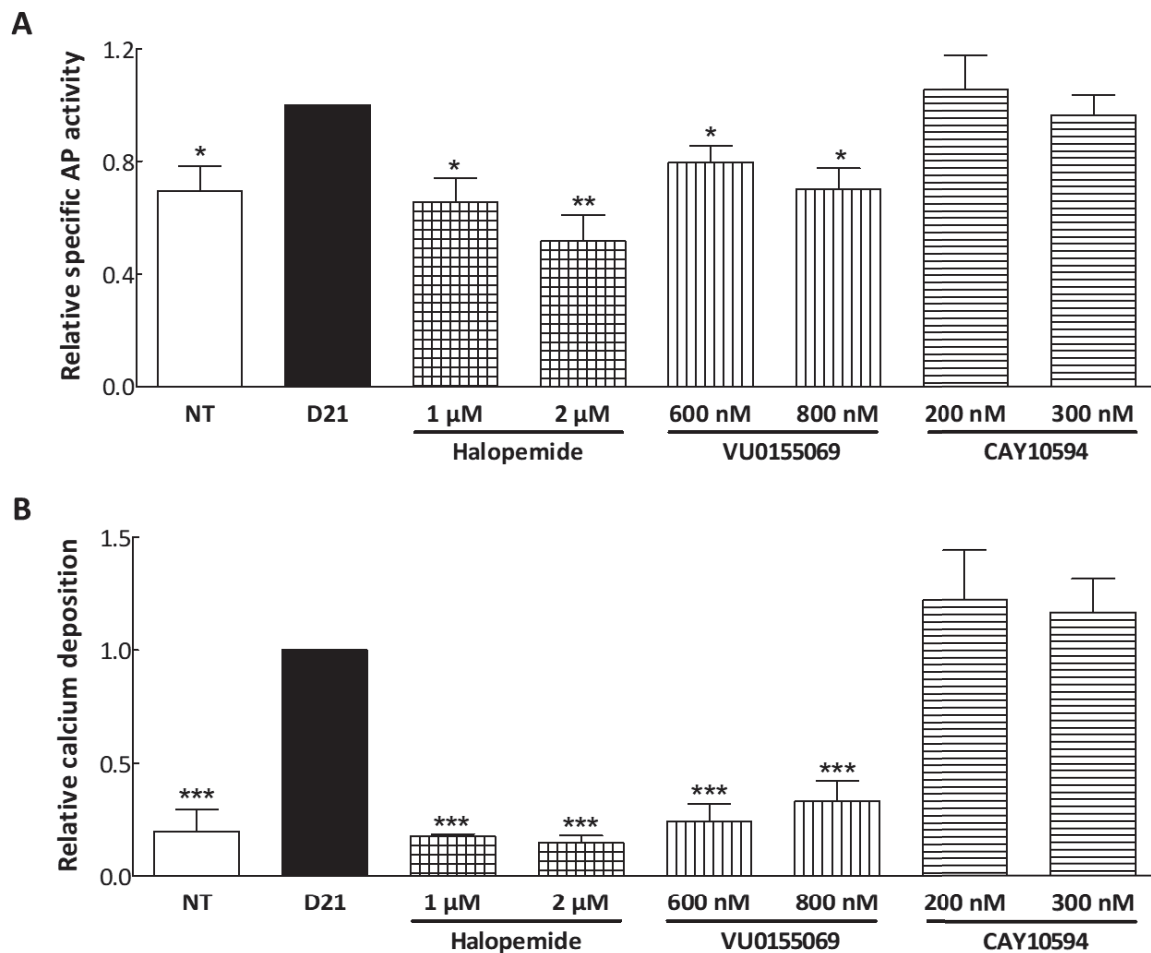


**Figure 19: The effects of different PLD inhibitors on calcification in MOVAS cells.** MOVAS cells were incubated with 10 mM  $\beta$ -GP and 50  $\mu$ g/ml AA during 21 days (D21) with or without PLD inhibitors: Halopemide, a pan-PLD inhibitor for PLD1 and PLD2 (used at 1 and 2  $\mu$ M), a PLD1-specific inhibitor VU0155069 (used at 600 and 800 nM) and a PLD2-specific inhibitor CAY10594 (used at 200 and 300 nM). NT are non-treated cells incubated in control medium for 21 days. (A) Relative specific AP activity was calculated by a colorimetric assay using pNPP as substrate and was normalized to total protein content. (B) Relative Ca deposition was quantified using o-cresolphthaline complexone in a colorimetric assay and was also normalized to total protein content. All results are represented as mean  $\pm$  SEM relative to cells stimulated for calcification during 21 days without treatment by any inhibitor (D21). At least 3 independent experiments were performed for each assay and statistical significance was estimated by student t test. \* Indicated  $p < 0.05$ , \*\* indicated  $p < 0.01$  and \*\*\* indicated  $p < 0.001$  with respect to D21.

We have seen that PLD expression and activity was decreasing beyond day14, thus it seems that it is especially important during the initial stages of calcification. During later steps, the decrease may be due to normal negative feedback regulation, in which its expression is decreased because it is no longer needed, or it may signify that PLD is playing opposite roles during different stages of calcification. To examine the latter possibility, MOVAS cells were stimulated to calcify during 28 days. Halopemide was added to culture medium during the whole culture time, only during the first 2 weeks or only during the last 2 weeks. Calcium deposition was inhibited equally in all these conditions (Figure 20B). Thus, PLD is important for calcification during all the 28 days. With respect to inhibiting AP activity, Halopemide

was effective mostly when given through the whole culture time. It was also partially effective when given during the first 2 weeks, but not effective when given only in the last 2 weeks (Figure 20A). These data indicate that PLD is not playing an opposite role during the late stages of calcification, because its late inhibition did not lead to an increase in AP activity and calcium deposition, but rather it was also effective in delaying calcium deposition. Therefore, PLD inhibitors can be given safely during any stage of calcification and they can still delay its progression even after VSMCs acquire increased calcification capacity.

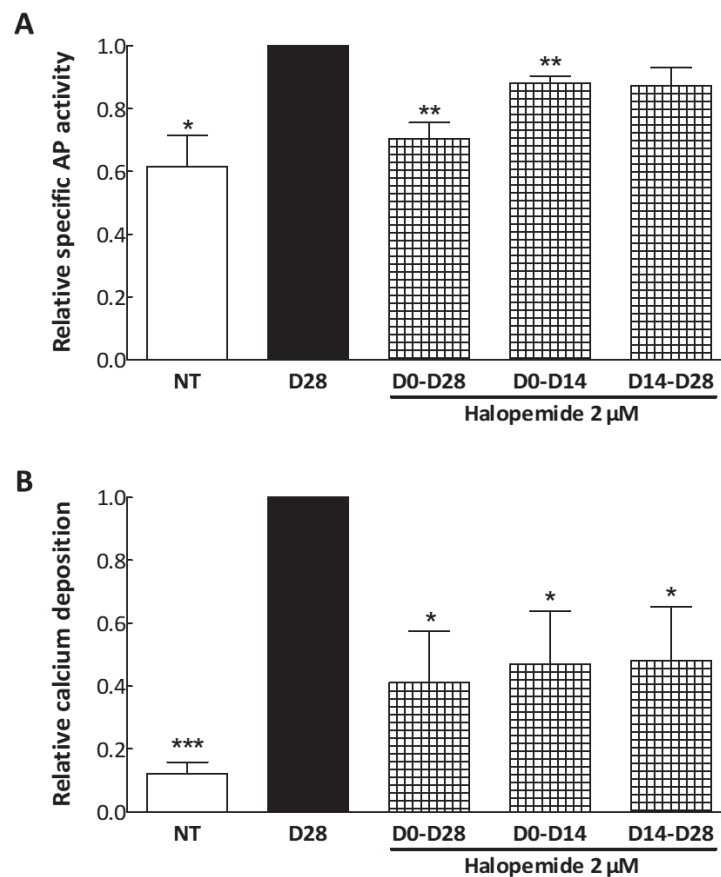


**Figure 20: The effects of the timing of PLD inhibition on calcification in MOVAS cells.** MOVAS cells were cultured for 28 days in stimulation medium (D28). D0-D28 cells were cultured in stimulation medium + Halopemide 2 μM for 28 days. D0-D14 cells were cultured in stimulation medium for 28 days, but treated with Halopemide 2 μM from day 0 until day 14 only. D14-D28 cells were also cultured in stimulation medium for 28 days but treated with Halopemide from day 14 until day 28. NT are non-treated cells incubated in control medium for 28 days. (A) Relative specific AP activity was calculated by a colorimetric assay using pNPP as substrate and was normalized to total protein content. (B) Relative Ca deposition was quantified using o-cresolphthaline complexone in a colorimetric assay and was also normalized to total protein content. All results are represented as mean ± SEM relative to D28 cells. At least 3 independent experiments were performed for each assay and statistical significance was estimated by student t test. \* Indicated p < 0.05, \*\* indicated p < 0.01 and \*\*\* indicated p < 0.001 with respect to D28.

## **2. The effects of PKC inhibition on calcification in MOVAS cells and on PLD activity.**

As PKC is one of the major PLD regulators, its involvement in PLD activation during MOVAS calcification was tested. Inhibition of PKC by Bisindolylmaleimide X hydrochloride, which normally inhibits PKC $\alpha$ ,  $\beta$ I,  $\beta$ II,  $\gamma$  and  $\epsilon$ , led to a concentration-dependent decline in AP activity and Ca deposition, which was significant when used at 5  $\mu$ M (Figure 21A and B). In contrast to AP activity, which was lowered to a level less than the control, Ca deposition was not abolished completely. Thus, PKC activity is involved in calcification in our model, however its role may not be as important as that of PLD. In consistence with this finding, the inhibition of PKC did not affect PLD activity (Figure 21C), when checked at day 14, at which the PLD activity was maximal. Therefore, PLD is activated during MOVAS calcification in a PKC-independent manner, and PKC also has a role in VC which did not involve activating PLD.

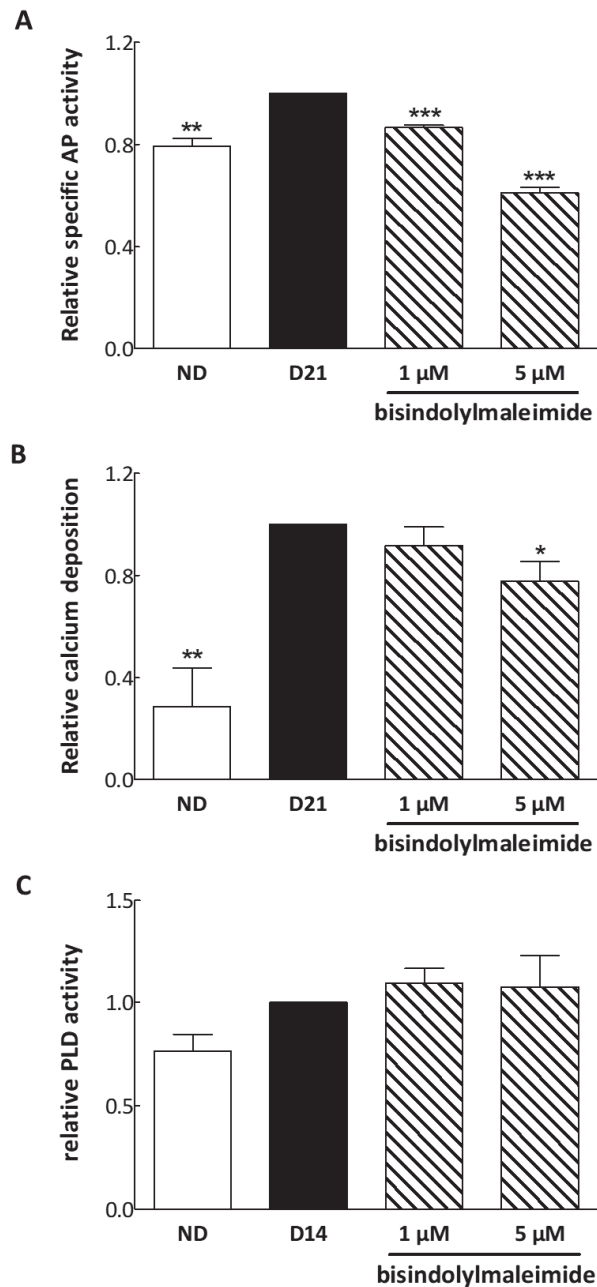


**Figure 21: The effects of PKC inhibition on calcification in MOVAS cells and on PLD activity.** MOVAS cells were incubated with 10 mM  $\beta$ -GP and 50  $\mu$ g/ml AA during 21 days (D21) (A and B) or 14 days (D14) (C) with or without the PKC inhibitor: Bisindolylmaleimide X hydrochloride at 1 or 5  $\mu$ M. NT are non-treated cells incubated in control medium for 21 days (A and B) or 14 days (C). (A) Relative specific AP activity was calculated by a colorimetric assay using pNPP as substrate and was normalized to total protein content. (B) Relative Ca deposition was quantified using o-cresolphthaline complexone in a colorimetric assay and was also normalized to total protein content. (C) PLD activity in MOVAS cells was measured as the amount of PtdButOH produced relative to total lipids. Results are represented as mean  $\pm$  SEM relative to D21 cells (A and B) or to D14 cells (C). At least 3 independent experiments were performed for each assay and statistical significance was estimated by student t test. \* Indicated  $p < 0.05$ , \*\* indicated  $p < 0.01$  and \*\*\* indicated  $p < 0.001$  with respect to D21 (A and B) or D14 (C).

### 3. The possible link between S1P and PLD during MOVAS calcification

S1P metabolic and signalling pathways are tightly linked to PLD signalling, and this link is bi-directional. As detailed in the introduction, S1P can activate PLD through binding its GPCRs. Also, PLD was seen to activate SK1. These facts combined with the role of S1P in bone homeostasis encouraged us to assess its role in vascular calcification and examine its possible link with PLD during this process.

First, we checked the gene expression of *Sphks* during calcification in MOVAS cells to find a stable expression of both *Sphk1* and *Sphk2* during the first 2 weeks, with a subsequent decline in both during the last 2 weeks (Figure 22A). Because the gene expression do not always correlate with protein expression due to post-transcriptional regulation, and SKs are enzymes that can show an increase in their activity even when no change in their expression was detected, we checked the activities of these kinases during calcification. The individual activity of each SK can be detected separately because they are differentially regulated; SK2, but not SK1, is strongly inhibited by detergents, thus SK1 activity was determined by using Triton X in the reaction mixture. On the other hand, SK1, but not SK2, can be inhibited by salts. Thus, SK2 activity was determined specifically by using KCl in the reaction mixture. We found a slight but significant increase in SK1 activity at day 7, with a later decrease down to its basal level until the end of the experiment (Figure 22B). SK2 showed a different profile; its activity increased significantly up to 2.7 fold with respect to the control at day 14 and then declined progressively until day 28 (Figure 22B). The timing of maximal SK2 activity is the same as that of PLD, which may predict a possible link between both enzymes. In this model, it seems that SK1 and SK2 have non-overlapping roles, and they may be involved in different stages of calcification.

S1P level in cells depends largely on the balance between its production and its degradation. It is degraded irreversibly by the action of SPL. Thus, we checked its gene (*Spg11*) expression. *Spg11* expression was stable during the first 2 weeks of calcification and decreased significantly and gradually until day 28 (Figure 22C). Although it is important to determine its activity, the decrease in its expression coupled with the increase seen in SK1/2 activities may signify an increase in S1P intracellular and/or extracellular levels.

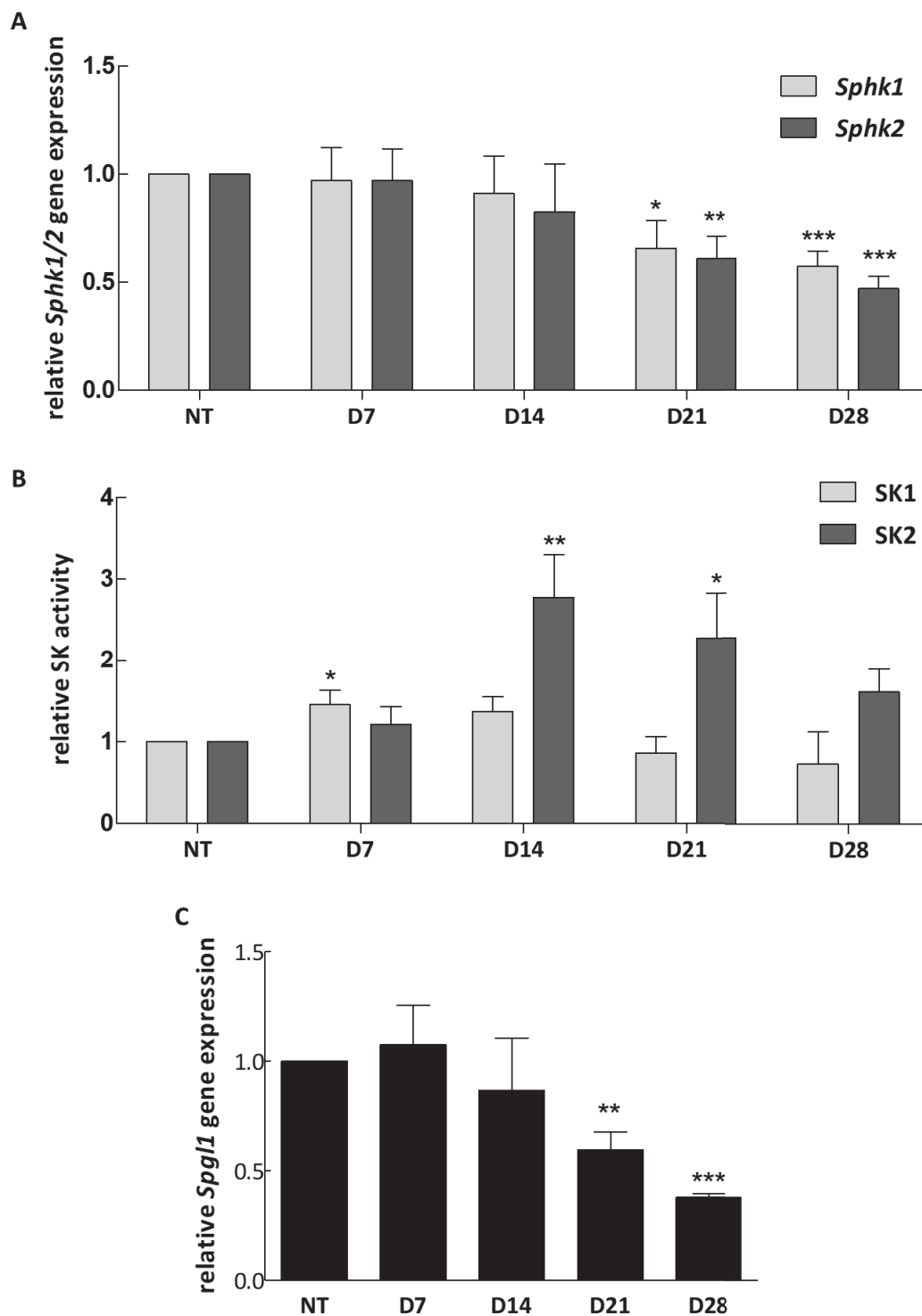


**Figure 22: The expression and activities of different S1P metabolic pathway effectors during calcification in MOVAS cells.** MOVAS cells were incubated with 10 mM  $\beta$ -GP and 50  $\mu$ g/ml AA during 28 days (D28). (A) *Sphk1* and *Sphk2* gene expression was relatively quantified by qPCR according to Livak's method and using *Gapdh* as a reference gene. (B) SK1/2 activities were measured by the amount of the radioactively labelled S1P produced, which was normalized to total protein content. (C) *Spg11* gene expression was relatively quantified by qPCR according to Livak's method and using *Gapdh* as a reference gene. All results are represented as mean  $\pm$  SEM relative to non-treated cells (NT), which were incubated with control medium for 7 days. At least 3 independent experiments were performed for each assay and statistical significance was estimated by student t test. \* Indicated  $p < 0.05$ , \*\* indicated  $p < 0.01$  and \*\*\* indicated  $p < 0.001$  with respect to NT cells.

Secreted S1P was collected during 24 hours in conditioned medium and dosed by ELISA. The preliminary data suggests an increase in S1P secretion between day 7 and day 21 (Figure 23A). These data needs to be confirmed. Although till now we can't be sure about the level of secreted S1P by MOVAS cells, S1P *in-vivo* can be produced by other cell types, like endothelial cells, and thus can affect VSMCs in a paracrine fashion. Thus, it was important to assess the expression of *S1prs*. *S1P*<sub>1-3</sub> are expressed in VSMCs, however the expression of *S1P*<sub>4,5</sub> in these cells is debated [371]. Therefore, the studies using VSMCs focused on *S1P*<sub>1-3</sub>, and so was done in our study. *S1pr1* expression did not change during calcification. However, *S1pr2* decreased significantly. *S1pr3* expression decreased during early stages of calcification but then increased significantly at day 28 (Figure 23B). Thus, S1PRs seem to have different roles during MOVAS cells trans-differentiation into calcifying cells.

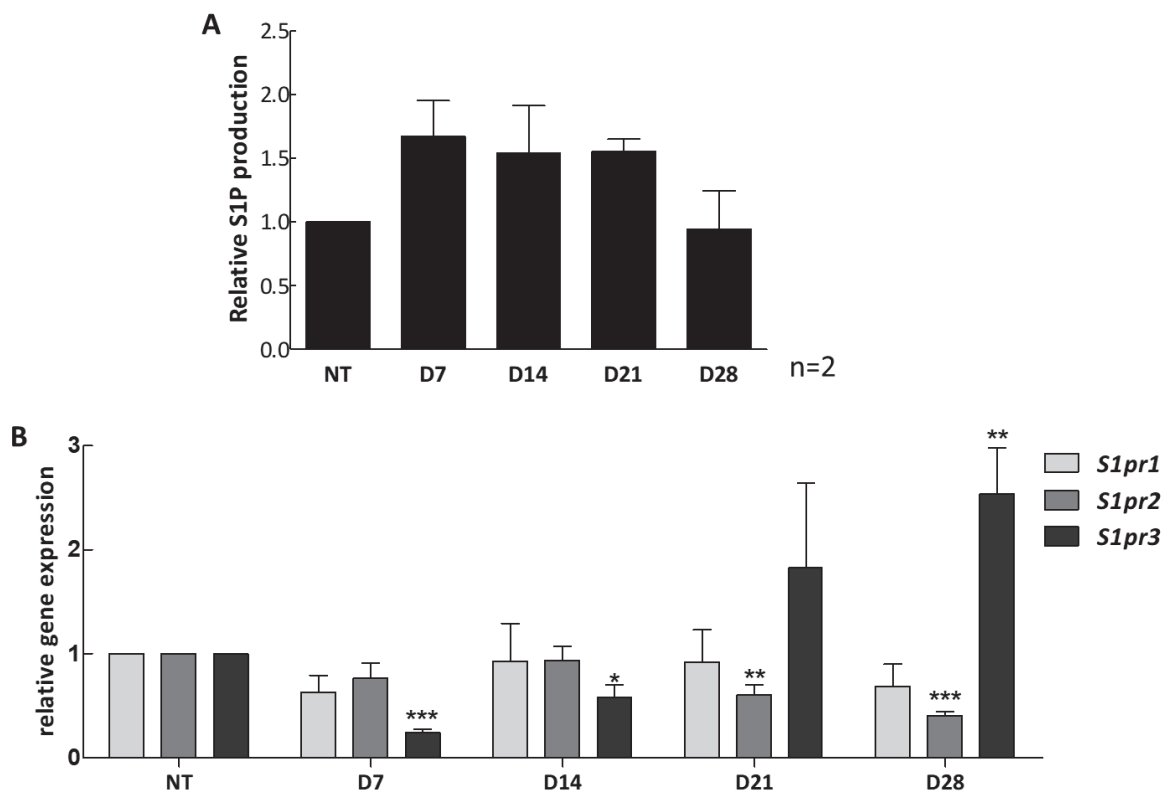


**Figure 23: extracellular S1P production and S1P receptors expression during calcification in MOVAS cells.** MOVAS cells were incubated with 10 mM  $\beta$ -GP and 50  $\mu$ g/ml AA during 28 days (D28). (A) Secreted S1P was dosed by ELISA in the conditioned media of MOVAS cells during calcification and normalized to total secreted proteins. Conditioned media was collected after 24 hours of incubation in serum-free medium. (B) *S1pr1,2,3* gene expression was relatively quantified by qPCR according to Livak's method and using *Gapdh* as a reference gene. All results are represented as mean  $\pm$  SEM relative to non-treated cells (NT), which were incubated with control medium for 7 days. In (B) 3 independent experiments were performed and statistical significance was estimated by student t test. \* Indicated  $p < 0.05$ , \*\* indicated  $p < 0.01$  and \*\*\* indicated  $p < 0.001$  with respect to NT cells.

The role of S1P produced during calcification was assessed by inhibiting SKs. The inhibition of SK1/2 activity for 3 weeks by pan-SK inhibitor SKi at 5  $\mu$ M abrogated calcification in terms of AP activity and Ca deposition. The use of K145 at 5  $\mu$ M, a specific inhibitor for SK2, had an even more prominent effect on calcification than Ski. However, SK1 inhibition by PF-543, 100 nM, did not affect calcification significantly (Figure 25A and B). To be sure that the absence of effect in case of PF-543 is not because it was used at a concentration that cannot inhibit SK1 efficiently, we checked the effects of PF-543 (100 nM) and SKi (5  $\mu$ M) on SK1 activity. The preliminary data showed that both inhibitors were able to block SK1 activity efficiently, 90% inhibition in case of SKi and 81% in case of PF-543 (Figure 24). Therefore, SK2 seems to be the isoform with the important role in calcification of MOVAS cells cultured with  $\beta$ -GP and AA.

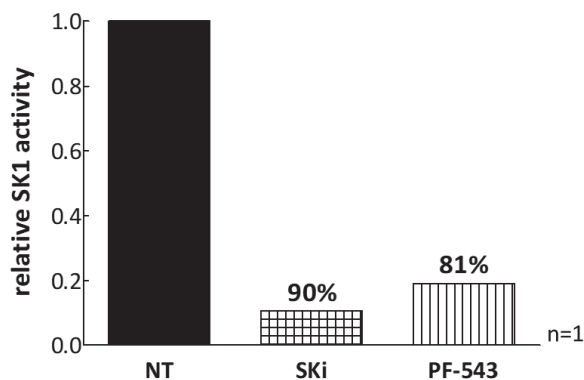


**Figure 24: The effect of SK1 inhibitors on SK1 activity.** MOVAS cells were incubated in control medium for 72 hours with or without the pan-SK inhibitor: Ski at 5  $\mu$ M or the SK1-specific inhibitor: PF-543 at 100 nM. SK1 activity was measured by the amount of the radioactively labelled S1P produced, which was normalized to total protein content. Results are presented relative to NT cells which was cultured in control medium for 72 hours without any inhibitor.

In order to study the possible role of extracellular S1P signalling, we used FTY720 (also called fingolimod). FTY720 is an immunosuppressant that was recently licensed by the Food and Drug Administration and the European Medicines Agency as Gilenya™. FTY720 is a sphingosine analogue which can be taken up by cells, phosphorylated by SK2 and released as FTY720-phosphate (FTY720-P). FTY720-P binds to all receptors except S1P<sub>2</sub> [349]. FTY720-P induces a later “functional antagonism” by promoting the polyubiquitination, endocytosis, and proteasomal degradation of S1P<sub>1</sub> [350]. Moreover, it can inhibit enzymatic activities of SKs, especially SK1 [351]. FTY720 at 2.5  $\mu$ M had a strong and significant inhibitory effect on AP activity that was lowered below the basal levels (Figure 25A). Also, it decreases significantly the amount of Ca deposited (Figure 25B). Its effect was more

important than that of Ski. Therefore, cellular signalling through S1P receptors, especially S1P<sub>1</sub> may be important for MOVAS calcification.

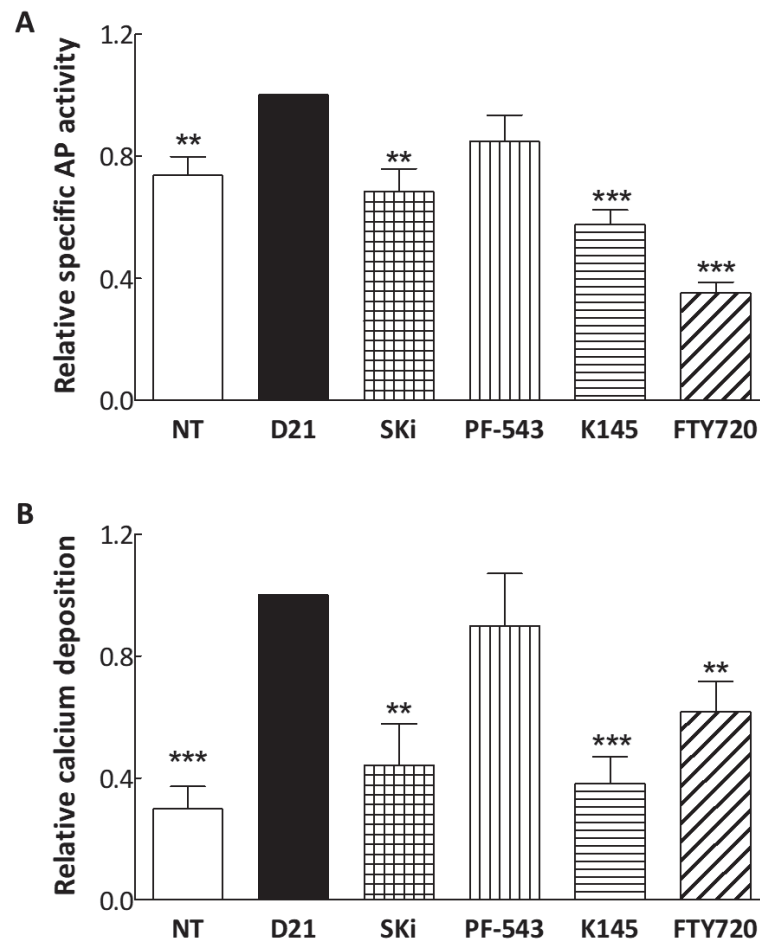


**Figure 25: The effects of modulation of S1P production and signalling on calcification in MOVAS cells.** MOVAS cells were cultured with 10 mM  $\beta$ -GP and 50  $\mu$ g/ml AA during 21 days with or without the pan-SK inhibitor Ski 5  $\mu$ M, the SK1 inhibitor PF-543 100 nM, the SK2 inhibitor, K145 5  $\mu$ M, or the general inhibitor of S1P metabolism and signalling, FTY720 2.5  $\mu$ M. Non-treated cells (NT) were cultured for 21 days in control medium. (A) Relative specific AP activity was calculated by a colorimetric assay using pNPP as substrate and was normalized to total protein content. (B) Relative Ca deposition was quantified using o-cresolphthaline complexone in a colorimetric assay and was also normalized to total protein content. Results are represented as mean  $\pm$  SEM relative to D21 cells. At least 3 independent experiments were performed for each assay and statistical significance was estimated by student t test. \* Indicated  $p < 0.05$ , \*\* indicated  $p < 0.01$  and \*\*\* indicated  $p < 0.001$  with respect to D21.

Then, we checked whether PLD activation in our model is mediated by extracellular S1P acting through its receptors or by intracellular S1P provided by the activity of SK2, which are both important for MOVAS calcification. So, we checked PLD activity during MOVAS calcification after using K145 or FTY720 for 14 days. This timing was chosen according to PLD maximal activity. However, neither K145 nor FTY720 had any effect on PLD activity during MOVAS calcification (Figure 26A).

In the other way round, it was previously proved that PLD can activate SK1 in other models. Thus, we checked the effects of different PLD inhibitors on SK1 and also SK2 activities in our cellular model (n=1). The preliminary data shows that the use of Halopemide or CAY10594 inhibited partially SK2 activity, however the use of the PLD1-specific inhibitor VU0155069 abolished SK2 activity far below the basal level (Figure 26C). Unexpectedly, PLD inhibition by any of the three inhibitors induced an increase in SK1 activity (Figure 26B). These data need to be confirmed, but it is possible the PLD1 role in VC depends on SK2 activation, especially that both enzymes were shown in our results to be crucial for calcification. The effect of PLD1 on SK1 may be due to some indirect actions. These opposing effects of PLD on SK1 and SK2 are not surprising, because SK1 and SK2 were shown to have opposing roles in different cellular functions like determining the cell fate [352,353].

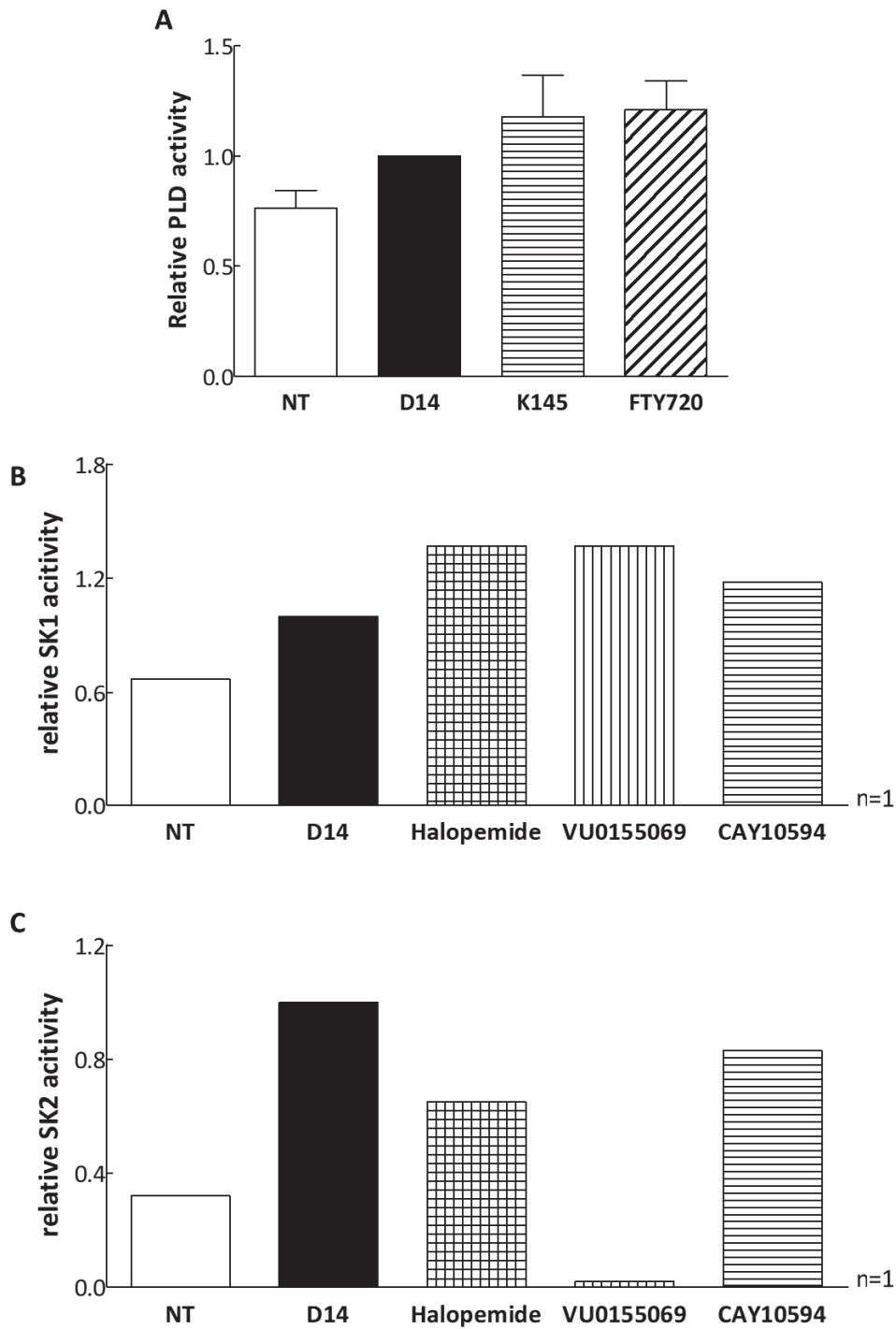


**Figure 26: The crosstalk between PLD and S1P signalling pathways.** MOVAS cells were cultured with 10 mM  $\beta$ -GP and 50  $\mu$ g/ml AA during 14 days with or without the SK2 inhibitor, K145 5  $\mu$ M, the general inhibitor of S1P metabolism and signalling, FTY720 2.5  $\mu$ M, the pan-PLD inhibitor, Halopemide 800 nM, the PLD1 inhibitor, VU0155069 2  $\mu$ M, and the PLD2-inhibitor, CAY10594 2  $\mu$ M. Non-treated cells (NT) were cultured for 14 days in control medium. (A) Relative PLD activity in MOVAS cells was measured as amount of PtdButOH produced and was normalized to total lipids. (B) And (C) SK1 and SK2 activity was measured by the amount of the radioactively labelled S1P produced, which was normalized to total protein content. Results are represented as mean  $\pm$  SEM relative D14 cells. In (A) 3 independent experiments were performed and statistical significance was estimated by student t test. \* Indicated  $p < 0.05$ , \*\* indicated  $p < 0.01$  and \*\*\* indicated  $p < 0.001$  with respect to D14.

## **Part 2: *Ex-vivo* rat aorta vascular calcification model**

### **1. Role of PLD during rat aorta calcification**

The extracellular matrix in blood vessels plays an important role in the progression of VC. So, we utilized a tissue culture model of aorta that preserves the components of extracellular matrix and protects the characteristics of SMCs. Full rat aortas were isolated and the adventitia layer was removed by gentle scraping while the intima is supposed to be removed by flushing in 37°C warmed PBS. Aortas were cultured either in control medium (1 mM Pi) or calcification stimulation medium containing 6 mM Pi for 6 days. When cultured in high Pi medium, aortas were able to calcify as demonstrated by a significant increase in Ca deposition and AP activity (Figure 27A and B). Moreover, aortic cells upregulated the expression of the osteo-chondrocytic markers *Runx2* and *Bglap*, evidencing that a trans-differentiation process is taking place (Figure 27C). Moreover, the gene expression of the calcification inhibitor *Spp1* decreased significantly (Figure 27C). It is expressed during initial stages of osteoblastic differentiation. Also, it is normally expressed in blood vessel by VSMCs and endothelial cells [358]. It is usually expressed in calcified tissues, but it inhibits calcium deposition by inhibiting crystals growth and stimulation of their resorption [359,360].

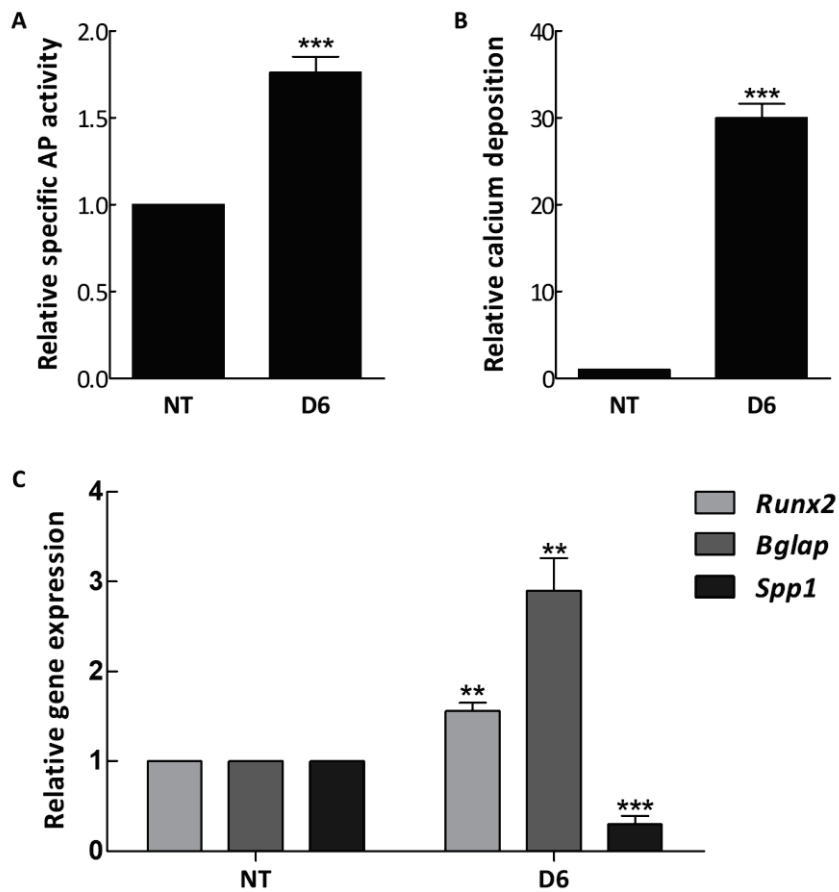


**Figure 27: Characterization of the rat aorta *ex-vivo* model of VC.** Rat aortas were incubated in 6 mM Pi for 6 days (D6) and were compared to non-treated aortas that were incubated in control medium (1 mM Pi) for 6 days also (NT). (A) The specific AP activity was calculated by a colorimetric assay using pNPP as substrate after smashing the tissues and was normalized to the total protein content. (B) Relative Ca deposition was quantified using o-cresolphthaline complexone in a colorimetric assay and was normalized to the tissue weight. (C) The gene expression of the osteochondrogenic markers, *Runx2* and *Bglap*, and of the calcification inhibitor, *Spp1*, was relatively quantified by qPCR according to Livak's method and using *Gapdh* as a reference gene. All results are represented as mean  $\pm$  SEM relative to non-treated aortas (NT). At least 3 independent experiments were performed for each assay and statistical significance was estimated by student t test. \* Indicated  $p < 0.05$ , \*\* indicated  $p < 0.01$  and \*\*\* indicated  $p < 0.001$  with respect to NT aortas.

Then, we checked PLD expression and activity during calcification in the aortic model. The gene expression of *Pld1* was augmented by 2.2 fold, however that of *Pld2* did not show any change (figure 28A). The increase in *Pld1* expression was accompanied with a significant increase in PLD activity by about 3.5-fold compared to NT aortas (Figure 28B). Thus, PLD may also have a role in calcification in this model, and PLD1 seems to be the involved isoform.

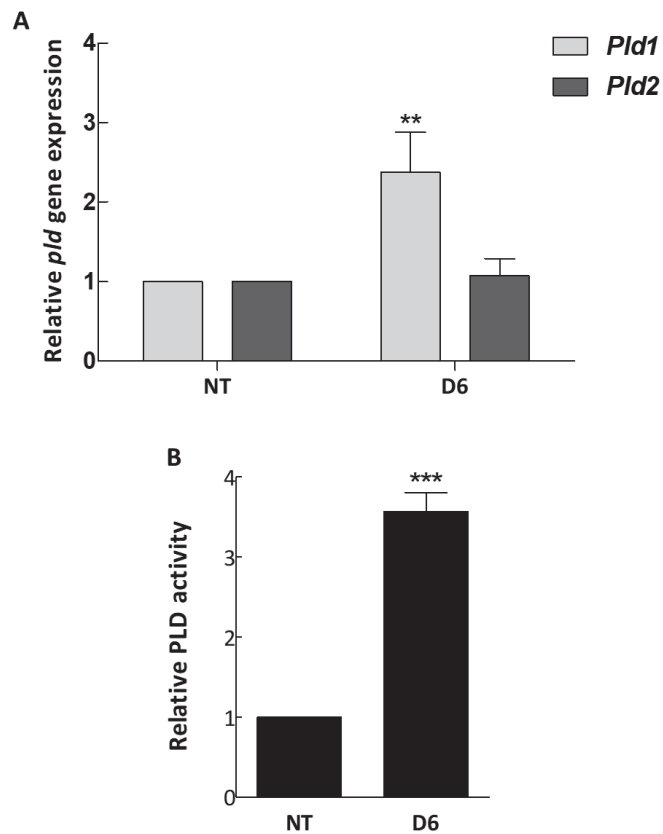


**Figure 28: PLD expression and activity during Pi-induced rat aorta calcification.** (A) The gene expression of *Pld1* and *Pld2* was relatively quantified using qPCR according to Livak's method and using *Gapdh* as a reference gene. (B) Relative PLD activity was estimated by measuring choline production and normalization to total protein amount. All results are represented as mean  $\pm$  SEM relative to non-treated aortas (NT). At least 3 independent experiments were performed for each assay and statistical significance was estimated by student t test. \* Indicated  $p < 0.05$ , \*\* indicated  $p < 0.01$  and \*\*\* indicated  $p < 0.001$  with respect to NT aortas.

The inhibition of PLD activity by using Halopemide, at 10  $\mu$ M, abolished the increase in AP activity and decreased significantly Ca deposition (Figure 29A and B). More importantly, PLD inhibition blocked the trans-differentiation as seen by a complete inhibition of *Runx2* and *Bglap* upregulation (Figure 29C and D). Moreover, Halopemide increased the expression the calcification inhibitor *Spp1* (Figure 29E). Thus, inhibiting PLD activity by a pan-PLD inhibitor could be efficient in blocking different aspects of VC and delaying its progression.

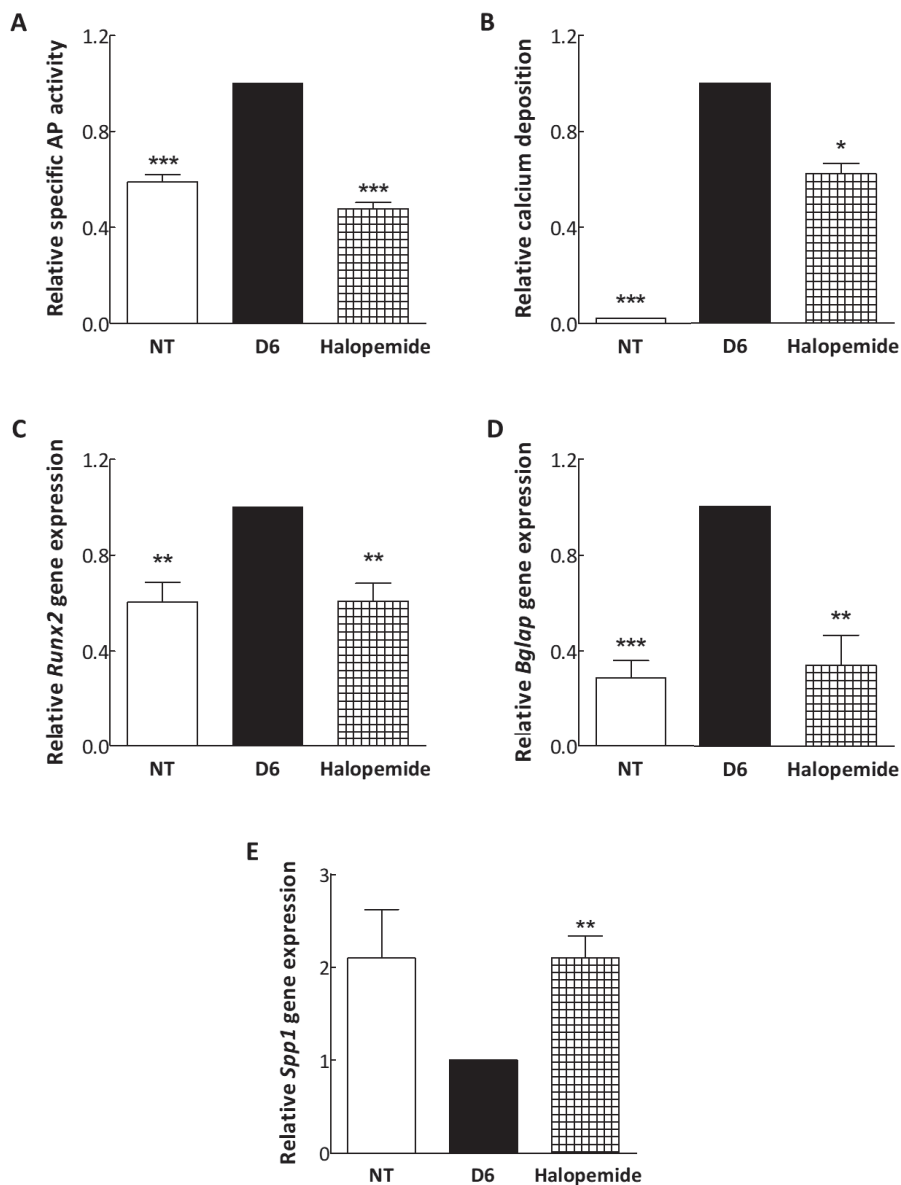


**Figure 29: The effects of PLD inhibition on Pi-induced rat aorta calcification.** Rat aortas were incubated in 6 mM Pi for 6 days (D6) with or without Halopemide 10  $\mu$ M. (A) Specific AP activity was calculated by a colorimetric assay using pNPP as substrate after smashing of the tissues and was normalized to the amount of total proteins. (B) Ca deposition was quantified using o-cresolphthaline complexone in a colorimetric assay and was normalized to the tissue weight. Gene expression of the osteo-chondrogenic markers, *Runx2* (C) and *Bglap* (D), and the calcification inhibitor, *Spp1* (E) was relatively quantified by qPCR using *Gapdh* as a reference gene. All results are represented as mean  $\pm$  SEM relative to D6 aortas. At least 3 independent experiments were performed for each assay and statistical significance was estimated by student t test. \* Indicated  $p < 0.05$ , \*\* indicated  $p < 0.01$  and \*\*\* indicated  $p < 0.001$  relative to D6.

Inhibitors had to be used at higher concentrations in tissue culture in order to be sure that they reach cells with efficient concentrations. However, VU0155069 and CAY10594 can lose their specificities when used at high concentrations, because we may pass their  $IC_{50}$  for both PLD isoforms. Therefore, in order to investigate the role of individual PLD isoforms, we used mouse models that are KO for either PLD1 or PLD2. From these mice, aortas were

isolated, cultured in high Pi medium (6 mM) and compared to WT aortas under the same culturing conditions. PLD1 KO aortas accumulated significantly less Ca than WT aortas. However, no difference was seen in PLD2 KO aortas compared to WT ones (Figure 30). The percentage of inhibition seen in Pld1 KO aortas is about 40% (figure 30), which is comparable to what was seen in case of Halopemide (figure 29B). Therefore, even in this model of VC, PLD activity seems to be important, and PLD1 is the major isoform involved in the process.

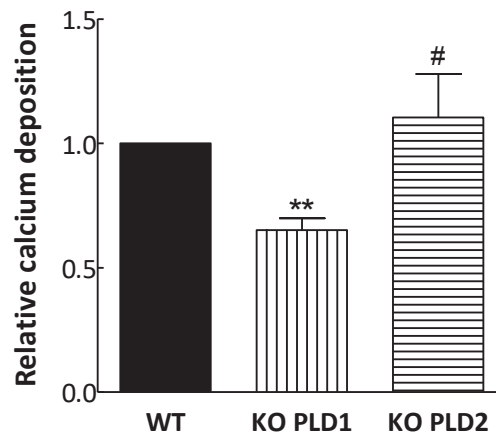


**Figure 30: The effect of PLD genetic ablation on calcium accumulation.** Aortas were isolated from WT, Pld1 KO and Pld2 KO mice. They were incubated in 6 mM Pi medium for 6 days. Ca deposition was quantified using o-cresolphthaline complexone in a colorimetric assay and was normalized to the amount of total protein. Results are represented relative to WT aortas as mean ± SEM. At least 3 independent experiments were performed for each measurement and statistical significance was estimated by student t test. \* Indicated p <0.05, \*\* indicated p<0.01 and \*\*\* indicated p<0.001 relative to WT aortas. # indicated p<0.05 relative to KO PLD1.

## 2. Role of S1P metabolic pathway during rat aorta calcification

As S1P signalling was important for calcification in MOVAS, we began to study its role in the aorta model. The preliminary data (n=2) displayed an increase in *Sphk2* expression with a rise in its activity (Figure 31A and B). *Sphk1* expression did not show a change, however its activity declined with calcification (Figure 31A and B). Therefore, they may have opposite roles in this model also similar to what was evidenced in MOVAS. With the absence of variation in *Spg11* expression (Figure 31C), the activities of SK1 and SK2 may give an indication about the S1P level present in different compartments.

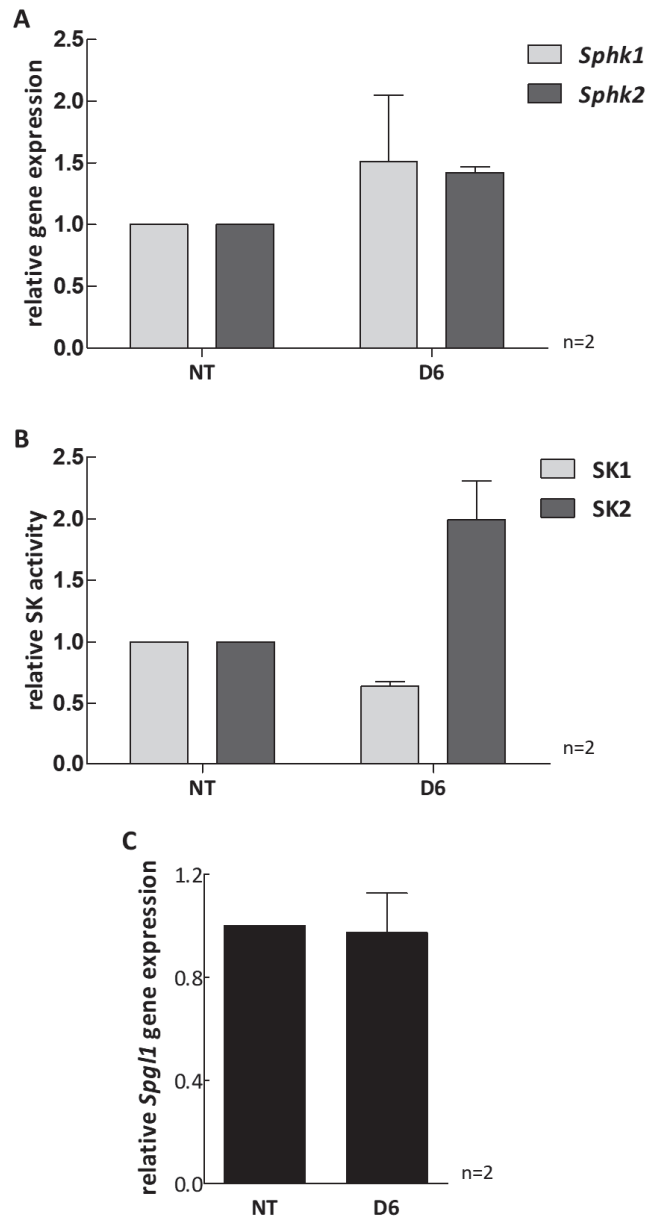


**Figure 31: Gene expressions and activities of enzymes of S1P metabolic pathway during rat aorta calcification.** Rat aortas were incubated in 6 mM Pi for 6 days (D6) and were compared to non-treated aortas that were incubated in control medium for 6 days also (NT). (A) The gene expression of *Sphk1* and *Sphk2*, was relatively quantified by qPCR according to Livak's method and using *Gapdh* as a reference gene. (B) SK1/2 activities were measured by the amount of the radioactively labelled S1P produced, which was normalized to total protein content. (C) The gene expression of *Spg11* was relatively quantified by qPCR using *Gapdh* as a reference gene. All results are represented relative to NT aortas as mean  $\pm$  SEM of 2 independent experiments.

### Part 3: Adenine-induced CKD rat model of vascular calcification

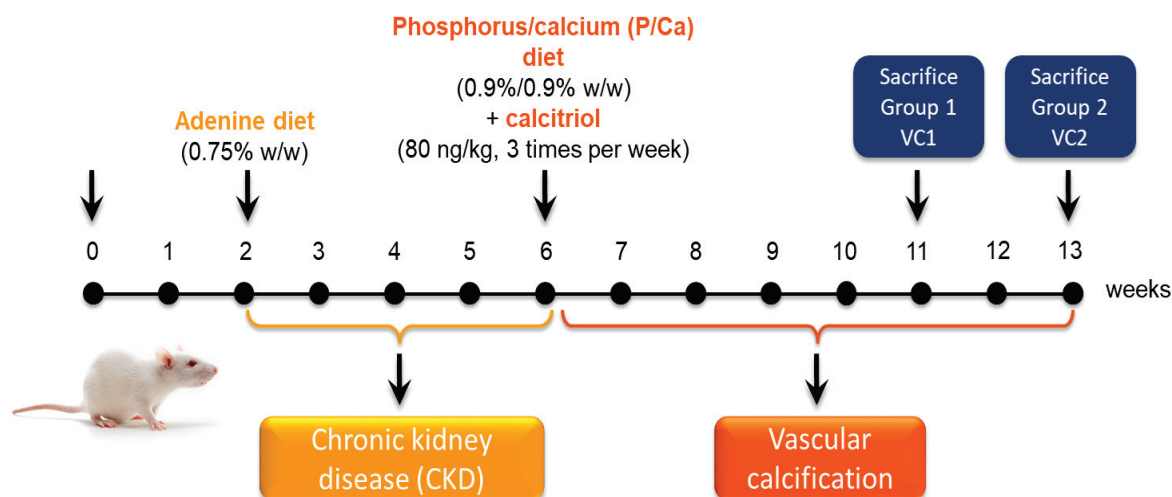


**Figure 32: Representation of the rat adenine-induced CKD model.** CKD was induced in rats by administration of high-adenine diet (0.75% by weight, w/w) for 4 weeks (CKD). After induction of CKD, rats were given high P/Ca diet (0.9%/0.9% by weight, w/w) with injections of calcitriol 3 times per week (80 ng/kg) for 5 or 7 weeks (VC1 and VC2, respectively). A group of rats were given only the high adenine diet (CKD) or only the high P/Ca diet with calcitriol (P/Ca + calcitriol). The control group was not given any special diet or calcitriol. All rats were kept during the whole experiment and were sacrificed at the same time.

CKD was induced in rats by giving them high-adenine diet (0.75% w/w) for 4 weeks (Figure 32). Adenine-induced CKD cannot be easily reversed by stopping the adenine diet, because 2,8-dihydroxyadenine produced after high-adenine ingestion persists in the kidney tubules causing severe kidney dysfunction. After 5 weeks of the stop of high-adenine diet, the kidneys of the rats were phenotypically abnormal. They were pale in colour, which may be due to insufficient supply of blood and decreased GFR (figure 33A). Moreover, they were slightly enlarged and weighted significantly more (by about 2 fold) than normal kidneys even after normalization to body weight (Table 2). Moreover, the plasma urea level of the rats that were previously given high-adenine diet was still significantly higher by 2.7-fold than the control groups at the end of the experiment (5 or 7 weeks after the termination of the high-adenine diet) (Figure 33B, Table 2). The weight of other organs, liver and heart, was similar to control rats when normalized to body weight (Figure 33B). The rats given high-adenine diet gained less weight than those with no CKD (figure 33B, Table 2). Interestingly, CKD rats had also increased plasma glucose and cholesterol (Table 2), thus signifying the occurrence of a metabolic syndrome. Unexpectedly, the plasma level of triglycerides decreased significantly in CKD rats compared to normal ones (Table 2).

VC was induced by further administration of high P/Ca diet (0.9%/ 0.9% w/w) and calcitriol injections 3 times per week (80 ng/kg) for 5 (VC1) or 7 weeks (VC2) (Figure 32). A group of rats had received only the high-adenine diet (CKD), another one received only the high P/Ca diet + calcitriol (P/Ca + calcitriol), and the control group was not given any special diet or injections (control).

Renal function	Control		CKD		Renal status	ANOVA-2	
	Standard diet	P/Ca diet +calcitriol	Standard diet	P/Ca diet +calcitriol		Treatment	Interaction
Treatment							
N	9	9	9	11			
<b>Biometry</b>							
BW. g	607 ± 15a	580 ± 28a	509 ± 16b	441 ± 18c	<b>0.002</b>	<b>0.021</b>	0.726
Body length. cm	27.6 ± 0.3a	27.4 ± 0.5a	25.9 ± 0.3b	25.2 ± 0.4b	<b>0.016</b>	0.117	0.321
Lee index	307 ± 2a	304 ± 1a	307 ± 1a	301 ± 2b	0.34	<b>0.008</b>	0.224
<b>Organ weight</b>							
Liver. g/100 g BW	2.89 ± 0.07	2.97 ± 0.1	2.85 ± 0.05	2.86 ± 0.07	0.109	0.916	0.334
Heart. g/100 g BW	0.26 ± 0.01	0.28 ± 0.02	0.28 ± 0.01	0.30 ± 0.02	0.608	0.320	0.086
Kidneys. g/100 g BW	0.53 ± 0.03a	0.54 ± 0.02a	0.93 ± 0.08b	1.04 ± 0.06b	<b>&lt;0.001</b>	0.066	0.614
<b>Plasma biochemistry</b>							
Urea. mmol/L	6.99 ± 0.40a	5.85 ± 0.20a	17.94 ± 2.14b	17.03 ± 3.64b	<b>&lt;0.001</b>	0.633	0.956
Glucose. mmol/L	6 ± 0.2a	6.4 ± 0.2a	7.3 ± 0.2b	7.1 ± 0.1b	<b>&lt;0.001</b>	0.173	0.389
Triglycerides. mmol/L	2.21 ± 0.22a	2.06 ± 0.20a	0.91 ± 0.10b	1.06 ± 0.11b	<b>&lt;0.001</b>	0.988	0.386
Total cholesterol. mmol/L	2.46 ± 0.18a	1.83 ± 0.13a	3.26 ± 0.27b	4.11 ± 0.49b	<b>&lt;0.001</b>	0.7343	0.023

**Table 2: General characteristics of control and CKD rats.** Measurements were made at the time or rats sacrifice. Data are presented as mean ± SEM. They were compared using 2-way ANOVA. Lee adiposity index was calculated as the cubic root of the BW divided by naso-anal length. The differences were considered statistically significant when the P<0.05 level. Abbreviation: BW, body weight. CKD, chronic kidney disease. Different letters (a, b and c) indicate a significant difference between group at the p<0.05 level.

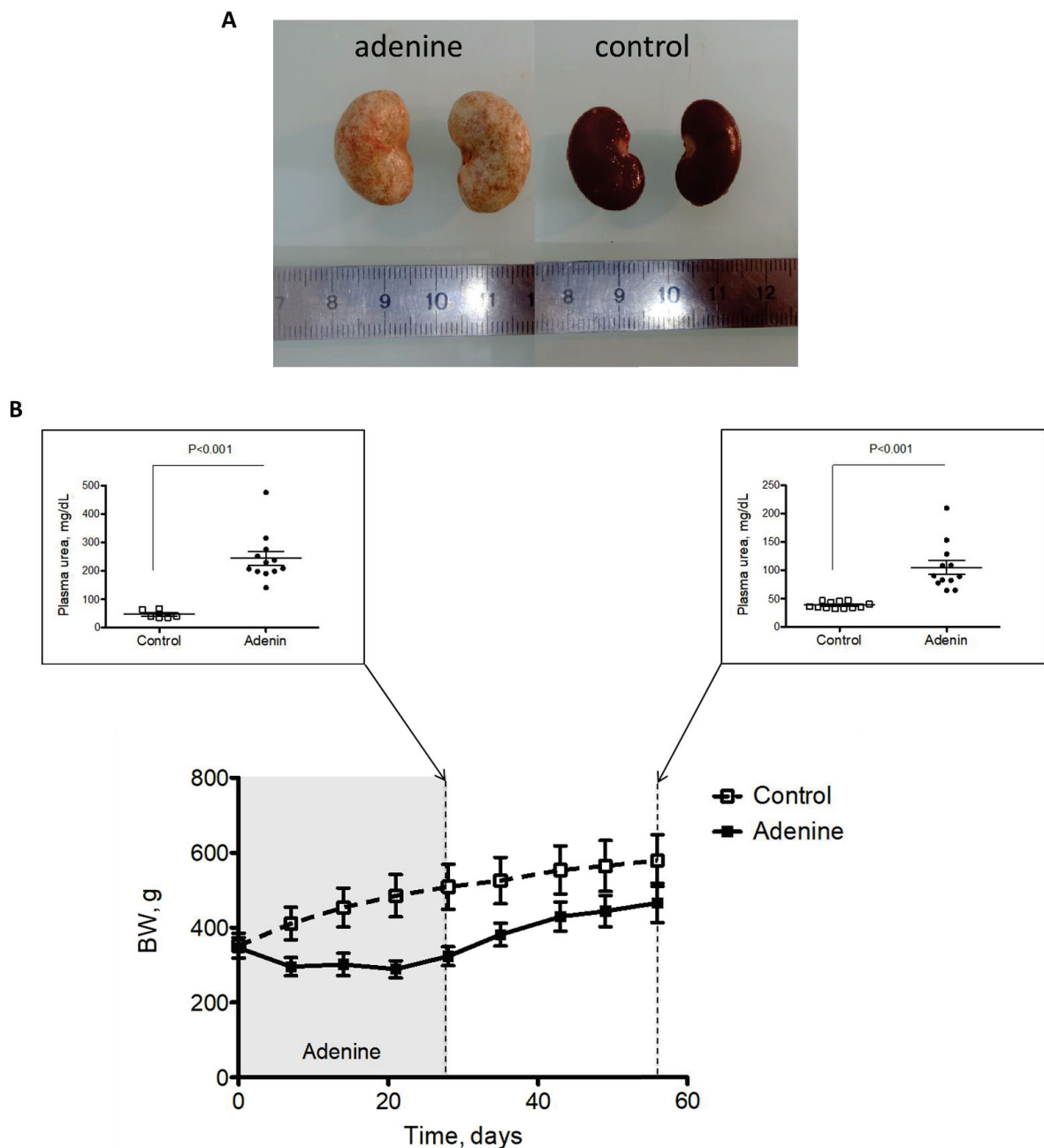


**Figure 33: The establishment of CKD in the rats given high-adenine diet.** Rats that were given in the first 4 week a high-adenine diet (0.75% by weight, w/w) are the (Adenine) group. Rats that were given normal diet during the first 4 weeks were considered the (Control) group. (A) A scaled image of the kidneys on control and adenine rats at the time of sacrifice. (B) The follow up of the change in body weight (BW) in control and adenine rat during 8 weeks of the experiment. Plasma urea measurements were done for these rat at week 4 and 8, and presented as mean  $\pm$  SEM. Data for plasma urea were compared using student t test. Differences were considered statistically significant when  $p < 0.05$ .

To assess VC in these rats, whole aortas were isolated from all the animals. Ca deposition was first assessed using o-cresolphthaline complexone in a colorimetric assay on small parts from different regions of the aorta pooled together to give a global idea about the state of the aorta. There was no difference between the control, CKD or P/Ca + calcitriol groups. Only a combination of both the high-adenine diet and the P/Ca diet + calcitriol induced an increase

in calcification. Both VC1 and VC2 aortas accumulated important amounts of Ca, which were significantly higher compared to all the 3 control groups (Figure 34A). In VC1, we noticed that there was a greater variations in the amount of calcium deposited compared to VC2 in which all aortas accumulated huge calcium amounts.

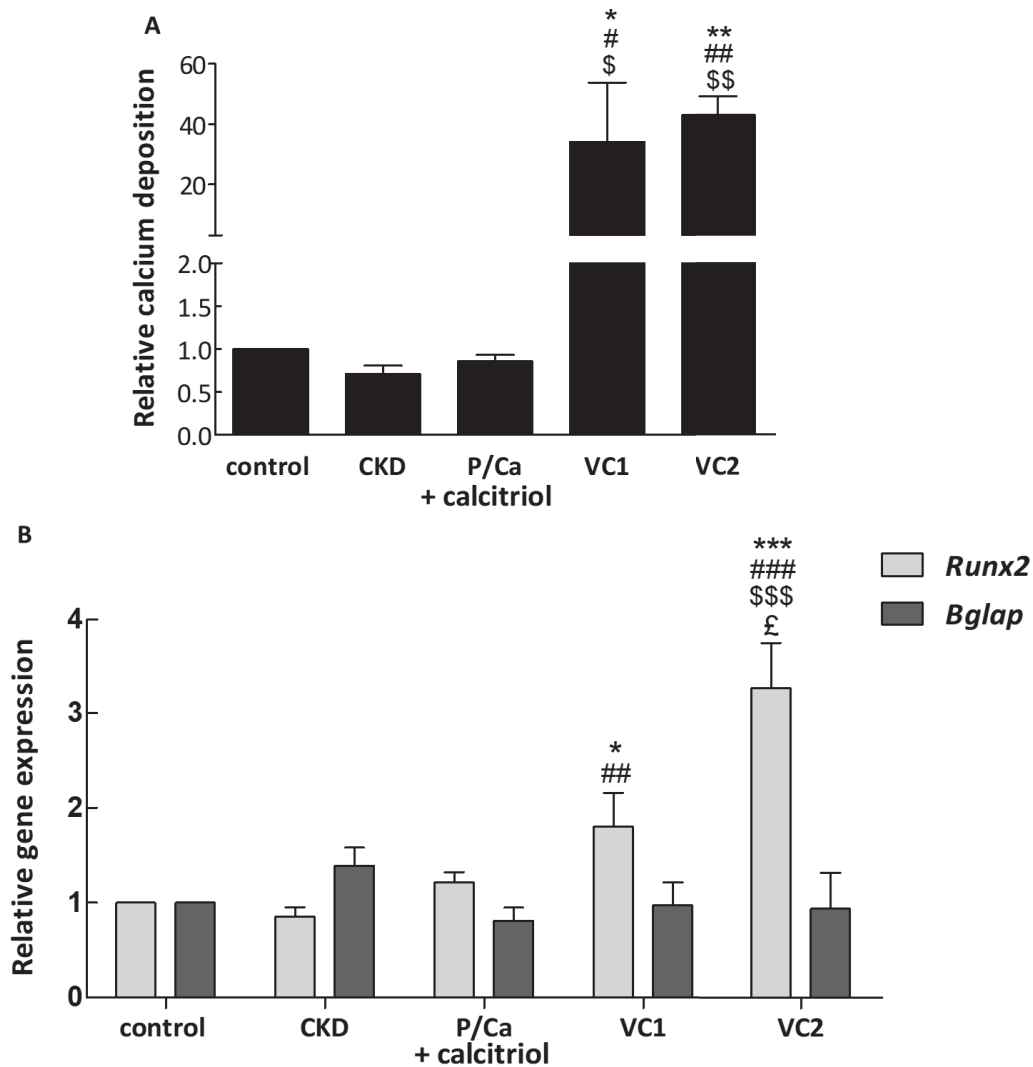


**Figure 34: VC in aortas of rat adenine-induced CKD model.** The details about rat treatments are present in the materials and methods part and in Figure 31. Whole aortas were isolated from all rats. (A) Relative Ca deposition was quantified using o-cresolphthaline complexone in a colorimetric assay using small parts from different regions on the aorta, and was normalized to tissue weight. (B) The rest of the aortic tissue was smashed in liquid nitrogen and RNA extraction was done and was followed by qPCR for quantification of the gene expression of *Runx2* and *Bglap*. All results are represented relative to control aortas as mean  $\pm$  SEM. At least 3 independent experiments were performed for each measurement. Statistical significance was assessed by student t test. \* Indicated  $p < 0.05$ , \*\* indicated  $p < 0.01$  and \*\*\* indicated  $p < 0.001$ , all relative to control. # indicated  $p < 0.05$ , ## indicated  $p < 0.01$  and ### indicated  $p < 0.001$ , all relative to CKD. \$ Indicated  $p < 0.05$ , \$\$ indicated  $p < 0.01$  and \$\$\$ indicated  $p < 0.001$ , all relative to P/Ca + calcitriol. £ Indicated  $p < 0.05$ , ££ indicated  $p < 0.01$  and £££ indicated  $p < 0.001$ , all relative to VC1.

The calcification seen in this model was not a passive process due to the increase in Pi and Ca, but it was accompanied by a significant increase in *Runx2* expression in both VC1 and VC2, which was more important in VC2 (more than the controls by 3-fold compared to the control) (Figure 34B). In our model, the *Bglap* expression was similar in all group (Figure 34B). The mechanism of calcification in our model may not include an upregulation of OCN, or the osteo-chondrocytic cells formed did not reach a stage in which they produce OCN.

Then we moved for checking PLD expression. Along with calcification, we detected an upregulation for both *Pld1* and *Pld2* expression in VC1 with a later decrease in VC2 back to the control levels (Figure 35A). The pattern of *Pld1* expression was similar to that seen in MOVAS cells, which suggests a possible common mechanism of calcification in these 2 models. Thus, PLD1 may be equally important for calcification *in-vivo*. The increase in *Pld2* expression may be due to the presence of different calcification stimulatory factors *in-vivo* which is not the case in the *in-vitro* and ex-vivo model. However, more experiments are indispensable to prove the implication of PLD in VC in case of CKD *in-vivo*.

Moreover, an increase in *Sphk2* expression was seen concomitant with the increase in *Pld1* and *Pld2* expression (Figure 35B). These enzymes may be working in coordination to promote VC in case of CKD *in-vivo*, similar to what was found in the MOVAS model. Therefore, giving PLD inhibitors *in-vivo* may possibly delay the progress of VC as seen in the other models.

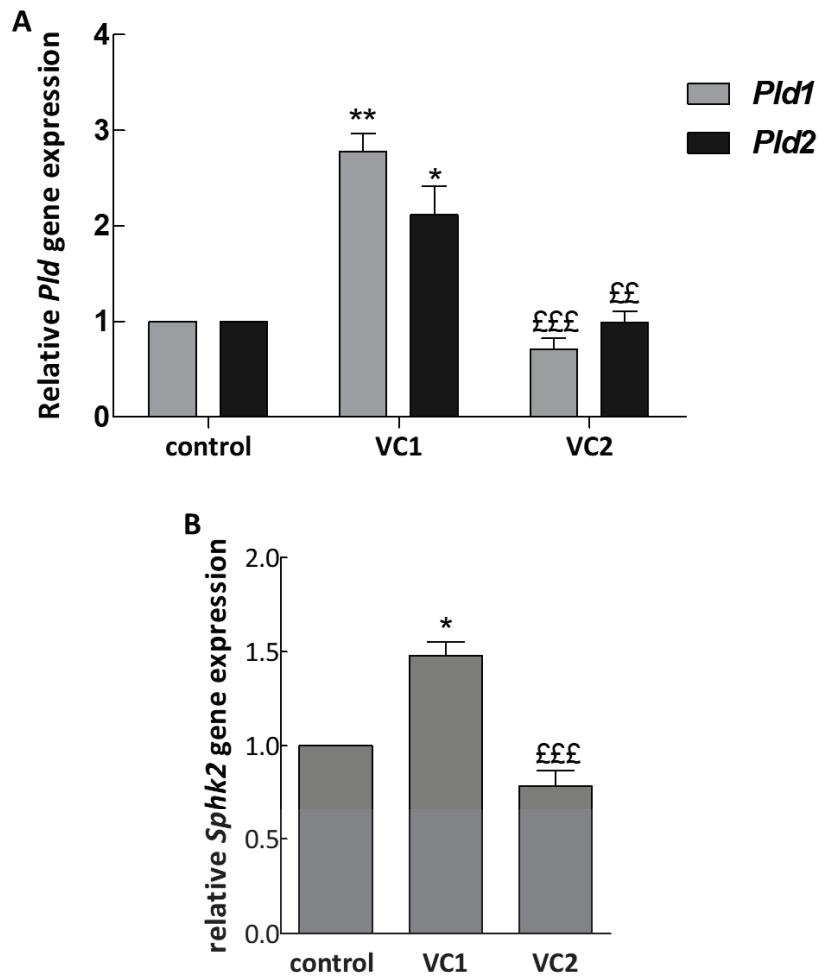


**Figure 35: *Pld* and *Sphk2* expression during VC in the aortas of adenine-induced CKD rats.** Rats were given high adenine diet (0.75% by weight, w/w) for 4 weeks to induce CKD, followed by 5 (VC1) or 7 (VC2) weeks of high P/Ca diet (0.9%/0.9% by weight, w/w) with injections of calcitriol 3 times per week (80 ng/kg) to induce VC. Different parts of the aorta of these rats were used for RNA extraction. The gene expression of *Pld1*, *Pld2* (A) and *Sphk2* (B) was relatively quantified using qPCR according to Livak's method and using *Gapdh* as a reference gene. Control rats are those that did not receive any special diets or injections. All results are represented as mean  $\pm$  SEM relative to control. At least 3 independent experiments were performed for each measurement. Statistical significance was assessed by student t test. \* Indicated  $p < 0.05$ , \*\* indicated  $p < 0.01$  and \*\*\* indicated  $p < 0.001$ , all relative to control. £ Indicated  $p < 0.05$ , ££ indicated  $p < 0.01$  and £££ indicated  $p < 0.001$ , all relative to VC1.

## **Discussion and conclusion**

VC can be found in many types of blood vessels where it may affect different layers. Its consequences on the organism's health do not only depend on its extent, but also on its location. In CKD, it mainly affects the medial layer of large arteries [63]. Proximal arteries near the heart depend largely on their elasticity to dampen the oscillations in blood flow produced due to the periodic heart function. Thus, they maintain an efficient diastolic blood flow, improve left ventricular relaxation and reduce heart work. When these arteries lose their elasticity, due to any reason including VC, they fail to perform the mentioned functions, leading to diastolic dysfunction, left ventricular hypertrophy and heart failure [50]. VC is a widespread disease, especially among CKD patients affecting about 80% of predialysis and dialysis CKD patients [354–356]. In these patients, cardiovascular diseases are the leading cause of death [67]. Until now, available treatments are limited to those that correct complications associated with CKD like inflammation, hyperphosphatemia and hyperparathyroidism [55,202]. However, these were not always effective in delaying VC. There is lack in specific targeted therapies for calcification that can directly affect its onset and progression, without interfering with bone homeostasis. In order to achieve this, a deep understanding of the molecular mechanisms that underlie VC is required. Therefore, we studied one of the possible mechanisms by which VC develops; the PLD signalling pathway.

PLD is involved in different cellular events and its function seems essential in the development of different diseases including cancer and neurodegenerative diseases (as detailed in chapter I, part 3.3). PLD is activated by different factors involved in osteogenesis including PTH, Wnt3a and PGE2 [298,303,307]. Also, it was activated by angiotensin, H<sub>2</sub>O<sub>2</sub> and oxidized LDL, all of which can enhance calcification directly [323,328,357]. Thus, PLD is a candidate culprit in the pathogenesis of VC.

In order to understand the role of PLD in this process, 3 different models were utilized. The first one is a murine SMC line (MOVAS) cultured with  $\beta$ -GP and AA. AA is used to induce the production of collagen I in order to create an appropriate support for calcium deposition, whereas  $\beta$ -GP is given to cells as an organic phosphate donor. Thus, our cellular model can be considered a model of high-Pi induced calcification. Among the complications seen in CKD, hyperphosphatemia have the strongest direct effects on SMCs (detailed in chapter I, Part2.2.2). As proved in earlier studies [185], MOVAS cells can calcify under these conditions, as detected by AP activity and Ca dosage (Figure 17A and B). This is a further

confirmation for the central role for SMCs in the calcification process, because they did not require any cooperation with other cells.

The second model is an organ culture of rat aorta incubated in high-Pi medium. This model provides an insight to the role of SMCs in their physiological environment; it do not neglect the role of ECM in VC. Also, it provides a natural support for HA crystals deposition. In VC, the role of ECM cannot be omitted, because it is now well known that elastin degradation products, which are produced during this process, can act both as signalling molecules and as high-affinity support to Ca [56,161]. Aortas were calcified massively upon culturing with high Pi, as demonstrated by increased AP activity and Ca deposition (figure 27A and B). Also, there was an evidence for a trans-differentiation process manifested by an increase in *Runx2* and *Bglap* expression (Figure 27C). These 2 genes are osteo-chondrocytic markers that are normally not expressed in vascular tissues. In MOVAS, we did not find any change in the expression of these 2 genes (data not shown). This may be due to one of two possibilities; the increase in *Runx2* expression can occur transiently between the studied time points and thus it can be missed, and *Bglap* expression may need more than 28 days to increase in these cells. Alternatively, the mechanism of calcification in MOVAS model may not include an upregulation of these genes. It is different from the aorta model by the absence of elastin, which is able to directly enhance SMCs trans-differentiation and upregulate *Bglap* and *Runx2* after being degraded [161]. Moreover, the gene expression of *Spp1* was decreased significantly with calcification in the aorta model (Figure 27C). OPN, whose gene is *Spp1*, is considered as inhibitor for vascular calcification.

In order to move closer toward the mechanisms of VC occurring in patients, an *in-vivo* rat model of CKD induced by high-adenine diet was used. When adenine is given in large quantities, it becomes oxidized by xanthine dehydrogenase into 2,8-hydroxyadenine which precipitates due to its low solubility in kidney tubules causing severe irreversible kidney dysfunction [358]. The irreversibility of the kidney disease was manifested in our model by an increase in plasma urea at 5 and 7 weeks after the stop of the high-adenine diet compared to control. Also, after sacrifice of the rats that were given high-adenine diet, their kidneys were phenotypically abnormal, enlarged and pale in colour. To induce VC, high P/Ca diet was given along with calcitriol injections. Toxic levels of calcitriol are already proved to induce VC [96]. Calcitriol facilitates the absorption of Pi and Ca at the intestine, thus achieving high serum levels. Normally, the organism is able to get rid of excess Pi and Ca, mainly by urinary excretion. However, when kidney function is compromised, Pi and Ca will persist in blood leading to hyperphosphatemia and hypercalcemia. Thus, a combination of

high-adenine diet, high P/Ca and active vitamin D (calcitriol) is needed to induce VC efficiently in the short time of the experiment. We detected calcification by quantification of deposited Ca in the aorta (Figure 34A). Small sections were taken from different regions of the aorta and were pooled together for Ca quantification. This was done to get a global idea about the state of aorta, because *in-vivo* calcification can occur in one part of the aorta only, with the other parts remaining healthy, so that the location of calcification cannot be predicted. The rest of the aortic tissues were used for RNA extraction, thus also providing a global idea about the state of aortic cells. We observed an upregulation in *Runx2*, which may indicate a process of trans-differentiation of aortic cells into calcifying cells (Figure 34B). There was no change in *Bglap* expression. This may be due to the short time of experiment which did not reach the point at which *Bglap* is upregulated. Alternatively, the mechanisms leading to calcification in this model may not involve OCN expression.

After confirming calcification in all the three models, we start analysing PLD expression during this process. The MOVAS model has two major advantages over other models apart from the relative easiness of cell lines manipulation; it allowed us to study of PLD status specifically in SMCs, and due to the possibility of assigning different time points for analysis, it provides the opportunity to follow PLD activity and expression during different steps of calcification. *Pld1* expression increased slightly at day 7 of culture in stimulation medium with a later decrease at day 28. At protein level, the upregulation was more prominent starting before the increase in AP activity and reaching maximum just before Ca deposition (Figure 18). The PLD activity followed approximately similar pattern, indicating that PLD may have role in initial steps of calcification. Although *Pld2* gene expression declined in late stages of calcification, its protein expression was not altered (Figure 18). Thus, PLD1 may be the involved isoform. In the rat aorta model, calcification at day 6 was also accompanied with an increase in *Pld1* expression and PLD total activity, with no change in *Pld2* expression (Figure 28). The possibility of contamination upon further incubation of the aorta limited the opportunity of having other time points that corresponds to the late stages seen in MOVAS. Thus, in the aorta the implication of PLD can be identified, however following its role during different stages of calcification is not feasible. Interestingly, in the CKD rat model, in VC1 we had an increase in *Pld1* expression which drop back to basal level in VC2 (Figure 35A). Thus, *Pld1* expression is seen increased only in early stages of calcification in CKD rats supporting the presence of a similar mechanism to that seen in MOVAS. The difference in the CKD model was in the expression of *Pld2* which followed the same pattern as *Pld1*. In MOVAS and the aorta model, Pi was the main causative agent for VC. However, in CKD rat

model, we have a complex disease, in which many factors can cause VC other than hyperphosphatemia. These factors need to be identified and may be responsible for the increase in *Pld2* expression. They may include: increased inflammation, hyperglycemia and/or hypercholesterolemia. Therefore, in the complex nature of kidney disease, both PLD1 and PLD2 may be involved in VC.

To assess whether the increase in PLD activity is just a consequence of VC or it has an active role, PLD activity was inhibited using small molecules of different specificities. Halopemide, a pan-PLD inhibitor, and VU0155069, a PLD1-specific inhibitor, were both able to abolish Ca accumulation and the increase in AP activity at day 21 of calcification (Figure 16). Thus, PLD1 has an important role in MOVAS calcification induced by AA and  $\beta$ -GP. Interestingly, PLD2 inhibition by CAY10594, did not affect calcification (Figure 19). PLD inhibition by Halopemide was also able to reduce calcification in the aorta model; it abolished AP activity and decreased significantly Ca accumulation. Also, it inhibited the upregulation of *Runx2* and *Bglap*, thus abolishing the trans-differentiation (Figure 29). Because Halopemide can inhibit the activity of both PLD1 and PLD2, we used another approach to test the implication of each isoform; aortas were isolated from *Pld1* KO, *Pld2* KO and WT mice, and were tested for their ability to calcify upon incubation in high Pi medium. *Pld2* KO aortas were able to accumulate Ca equally to WT ones. However, *Pld1* KO aortas accumulated significantly less Ca than both WT and *Pld2* KO aortas. The extent of inhibition in Ca deposition in case of *Pld1* KO aortas (about 40%) was comparable to that seen with Halopemide, indicating that the effect seen with Halopemide is more probably due to PLD1 inhibition (Figure 30).

After discovering a role for PLD, especially PLD1, in VC, we tried to find out how it was activated during this process. PKC is a major activator of PLD (as described in chapter I, Part 3.2.1). The role of PKC in osteogenesis is controversial even for a single isoform. For example in one study, the specific overexpression of PKC $\alpha$  in human and murine MSCs and in murine mesenchymal C3H10T1/2 cell line led to an increase in osteogenic differentiation [359]. In contrast, in another study, its overexpression in MC3T3-E1 decreased osteoblastic differentiation [360]. These studies may depend largely on the cellular model used or the culture conditions. In the MOVAS model, PKC inhibition by bisindolylmaleimide X, decreased both AP activity and Ca deposition significantly (Figure 21A and B). However, it did not affect PLD activity (Figure 21 C). Thus, PLD activation during MOVAS calcification is PKC-independent.

Another possible mechanism by which PLD may be activated is S1P signalling pathway. We were especially interested in this pathway because S1P is involved in chondrocytic and osteoblastic differentiation [279,361]. Thus, we started analysing the role of S1P metabolic and signalling pathway in VC.

S1P is formed via phosphorylation by SK1 or SK2, and can be degraded reversibly by SPPs or irreversibly by SPL. The gene expression of *Sphk1* and *Sphk2* did not change during the first 2 weeks of calcification but decreased later during the last 2 weeks in MOVAS cells (Figure 22A). However, the activities of SKs followed a different pattern; SK1 activity increased significantly only at day 7, whereas that of SK2 increased at day 14 till the end of the experiment time (Figure 22B). The increase in SK activities indicates an increase in S1P formation, which coupled with the decrease seen in *Spg11* expression, can signify an increase in S1P level (Figure 22C). Similarly, in aorta, our preliminary results showed an increase in SK2 expression and activity with no change in *Spg11* expression. Even in case of a decrease in SK1 activity, these results may indicate an increase in S1P level in compartments dominated by SK2 such as mitochondria or nucleus [250] (Figure 31). In the CKD rat model, *Sphk2* expression was also increased in VC1 (figure 35B), which indicates that it may have a role also *in-vivo*.

SKs activities were inhibited to assess their role in calcification. The inhibition of both isoforms by SKi or SK2-specific inhibition by K145 inhibited both AP activity and Ca deposition. However, SK1-specific inhibition did not induce any significant effect (Figure 24). Thus, it seems that S1P produced by SK2 is the one responsible for the effects on calcification. The effect of K145 on PLD activity was also tested without finding any significant influence (Figure 19C). However, PLD can also have a role in activating SKs [272]. Thus, we examined the effect of PLD inhibition on SK1 and SK2 activity. The preliminary results showed a decrease in SK2 activity upon usage PLD inhibitors especially PLD1-specific inhibition (Figure 26). PLD inhibition had an opposing effect on SK1 activity. These results need to be confirmed, but the possibility that PLD is promoting calcification by enhancing S1P production via SK2 must be considered.

S1P can act intracellularly or extracellularly, after being secreted, by binding to one of its receptors. Although SK2-derived S1P usually act intracellularly [250]. Our preliminary data showed a possible increase in the amount of S1P secreted by MOVAS cells, however S1P received by VSMCs *in-vivo* are not restricted to those produced by them (Figure 23A). Different cell types may act as a source for extracellular S1P such as endothelial cells.

Therefore, we started examining the expression of these S1P receptors on SMCs during calcification. *Slpr1* expression did not change, whereas there was a significant decrease in *Slpr2* starting from day 21 in MOVAS cells. *Slpr3* expression declined at day 7 and 14 with a later upregulation at day 28 (Figure 23B). Although a protein expression assessment is necessary, these data may indicate different roles for S1PRs during trans-differentiation and calcification stages in MOVAS cells. FTY720 is a sphingosine analogue, it can inhibit the activities of SKs [362,363]. After being phosphorylated by SK2 and released, it acts mainly as a functional antagonist to S1P<sub>1</sub>; after binding to this receptor, it induces S1P<sub>1</sub> polyubiquitination, internalization and degradation [364,365]. FTY720 inhibited significantly AP activity and Ca deposition but did not affect PLD activity (Figure 19). The inhibition seen with FTY720 is more important than that found with SK inhibitors indicating a possible role for S1P<sub>1</sub> in the calcification process. A deeper evaluation of the effects of different specific S1PRs antagonists is necessary. The activity of S1PR in our model may not be driven only by S1P produced by the cells but rather by S1P provided from FBS in culture medium.

In our work, we identified a central role for PLD in VC in the setting of high-Pi conditions *in-vitro* and *ex-vivo*. This role needs to be validated also *in-vivo*. PLD can be a novel target for preventing the onset or slowing down the progression of VC. *Pld1/2*-double KO mice are phenotypically normal without obvious health problems [213]. Interestingly, they were protected against diseases such as cancer, brain and cardiovascular disorders [213,292,293,366]. A possible explanation for these observations is the compensation for the chronic loss in PLD activity by other enzymes involved in PA metabolism. These may include an increase in activity of enzymes that produce PA, like DAG kinase, and/or a decrease in activity of enzymes that degrade it, like PA phosphatase, thus keeping a constant PA level [213]. However, in the setting of diseases, the production of excess PA and/or the non-lipase activity of PLD may not be compensated. In accordance to this, Halopemide was used for blocking dopamine receptor as treatment of neurological disorders in dosages enough to inhibit PLD activity, and it did not have adverse health effects in patients [366,367]. Thus, it will be interesting to identify PLD as a new effector in VC because it can be targeted safely in patients.

## Perspectives

We discovered an important role for PLD1 during calcification induced by high Pi in MOVAS cells and aorta *ex-vivo* model. However, the role of PLD in the adenine-induced CKD rat model still needs to be identified. An analysis of PLD activity during calcification is needed for this model. Also, because PLD inhibition seems to be safe *in-vivo* [368], PLD inhibitors, like Halopemide and FIPI, can be given to rats during the induction of calcification. The effects of these inhibitors on Ca accumulation, AP activity and *Runx2* expression in aorta can be checked to confirm the implication of PLD in vascular calcification *in-vivo*.

Until now we did not detect how PLD is activated during VC. After discovering that PLD was activated in a PKC- and SIP- independent pathways, we can now assess the possibility of regulation by small G proteins. This can be done by using different small G proteins inhibitors and addressing their effect on calcification and PLD activity.

After finding a positive role for PLD in VC, it is important to understand how PLD is acting during this process. The main mediator of PLD functions in cells is PA. Thus, it may also mediate its actions in VC. PA can act in different ways like affecting membrane curvature, being a precursor for the synthesis of other lipid effectors or activating a repertoire of proteins.

PA can directly bind and activate the mammalian target of rapamycin (mTOR) [369–371]. mTOR complex 1 (mTORC1), when active, phosphorylates and inhibits the activity of (UNC-51 like kinase-1/2) ULK1/2, a key kinase needed in autophagy initiation [372]. Therefore, PA aids in inhibiting autophagy through mTOR. Autophagy has a role in enhancing mineralisation in osteoblasts, since autophagy-deficient osteoblasts had decreased mineralization capacity, and mice with autophagy-deficient osteoblasts had low bone mass with reduced mineralization [373]. Autophagy induction by kaempferol as detected by increased LC3II/LC3I ratio and Beclin-1 expression, enhanced osteogenic differentiation in MC3T3-E1 cells [374]. Moreover, it was involved in the differentiation of MSCs into osteoblasts [375]. However, autophagy had a negative effect on pathological calcification by SMCs. In fact, an increase of autophagy, manifested by increase in of light-chain 3-II (LC3II) and autophagosome formation, was observed in SMCs cultured in high Pi conditions and also in renal artery walls of CKD patients. Induction of autophagy was dependent on the Pi-mediated ROS production. However, autophagy in this model was a protective mechanism counteracting VC, since its blockage increased Ca deposition and its further induction

inhibited Ca deposition. They attributed the reduction of calcification by autophagy to the inhibition of MVs release [376]. In another study, atorvastatin inhibited calcification in VSMCs by induction of autophagy, as seen by increased Beclin1, ATG5 and LC3II/LC3I ratio, via the inhibition of  $\beta$ -catenin expression [377]. In our models, PLD may be inducing VC by inhibiting autophagy. Thus, it will be interesting to evaluate autophagy during MOVAS calcification by assessing autophagy-related proteins expression like Beclin-1, calculating LC3II/LC3I ratio and evaluating autophagosome formation. Investigation of the effects of PLD inhibitors on these markers during calcification may give an idea about the link between PLD and autophagy during this process.

Another way by which PLD and PA can help in the initiation of VC is by helping in MV secretion. PLD activity was found increased just before the elevation in AP activity, and it reached its peak before Ca accumulation. After this point, PLD activity decreased again. The timing of maximal PLD activity seems overlapping with the stage at which MVs may be released to initiate Ca deposition. The biogenesis of MV is still controversial. The most accepted origin is the plasma membrane. Some reports pointed to that they originate by budding directly from plasma membrane [378,379], whereas others showed that they originate from microvilli. The microvilli hypothesis had more evidences and it was proved in osteoblast-like cells Saos-2 [380,381] and in chondrocytes [382,383][383]. In both cell types, the inhibition of actin polymerization by Cytochalasin D led to the release of MV [380,382]. PLD and its product, PA, have important roles in actin cytoskeletal reorganization proved in many cell types. PA and other lipids, like DAG and phosphoinositides, are important in recruitment and orientation of different of molecules involved in actin remodelling [384]. In fact, PLD and PA were shown to have important roles in actin stress fibre formation in response to LPA in porcine aortic endothelial cells [385], in Rat-2 fibroblasts [386] and in CFNPE90<sup>-</sup> cell line derived from a nasal polyp [264]. One of the studied mechanisms for the role of PLD-produced PA in actin reorganization pointed for the recruitment and activation of PIPKI (PI4P kinase I). Overexpression of wild-type PIPKI led to actin polymerization and formation of actin comets and foci (actin-based structures found in cells infected by an intracellular pathogen) in Cos7 cells, whereas mutant PIPKI that cannot bind PA was unable to induce these effects. PLD inhibition prevented membrane association of PIPKI and formation of comets and foci. Thus, PA, produced by PLD, was important in recruiting and activating PIPKI, which have important roles in actin cytoskeleton reorganisation [387]. Moreover, another study showed an important role for PLD-produced PA in the formation of PI4,5P<sub>2</sub> and in the organization of actin cytoskeleton needed for *Dictyostelium* motility,

phagocytosis and micropinocytosis [388]. Thus, PLD could be helping in calcification by regulation of actin reorganisation during the biogenesis of MV. In this regard, the effect of PLD inhibitors on MVs formation could be evaluated in our models.

Elastin degradation by MMPs is an important step for the progression of VC. As discussed before, the elastin degradation products have high affinity to Ca and thus can enhance its deposition [56]. Moreover, elastin-derived peptides can bind to elastin laminin receptor which is expressed on SMCs. *In-vitro*, these peptides induces trans-differentiation and calcification when applied to SMCs, manifested by an increase in osteo-chondrogenic marker expression (*Bglap* and *Runx2*) and an elevation in AP activity [162]. Moreover, the addition of  $\alpha$ -elastin, which is an elastin-derived peptide, enhanced Pi-induced calcification VSMCs as seen by an increase in AP activity and Von Kossa staining for deposited Ca [111]. During calcification, elastin is mainly degraded by MMP2 and MMP9 [56,389,390]. The inhibition of MMPs by doxycycline in CKD rats inhibited calcification induced by calcitriol and high-phosphorus diet [158]. Therefore, elastin degradation by metalloproteases is a key step for enhancing calcification, which may explain why we had an increased rate of calcification in the aorta model compared to MOVAS cells at day 7. PLD induced the production of MMP2 and MMP9 in different cancer cells [290,291,391,392]. Therefore, in SMCs PLD may also enhance calcification by inducing the expression of MMPs and prompting elastin degradation. Thus, the expression and activity of MMPs can be tested during calcification in absence and presence of PLD inhibitors. This mechanism could not be the only one, because PLD had an important effect in MOVAS model in which elastin is not present.

In MOVAS, the preliminary results showed that inhibition of PLD1 abolished SK2 activity, which we found to be important for calcification in this model. Thus, PLD action may be mediated by activating SK2. Therefore, this experiment needs to be repeated in order to check if this effect is statistically significant.

The S1P extracellular signalling pathway may be actively involved in calcification. The effects of FTY720 can give some clues about a positive role for S1P<sub>1</sub> in VC. However, FTY720 can also inhibit SKs, and it may act as agonist for S1P<sub>3-5</sub>. Therefore, the use of other antagonists that can specifically block S1PRs without other effects on S1P metabolic and signalling pathways is needed. The antagonists that can be used include: W146, a specific S1P<sub>1</sub> antagonist, JTE-013, a specific S1P<sub>2</sub> antagonist, VPC23019, an antagonist for S1P<sub>1/3</sub> and BML-241, a specific S1P<sub>3</sub> antagonist [364,393]. The usage of these antagonists and the

comparison of their effects in calcification can give clues about the specific roles of S1P receptors during this process.

# Sommaire

## Introduction

La minéralisation est normalement limitée à l'os, au cartilage et aux dents. Il s'agit d'un processus qui dure toute la vie: depuis la formation osseuse au cours de la vie prénatale et postnatale précoce se poursuivant pendant la croissance osseuse, le remodelage et la réparation jusqu'à la mort. Les os sont constitués d'une matrice extracellulaire étroitement organisée (MEC) avec des cellules résidentes (ostéocytes et cellules de la muqueuse osseuse), minéralisantes (ostéoblastes) et des cellules de résorption osseuse (ostéoclastes). Le cartilage a une MEC différente avec un seul type de cellules (chondrocytes).

La formation osseuse se produit principalement selon l'un des deux processus; La formation osseuse intramembraneuse qui prend place dans les os plats, comme les os craniofaciaux et la clavicule, ou la formation osseuse endochondrale qui a lieu dans le reste des os [3,7].

La formation osseuse intramembraneuse s'effectue directement dans le mésenchyme condensé sans une étape de transition du cartilage. Les cellules souches mésenchymateuses (CSM) d'origine ectoderme migrent vers le site de formation osseuse et se condensent autour d'un réseau de capillaires. Les cellules au centre de l'agrégat commencent à se différencier en préostéoblastes [3]. L'engagement primaire est déterminé par l'expression de RUNX2, le facteur de transcription principal de la lignée des ostéoblastes [8]. Son expression commence dans les CSM pendant la condensation, se poursuit dans les préostéoblastes et à travers les différentes étapes de la maturation et diminue dans les derniers stades de la maturation des ostéoblastes [10]. Il est absolument nécessaire pour l'engagement ostéoblastique et la formation osseuse, car les souris *Runx2* KO sont dépourvues d'os et meurent à la naissance par échec respiratoire [11,12]. RUNX2 peut activer l'expression de différents gènes importants dans la différenciation et la fonction ostéoblastique, tels que: *Spp1* (gène codant pour OPN), *coll1a1* (gène du collagène type 1), *Ibsp* (gène codant pour BSP1), *Bglap* (gène d'OCN), et ceci par lien direct de RUNX2 aux promoteurs de ces gènes [13]. Les préostéoblastes se différencient en OB matures en passant par 3 stades; les ostéoblastes du stade I exprimant la fibronectine, le collagène 1, le récepteur 1 du facteur de croissance transformant (TGF $\beta$ ) et l'OPN, et ils continuent à proliférer. Les ostéoblastes de stade II arrêtent de proliférer et commencent la maturation avec plus de sécrétion de collagène 1 et de la TNAP. Au stade III, les ostéoblastes sont matures et cuboïdes. Ils sécrètent l'OCN à la matrice extracellulaire et favorisent la formation et le dépôt de cristaux d'hydroxyapatite (HA) [8]. La TNAP est une enzyme cruciale pour la minéralisation puisqu'elle hydrolyse l'inhibiteur de minéralisation le plus puissant, le pyrophosphate (PPi), pour produire du

phosphate inorganique (Pi), un promoteur de minéralisation. Il est exprimé à la surface des ostéoblastes et des chondrocytes hypertrophiques, et il est enrichi sur les membranes sécrétées par ces cellules, appelées vésicules matricielles (VMs).

La minéralisation se produit principalement en deux étapes. Tout d'abord, les cristaux d' HA sont formés à l'intérieur des VMs (intravésiculaires) puis ils s'étendent à travers l'MEC (extravésiculaire) [24]. Les VM sont des petites structures spécialisées (20-200 nm), liées à la membrane [28] et produites par les ostéoblastes, les chondrocytes hypertrophiques et les odontoblastes. Ces vésicules sont le site initial où les cristaux de HA sont formés [24]. Les VM contiennent des annexines qui forment des canaux de calcium (Ca) dans leur membrane et importent du Ca de la matrice extracellulaire. En outre, elles contiennent des lipides et des protéines de liaison au Ca, tels que la phosphatidylsérine (PS) et la calbindine D9k, respectivement. Les VMs peuvent ainsi concentrer le Ca dans leur lumière. De plus, elles peuvent concentrer le Pi. Par exemple, la phosphoéthanolamine (PE) et la phosphatidylcholine (PC) peuvent produire du Pi lorsqu'elles sont hydrolysées par une phosphatase PE / PC (PHOSPHO1), une enzyme abondamment présente dans les VMs. En outre, le Pi est importé de l'espace extracellulaire au moyen de transporteurs Na / Pi de type III présents dans la membrane de ces VMs. Lorsqu'une certaine concentration de Pi et de Ca est atteinte à l'intérieur des VM, ils précipitent sous forme de cristaux de HA. À la deuxième étape de la minéralisation, ces cristaux commencent à sortir des VMs et s'étendent entre les fibrilles de collagène. Dans cette étape, le principal déterminant de la formation de cristaux HA est le rapport Pi / PPI. La TNAP est la principale enzyme d'hydrolyse de PPI. Elle hydrolyse PPI en Pi, élevant ainsi le rapport Pi / PPI et permettant la minéralisation [24,28,29]. Lorsque la matrice extracellulaire est correctement minéralisée, les ostéoblastes matures qui en sont entourés se différencient en ostéocytes et les cellules qui se trouvent sur la surface de l'os subissent une apoptose ou se différencient en cellules de la muqueuse osseuse. [8].

La formation osseuse endochondrale implique la formation osseuse à partir d'un modèle de cartilage construit précédemment. Les cellules mésenchymateuses s'agrègent et se condensent sous la forme d'une tige. La condensation n'est pas entraînée par une augmentation de la prolifération des cellules souches mésenchymateuses mais par une agrégation active des cellules. L'atteinte d'une certaine densité cellulaire est nécessaire pour la chondrogenèse ultérieure. A ce stade, les cellules du centre de l'agrégat commencent à se différencier en chondrocytes avec une diminution de l'expression du collagène I. Les cellules qui sont à la frontière forment le périchondre, conservent l'expression du collagène I et maintiennent la

capacité de se différencier en ostéoblastes ou en chondrocytes. Les chondrocytes commencent à sécréter le collagène de type II, IX et XI, la protéine gla de la matrice et l'aggrécane, en construisant une tige de cartilage hyalin [4,33]. Puis ce modèle cartilagineux croît en longueur (croissance interstitielle) en raison de la prolifération des chondrocytes pour atteindre la bonne taille, et en épaisseur (croissance appositive) en raison de l'ajout de matrice par les chondrocytes à la périphérie du modèle du cartilage [3]. En outre, plus de chondrocytes peuvent encore se différencier des cellules périchondriales. Les chondrocytes au milieu de la diaphyse quittent le cycle cellulaire et commencent leur maturation. Lorsque les chondrocytes deviennent hypertrophiques, ils commencent à sécréter le collagène de type X, la métalloprotéase Matrix 13 (MMP13) et la TNAP qui induit une minéralisation dans le cartilage hypertrophique. Ces événements s'accompagnent d'une invasion vasculaire du cartilage hypertrophique facilitée par la dégradation de la matrice extracellulaire par MMP13. Les vaisseaux sanguins apportent avec eux des ostéoprogénateurs qui se différencient en ostéoblastes et forment le centre d'ossification primaire, produisant l'os trabéculaire. Les chondrocytes hypertrophiques subissent alors une apoptose, alors que peu se différencient en ostéoblastes et contribuent à la formation de l'os trabéculaire [33,34]. Les cellules périchondriales de la couche interne du périchondre se différencient en ostéoblastes et sécrètent une matrice osseuse formant le collier osseux [4]. SRY (région déterminant le sexe Y) -box 9 (SOX9) est le facteur de transcription chondrogénique le plus crucial et le marqueur le plus précoce de la chondrogenèse. Il conduit l'engagement initial des CSM dans la lignée chondrocytaire, ce qui peut donner soit des chondrocytes ou des cellules périchondriales [4,8]. RUNX2 peut agir comme un facteur de transcription pro-hypertrophique. Son expression commence au cours des premiers stades de condensation du mésenchyme, se poursuit seulement dans les cellules périchondriales, et il est ré-exprimé dans les cellules préhypertrophiques et hypertrophiques précoces [33]. De même, dans ce type de formation osseuse, les ostéoblastes se forment d'abord sous forme de préostéoblastes, puis ils se différencient en trois étapes similaires à celles décrites pour l'ossification intramembranaire et deviennent matures.

La calcification est le terme utilisé pour l'accumulation ectopique de cristaux de calcium dans les tissus extrasquelettiques. Dans le système cardio-vasculaire, elle se produit principalement dans les vaisseaux sanguins et dans les valves cardiaques. Au niveau des artères, la calcification peut être trouvée dans différentes couches. La calcification dans la couche intimale est associée à l'athérosclérose. Elle peut affecter la stabilité des plaques en fonction de son profil. Alors que les microcalcifications, caractérisées par des taches ou des granules

de calcification, déstabilisent les plaques atherosclérotiques et provoquent leur rupture, les macrocalcifications, caractérisées par une calcification diffuse et continue, stabilisent les plaques et empêchent leur rupture [53]. La calcification dans la couche médiale est surtout observée chez les patients atteints de diabète et d'insuffisance rénale chronique (IRC) [51,56]. La maladie rénale est caractérisée par un dommage des reins qui affecte leur fonction. Le processus de développement de l'insuffisance rénale chronique évolue en 5 stades en fonction de la gravité des dommages, comme en témoigne la capacité des reins à filtrer le sang mesurée par le taux de filtration glomérulaire (GFR). La IRC de stade 5 est définie comme une maladie rénale terminale (IRT) dans laquelle la dialyse est le seul moyen de filtration du sang [58]. La calcification médiale affecte principalement l'élasticité des vaisseaux [61,62]. Normalement, l'aorte a une grande élasticité en raison de l'énorme quantité d'élastine présente, en particulier dans sa partie proximale. En systole, lorsque le ventricule gauche (VG) éjecte du sang dans l'aorte, le changement de pression (pression pulsée) provoque la distension de la paroi aortique afin de recevoir une partie du sang éjecté. Habituellement, seulement environ 50% du sang éjecté est envoyé directement à la circulation périphérique, tandis que le reste est stocké dans l'aorte et les grandes artères qui se développent en utilisant une partie de l'énergie cinétique fournie par le sang éjecté. Cette énergie est stockée dans la paroi aortique comme énergie potentielle. Puis en diastole, l'aorte recule en éjectant le sang dans la circulation périphérique et dans l'artère coronaire, qui dépend principalement de l'apport sanguin diastolique [59,60]. Ainsi, un flux sanguin continu et une perfusion suffisante du myocarde sont maintenus quelle que soit la fonction intermittente du coeur. Ceci permet d'améliorer la relaxation ventriculaire gauche et minimise le travail cardiaque. Cela se produit parfaitement lorsque l'élasticité de l'aorte est optimale. Cependant, ces fonctions sont affectées dans différentes conditions qui modifient l'élasticité [59,60], ce qui entraînera une réduction du flux artériel coronaire et un flux sanguin périphérique quasi-discontinu (dysfonction diastolique). Pour compenser ces défauts, le ventricule gauche doit augmenter la pression à laquelle il éjecte le sang entraînant une post-charge et une hypertrophie [64,65]. De plus, le cœur doit travailler plus rapidement afin de maximiser l'apport sanguin pour la circulation périphérique menant à l'insuffisance cardiaque, surtout qu'il est sous ischémie coronarienne partielle en raison d'un faible dysfonctionnement diastolique [65].

La calcification vasculaire (CV) était considérée comme une précipitation passive du Ca et du Pi lorsque leur concentration augmentait au-delà des niveaux physiologiques. Cependant, il a été démontré que plusieurs événements cellulaires et moléculaires étaient impliqués, des

événements similaires à ceux observés dans la formation osseuse normale [67]. Bien que les calcifications médiale et intinale impliquent différents facteurs et mécanismes, elles englobent une étape clé de trans-différenciation des CMLs en cellules osseuses ou cartilagineuses, ostéoblastes ou chondrocytes, hypothèse la plus acceptée pour l'origine des cellules vasculaires calcifiantes. Les cellules musculaires lisses vasculaires (CMLV) sont des cellules dérivées du mésenchyme qui sont, sous contrainte, capables de se différencier en ostéoblastes, en chondrocytes ou en adipocytes [51]. Les CMLV se trans-différencient sous différents types de stress en cellules de type ostéo-chondrocytaire. Elles perdent l'expression de protéines spécifiques de CMLs, telles que  $\alpha$ SMA et SM22 $\alpha$ , et leurs propriétés contractiles et gagnent un phénotype synthétique prolifératif. Sous l'effet de facteurs de transcription ostéo-chondrocytaires tels que RUNX2, Osterix, MSX2 et SOX9, elles peuvent produire et sécréter des protéines MEC spécifiques de l'os ou du cartilage, comme l'OPN, BSP11, l'ostéonectine, le collagène I et l'OCN, et des VMs compétentes pour la minéralisation [50,51,55,56]. Un large répertoire de facteurs différents peuvent induire de tels changements phénotypiques dans les CML en fonction du contexte et de la maladie sous-jacente. En IRC, l'hyperphosphatémie et probablement l'inflammation sont considérés comme les principaux facteurs directs, cependant dans l'athérosclérose, les principaux facteurs directs pourraient être l'inflammation et le stress oxydatif. Dans le diabète, l'hyperglycémie peut également induire directement la différenciation ostéo-chondrogénique des CMLs [50]. La calcification s'accompagne également d'un certain degré d'apoptose des CMLs et des macrophages, ce qui contribuerait à la calcification ectopique. De plus, la dégradation de l'élastine est une caractéristique de la calcification médiale, mais qui agit également comme un médiateur pour elle, et contribue beaucoup à la raideur observée en cas d'artériosclérose. La calcification peut aussi être favorisée par une diminution systémique ou locale de différents inhibiteurs de la minéralisation [55,56].

La vitamine D peut parfois être un contributeur à la calcification vasculaire. Le calcitriol, la vitamine D active et d'autres agonistes du récepteur VitD (VDR) peuvent se lier directement au VDR intracellulaire et l'activer [79,81]. La VitD active agit sur l'intestin pour augmenter l'absorption du Pi et du Ca. En outre, elle active l'ostéoclastogénèse dans l'os, mobilisant ainsi de grandes quantités de Pi et de Ca dans la circulation [82]. Avec la baisse de la fonction rénale, de nombreux patients développent un déficit en VitD [79,81,83,84]. La carence en VitD dans le contexte de l'IRC est la principale cause d'hyperthyroïdie secondaire observée dans cette maladie. La carence en VitD est le résultat d'une augmentation du FGF23 et d'une diminution de la réponse à la parathormone (PTH) au niveau du rein [79,82]. Le rôle de VitD dans la CV est controversé, avec des divergences entre différentes doses et différents modèles

utilisés. Il y a différentes raisons à ces écarts; Le VDR est exprimé dans les CMLVs, donc les agonistes des VDR (VDRA), avec leur effet systématique, peuvent agir directement sur ces cellules. En outre, la dose de ces agonistes VDRA et la présence d'autres facteurs de risque peuvent affecter énormément les résultats. De plus, différents analogues de VDR peuvent avoir des effets différents sur la CV [88]. *In vivo*, le calcitriol induit une CV et augmente la VOP dans différentes études utilisant des rats dans lesquels l'IRC est induite par une néphrectomie ou un régime riche en adénine [95–97]. Cependant, dans une étude chez des souris IRC, de faibles doses de calcitriol, qui étaient suffisantes pour diminuer la PTH, ont protégé contre le CV, mais des doses plus élevées augmentent le fardeau de la calcification aortique [98]. Une étude délicate des rôles systématiques et directs du calcitriol a été réalisée par Lomashvili et al. Dans cette étude, le calcitriol induit une calcification aortique chez les souris urémiques mais pas chez les souris normales. De plus, des segments *Vdr*<sup>-/-</sup> aortiques ont été transplantés chez des souris *Vdr*<sup>+/+</sup>, puis ils ont été rendus urémiques. Chez ces souris, le calcitriol induit le même niveau de calcification dans l'aorte native et dans l'allogreffe, indiquant que le rôle inducteur de la calcification du calcitriol est dû à un effet systématique plutôt que direct [102]. Ainsi, interpréter le rôle exact de la VitD dans la calcification est difficile en raison des effets systématiques et locaux qui peuvent différer dans leurs résultats et qui dépendent aussi largement de la dose utilisée.

Un autre contributeur majeur à la calcification est la concentration élevée en phosphate. Chez les patients atteints d'IRC, le taux de Pi dans le sérum reste dans la plage normale jusqu'au stade 4 et augmente encore chez les patients atteints de maladie rénale chronique de stade 5 (IRC) [394]. Pi est le constituant principal des HA, le minéral principal trouvé dans les os et les vaisseaux sanguins calcifiés. Une augmentation de Pi extracellulaire peut favoriser la formation d'hydroxyapatite, en particulier lorsque le niveau de PPI est rendu bas par une expression et une activité plus élevées de TNAP. Cependant, le rôle de Pi dans CV n'est pas limité à ceci; Pi peut jouer un rôle actif dans la différenciation ostéo-chondrogénique des CMLV.

Un taux élevé de calcium peut également induire une calcification vasculaire. La dialyse et la supplémentation du VDRA actif et d'un liant phosphate à base de calcium peuvent entraîner une hypercalcémie sporadique [56,129,130]. Un taux élevé de calcium extracellulaire dans les vaisseaux des patients atteints de néphropathie chronique est non seulement dû à un taux élevé de Ca sérique, mais aussi à une augmentation locale de Ca libéré par les CMLs apoptotiques. Ca peut induire l'apoptose en provoquant une augmentation supplémentaire de Ca local et la libération de corps apoptotiques, qui peuvent potentiellement agir comme foyers pour le dépôt de cristaux HA. Il a aussi été démontré d'augmenter la production de

vésicules matricielles compétentes de minéralisation contenant des cristaux HA préformés en particulier avec la perte d'inhibiteurs de calcification observée chez les patients atteints d'IRC [56,129,130,135]. Encore plus important, il a été démontré que des taux élevés de Ca augmentaient la calcification induite par le Pi de l'aorte de rat *ex-vivo* d'une manière dépendante de la concentration en augmentant l'expression de Pit1 [136,137].

L'apoptose est évidente dans les artères de patients dialysés [138]. *In vitro*, les CMLV cultivées ont montré un certain degré d'apoptose dans des conditions stimulatrices de la calcification, telles que Pi élevé, Ca élevé, glucose élevé ou en présence de nanocristaux de calcium-phosphate qui peuvent être phagocytés et dégradés dans le lysosome pour générer un niveau élevé de Ca intracellulaire [115,135,139–142]. L'apoptose des CMLV peut contribuer à la calcification de différentes manières; les cellules apoptotiques libèrent une quantité élevée de Ca, augmentant ainsi davantage la charge en Ca locale. De plus, la perte des CMLV entraîne une diminution de la production de MGP, un inhibiteur important de la calcification. De plus, les corps apoptotiques libérés par les cellules mourantes peuvent agir comme foyers pour la calcification, car des cristaux de HA ont été trouvés dans les vésicules libérées par les cellules mortes dans les artères dialysées. [138].

L'inflammation est également liée à la CV associée à l'athérosclérose, au diabète et à l'IRC. L'inflammation accrue dans IRC a différentes causes, y compris, une production accrue et une clairance réduite des cytokines inflammatoires, la rétention des toxines urémiques et l'acidose métabolique de développement. En outre, le processus de dialyse par lui-même peut induire une inflammation aiguë [144]. Les cytokines inflammatoires peuvent avoir des effets directs sur les CMLV et peuvent induire un changement phénotypique. Par exemple, le TNF $\alpha$  peut induire un changement phénotypique ostéo-chondrogénique des CMLV cultivées régulant à la hausse l'expression de *RUNX2*, *SP7*, *ALPL*, *MSX2* et *BSP1*. Il induit également l'activité PA et la calcification de la matrice par ces cellules [150,151].

La progression de l'IRC s'accompagne également d'une augmentation du stress oxydatif systémique qui se manifeste par une augmentation du taux sérique de malondialdéhyde (MDA) et de 15- (F) 2t-isoprostane, des marqueurs du stress oxydatif et une diminution du taux sérique des marqueurs de l'antioxydant, superoxyde dismutase (SOD) et glutathion peroxydase (GSH-PX)[153,154]. Les ROS peuvent agir directement sur les CMLV pour induire un changement phénotypique. Le peroxyde d'hydrogène, un ROS commun, induit une calcification dans les CML cultivées avec une augmentation de l'expression de Runx2, Alpl, Bglap et Coll1 $\alpha$ 1, et une diminution de l'expression de Sm22 $\alpha$  et  $\alpha$ Sma [157].

L'élastine est le constituant principal des grosses artères qui leur confèrent leurs propriétés élastiques. La dégradation de l'élastine est un processus majeur de la calcification médiale

contribuant directement à la raideur artérielle. Les CMLV subissant un changement phénotypique régularisent l'expression des MMPs, en particulier les MMP2 et MMP9, qui sont les principaux acteurs de la dégradation de l'élastine [56,158–160]. L'élastine dégradée a une forte affinité pour le Ca facilitant le dépôt de cristaux de HA le long de la lamelle élastique. De plus, les peptides dérivés de l'élastine peuvent se lier aux récepteurs de l'élastine-laminine sur les CMLV et altérer activement l'expression de différents gènes aboutissant à un phénotype ostéo-chondrogénique [161,162].

La calcification ectopique n'est pas induite par une simple augmentation du Ca et du Pi sériques, car les inhibiteurs de la calcification sont présents en quantité suffisante pour inhiber la formation de cristaux de HA. PPI est l'un des inhibiteurs les plus puissants. Lorsque les CML commencent à acquérir un phénotype semblable à celui des ostéochondrocytes, ils expriment progressivement la TNAP qui peut hydrolyser PPI en Pi, ce qui augmente le rapport Pi / PPI et crée un environnement favorable à la calcification. De plus, pendant la HD, le PPI est éliminé, ce qui entraîne une diminution de son niveau de circulation [56]. Fetuin A est un autre inhibiteur systématique important. C'est une glycoprotéine sécrétée par le foie. Elle agit en liant le Ca libre et en augmentant les cristaux de HA pour inhiber leur croissance ultérieure. Fetuin A est une protéine de phase aiguë négative, donc chez les patients dialysés, elle se trouve en quantité réduite peut-être en raison de l'inflammation accrue [56]. La MGP est un inhibiteur important de la calcification produit par différentes cellules, y compris les CMLV. La phosphorylation et la  $\gamma$ -carboxylation sont obligatoires pour la sécrétion et la fonction de MGP. La  $\gamma$ -carboxylation nécessite de la vitamine K comme cofacteur. Elle inhibe également la calcification en se liant directement aux cristaux de Ca et de calcium-phosphate [56,168]. La warfarine, qui est administrée aux patients atteints d'IRC, inhibe l'action de la vitamine K, inhibant ainsi la carboxylation et la fonction de la MGP [56].

La CV peut être détectée par divers types de systèmes d'imagerie, tels que: la radiographie conventionnelle, l'échographie, la tomодensitométrie, l'échographie intravasculaire et la tomographie par cohérence optique.

Les traitements actuels de CV sont en quelque sorte limités à ceux qui corrigent les facteurs de risque comme le contrôle de l'hyperphosphatémie, de l'hyperparathyroïdie et de l'inflammation. De nombreuses études sont maintenant à la recherche de nouvelles cibles de CV. Etant donné les similitudes entre la CV et la formation osseuse, il est plus compliqué de la cibler systématiquement sans poser d'effets préjudiciables sur les os et les dents.

La CV est l'un des principaux contributeurs à la mortalité cardiovasculaire, notamment en raison de ses effets sur la dynamique cardiovasculaire, et jusqu'à présent, il n'y a pas de traitement spécifique, efficace et approuvé. Comprendre les mécanismes moléculaires

derrière cette maladie complexe est indispensable pour la conception de nouveaux traitements ou de stratégies préventives, en particulier que son apparition est prévue chez les patients atteints de MRC ou de diabète.

La superfamille de PLD est constituée de 6 membres: PLD1 à 6, parmi lesquels seuls PLD1 et PLD2 sont responsables de l'activité phosphodiesterase principalement responsable de l'hydrolyse de la phosphatidylcholine en acide phosphatidique et en choline. L'activité de la lipase catalytique est commandée par un site catalytique dimérisé constitué de deux motifs HKD hautement conservés qui contiennent une séquence spécifique d'acides aminés: His-x-Lys-x-x-x-Asp. Ainsi, chacun de PLD1 et PLD2 ont 2 motifs HKD. L'acide phosphatidique est impliquée dans différentes fonctions cellulaires. L'AP peut lier des protéines pour les recruter dans des membranes cellulaires où elles sont nécessaires pour transduire des signaux. En outre, cette interaction est capable d'activer différentes protéines. Ainsi, l'acide phosphatidique agit comme messager secondaire dans différentes voies de signalisation cellulaire. En outre, l'acide phosphatidique peut être hydrolysé en d'autres messagers lipidiques comme le DAG et le LPA, qui peuvent également réguler différentes voies de signalisation. De plus, le fait d'avoir une petite tête chargée négativement aide l'acide phosphatidique à adopter une forme de cône favorisant la courbure de la membrane négative lorsque son niveau augmente, ce qui facilite la formation et la fusion des vésicules [213]. D'autre part, les fonctions de PLD1 et 2 ne sont pas limitées à son activité lipase, mais elles ont également des activités indépendantes de la lipase. La PLD peut être impliquée dans différentes voies de signalisation par des interactions directes protéine-protéine. En outre, PLD2, mais pas PLD1, a une activité supplémentaire de facteur d'échange de nucléotides guanine (GEF), de sorte qu'il peut activer les protéines G [214]. L'activité de la PLD est contrôlée par différentes voies de signalisation, y compris les PKC, les petites protéines G, les RCPG et les récepteurs de la tyrosine kinase. Ainsi, il peut être impliqué dans les processus cellulaires contrôlés par toutes ces molécules. En outre, il peut être activé par S1P lorsqu'il agit de manière extracellulaire en se liant à l'un de ses récepteurs S1P1-5, qui sont des RCPG. De plus, il a été montré que la PLD active la sphingosine kinase 1 (SK1), l'une des enzymes responsables de la production de S1P [272].

L'expression et l'activité de la PLD ont été retrouvées régulées positivement dans divers cancers humains [214,285]. En raison de sa large intégration dans différentes voies de signalisation cellulaire, PLD a été impliquée dans diverses étapes de la progression du cancer, y compris la survie des cellules, la prolifération, l'invasion, l'angiogenèse et la métastase. De plus, les deux PLD1 et PLD2 ont été impliquées dans la pathogenèse de la maladie d'Alzheimer, et ils ont tous deux des rôles dans les maladies infectieuses.

L'activité de la PLD est présente dans les ostéoblastes et les chondrocytes, dans lesquels elle est induite par différents facteurs impliqués dans l'homéostasie osseuse. Parmi ceux-ci, la PTH a activé la PLD dans la lignée cellulaire de type ostéoblaste UMR-106 dans un mécanisme impliquant  $G\alpha_{12}$ ,  $G\alpha_{13}$  et RhoA et les GTPases Arf. [298–300]. La PTH était capable d'améliorer la différenciation ostéoblastique de la cellule ressemblant aux ostéoblastes, MC3T3-E1, par un mécanisme impliquant la voie Wnt /  $\beta$ -caténine [301]. Il peut également induire la différenciation ostéoblastique dans les cellules précurseurs humaines dérivées de la peau, et il est utilisé pour traiter l'ostéoporose en raison de sa fonction anabolique sur les os *in vivo* [302]. Fait important, Wnt3a a amélioré l'expression et l'activité de PLD1 dans un mécanisme impliquant la  $\beta$ -caténine. A son tour, acide phosphatidique produit par PLD1 peut améliorer l'activité transcriptionnelle de  $\beta$ -caténine [303]. Ainsi, PLD1 peut améliorer à la fois l'expression et l'activité de la  $\beta$ -caténine, et peut être activé par la signalisation Wnt /  $\beta$ -caténine. Wnt3a a provoqué une calcification et une trans-différenciation ostéo-chondrogénique dans les CMLV, avec une augmentation de l'expression de RUNX2 et de l'OCN. De plus, l'inhibition de la signalisation Wnt /  $\beta$ -caténine a réduit l'expression de l'OCN induite par le Pi. [121]. Collectivement, ces études peuvent proposer un rôle de la PLD dans la différenciation ostéoblastique à partir de cellules précurseurs ou de CMLV.

D'autre part, l'acide phosphatidique produite par PLD peut être traitée pour donner naissance à la prostaglandine E2 (PGE2) dans la lignée cellulaire ostéoblastique UMR-106, les cellules MC3T3-E1 et les ostéoblastes primaires isolés de la calvaria de rat en réponse aux esters de phorbol ou à l'endothéline 1 [305,306]. Dans l'autre sens, PGE2 était également capable d'activer PLD dans les cellules MC3T3-E1 [307]. La PGE2 a une action anabolique sur la formation osseuse chez des rats jeunes, en croissance et vieillissants [308]. En résumé, ces données indiquent que la PGE2 a un effet sur la différenciation ostéoblastique, et le lien bidirectionnel entre PGE2 et PLD, peut également fournir une indication supplémentaire pour l'implication de la PLD dans l'ostéogénèse.

En fait, PLD était activement impliquée dans certains modèles de différenciation ostéoblastique. La N-formyl-méthionyl-leucyl-phénylalanine (fMLP) a induit une différenciation ostéoblastique chez les CSM humains en agissant par l'intermédiaire de son récepteur, le récepteur du peptide N-formyle (FRP). Ces effets étaient accompagnés d'une augmentation de l'activité PLD. La régulation négative de la PLD1 par le siRNA a inhibé l'augmentation induite par le fMLP de l'activité PA et l'inhibition de la PLD par le FIPI, qui peut inhiber les deux isoformes, abolir l'accumulation de calcium induite par le fMLP. Ainsi, la PLD est un facteur important dans la différenciation ostéoblastique en réponse à fMLP

[316]. De plus, la PLD était importante dans la différenciation ostéoblastique en réponse à la rugosité de surface du titane. En réponse à l'augmentation de la rugosité des surfaces de titane sablées avec de l'oxyde d'aluminium, les cellules semblables aux ostéoblastes MG63 présentaient une différenciation ostéogénique accrue manifestée par une production accrue d'OCN et une activité PA. Ces événements étaient accompagnés d'une augmentation de l'expression et de l'activité de la PLD, et ils étaient renforcés par l'activation de la PLD et inhibés par l'inhibition de la PLD [317]. Ces résultats ont été confirmés dans une étude similaire dans laquelle la PLD était activée dans les cellules MG63 par une augmentation de la rugosité de surface et de l'énergie, ainsi qu'une différenciation ostéoblastique accrue manifestée par une activité PA améliorée et une expression d'OCN et d'ostéoprotégérine. L'utilisation d'éthanol pour bloquer la production de acide phosphatidique par PLD a inhibé ces événements. En outre, l'utilisation de siRNA contre PLD1 et PLD2 inhibe la différenciation ostéoblastique en réponse à la rugosité de surface et de l'énergie [318]. Ainsi, la PLD pourrait être importante dans la différenciation ostéoblastique en réponse à différents stimulants.

L'activité et l'expression de la PLD ont également été détectées dans les chondrocytes, les cellules de la zone de repos ayant une activité PLD plus élevée que les chondrocytes de la zone de croissance. Dans les cellules de la zone de repos, PLD peut être activé par 24,25diOHD3 qui joue un rôle dans la prolifération et la différenciation des chondrocytes [319–321]. Ainsi, PLD peut également avoir un rôle dans la différenciation chondrocytaire.

Il est important de noter que la PLD était également activée par des facteurs pouvant être impliqués directement dans CV. La PLD était activée par le peroxyde d'hydrogène dans les CMLV. La migration induite par le stress oxydatif a été inhibée par le 1-butanol, mais pas par le 3-butanol, ce qui indique que la PLD est un effecteur important de la signalisation du stress oxydatif dans les CMLV. [322]. En outre, le peroxyde d'hydrogène peut activer la PLD dans d'autres types de cellules, comme les cellules phéochromocytome PC12 [323]. Le stress oxydatif peut causer directement CV, et le peroxyde d'hydrogène peut directement induire une trans-différenciation ostéogénique des CML [157]. De plus, l'angiotensine II (AngII), un peptide qui peut augmenter la tension artérielle, peut également induire une trans-différenciation ostéogénique lorsqu'elle est appliquée aux CMLV dans une voie impliquant la liaison au récepteur AngII de type 1 (AT1) et l'inhibition de la production de MGP par les CMLV [324,325]. AngII était également capable d'activer la PLD dans les CMLV dans une voie impliquant AT1,  $G\alpha_{12}$ ,  $G\beta\gamma$  et RhoA [328–330]. De plus, les LDL oxydées, connues pour leur action athérogène, ont récemment montré qu'elles induisaient une différenciation

ostéogénique et une calcification par action directe sur les CMLV [183,332,333]. Les LDL oxydées ont également montré qu'ils activaient la PLD dans les CMLV et les macrophages [334,335]. Par conséquent, étant donné le lien étroit entre la PLD et ces inducteurs de calcification, PLD pourrait être activement impliquée dans CV.

## Matériel et méthodes

### 1. Culture cellulaire

La lignée murine de CMLV MOVAS (ATCC® CRL-2797™) a été cultivée dans du milieu DMEM (*Dulbecco's Modified Eagle Medium*) à haute teneur en glucose (4,5 g / L). Ce milieu contient de la glutamine à 2 mM, de la pénicilline à 10 U / mL, de la streptomycine à 10 mg / mL et 10 % de serum de veau fœtal SVF (v / v), (proviennent tous de Sigma Aldrich, Lyon, FR). Il s'agit du milieu contrôle. Pour stimuler la calcification, 50 µg / mL d'acide ascorbique et 10 mM de β-glycérophosphate ont été ajoutés au milieu contrôle : c'est le milieu de stimulation. Le temps de culture est choisi en fonction du but. Pour étudier la calcification et l'expression des différents gènes et protéines et ainsi que leurs activités au cours du processus de calcification, les cellules ont été cultivées pendant 28 jours dans le milieu de stimulation et ont été récupérées tous les 7 jours pour l'analyse. Dans ces expériences, des cellules non traitées (NT) ont été cultivées dans un milieu témoin pendant 7 jours. Pour étudier les effets de différents traitements sur la calcification, les cellules ont été cultivées pendant 21 jours dans le milieu de stimulation, et l'analyse n'a été effectuée qu'à la fin de cette période. Des cellules NT dans ces expériences ont été cultivées pendant 21 jours dans un milieu témoin. Pour étudier les effets des différents traitements sur les activités PLD ou SK, les cellules ont été cultivées pendant 14 jours dans un milieu de stimulation. Les cellules NT ont été cultivées pendant 14 jours dans un milieu témoin. Différents traitements ont été réalisés, tout d'abord la PLD a été inhibée. Différents inhibiteurs ont été utilisés : l'Halopémide, un inhibiteur de PLD1 et PLD2 (utilisé à 1 et 2 µM), VU0155069, un inhibiteur spécifique de PLD1 (utilisé à 600 et 800 nM), CAY10594, un inhibiteur spécifique de PLD2 (utilisé à 200 et 300 nM), (ces inhibiteurs proviennent de Cayman chemical (Montluçon, FR)). Dans un deuxième temps, la voie de la PKC a été inhibée en utilisant le chlorhydrate de bisindolylmaléimide X (utilisé à 1 et 5 µM), obtenu auprès d'Enzo Life (Villeurbanne, FR). Dans un troisième, la voie métabolique de la S1P a été bloquée par Ski un pan-inhibiteur des SK (utilisé à 5 µM), PF-543 un inhibiteur de SK1 (utilisé à 100 nM), K145 un inhibiteur de SK2 (utilisé à 5 µM) et FTY720 l'inhibiteur général du métabolisme de la S1P (utilisé à 2,5 µM). Ces inhibiteurs et antagonistes ont été achetés chez Merck Millipore (Fontenay Sous Bois, FR). Les cellules

ont été cultivées à 37 °C dans une atmosphère humidifiée constituée de 95% d'air et de 5% de CO<sub>2</sub>.

## 2. Culture d'explant aortique

Des aortes entières ont été isolées à partir de rats males de la souche Sprague Dawley (Janvier-Labs, Le Genest-Saint-Isle, FR). Elles ont été nettoyées dans du tampon phosphate salin (PBS). La couche d'adventice a été enlevée par un léger grattage et l'intima a été éliminée par rinçage avec du PBS à 37 ° C, ne laissant que la couche médiane pour la culture *ex-vivo*. Ensuite, les aortes ont été cultivées dans du DMEM riche en glucose (4,5 g / L) contenant 10 % (v / v) de FBS, 10 U / ml de pénicilline et 10 mg / ml de streptomycine (tous de Sigma Aldrich, Lyon, FR) pendant 6 jours (milieu de contrôle). La calcification a été stimulée par l'ajout de 6 mM de Pi pendant 6 jours (milieu de stimulation pour l'aorte). L'halopémide à 10 µM a été utilisé pour inhiber l'activité de la PLD dans ces conditions. Les aortes ont également été isolées à partir de souris KO PLD1 et KO PLD2 en utilisant un protocole similaire [336,337].

## 3. Expérimentation animale

Toutes les expériences ont été réalisées sous l'autorisation n ° 69-266-0501 et étaient en accord avec les lignes directrices du Ministère de l'Agriculture (n ° 2013-118) et la Directive du Conseil de l'Union Européenne pour la protection des animaux utilisés à des fins scientifiques du 22 septembre 2010 (2010 / 63UE). Le protocole a été approuvé par le comité éthique local (Comité Ethique de l'INSA-Lyon - CETIL, CRNEEA n ° 102) sous la référence APAFIS # 4601-2016032110173355. Des rats mâles de la souche Sprague Dawley (150-175 g) ont été achetés chez Janvier-Labs et logés dans une pièce climatisée dans un environnement contrôlé de 21 ± 0,5 ° C et 60-70 % d'humidité, sous un cycle lumière / obscurité de 12h (lumière de 7h à 19h) avec un accès gratuit à la nourriture et à l'eau. L'IRC (insuffisance rénale chronique) a été induite chez les rats suite à un régime riche en adénine. Les rats ont été randomisés soit à une IRC soit à un groupe témoin. Les animaux affectés au groupe IRC ont été nourris avec de l'adénine à 0,75% (p / p) contenant de la nourriture pour rats, sur une base A04 (SAFE, Augy, FR) pendant 4 semaines. Les animaux témoins ont été nourris avec de la nourriture de rat régulière (A04, 13,4 kJ / g) pendant toute la période d'observation (A04, Safe, Augy, FR).

Pour induire la calcification vasculaire, les animaux ont été nourris pendant 5 ou 7 semaines avec un régime personnalisé contenant 0,9 % (p / p) de calcium et 0,9 % (p / p) de phosphore

sur A04 (régime P / Ca). Ils ont reçus trois injections par semaine de 80 ng / kg de calcitriol (Rocaltrol, Roche, FR) dilué dans du propylène glycol. Les animaux témoins ont été nourris avec le régime standard (A04, Safe, Augy, FR) contenant 0,71 % (p / p) de calcium et 0,55 % (p / p) de phosphore.

Les animaux ont été sacrifiés après 5 ou 7 semaines de régime P / Ca. Les rats ont été profondément anesthésiés avec du pentobarbital de sodium (200 mg / kg ip). Environ 10 mL de sang ont été collectés par ponction cardiaque à l'aide d'une seringue héparinisée. Le sang a été centrifugé pendant 5 minutes à 2 000 g pour séparer le plasma, congelé instantanément dans de l'azote liquide et stocké à -80 °C jusqu'à l'analyse. La concentration plasmatique d'urée a été déterminée à l'aide du kit UREA S180 (Sobioda, Montbonnot, FR). Le soin des animaux et les analyses de la fonction rénale ont été respectivement effectués par M. Alexandre Debain et M. Christophe Soulage. Des aortes entières ont été isolées chez tous les rats, et de minuscules parties provenant de différentes régions de chaque aorte ont été regroupées et utilisées pour le dosage du calcium. Le reste de chaque aorte a été utilisé pour l'extraction de l'ARN et l'analyse par RT-qPCR subséquente.

#### 4. Test d'activité de la phosphatase alcaline (PA)

Pour la détermination de l'activité PA [339], les cellules ont été récoltées dans du Nonidet P-40 à 0,2 % (v / v) (Sigma Aldrich, Lyon, FR) et dissociées par sonication. Pour les aortes, les tissus ont été boryés dans l'azote liquide, puis 0,2 % de Nonidet P-40 ont été ajoutés au broyat qui a été dissocié suite à une sonication. L'homogénat a été centrifugé à 1 500 g pendant 5 minutes et le surnageant contenant la PA a été récupéré. L'activité PA a été déterminée en utilisant le *para*-nitrophénylphosphate (*p*NPP) (Sigma Aldrich, Lyon, FR) comme substrat à pH = 10,4. L'absorbance a été mesurée à 405 nm. Pour déterminer l'activité spécifique, un dosage de protéines à l'acide bicinchoninique (BCA) a été réalisé dans les mêmes échantillons [340] (BCA, Sigma-Aldrich, Lyon, FR). Les résultats ont été exprimés en nmol de *para*-nitrophénol (pNP) produit / min / mg de protéine et ont été normalisés par rapport à leurs témoins respectifs.

#### 5. Dosage de calcium

Pour les explants aortiques et les cellules MOVAS, le calcium déposé a été extrait de la matrice extracellulaire en ajoutant 0,6 M de HCl une nuit à température ambiante. La teneur en calcium des surnageants de HCl a été détectée par un dosage colorimétrique en utilisant la méthode du complexe o-crésolphthaline complexone (Sigma-Aldrich, Lyon, FR) [341]. L'absorbance a été mesurée à 570 nm. Le dépôt de calcium a été normalisé par rapport à la

masse des aortes ou à la quantité de protéines dans les cellules. Pour les cellules, les protéines ont été récoltées dans du NaOH 0,1 M / SDS 0,1% et centrifugées à 700 g pendant 5 min à 4 ° C. Le surnageant contenant les protéines a été récolté et la quantité de protéines a été déterminée par un dosage BCA.

#### 6. Extraction de l'ARN total, transcription inverse et analyse quantitative en temps réel de la réaction en chaîne par polymérase (RT-qPCR)

L'ARN a été extrait des cellules en utilisant le kit d'isolement d'ARN NucleoSpin de Macherey-Nagel (Villeurbanne, FR) selon les instructions du fabricant. Pour les aortes, les tissus ont été broyés dans de l'azote liquide puis transférés dans des tubes contenant du réactif TRI (Sigma Aldrich, Lyon, FR), puis l'ARN a été extrait selon les instructions du fabricant. L'ARN total a été quantifié à l'aide d'un spectrophotomètre sur microvolume à 260 nm et sa pureté a été déterminée par les rapports A260 / A280 et A260 / A230 (A: Absorbance). 1 µg de l'ARN résultant a été utilisé pour la transcription inverse, en utilisant la transcriptase inverse Superscript II (Invitrogen, Villebon-sur-Yvette, FR) et les hexamères aléatoires (Invitrogen) dans un volume final de 20 µL. La réaction a été effectuée à 42 ° C pendant 30 minutes et l'enzyme a été inactivée à 99 ° C pendant 5 minutes. 1 µL de l'ADNc a été utilisé dans les qPCR suivantes. L'appareil « Light Cycler » (Roche Diagnostics, Meylan, FR), qui est un système en capillaires, a été utilisé pour réaliser les qPCR. Les réactions ont été effectuées dans un volume final de 20 µL avec des amorces à 0,3 µM, du MgCl<sub>2</sub> (2 mM) et 2 µL du mélange ADN Master SYBR Green I de Light Cycler Fast Start (Roche, Lyon, FR). Les séquences d'amorces utilisées dans la qPCR sont montrées dans le tableau 1. En premier lieu, l'enzyme polymérase est activée à 90°C pendant 10 min. Ensuite, quarante-cinq cycles de PCR sont réalisés, et chacun comprend trois étapes : tout d'abord, une étape de dénaturation à 95°C a lieu pendant 10 secondes, permettant l'ouverture des deux brins d'ADN. Ensuite, la température est abaissée jusqu'à 60°C pendant 10 secondes, conduisant à l'hybridation des amorces (sens et anti-sens). Enfin, l'ADN polymérase synthétise le brin complémentaire à partir des extrémités libres des amorces, c'est l'extension, qui se fait à 72°C pendant 25 secondes. À l'issue de l'amplification, une étape de fusion, qui permet de passer de 60°C à 95°C avec une augmentation de 0,1°C par seconde, est ajoutée pour vérifier la spécificité des amorces utilisées.

La quantification relative a été réalisée selon la méthode de Livak en utilisant la *Gapdh* comme gène de référence.

#### 7. Western blot

Les cellules ont été homogénéisées dans un tampon Tris / HCl 20 mM à pH 7,6 contenant du NaCl (100 mM), du Triton X-100 (1 %) et un cocktail d'inhibiteurs de protéases (1 %) (Sigma Aldrich, Lyon FR). Les lysats cellulaires ont été mélangés avec du tampon Laemmli (BioRad, Californie, US), chauffés à 100 °C pendant exactement 1 min, et séparés sur un gel SDS-polyacrylamide (8 %) contenant 4 M d'urée. Les transferts de type western ont été sondés avec des anticorps polyclonaux anti-PLD1 et anti-PLD2 spécifiquement fournis par S. Bourgoïn (Université Laval, CA), utilisés à des dilutions de 1/10 000 et 1/5 000, respectivement. La révélation se fait en mélangeant les produits du kit de chimiluminescence « *ECL (enhanced chimiluminescence) prime Western Blotting Detection Reagent* » (GE Healthcare, Limonest, FR), en proportions égales, sur des films autoradiographiques. Les membranes ont été incubées avec un anticorps monoclonal anti- $\beta$ -actine (clone AC-74) de Sigma Aldrich pour la normalisation. Les bandes ont ensuite été quantifiées à l'aide du logiciel Image J (<https://imagej.nih.gov/ij/>).

#### 8. Test d'activité PLD

Pour les cellules:

L'activité de la PLD a été déterminée en mesurant la production du  $^{14}\text{C}$ -phosphatidylbutanol, qui est le produit de son activité de transphosphatidylation. Brièvement, les cellules ont été incubées pendant 16 h avec 0,5 mCi de  $^{14}\text{C}$ -palmitate / L (Perkin Elmer, Villebon Sur Yvette, FR) pour marquer la phosphatidylcholine. Le milieu radioactif a ensuite été retiré et les cellules ont été lavées 3 fois avec du DMEM contenant 0,2 % de BSA. Du 1-butanol, à une concentration finale de 0,8 %, a été ajouté et les cellules ont été incubées davantage pendant 30 minutes, temps optimal pour récupérer la formation maximale de phosphatidylbutanol (PtdButOH). Les lipides ont ensuite été extraits comme décrit par Bligh et Dyer [342], sauf que 2 M de KCl dans 0,2 M d'HCl ont été ajoutés au mélange d'extraction à la place de l'eau pour la séparation des phases aqueuse et organique. Les phases de chloroforme ont ensuite été évaporées pendant une nuit et remises en suspension dans 50  $\mu\text{L}$  de chloroforme. Les lipides ont été séparés par chromatographie sur couche mince (CCM) en utilisant des plaques de gel de silice. Les plaques de CCM ont été développées avec la phase supérieure contenant le mélange d'acétate d'éthyle / isooctane / acide acétique / eau (55/25/10/50). Les positions des lipides ont été identifiées après coloration à la vapeur d'iode par comparaison avec des étalons authentiques. Le gel de silice contenant des lipides radioactifs a été quantifié à l'aide d'un compteur à scintillation liquide après grattage des taches sur les plaques.

Pour les aortes:

Le kit Amplex Red PLD (Molecular Probes, Eugene, OR, US) a été utilisé pour mesurer le taux de production de choline à partir de l'hydrolyse du PC par la PLD, selon les instructions du fabricant avec de légères modifications [343].

Les tissus ont été broyés dans de l'azote liquide et ajoutés à du tampon Tris 50 mM pH = 8,0. Les broyats ont été lysés par 3 cycles de congélation / décongélation. Les échantillons ont été incubés en présence de 0,5 mM de PC (Avanti Polar Lipids, Alabaster, AL, US) et de 2 mM de lévamisol pendant 30 minutes à 37 °C. Ensuite, des aliquotes de 100 pL ont été recueillies. Les extraits ont été mélangés avec 100 µL de tampon de réaction contenant 100 µM de réactif Amplex Red, 2 U / mL de peroxydase du raifort (HRP) (Molecular Probes, Eugene, OR, US) et 0,2 U / ml de choline oxydase d'*Alcaligenes* sp. (MP Biomedicals, Ilkirch-Graffenstaden, FR). 2 mM de lévamisol (Sigma Aldrich, Lyon, FR) ont été ajoutés dans le tampon de réaction, pour empêcher la déphosphorylation de la phosphocholine induite par la PLC. L'activité PLD a été estimée en mesurant la fluorescence de la résorufine après 30 min d'incubation à 37 °C en utilisant un lecteur de plaques de microtitrage (NanoQuant Infinite M200, Tecan, Salzburg, AU) à 590 nm après excitation de l'échantillon à 530 nm. Une courbe standard a été réalisée en utilisant la choline. L'activité de la PLD a été normalisée par rapport à la quantité totale de protéines (BCA, Sigma-Aldrich, Lyon, FR).

#### 9. Test d'activité SK

Les activités SK ont été mesurées par leur capacité à phosphoryler la sphingosine et ont été obtenues sous forme de picomoles de S1P formée / min / mg de protéines totales. Pour déterminer l'activité de la SK1, le mélange réactionnel a été réalisé de façon à inhiber l'activité de la SK1. Il contenait de la sphingosine à 50 mM (Enzo Life Sciences, Villeurbanne, FR), 0,25% de Triton X-100 (qui inhibe l'activité de la SK2), [ $\gamma$ -<sup>32</sup>P] -ATP (5 mCi / L, 10 mM) (Perkin-Elmer, Courtaboeuf, FR) et 10 mM de MgCl<sub>2</sub>.

Pour déterminer l'activité de la SK2, le même mélange est utilisé mais à la place du Triton X-100, il contient 0,1 % d'albumine sérique bovine sans acides gras et 1M de KCl (qui inhibe l'activité de la SK1). La S1P marquée a été séparée par chromatographie en couche mince sur du gel de silice 60 (Dutscher, Brumath, FR) réalisée dans du 1-butanol / éthanol / acide acétique glacial / eau (8: 2: 1: 1 en volume). La mise en place de la S1P sur les plaques a été visualisée par autoradiographie et le gel de silice contenant des lipides radioactifs a été quantifié à l'aide d'un compteur à scintillation liquide après grattage des taches sur les plaques. Leyre Brizuela Madrid a effectué toutes les expériences en présence du <sup>32</sup>P.

#### 10. Dosage de S1P

Les MOVAS ont été cultivées dans du milieu sans sérum pendant 24 heures afin de recueillir la S1P sécrétée. Ensuite, la quantité de S1P dans le milieu conditionné a été déterminée en utilisant un kit ELISA compétitif qui détecte la S1P de Tebu-bio (Le Perray En Yvelines, France) selon les instructions du fabricant. La quantité de S1P a été normalisée par rapport à la quantité de protéines totales sécrétées après le dosage des protéines dans le milieu conditionné.

#### 11. Analyse statistique

L'analyse statistique est effectuée pour les mesures pour lesquelles au moins trois expériences indépendantes ont été réalisées. Les groupes ont été comparés en utilisant un t-test non apparié recto-verso. Les résultats sont exprimés en moyenne  $\pm$  erreur-type de la moyenne (SEM). Les résultats ont été considérés comme significatifs lorsque la *p*-value (*p*) était inférieure à 0,05.

### Résultats

La calcification a été induite en cultivant des cellules MOVAS en présence de 10 mM de  $\beta$ -GP et de 50  $\mu$ g / mL d'AA pendant 28 jours. La capacité des MOVAS à induire la calcification a été évaluée en mesurant l'activité PA et la quantité de Ca déposée dans la matrice extracellulaire. Il y avait une augmentation significative de l'activité spécifique de la PA et du dépôt de Ca en fonction du temps de culture à partir du jour 14 et du jour 21, respectivement. Ainsi, la calcification a été induite dans le modèle cellulaire MOVAS. L'expression génique de *Pld1* a montré une légère augmentation au jour 7 de culture avec un déclin ultérieur de l'expression de *Pld1* et *Pld2*. L'augmentation de l'expression de *Pld1* s'est manifestée également au niveau protéique à partir du jour 7 et a atteint le maximum au 14<sup>ème</sup> jour de culture, et elle s'est accompagnée d'une augmentation de l'activité PLD, qui a suivi le même profil. Cependant, il n'y avait pas de changement dans l'expression protéique de la PLD2 par rapport au contrôle pendant le temps de culture.

Pour vérifier si l'augmentation de l'activité de la PLD n'accompagne que la calcification ou si elle a un rôle actif au cours de ce processus, l'effet de l'inhibition de la PLD sur la calcification a été étudié. L'activité de la PLD s'élevait jusqu'au jour 21, et à ce stade de différenciation, la quantité de Ca déposée et l'activité de la PA étaient déjà augmentées. Ainsi, la durée de 21 jours a été choisie pour vérifier l'effet de l'inhibition de la PLD sur le processus de calcification. L'utilisation de l'Halopémide, un pan-inhibiteur qui peut inhiber à la fois PLD1 et PLD2, a permis d'abolir l'activité PA et le dépôt de Ca induits par le  $\beta$ -GP et l'AA aux deux concentrations testées: 1  $\mu$ M et 2  $\mu$ M. L'inhibiteur spécifique de la PLD1, VU0155069, qui a été utilisé à 600 nM et 800 nM, a eu un effet similaire à celui de l'halopémide. Cependant, l'inhibition spécifique de la PLD2 par CAY10594 n'a pas affecté la

calcification des cellules MOVAS. Ainsi, la PLD a un rôle actif au cours de la calcification des MOVAS, et les données obtenues suggèrent fortement que c'est l'isoforme PLD1 qui y est impliquée.

Étant donné que la PKC est l'un des principaux régulateurs de la PLD, son implication dans l'activation de la PLD au cours de la calcification des MOVAS a été testée. L'inhibition de la PKC par le chlorhydrate de bisindolylmaléimide X a conduit à une diminution de l'activité PA et du dépôt de Ca. Cette diminution dépend de la concentration d'inhibiteur utilisée, et elle était significative lorsqu'il était utilisé à 5  $\mu$ M. Contrairement à l'activité PA, qui a été réduite à un niveau inférieur à celui du contrôle, le dépôt de Ca n'a pas été complètement diminué. Donc, l'activité de la PKC est impliquée dans la calcification dans notre modèle, mais son rôle peut ne pas être aussi important que celui de la PLD. De plus, l'inhibition de la PKC n'affecte pas l'activité de la PLD, lorsqu'elle est vérifiée au jour 14 où l'activité PLD était maximale. Par conséquent, la PLD est activée au cours de la calcification des MOVAS d'une manière indépendante de la PKC.

Les voies métaboliques et de signalisation de la S1P sont étroitement liées à la signalisation de la PLD. Ainsi, nous avons cherché à étudier le rôle de la S1P au cours de la calcification dans les MOVAS et à évaluer son interférence possible avec la signalisation PLD. Au cours de la calcification, l'expression génique de *Sphk1* et de *Sphk2* étaient stables jusqu'au jour 14. Au delà de ce temps, elles commençaient à diminuer. Cependant, les activités SK1 / 2 ont été augmentées mais à des temps différents. L'activité de la SK1 a légèrement augmenté de manière significative au jour 7 avant de revenir à son niveau basal au jour 21. Cependant, l'activité de la SK2 a commencé à augmenter significativement à partir du jour 14 et est restée élevée jusqu'à la fin de l'expérience. Ces résultats suggèrent différents rôles pour la SK1 et la SK2 au cours de la différenciation des cellules MOVAS en cellules calcifiantes. Avec l'augmentation observée dans les activités SK, l'expression génique de S1P lyase (*Spg11*) a été diminuée de manière significative. Bien que la détermination de son niveau protéique soit importante, cette découverte couplée à l'augmentation de l'activité SK peut signifier une augmentation du taux de S1P, au niveau intracellulaire et / ou extracellulaire. Les S1PR étaient impliqués dans l'activation de PLD dans différents modèles. Ainsi, nous avons étudié leur expression génique par RT-qPCR pour en prédire un rôle possible dans la calcification. L'expression de *S1pr1* n'a pas changé pendant la calcification. Cependant, *S1pr2* a diminué de manière significative, avec une augmentation significative de *S1pr3*. Ainsi, les S1PR semblent également jouer des rôles différents lors de la trans-différenciation des cellules MOVAS en cellules calcifiantes.

L'inhibition de l'activité de SK1 / 2 pendant 3 semaines par le pan-inhibiteur SKi à 5  $\mu$ M, a annulé la calcification en termes d'activité PA et de dépôt de Ca. K145, utilisé à 5  $\mu$ M, un inhibiteur spécifique de SK2, a eu un effet plus important sur la calcification que SKi. Cependant, l'inhibition de SK1 par PF-543, 100 nM, n'a pas affecté la calcification de manière significative. Par conséquent, SK2 semble jouer un rôle important dans la calcification des cellules MOVAS cultivées en présence de  $\beta$ -GP et d'AA. Afin d'étudier l'effet possible de la signalisation S1P extracellulaire, nous avons utilisé FTY720. Lorsque ce dernier est phosphorylé, il induit un «antagonisme fonctionnel» en favorisant la polyubiquitination, l'endocytose et la dégradation protéasomale de S1P<sub>1</sub> [350]. De plus, il inhibe également d'autres activités enzymatiques des SK, en particulier SK1 [351]. FTY720 à 2,5  $\mu$ M a eu un effet fort et significatif sur l'activité PA qui a été abaissée au-dessous des niveaux de base. En outre, il diminue de manière significative la quantité de Ca déposée. Par conséquent, la signalisation extracellulaire à travers les récepteurs de la S1P peut être importante pour la calcification des MOVAS.

Ensuite, nous avons vérifié l'activité de la PLD au cours de la calcification des MOVAS après l'utilisation de K145 ou FTY720 pendant 2 semaines. Cependant, aucun d'entre eux n'a eu d'effets sur l'activité de la PLD. SK2 semble être l'isoforme importante de notre modèle. Ainsi, nous avons vérifié les effets des inhibiteurs de la PLD sur l'activité SK2 dans notre modèle cellulaire (n = 1). Nos données préliminaires indiquent que l'inhibition de PLD1 a aboli l'activité SK2. Par conséquent, dans notre modèle, SK2 semble agir en aval de la PLD1, et les S1PR agissent indépendamment de la PLD pour favoriser la calcification.

La matrice extracellulaire dans les vaisseaux sanguins joue un rôle important dans la progression de la calcification vasculaire. Ainsi, nous avons utilisé un modèle de culture tissulaire de l'aorte qui préserve les composants de la matrice extracellulaire et protège les caractéristiques des cellules musculaires lisses. Les aortes ont été cultivées soit dans un milieu témoin (Pi 1 mM), soit dans un milieu de stimulation de la calcification contenant du Pi à 6 mM pendant 6 jours. Lorsqu'elles sont cultivées dans un milieu à une forte concentration en Pi, les aortes sont capables de se calcifier, comme le démontre une augmentation significative du dépôt de Ca et de l'activité PA. De plus, dans les cellules aortiques nous avons une surexpression des marqueurs ostéo-chondrocytaires *Runx2* et *Bglap*, ce qui prouve qu'un processus de trans-différenciation a lieu. Avec la calcification, l'expression de la *Pldl* a été augmentée et a été accompagnée d'une augmentation de l'activité

PLD. Cependant, l'expression de la *Pld2* n'a pas été modifiée. Ainsi, la PLD peut également avoir un rôle dans la calcification dans ce modèle.

L'inhibition de l'activité de la PLD en utilisant de l'Halopéride, à 10  $\mu$ M, abolit l'augmentation de l'activité PA et diminue de manière significative le dépôt de Ca. De plus, l'inhibition de la PLD a bloqué la trans-différenciation comme on le voit par une inhibition complète de la surexpression de *Runx2* et de *Bglap*. Afin d'étudier le rôle des isoformes individuelles de la PLD, nous avons utilisé des modèles de souris KO pour PLD1 ou PLD2. À partir de ces souris, les aortes ont été isolées, cultivées en milieu contenant une forte concentration en Pi et comparées aux aortes WT dans les mêmes conditions de culture. Les aortes de PLD1 KO accumulaient de façon significative moins de Ca que les aortes WT et PLD2 KO. Par conséquent, l'activité de la PLD semble être importante dans le modèle aortique, et PLD1 est l'isoforme majeure impliquée dans le processus.

Pour la voie métabolique S1P, les données préliminaires (n = 2) ont montré une augmentation de l'expression de *Sphk2* avec une augmentation de son activité. De manière inattendue, l'activité de SK1 a diminué avec la calcification. En l'absence de variation de l'expression de *Spgl1*, les activités de SK1 et SK2 peuvent donner une indication sur le niveau de S1P présent dans différents compartiments.

L'IRC a été induite chez le rat *via* un régime riche en adénine (0,75% p / p) pendant 4 semaines. Les reins de rats ayant reçu un régime riche en adénine étaient phénotypiquement anormaux, élargis et de couleur pâle. En outre, le niveau d'urée plasmatique des rats qui avaient reçu un régime alimentaire riche en adénine était significativement plus élevé (2 fois plus) que les groupes témoins à la fin de l'expérience.

La calcification vasculaire a été induite par une administration ultérieure d'un régime riche en P / Ca (0,9% / 0,9% w / w) et des injections de calcitriol 3 fois par semaine (80 ng / kg) pour 5 (VC1) ou 7 semaines (VC2).

Pour évaluer la CV chez ces rats, des aortes entières ont été isolées chez tous les animaux. Les deux aortes VC1 et VC2 ont accumulé des quantités importantes de Ca, qui étaient significativement plus élevés par rapport à tous les 3 groupes témoins. Cette calcification n'était pas un processus passif, mais elle était accompagnée d'une augmentation significative de l'expression de *Runx2* à la fois dans VC1 et VC2. Cette augmentation était plus importante dans VC2, et elle était 3 fois plus importante que les contrôles. Avec la calcification, nous avons détecté une régulation positive à la fois pour *Pld1* et *Pld2* dans VC1 avec une diminution ultérieure de VC2. Bien que l'augmentation de l'expression de *Pld2* n'a pas été

observée chez les MOVAS, le profil d'expression de *Pld1* était similaire à celui observé chez les MOVAS, ce qui suggère un possible mécanisme commun de calcification dans nos modèles, impliquant également PLD *in-vivo*. Cependant, plus d'expériences sont indispensables pour démontrer l'implication de la PLD dans la CV dans le modèle IRC *in-vivo*. De plus, une augmentation de l'expression de *Sphk2* a été observée concomitante avec l'augmentation de l'expression de *Pld*. Ces deux enzymes peuvent travailler en coordination pour promouvoir la calcification vasculaire dans le cas d'une IRC *in-vivo*.

### **Discussion et conclusion**

La calcification vasculaire peut être rencontrée dans de nombreux types de vaisseaux sanguins où elle peut affecter différentes couches. Dans le cas d'une IRC, elle affecte principalement la couche médiane des grosses artères [63]. Les artères proximales près du cœur dépendent en grande partie de leur élasticité pour amortir les oscillations du flux sanguin produites en raison de la fonction cardiaque périodique. Ainsi, elles maintiennent un flux sanguin diastolique efficace, améliorent la relaxation ventriculaire gauche et réduisent le travail cardiaque. Lorsque ces artères perdent leur élasticité, pour une raison quelconque, y compris une calcification, elles ne parviennent pas à remplir les fonctions mentionnées, ce qui conduit à un dysfonctionnement diastolique, à une hypertrophie ventriculaire gauche et à une insuffisance cardiaque [50]. La calcification vasculaire est une maladie très répandue, en particulier chez les patients atteints d'IRC. Elle affecte 80 % des patients IRC de paradialyse et de dialyse [354–356]. Jusqu'à présent, les traitements disponibles sont limités à ceux qui corrigent les complications associées à l'IRC. [55,202]. Il y a un manque de thérapies ciblées spécifiques dirigées contre la calcification qui peuvent affecter directement son apparition et sa progression, sans interférer avec l'homéostasie osseuse. C'est pourquoi, une compréhension approfondie des mécanismes moléculaires qui régissent la calcification vasculaire est nécessaire. Par conséquent, nous avons étudié l'un des mécanismes possibles par lesquels la calcification vasculaire se développe ; la voie de la PLD.

La PLD est activée par différents facteurs impliqués dans l'ostéogenèse, y compris PTH, Wnt3a et PGE2 [298,303,307]. En outre, la PLD est activée par l'angiotensine, le peroxyde d'hydrogène (H<sub>2</sub>O<sub>2</sub>) et le LDL oxydé, qui peuvent tous directement activer la calcification [323,328,357]. Ainsi, PLD est un candidat participant à la pathogenèse de la calcification vasculaire.

Afin de comprendre le rôle de la PLD dans ce processus, 3 modèles différents ont été utilisés. Le premier est une lignée murine de CMLs (cellules musculaires lisses) (MOVAS) cultivée en présence de  $\beta$ -GP et d'AA. L'AA a été administré aux cellules afin d'améliorer la production de collagène I. Le collagène produit peut servir de matrice pour le dépôt tardif de Ca et ainsi améliorer la minéralisation. Le  $\beta$ -GP est considéré comme un donneur de phosphate. Il fournit Pi après avoir été hydrolysé par des phosphatases comme la TNAP [347]. Ainsi, notre modèle cellulaire peut être considéré comme un modèle de calcification induite par le Pi élevé. Parmi les complications observées en IRC, l'hyperphosphatémie a les effets directs les plus importants sur les CML. Les cellules MOVAS peuvent se calcifier dans ces conditions, comme détecté par l'activité PA et la dosage du Ca extracellulaire.

Le deuxième modèle est une culture oragnotypique d'aorte de rat incubée dans un milieu à forte concentration en Pi. Ce modèle donne un aperçu du rôle des CML dans leur environnement physiologique. il ne néglige pas le rôle de la MEC (matrice extracellulaire) dans la calcification vasculaire. En outre, il fournit un support naturel pour le dépôt de cristaux d'hydroxyapatite. Dans la calcification vasculaire, le rôle de la MEC ne peut pas être omis, car il est maintenant bien connu que les produits de dégradation d'élastine, qui sont produits pendant ce processus, peuvent agir à la fois comme molécules de signalisation et comme support de haute affinité pour le Ca [56,161]. Les aortes ont été massivement calcifiées lors de la culture en présence d'une forte concentration en Pi, comme démontré par l'augmentation de l'activité PA et le dépôt de Ca. En outre, il y avait une évidence pour un processus de trans-différenciation manifesté par une augmentation de l'expression *Runx2* et *Bglap*. Ces 2 gènes sont des marqueurs ostéo-chondrocytaires qui ne sont normalement pas exprimés dans les tissus vasculaires. En MOVAS, nous n'avons trouvé aucun changement dans l'expression de ces 2 gènes (données non présentées). Cela peut être dû à l'une des deux possibilités ; l'augmentation de l'expression de *Runx2* peut se produire de manière transitoire entre les points temporels étudiés et ainsi, elle peut être manquée, et l'expression de *Bglap* peut nécessiter plus de 28 jours pour augmenter dans ces cellules. Alternativement, le mécanisme de calcification dans ce modèle peut ne pas inclure une régulation positive de ces gènes. Il est différent du modèle de l'aorte par l'absence d'élastine, qui est capable d'améliorer directement la trans-différenciation des CML et de réguler positivement *Bglap* et *Runx2* après avoir été dégradée. [161].

Afin de se rapprocher des mécanismes de la calcification vasculaire chez les patients, un modèle d'IRC *in vivo* chez le rat, induit par un régime riche en adénine, a été utilisé. Lorsque l'adénine est administrée en grandes quantités, elle est oxydée par la xanthine déshydrogénase

en 2,8-hydroxyadénine qui précipite en raison de sa faible solubilité dans les tubules rénaux, ce qui cause un dysfonctionnement rénal grave et irréversible. [358]. L'irréversibilité de la maladie rénale s'est manifestée dans notre modèle par une augmentation de l'urée plasmatique à 5 semaines après l'arrêt du régime riche en adénine par rapport au contrôle. En outre, après le sacrifice des rats qui ont reçu un régime riche en adénine, leurs reins étaient phénotypiquement anormaux, élargis et de couleur pâle. Pour induire la calcification vasculaire, un régime riche en P / Ca a été administré en même temps que des injections de calcitriol. Les niveaux toxiques de calcitriol sont connus pour induire la calcification vasculaire [96]. Nous avons détecté une calcification suite à la quantification du Ca déposé dans l'aorte. De petites sections ont été prises de différentes régions de l'aorte et ont été regroupées pour la quantification du Ca. Cela a été fait pour avoir une idée globale de l'état de l'aorte, car la calcification *in vivo* peut se produire dans une partie de l'aorte seulement, de sorte que l'emplacement de la calcification ne peut pas être prédit. Le reste des tissus aortiques ont été utilisés pour l'extraction de l'ARN, fournissant ainsi également une idée globale de l'état des cellules de l'aorte. Nous avons observé une régulation positive de l'expression génique de *Runx2*, ce qui peut indiquer un processus de trans-différenciation des cellules aortiques en cellules calcifiantes. Il n'y avait aucun changement dans l'expression de *Bglap*. Cela peut être dû à la courte période d'expérimentation qui n'a pas atteint le point où l'expression génique de *Bglap* est augmentée. Alternativement, les mécanismes menant à la calcification dans ce modèle peuvent ne pas impliquer l'expression de l'ostéocalcine.

Après confirmation de la calcification dans tous les trois modèles, nous avons commencé à analyser l'expression de la PLD au cours de ce processus. Le modèle MOVAS a deux avantages par rapport aux autres modèles ; il nous a permis d'étudier le statut de la PLD spécifiquement dans les CML, et en raison de la possibilité d'assigner différents points de temps pour l'analyse, il offre l'opportunité de suivre l'activité et l'expression de la PLD au cours des différentes étapes de la calcification. L'expression de *Pld1* augmente légèrement au jour 7 de culture en milieu de stimulation avec une diminution ultérieure au jour 28. Au niveau protéique, la régulation positive est plus importante avant l'augmentation de l'activité PA et atteint son maximum juste avant le dépôt de Ca. L'activité de la PLD a suivi un schéma approximativement similaire, indiquant que la PLD peut avoir un rôle dans les étapes initiales de la calcification. Bien que l'expression du gène *Pld2* ait diminué au cours des derniers stades de la calcification, son expression protéique n'a pas été altérée. Ainsi, PLD1 peut être l'isoforme impliquée. Dans le modèle de l'aorte de rat, la calcification au jour 6 était accompagnée d'une augmentation de l'expression de *Pld1* et de l'activité totale de la PLD,

sans changement de l'expression de *Pld2*. La possibilité d'une contamination lors d'une incubation supplémentaire de l'aorte a limité l'opportunité d'avoir d'autres points temporels correspondant aux stades tardifs observés chez les MOVAS. Ainsi, dans l'aorte, l'implication de la PLD peut être identifiée, mais il n'est pas possible de suivre ce rôle à différents stades de la calcification. Ce qui est intéressant c'est que dans le modèle IRC de rat, dans CV1 nous avons eu une augmentation de l'expression de *Pld1* qui retombe au niveau basal dans CV2. Ainsi, l'expression de *Pld1* n'est augmentée que dans les stades précoces de la calcification chez les rats IRC soutenant la présence d'un mécanisme similaire à celui observé chez les MOVAS. La différence dans le modèle IRC était dans l'expression de *Pld2* qui a suivi le même modèle que *Pld1*. Dans les MOVAS et le modèle de l'aorte, Pi était le principal l'agent causant la calcification vasculaire. Cependant, dans le modèle IRC de rat, nous avons une maladie complexe, dans laquelle de nombreux facteurs peuvent provoquer une calcification vasculaire autre que l'hyperphosphatémie. Ces facteurs doivent être identifiés et peuvent être responsables de l'augmentation de l'expression de *Pld2*. Par conséquent, dans la nature complexe de la maladie rénale, à la fois PLD1 et PLD2 peuvent être impliqués dans la calcification vasculaire. Pour évaluer si l'augmentation de l'activité PLD est juste une conséquence de la calcification vasculaire ou si elle a un rôle actif, l'activité PLD a été inhibée en utilisant de petites molécules de différentes spécificités. L'halopémide, un pan-inhibiteur de PLD, et le VU0155069, un inhibiteur spécifique de PLD1, étaient tous les deux capables d'abolir l'accumulation du Ca et l'augmentation de l'activité PA au jour 21 de la calcification. Ainsi, la PLD1 a un rôle important dans la calcification MOVAS induite par l'AA et le  $\beta$ -GP. Par contre, l'inhibition de la PLD2 par CAY10594, n'a pas affecté la calcification. L'inhibition de la PLD par Halopémide était également capable de réduire la calcification dans le modèle de l'aorte; elle a aboli l'activité PA et diminué de façon significative l'accumulation du Ca. En outre, elle a inhibé la surexpression de *Runx2* et de *Bglap*, abolissant ainsi la trans-différenciation. Parce que l'halopémide peut inhiber l'activité de PLD1 et de PLD2, nous avons utilisé une autre approche pour tester l'implication de chaque isoforme; les aortes ont été isolées à partir de souris KO *Pld1*, KO *Pld2* et WT, et ont été testés pour leur capacité à se calcifier lors de l'incubation dans un milieu à haute teneur en Pi. Les aortes des souris KO *Pld2* étaient capables d'accumuler le Ca aussi bien que celles des souris WT. Cependant, les aortes des souris KO *Pld1* accumulaient significativement moins de Ca que les aortes des souris WT et KO *Pld2*. Le pourcentage d'inhibition du dépôt de Ca dans les aortes issues des souris KO *Pld1* (environ 40%) était comparable à celle observée avec l'Halopémide, indiquant que l'effet observé avec l'Halopémide est plus probablement dû à l'inhibition de la PLD1.

Après avoir découvert un rôle pour la PLD, en particulier la PLD1, dans la calcification vasculaire, nous avons essayé de découvrir comment elle était activée. La PKC est un activateur majeur de la PLD comme décrit dans le chapitre I, partie 3.2.A. Le rôle de la PKC dans l'ostéogenèse est controversé même pour une seule isoforme. Par exemple, dans une étude, la surexpression spécifique de la PKC $\alpha$  dans les cellules souches mésenchymateuses murines et humaines et dans la lignée cellulaire C3H10T1 / 2 mésenchymateuse murine a conduit à une augmentation de la différenciation ostéogénique [359]. En revanche, dans une autre étude, sa surexpression dans MC3T3-E1 a diminué la différenciation ostéoblastique [360]. Ces études peuvent dépendre en grande partie du modèle cellulaire utilisé ou des conditions de culture. Dans le modèle MOVAS, l'inhibition de la PKC (par le bisindolylmaléimide X, qui inhibe normalement la PKC $\alpha$ , la  $\beta$ I, la  $\beta$ II, la  $\gamma$  et la  $\epsilon$ ) diminue significativement l'activité de la PA et le dépôt de Ca. Cependant, cela n'a pas affecté l'activité PLD. Ainsi, l'activation de la PLD au cours de la calcification des MOVAS est indépendante de la PKC. Un autre mécanisme possible par lequel la PLD peut être activée est la voie de signalisation de la S1P. Nous nous sommes particulièrement intéressés à cette voie car la S1P est impliqué dans la différenciation chondrocytaire et ostéoblastique [279,361]. Ainsi, nous avons commencé à analyser le rôle de la voie métabolique et de signalisation S1P dans le cadre de la calcification vasculaire.

S1P est formée suite à la phosphorylation de la sphingosine par SK1 ou SK2, et peut être dégradée de manière réversible par SPP ou de manière irréversible par SPL. L'expression des gènes de *Sphk1* et *Sphk2* n'a pas changé au cours des 2 premières semaines de calcification, mais a diminué plus tard au cours des 2 semaines suivantes dans les cellules MOVAS. Cependant, les activités des SK ont suivi un modèle différent. L'activité de SK1 n'a augmenté significativement qu'au jour 7 de culture, tandis que celle de SK2 a augmenté à partir du jour 14 et a continué d'augmenter jusqu'à la fin de l'expérience. L'augmentation des activités SK indique une augmentation de la formation de S1P, qui, couplée à la diminution observée dans l'expression de *Spg11*, peut signifier une augmentation du niveau de S1P. De même, dans l'aorte, nos résultats préliminaires ont montré une augmentation de l'expression et de l'activité de SK2 sans modification de l'expression de *Spg11*. Même en cas de diminution de l'activité de SK1, ces résultats peuvent indiquer une augmentation du niveau de S1P dans les compartiments dominés par SK2 comme les mitochondries ou le noyau, entre autres [250].

Les activités des SK ont été inhibées pour évaluer leur rôle dans la calcification. L'inhibition des deux isoformes par SKi ou l'inhibition spécifique de SK2 par K145 a inhibé à la fois l'activité PA et le dépôt de Ca. Cependant, l'inhibition spécifique de SK1 n'a induit aucun

effet significatif. Ainsi, il semble que c'est la S1P produite par SK2 qui est responsable des effets sur la calcification. L'effet de K145 sur l'activité de la PLD a également été testé sans trouver d'effets significatifs. Cependant, la PLD peut également jouer un rôle dans l'activation des SK [272]. Ainsi, nous avons examiné l'effet de l'inhibition de la PLD sur l'activité SK2. Les résultats préliminaires ont montré une diminution de l'activité de SK2 lors de l'utilisation de Halopemide ou CAY10594, tandis que l'inhibition spécifique de PLD1 a induit une forte inhibition de dans cette activité bien en dessous du niveau de base. Ces résultats doivent être confirmés, mais la possibilité que PLD favorise la calcification en augmentant la production de S1P *via* SK2 doit être considérée.

La S1P peut agir de manière intracellulaire ou extracellulaire, après avoir été sécrétée, en se liant à l'un de ses récepteurs. Bien que la S1P provenant de SK2 agit habituellement dans le milieu intracellulaire [250], différents types de cellules peuvent agir comme une source de S1P extracellulaire *in vivo* comme les cellules endothéliales et pourraient affecter les CMLs par voie paracrine. Par conséquent, il était important d'étudier l'expression des récepteurs de la S1P sur les CMLs pendant la calcification. Ces récepteurs ne sont pas exprimés de la même façon pendant la calcification. S1P1-3 sont exprimés dans les CML vasculaires, mais l'expression de S1P4,5 dans ces cellules est discutée [395]. Par conséquent, les études utilisant des CML vasculaires se sont concentrées sur S1P1-3, et c'est ce qui a été fait dans notre étude. L'expression génique de *S1pr1* n'a pas changé, alors qu'il y avait une diminution significative de celle de *S1pr2* à partir du jour 21 dans les cellules MOVAS. L'expression de *S1pr3* a diminué aux jours 7 et 14 avec une augmentation ultérieure au jour 28. Bien qu'une évaluation de l'expression des protéines soit nécessaire, ces données peuvent indiquer des rôles différents pour les S1PR au cours des étapes de trans-différenciation et de calcification dans les cellules MOVAS. FTY720 est un analogue de la sphingosine, il peut inhiber les activités des SK [362,363]. Après avoir été phosphorylé par la SK2 et libéré, il agit principalement comme un antagoniste fonctionnel de S1P<sub>1</sub> ; après liaison à ce récepteur, il induit la polyubiquitinylation de ce récepteur, son internalisation et sa dégradation [364,365]. FTY720 a inhibé de manière significative l'activité PA et le dépôt de Ca mais n'a pas affecté l'activité de la PLD. L'inhibition observée avec FTY720 est plus importante que celle observée avec les inhibiteurs de SK indiquant un rôle possible de S1P<sub>1</sub> dans le processus de calcification. Une évaluation plus approfondie des effets des différents antagonistes S1PR spécifiques est nécessaire. Dans notre modèle, les récepteurs ne sont pas uniquement activés la S1P provenant des cellules, mais plutôt par la S1P présente dans le serum du milieu de culture.

La PLD peut être une nouvelle cible pour prévenir l'apparition ou ralentir la progression de la calcification vasculaire. Les souris double-KO *Pld1/2* sont phénotypiquement normales sans problèmes de santé évidents [213]. Elles étaient protégées contre les maladies telles que le cancer, les troubles cérébraux et cardiovasculaires [213,292,293,366]. De ce fait, l'Halopemide est utilisé pour bloquer le récepteur de la dopamine dans le traitement des troubles neurologiques à des doses qui peuvent inhiber l'activité de la PLD, et il n'a pas eu d'effets néfastes sur la santé chez les patients [366,367]. Ainsi, il serait intéressant d'identifier la PLD comme un nouvel effecteur dans la calcification vasculaire car elle peut être ciblée sans causer des problèmes chez les patients.

### Perspectives

Nous avons découvert un rôle important pour la PLD1 au cours de la calcification induite par le Pi dans les cellules MOVAS et le modèle *ex vivo* de l'aorte. Cependant, le rôle des isoformes de la PLD dans le modèle d'IRC de rat induite par l'adénine doit encore être identifié. Une analyse de l'activité de la PLD pendant la calcification est nécessaire pour ce modèle. En outre, étant donné que l'inhibition de PLD semble être inoffensive *in vivo* [368], les inhibiteurs de la PLD, comme l'Halopémide et le FIPI, peuvent être administrés à des rats pendant l'induction de la calcification. L'effet de ces inhibiteurs sur l'accumulation du Ca, l'activité PA et l'expression de *Runx2* dans l'aorte peut être vérifié pour confirmer l'implication de la PLD dans la calcification vasculaire *in-vivo*.

Il est important de comprendre comment la PLD agit pendant ce processus. Le principal médiateur des fonctions la PLD dans les cellules est l'acide phosphatidique. Ainsi, il peut également médier ses effets dans la calcification vasculaire. L'acide phosphatidique peut agir de différentes manières comme affecter la fluidité de la membrane, étant un précurseur pour la synthèse d'autres effecteurs lipidiques ou l'activation d'un répertoire de protéines.

L'acide phosphatidique aide à inhiber l'autophagie en se liant à mTOR et causant par la suite son activation [369–371]. Par conséquent, l'autophagie a un rôle dans l'amélioration de la minéralisation des ostéoblastes, car les ostéoblastes déficients en autophagie avaient une capacité de minéralisation réduite, et les souris avec des ostéoblastes déficients en autophagie avaient une faible masse osseuse avec une minéralisation réduite [373]. Cependant, l'autophagie a eu un effet négatif sur la calcification pathologique par les CML. En fait, une augmentation de l'autophagie a été observée dans les CML cultivées dans des conditions de Pi élevé et également dans les parois des artères rénales des patients atteints d'une IRC. L'induction de l'autophagie dépendait de la production de ROS médiée par le Pi. Cependant,

l'autophagie dans ce modèle était un mécanisme protecteur contre la calcification vasculaire, puisque son blocage augmentait le dépôt de Ca et son induction supplémentaire inhibait le dépôt de Ca. Cependant, l'autophagie a inhibé la calcification pathologique induite par les CML. En effet, une augmentation de l'autophagie, manifestée par l'augmentation de la formation de chaînes légères 3-II (LC3II) et autophagosomales, a été observée dans les CML cultivées dans des conditions de Pi élevées et également dans les parois des artères rénales des patients atteints d'une IRC. L'induction de l'autophagie dépendait de la production de ROS médiée par le Pi. Cependant, l'autophagie dans ce modèle était un mécanisme protecteur contre la calcification vasculaire, puisque son blocage augmentait le dépôt de Ca et son induction supplémentaire inhibait le dépôt de Ca. Ils ont attribué l'inhibition de la calcification par l'autophagie à l'inhibition de la libération de vésicules matricielles (VM) [376]. Dans une autre étude, l'atorvastatine a inhibé la calcification dans les CMLvasculaires en induisant l'autophagie en inhibant l'expression de la  $\beta$ -caténine [377]. Dans nos modèles, la PLD peut induire la calcification vasculaire en inhibant l'autophagie. Ainsi, il sera intéressant d'évaluer l'autophagie au cours de la calcification des MOVAS en évaluant l'expression des protéines liées à l'autophagie comme Beclin-1, en calculant le rapport LC3II / LC3I et en évaluant la formation d'autophagosomes. L'étude des effets des inhibiteurs de la PLD sur ces marqueurs pendant la calcification peut donner une idée du lien entre la PLD et l'autophagie au cours de ce processus.

Une autre façon par laquelle la PLD et l'acide phosphatidique peuvent aider à l'initiation de la calcification vasculaire est en aidant à la sécrétion des VM. L'activité de la PLD a été vue augmentée juste avant l'élévation de l'activité PA, et elle a atteint son pic avant l'accumulation du Ca. Après ce point, l'activité PLD a diminué à nouveau. Le moment de l'activité maximale de la PLD semble se chevaucher avec le stade auquel les VM peuvent être libérés pour amorcer le dépôt de Ca. La biogenèse des VM est encore controversée. L'origine la plus acceptée est la membrane plasmique. Certains rapports ont souligné qu'elles proviennent de bourgeons directement à partir de la membrane plasmique [378,379], tandis que d'autres ont montré qu'elles proviennent de microvillosités dans des cellules ressemblant aux ostéoblastes Saos-2 [380,381] et dans les chondrocytes [382,383][383]. Dans les deux cellules, l'inhibition de la polymérisation de l'actine par la cytochalasine D a conduit à la libération des VM [380,382]. La PLD et son produit, l'acide phosphatidique, ont des rôles importants dans la réorganisation du cytosquelette d'actine prouvée dans de nombreux types de cellules. L'acide phosphatidique et d'autres lipides, comme le DAG et phosphoinositides, sont importants dans le recrutement et l'orientation de différentes molécules impliquées dans

le remodelage de l'actine [384]. En effet, il a été démontré que la PLD et l'acide phosphatidique jouent un rôle important dans la formation de fibres de stress d'actine en réponse au LPA dans différents types de cellules. [385] [386] [264]. L'un des mécanismes étudiés pour le rôle de l'acide phosphatidique produit par la PLD dans la réorganisation de l'actine a indiqué le recrutement et l'activation de PIPKI (PI4P kinase I). La surexpression de PIPKI de type sauvage a conduit à la polymérisation de l'actine et à la formation de cellules Cos7, alors que le PIPKI mutant qui ne peut pas se lier à l'acide phosphatidique était incapable d'induire ces effets. L'inhibition de la PLD a empêché l'association membranaire de PIPKI et la formation de comètes et de foyers. Ainsi, l'acide phosphatidique, produit par la PLD, était important dans le recrutement et l'activation de PIPKI, qui ont des rôles importants dans la réorganisation du cytosquelette d'actine [387]. En outre, une autre étude a montré un rôle important pour l'acide phosphatidique produit par la PLD dans la formation de PI4,5P2 et dans l'organisation du cytosquelette d'actine nécessaire pour la motilité du *Dictyostelium*, la phagocytose et la micropinocytose [388]. Ainsi, la PLD participerait à la calcification par la régulation de la réorganisation de l'actine au cours de la biogenèse des VM. À cet égard, l'effet des inhibiteurs de la PLD sur la formation des VM pourrait être évalué dans nos modèles.

La dégradation de l'élastine par les MMP est une étape importante dans la progression de la calcification vasculaire. Comme discuté précédemment, les produits de dégradation de l'élastine ont une forte affinité pour le Ca et peuvent ainsi faciliter son dépôt [56]. De plus, les peptides dérivés de l'élastine peuvent se lier au récepteur de la laminine élastine qui est exprimé sur les CML. *In vitro*, les CML se trans-différencient et se calcifient en présence de ces peptides, se manifestant par une augmentation de l'expression du marqueur ostéochondrogène (*Bglap* et *Runx2*) et une élévation de l'activité PA [162]. De plus, l'ajout de l' $\alpha$ -élastine, qui est un peptide dérivé de l'élastine, a augmenté la calcification des CML vasculaires induite par le Pi, en observant l'augmentation de l'activité PA et la coloration de Von Kossa pour le Ca déposé [111]. Pendant la calcification, l'élastine est dégradée par MMP-2 et MMP-9 [56,389,390]. L'inhibition des MMP par la doxycycline chez les rats atteints d'IRC a inhibé la calcification induite par le calcitriol et un régime riche en phosphore [158]. La PLD est impliquée dans l'induction de la production de MMP-2 et de MMP-9 dans différentes cellules cancéreuses [290,291,391,392]. Par conséquent, dans les CMLs, la PLD peut également améliorer la calcification en induisant l'expression des MMP et en provoquant la dégradation de l'élastine. Ainsi, l'expression et l'activité des MMP peuvent être testées lors de la calcification en absence et en présence d'inhibiteurs de la PLD.

Dans les MOVAS, les résultats préliminaires ont montré que l'inhibition de la PLD1 abolissait l'activité de SK2 que nous avons trouvée importante pour la calcification dans ce modèle. Ainsi, l'action de la PLD peut être médiée par l'activation de SK2. Par conséquent, cette expérience doit être répétée afin de vérifier si cet effet est statistiquement significatif.

La voie de signalisation extracellulaire de la S1P peut être activement impliquée dans la calcification. Les effets de FTY720 peuvent donner quelques indices sur un rôle positif dans la calcification vasculaire. Cependant, FTY720 peut également inhiber SK, et il peut agir comme agoniste pour S1P<sub>3-5</sub>. Par conséquent, l'utilisation d'autres antagonistes qui peuvent bloquer spécifiquement les S1PR sans autres effets sur la voie métabolique et la voie de signalisation S1P est nécessaire. Les antagonistes pouvant être utilisés sont : W146, un antagoniste spécifique de S1P<sub>1</sub>, JTE-013, un antagoniste spécifique de S1P<sub>2</sub>, VPC23019, un antagoniste de S1P<sub>1/3</sub> et BML-241, un antagoniste spécifique de S1P<sub>3</sub> [364,393]. L'utilisation de ces antagonistes et la comparaison de leurs effets sur la calcification peuvent donner des indices sur les rôles spécifiques des récepteurs S1P au cours de ce processus.

## List of References

- [1] R. Florencio-Silva, G.R. da S. Sasso, E. Sasso-Cerri, M.J. Simões, P.S. Cerri, *Biology of Bone Tissue: Structure, Function, and Factors That Influence Bone Cells*, *BioMed Res. Int.* 2015 (2015). doi:10.1155/2015/421746.
- [2] B. Clarke, *Normal Bone Anatomy and Physiology*, *Clin. J. Am. Soc. Nephrol. CJASN.* 3 (2008) S131–S139. doi:10.2215/CJN.04151206.
- [3] U. Kini, B.N. Nandeesh, *Physiology of Bone Formation, Remodeling, and Metabolism*, in: I. Fogelman, G. Gnanasegaran, H. van der Wall (Eds.), *Radionucl. Hybrid Bone Imaging*, Springer Berlin Heidelberg, 2012: pp. 29–57. doi:10.1007/978-3-642-02400-9\_2.
- [4] S. Egawa, S. Miura, H. Yokoyama, T. Endo, K. Tamura, *Growth and differentiation of a long bone in limb development, repair and regeneration*, *Dev. Growth Differ.* 56 (2014) 410–424. doi:10.1111/dgd.12136.
- [5] *Long Bone Structure*, *Hum. Anat. Chart.* (2015). <http://humananatomychart.us/long-bone-structure/>.
- [6] M.J. Olszta, X. Cheng, S.S. Jee, R. Kumar, Y.-Y. Kim, M.J. Kaufman, E.P. Douglas, L.B. Gower, *Bone structure and formation: A new perspective*, *Mater. Sci. Eng. R Rep.* 58 (2007) 77–116. doi:10.1016/j.mser.2007.05.001.
- [7] M.T. Valenti, L. Dalle Carbonare, M. Mottes, *Osteogenic Differentiation in Healthy and Pathological Conditions*, *Int. J. Mol. Sci.* 18 (2016). doi:10.3390/ijms18010041.
- [8] A. Rutkovskiy, K.-O. Stensl kken, I.J. Vaage, *Osteoblast Differentiation at a Glance*, *Med. Sci. Monit. Basic Res.* 22 (2016) 95–106. doi:10.12659/MSMBR.901142.
- [9] M. Fakhry, E. Hamade, B. Badran, R. Buchet, D. Magne, *Molecular mechanisms of mesenchymal stem cell differentiation towards osteoblasts*, *World J. Stem Cells.* 5 (2013) 136–148. doi:10.4252/wjsc.v5.i4.136.
- [10] T. Komori, *Regulation of bone development and extracellular matrix protein genes by RUNX2*, *Cell Tissue Res.* 339 (2010) 189–195. doi:10.1007/s00441-009-0832-8.
- [11] F. Otto, A.P. Thornell, T. Crompton, A. Denzel, K.C. Gilmour, I.R. Rosewell, G.W.H. Stamp, R.S.P. Beddington, S. Mundlos, B.R. Olsen, P.B. Selby, M.J. Owen, *Cbfa1, a Candidate Gene for Cleidocranial Dysplasia Syndrome, Is Essential for Osteoblast Differentiation and Bone Development*, *Cell.* 89 (1997) 765–771. doi:10.1016/S0092-8674(00)80259-7.
- [12] T. Komori, H. Yagi, S. Nomura, A. Yamaguchi, K. Sasaki, K. Deguchi, Y. Shimizu, R.T. Bronson, Y.H. Gao, M. Inada, M. Sato, R. Okamoto, Y. Kitamura, S. Yoshiki, T. Kishimoto, *Targeted disruption of Cbfa1 results in a complete lack of bone formation owing to maturational arrest of osteoblasts*, *Cell.* 89 (1997) 755–764.
- [13] P. Ducy, R. Zhang, V. Geoffroy, A.L. Ridall, G. Karsenty, *Osf2/Cbfa1: a transcriptional activator of osteoblast differentiation*, *Cell.* 89 (1997) 747–754.
- [14] W. Liu, S. Toyosawa, T. Furuichi, N. Kanatani, C. Yoshida, Y. Liu, M. Himeno, S. Narai, A. Yamaguchi, T. Komori, *Overexpression of Cbfa1 in osteoblasts inhibits osteoblast maturation and causes osteopenia with multiple fractures*, *J. Cell Biol.* 155 (2001) 157–166. doi:10.1083/jcb.200105052.
- [15] Z. Maruyama, C.A. Yoshida, T. Furuichi, N. Amizuka, M. Ito, R. Fukuyama, T. Miyazaki, H. Kitaura, K. Nakamura, T. Fujita, N. Kanatani, T. Moriishi, K. Yamana, W. Liu, H. Kawaguchi, K. Nakamura, T. Komori, *Runx2 determines bone maturity and turnover rate in postnatal bone development and is involved in bone loss in estrogen deficiency*, *Dev. Dyn. Off. Publ. Am. Assoc. Anat.* 236 (2007) 1876–1890. doi:10.1002/dvdy.21187.
- [16] Y. Nishio, Y. Dong, M. Paris, R.J. O’Keefe, E.M. Schwarz, H. Drissi, *Runx2-mediated regulation of the zinc finger Osterix/Sp7 gene*, *Gene.* 372 (2006) 62–70. doi:10.1016/j.gene.2005.12.022.
- [17] K. Nakashima, X. Zhou, G. Kunkel, Z. Zhang, J.M. Deng, R.R. Behringer, B. de Crombrughe, *The novel zinc finger-containing transcription factor osterix is required for osteoblast differentiation and bone formation*, *Cell.* 108 (2002) 17–29.

- [18] X. Yang, K. Matsuda, P. Bialek, S. Jacquot, H.C. Masuoka, T. Schinke, L. Li, S. Brancorsini, P. Sassone-Corsi, T.M. Townes, A. Hanauer, G. Karsenty, ATF4 is a substrate of RSK2 and an essential regulator of osteoblast biology; implication for Coffin-Lowry Syndrome, *Cell*. 117 (2004) 387–398.
- [19] G. Xiao, D. Jiang, C. Ge, Z. Zhao, Y. Lai, H. Boules, M. Phimphilai, X. Yang, G. Karsenty, R.T. Franceschi, Cooperative interactions between activating transcription factor 4 and Runx2/Cbfa1 stimulate osteoblast-specific osteocalcin gene expression, *J. Biol. Chem.* 280 (2005) 30689–30696. doi:10.1074/jbc.M500750200.
- [20] T. Gaur, C.J. Lengner, H. Hovhannisyan, R.A. Bhat, P.V.N. Bodine, B.S. Komm, A. Javed, A.J. van Wijnen, J.L. Stein, G.S. Stein, J.B. Lian, Canonical WNT signaling promotes osteogenesis by directly stimulating Runx2 gene expression, *J. Biol. Chem.* 280 (2005) 33132–33140. doi:10.1074/jbc.M500608200.
- [21] T.F. Day, X. Guo, L. Garrett-Beal, Y. Yang, Wnt/beta-catenin signaling in mesenchymal progenitors controls osteoblast and chondrocyte differentiation during vertebrate skeletogenesis, *Dev. Cell*. 8 (2005) 739–750. doi:10.1016/j.devcel.2005.03.016.
- [22] M.-H. Lee, T.-G. Kwon, H.-S. Park, J.M. Wozney, H.-M. Ryoo, BMP-2-induced Osterix expression is mediated by Dlx5 but is independent of Runx2, *Biochem. Biophys. Res. Commun.* 309 (2003) 689–694.
- [23] J.L. Millán, M.P. Whyte, Alkaline Phosphatase and Hypophosphatasia, *Calcif. Tissue Int.* 98 (2016) 398–416. doi:10.1007/s00223-015-0079-1.
- [24] H. Orimo, The mechanism of mineralization and the role of alkaline phosphatase in health and disease, *J. Nippon Med. Sch. Nippon Ika Daigaku Zasshi.* 77 (2010) 4–12.
- [25] S. Narisawa, N. Fröhlander, J.L. Millán, Inactivation of two mouse alkaline phosphatase genes and establishment of a model of infantile hypophosphatasia, *Dev. Dyn. Off. Publ. Am. Assoc. Anat.* 208 (1997) 432–446. doi:10.1002/(SICI)1097-0177(199703)208:3<432::AID-AJA13>3.0.CO;2-1.
- [26] K.N. FEDDE, L. BLAIR, J. SILVERSTEIN, S.P. COBURN, L.M. RYAN, R.S. WEINSTEIN, K. WAYMIRE, S. NARISAWA, J.L. MILLÁN, G.R. MACGREGOR, M.P. WHYTE, Alkaline Phosphatase Knock-Out Mice Recapitulate the Metabolic and Skeletal Defects of Infantile Hypophosphatasia, *J. Bone Miner. Res. Off. J. Am. Soc. Bone Miner. Res.* 14 (1999) 2015–2026. doi:10.1359/jbmr.1999.14.12.2015.
- [27] C. Wennberg, L. Hesse, P. Lundberg, S. Mauro, S. Narisawa, U.H. Lerner, J.L. Millán, Functional characterization of osteoblasts and osteoclasts from alkaline phosphatase knockout mice, *J. Bone Miner. Res. Off. J. Am. Soc. Bone Miner. Res.* 15 (2000) 1879–1888. doi:10.1359/jbmr.2000.15.10.1879.
- [28] E.E. Golub, Role of matrix vesicles in biomineralization, *Biochim. Biophys. Acta.* 1790 (2009) 1592–1598. doi:10.1016/j.bbagen.2009.09.006.
- [29] J.L. Millán, The role of phosphatases in the initiation of skeletal mineralization, *Calcif. Tissue Int.* 93 (2013) 299–306. doi:10.1007/s00223-012-9672-8.
- [30] H.C. Anderson, H.H. Hsu, D.C. Morris, K.N. Fedde, M.P. Whyte, Matrix vesicles in osteomalacic hypophosphatasia bone contain apatite-like mineral crystals, *Am. J. Pathol.* 151 (1997) 1555–1561.
- [31] H.C. Anderson, J.B. Sipe, L. Hesse, R. Dhanyamraju, E. Atti, N.P. Camacho, J.L. Millán, R. Dhanyamraju, Impaired calcification around matrix vesicles of growth plate and bone in alkaline phosphatase-deficient mice, *Am. J. Pathol.* 164 (2004) 841–847.
- [32] K.N. Weilbaecher, T.A. Guise, L.K. McCauley, Cancer to bone: a fatal attraction, *Nat. Rev. Cancer.* 11 (2011) 411–425. doi:10.1038/nrc3055.
- [33] F. Long, D.M. Ornitz, Development of the endochondral skeleton, *Cold Spring Harb. Perspect. Biol.* 5 (2013) a008334. doi:10.1101/cshperspect.a008334.
- [34] X. Zhou, K. von der Mark, S. Henry, W. Norton, H. Adams, B. de Crombrugge, Chondrocytes Transdifferentiate into Osteoblasts in Endochondral Bone during Development, Postnatal Growth and Fracture Healing in Mice, *PLoS Genet.* 10 (2014). doi:10.1371/journal.pgen.1004820.

- [35] S. Pizette, L. Niswander, BMPs are required at two steps of limb chondrogenesis: formation of prechondrogenic condensations and their differentiation into chondrocytes, *Dev. Biol.* 219 (2000) 237–249. doi:10.1006/dbio.2000.9610.
- [36] M. Barna, L. Niswander, Visualization of cartilage formation: insight into cellular properties of skeletal progenitors and chondrodysplasia syndromes, *Dev. Cell.* 12 (2007) 931–941. doi:10.1016/j.devcel.2007.04.016.
- [37] Q. Zhao, H. Eberspaecher, V. Lefebvre, B. De Crombrughe, Parallel expression of Sox9 and Col2a1 in cells undergoing chondrogenesis, *Dev. Dyn. Off. Publ. Am. Assoc. Anat.* 209 (1997) 377–386. doi:10.1002/(SICI)1097-0177(199708)209:4<377::AID-AJA5>3.0.CO;2-F.
- [38] H. Akiyama, M.-C. Chaboissier, J.F. Martin, A. Schedl, B. de Crombrughe, The transcription factor Sox9 has essential roles in successive steps of the chondrocyte differentiation pathway and is required for expression of Sox5 and Sox6, *Genes Dev.* 16 (2002) 2813–2828. doi:10.1101/gad.1017802.
- [39] B.K. Zehentner, C. Dony, H. Burtscher, The transcription factor Sox9 is involved in BMP-2 signaling, *J. Bone Miner. Res. Off. J. Am. Soc. Bone Miner. Res.* 14 (1999) 1734–1741. doi:10.1359/jbmr.1999.14.10.1734.
- [40] P. Dy, W. Wang, P. Bhattaram, Q. Wang, L. Wang, R.T. Ballock, V. Lefebvre, Sox9 directs hypertrophic maturation and blocks osteoblast differentiation of growth plate chondrocytes, *Dev. Cell.* 22 (2012) 597–609. doi:10.1016/j.devcel.2011.12.024.
- [41] B.S. Yoon, D.A. Ovchinnikov, I. Yoshii, Y. Mishina, R.R. Behringer, K.M. Lyons, Bmpr1a and Bmpr1b have overlapping functions and are essential for chondrogenesis in vivo, *Proc. Natl. Acad. Sci. U. S. A.* 102 (2005) 5062–5067. doi:10.1073/pnas.0500031102.
- [42] K.N. Retting, B. Song, B.S. Yoon, K.M. Lyons, BMP canonical Smad signaling through Smad1 and Smad5 is required for endochondral bone formation, *Dev. Camb. Engl.* 136 (2009) 1093–1104. doi:10.1242/dev.029926.
- [43] T.P. Hill, D. Später, M.M. Taketo, W. Birchmeier, C. Hartmann, Canonical Wnt/beta-catenin signaling prevents osteoblasts from differentiating into chondrocytes, *Dev. Cell.* 8 (2005) 727–738. doi:10.1016/j.devcel.2005.02.013.
- [44] Y. Dong, A.M. Jesse, A. Kohn, L.M. Gunnell, T. Honjo, M.J. Zuscik, R.J. O’Keefe, M.J. Hilton, RBPjkappa-dependent Notch signaling regulates mesenchymal progenitor cell proliferation and differentiation during skeletal development, *Dev. Camb. Engl.* 137 (2010) 1461–1471. doi:10.1242/dev.042911.
- [45] A.C. Karaplis, A. Luz, J. Glowacki, R.T. Bronson, V.L. Tybulewicz, H.M. Kronenberg, R.C. Mulligan, Lethal skeletal dysplasia from targeted disruption of the parathyroid hormone-related peptide gene, *Genes Dev.* 8 (1994) 277–289.
- [46] M. Inada, T. Yasui, S. Nomura, S. Miyake, K. Deguchi, M. Himeno, M. Sato, H. Yamagiwa, T. Kimura, N. Yasui, T. Ochi, N. Endo, Y. Kitamura, T. Kishimoto, T. Komori, Maturation disturbance of chondrocytes in Cbfa1-deficient mice, *Dev. Dyn. Off. Publ. Am. Assoc. Anat.* 214 (1999) 279–290. doi:10.1002/(SICI)1097-0177(199904)214:4<279::AID-AJA1>3.0.CO;2-W.
- [47] M.A. Arnold, Y. Kim, M.P. Czubyrt, D. Phan, J. McAnally, X. Qi, J.M. Shelton, J.A. Richardson, R. Bassel-Duby, E.N. Olson, MEF2C transcription factor controls chondrocyte hypertrophy and bone development, *Dev. Cell.* 12 (2007) 377–389. doi:10.1016/j.devcel.2007.02.004.
- [48] R.B. Vega, K. Matsuda, J. Oh, A.C. Barbosa, X. Yang, E. Meadows, J. McAnally, C. Pomajzl, J.M. Shelton, J.A. Richardson, G. Karsenty, E.N. Olson, Histone deacetylase 4 controls chondrocyte hypertrophy during skeletogenesis, *Cell.* 119 (2004) 555–566. doi:10.1016/j.cell.2004.10.024.
- [49] B. St-Jacques, M. Hammerschmidt, A.P. McMahon, Indian hedgehog signaling regulates proliferation and differentiation of chondrocytes and is essential for bone formation, *Genes Dev.* 13 (1999) 2072–2086.
- [50] L.L. Demer, Y. Tintut, Vascular calcification: pathobiology of a multifaceted disease, *Circulation.* 117 (2008) 2938–2948. doi:10.1161/CIRCULATIONAHA.107.743161.
- [51] R. Shroff, D.A. Long, C. Shanahan, Mechanistic insights into vascular calcification in CKD, *J. Am. Soc. Nephrol. JASN.* 24 (2013) 179–189. doi:10.1681/ASN.2011121191.

- [52] M.K. Pugsley, R. Tabrizchi, The vascular system. An overview of structure and function, *J. Pharmacol. Toxicol. Methods.* 44 (2000) 333–340.
- [53] G. Pugliese, C. Iacobini, C. Blasetti Fantauzzi, S. Menini, The dark and bright side of atherosclerotic calcification, *Atherosclerosis.* 238 (2015) 220–230. doi:10.1016/j.atherosclerosis.2014.12.011.
- [54] J.E. WAGENSEIL, R.P. MECHAM, Vascular Extracellular Matrix and Arterial Mechanics, *Physiol. Rev.* 89 (2009) 957–989. doi:10.1152/physrev.00041.2008.
- [55] R.B. de Oliveira, H. Okazaki, A.E.M. Stingham, T.B. Drüeke, Z.A. Massy, V. Jorgetti, Vascular calcification in chronic kidney disease: a review, *J. Bras. Nefrol. 'orgão Of. Soc. Bras. E Lat.-Am. Nefrol.* 35 (2013) 147–161. doi:10.5935/0101-2800.20130024.
- [56] N.J. Paloian, C.M. Giachelli, A current understanding of vascular calcification in CKD, *Am. J. Physiol. Renal Physiol.* 307 (2014) F891-900. doi:10.1152/ajprenal.00163.2014.
- [57] Histology of Blood Vessels, (n.d.). <http://cmapspublic.ihmc.us/rid=1NG0K2PP0-1SL1781-8VH/Histology%20of%20Blood%20Vessels.cmap> (accessed October 5, 2017).
- [58] A.S. Levey, K.-U. Eckardt, Y. Tsukamoto, A. Levin, J. Coresh, J. Rossert, D.D.E. Zeeuw, T.H. Hostetter, N. Lameire, G. Eknoyan, Definition and classification of chronic kidney disease: A position statement from Kidney Disease: Improving Global Outcomes (KDIGO), *Kidney Int.* 67 (2005) 2089–2100. doi:10.1111/j.1523-1755.2005.00365.x.
- [59] G.G. Belz, Elastic properties and Windkessel function of the human aorta, *Cardiovasc. Drugs Ther. Spons. Int. Soc. Cardiovasc. Pharmacother.* 9 (1995) 73–83.
- [60] G.M. London, B. Pannier, Arterial functions: how to interpret the complex physiology, *Nephrol. Dial. Transplant. Off. Publ. Eur. Dial. Transpl. Assoc. - Eur. Ren. Assoc.* 25 (2010) 3815–3823. doi:10.1093/ndt/gfq614.
- [61] N.D. Toussaint, P.G. Kerr, Vascular calcification and arterial stiffness in chronic kidney disease: implications and management, *Nephrol. Carlton Vic.* 12 (2007) 500–509. doi:10.1111/j.1440-1797.2007.00823.x.
- [62] G.M. London, A.P. Guérin, S.J. Marchais, F. Métivier, B. Pannier, H. Adda, Arterial media calcification in end-stage renal disease: impact on all-cause and cardiovascular mortality, *Nephrol. Dial. Transplant. Off. Publ. Eur. Dial. Transpl. Assoc. - Eur. Ren. Assoc.* 18 (2003) 1731–1740.
- [63] M. Leroux-Berger, I. Queguiner, T.T. Maciel, A. Ho, F. Relaix, H. Kempf, Pathologic calcification of adult vascular smooth muscle cells differs on their crest or mesodermal embryonic origin, *J. Bone Miner. Res. Off. J. Am. Soc. Bone Miner. Res.* 26 (2011) 1543–1553. doi:10.1002/jbmr.382.
- [64] G.M. London, S.J. Marchais, M.E. Safar, A.F. Genest, A.P. Guerin, F. Metivier, K. Chedid, A.M. London, Aortic and large artery compliance in end-stage renal failure, *Kidney Int.* 37 (1990) 137–142.
- [65] L.L. Demer, Y. Tintut, Vascular calcification: pathobiology of a multifaceted disease, *Circulation.* 117 (2008) 2938–2948. doi:10.1161/CIRCULATIONAHA.107.743161.
- [66] R.N. Foley, P.S. Parfrey, M.J. Sarnak, Clinical epidemiology of cardiovascular disease in chronic renal disease, *Am. J. Kidney Dis. Off. J. Natl. Kidney Found.* 32 (1998) S112-119.
- [67] M. Mizobuchi, D. Towler, E. Slatopolsky, Vascular calcification: the killer of patients with chronic kidney disease, *J. Am. Soc. Nephrol. JASN.* 20 (2009) 1453–1464. doi:10.1681/ASN.2008070692.
- [68] J. Blacher, A.P. Guerin, B. Pannier, S.J. Marchais, G.M. London, Arterial Calcifications, Arterial Stiffness, and Cardiovascular Risk in End-Stage Renal Disease, *Hypertension.* 38 (2001) 938–942. doi:10.1161/hy1001.096358.
- [69] A.P. Guérin, G.M. London, S.J. Marchais, F. Metivier, Arterial stiffening and vascular calcifications in end-stage renal disease, *Nephrol. Dial. Transplant. Off. Publ. Eur. Dial. Transpl. Assoc. - Eur. Ren. Assoc.* 15 (2000) 1014–1021.
- [70] B. Pannier, A.P. Guérin, S.J. Marchais, M.E. Safar, G.M. London, Stiffness of capacitive and conduit arteries: prognostic significance for end-stage renal disease patients, *Hypertens. Dallas Tex* 1979. 45 (2005) 592–596. doi:10.1161/01.HYP.0000159190.71253.c3.

- [71] A. Gauthier-Bastien, R.-V. Ung, R. Larivière, F. Mac-Way, M. Lebel, M. Agharazii, Vascular remodeling and media calcification increases arterial stiffness in chronic kidney disease, *Clin. Exp. Hypertens. N. Y. N* 1993. 36 (2014) 173–180. doi:10.3109/10641963.2013.804541.
- [72] N. Li, W. Cheng, T. Huang, J. Yuan, X. Wang, M. Song, Vascular Adventitia Calcification and Its Underlying Mechanism, *PloS One*. 10 (2015) e0132506. doi:10.1371/journal.pone.0132506.
- [73] C.I. Han, G.R. Campbell, J.H. Campbell, Circulating bone marrow cells can contribute to neointimal formation, *J. Vasc. Res.* 38 (2001) 113–119. doi:51038.
- [74] K. Tanaka, M. Sata, T. Natori, J.-R. Kim-Kaneyama, K. Nose, M. Shibamura, Y. Hirata, R. Nagai, Circulating progenitor cells contribute to neointimal formation in nonirradiated chimeric mice, *FASEB J. Off. Publ. Fed. Am. Soc. Exp. Biol.* 22 (2008) 428–436. doi:10.1096/fj.06-6884com.
- [75] S.N. Pal, J. Golledge, Osteo-progenitors in vascular calcification: a circulating cell theory, *J. Atheroscler. Thromb.* 18 (2011) 551–559.
- [76] S. Lim, S. Park, Role of vascular smooth muscle cell in the inflammation of atherosclerosis, *BMB Rep.* 47 (2014) 1–7. doi:10.5483/BMBRep.2014.47.1.285.
- [77] W.L. Lau, M.H. Festing, C.M. Giachelli, Phosphate and vascular calcification: Emerging role of the sodium-dependent phosphate co-transporter PiT-1, *Thromb. Haemost.* 104 (2010) 464–470. doi:10.1160/TH09-12-0814.
- [78] D.A. Towler, Vascular calcification: A perspective on an imminent disease epidemic, *IBMS BoneKEy.* 5 (2008) 41–58. doi:10.1138/20080298.
- [79] Y.-C. Hou, W.-C. Liu, C.-M. Zheng, J.-Q. Zheng, T.-H. Yen, K.-C. Lu, Role of Vitamin D in Uremic Vascular Calcification, *BioMed Res. Int.* 2017 (2017). doi:10.1155/2017/2803579.
- [80] K. Nitta, N. Nagano, K. Tsuchiya, Fibroblast growth factor 23/klotho axis in chronic kidney disease, *Nephron Clin. Pract.* 128 (2014) 1–10. doi:10.1159/000365787.
- [81] C.S. Kim, S.W. Kim, Vitamin D and chronic kidney disease, *Korean J. Intern. Med.* 29 (2014) 416–427. doi:10.3904/kjim.2014.29.4.416.
- [82] R.B. de Oliveira, H. Okazaki, A.E.M. Stinghen, T.B. Drüeke, Z.A. Massy, V. Jorgetti, Vascular calcification in chronic kidney disease: a review, *J. Bras. Nefrol. 'orgão Of. Soc. Bras. E Lat.-Am. Nefrol.* 35 (2013) 147–161. doi:10.5935/0101-2800.20130024.
- [83] E.A. González, A. Sachdeva, D.A. Oliver, K.J. Martin, Vitamin D insufficiency and deficiency in chronic kidney disease. A single center observational study, *Am. J. Nephrol.* 24 (2004) 503–510. doi:10.1159/000081023.
- [84] R.E. LaClair, R.N. Hellman, S.L. Karp, M. Kraus, S. Ofner, Q. Li, K.L. Graves, S.M. Moe, Prevalence of calcidiol deficiency in CKD: a cross-sectional study across latitudes in the United States, *Am. J. Kidney Dis. Off. J. Natl. Kidney Found.* 45 (2005) 1026–1033.
- [85] A. Jayedi, S. Soltani, S. Shab-Bidar, Vitamin D status and all-cause mortality in patients with chronic kidney disease: A systematic review and dose-response meta-analysis, *J. Clin. Endocrinol. Metab.* (2017). doi:10.1210/jc.2017-00105.
- [86] F. Durantou, M.E. Rodríguez-Ortiz, Y. Duny, M. Rodríguez, J.-P. Daurès, A. Argilés, Vitamin D treatment and mortality in chronic kidney disease: a systematic review and meta-analysis, *Am. J. Nephrol.* 37 (2013) 239–248. doi:10.1159/000346846.
- [87] Z. Zheng, H. Shi, J. Jia, D. Li, S. Lin, Vitamin D supplementation and mortality risk in chronic kidney disease: a meta-analysis of 20 observational studies, *BMC Nephrol.* 14 (2013) 199. doi:10.1186/1471-2369-14-199.
- [88] M. Rodríguez, J.M. Martínez-Moreno, M.E. Rodríguez-Ortiz, J.R. Muñoz-Castañeda, Y. Almaden, Vitamin D and vascular calcification in chronic kidney disease, *Kidney Blood Press. Res.* 34 (2011) 261–268. doi:10.1159/000326903.
- [89] J.-K. Kim, M.J. Park, Y.R. Song, H.J. Kim, S.G. Kim, Vitamin D: a possible modifying factor linking obesity to vascular calcification in hemodialysis patients, *Nutr. Metab.* 14 (2017) 27. doi:10.1186/s12986-017-0181-7.
- [90] J.H. Chang, H. Ro, S. Kim, H.H. Lee, W. Chung, J.Y. Jung, Study on the relationship between serum 25-hydroxyvitamin D levels and vascular calcification in hemodialysis patients with

- consideration of seasonal variation in vitamin D levels, *Atherosclerosis*. 220 (2012) 563–568. doi:10.1016/j.atherosclerosis.2011.11.028.
- [91] R. Shroff, M. Egerton, M. Bridel, V. Shah, A.E. Donald, T.J. Cole, M.P. Hiorns, J.E. Deanfield, L. Rees, A bimodal association of vitamin D levels and vascular disease in children on dialysis, *J. Am. Soc. Nephrol. JASN*. 19 (2008) 1239–1246. doi:10.1681/ASN.2007090993.
- [92] P. Raggi, G.M. Chertow, P.U. Torres, B. Csiky, A. Naso, K. Nossuli, M. Moustafa, W.G. Goodman, N. Lopez, G. Downey, B. Dehmel, J. Floege, ADVANCE Study Group, The ADVANCE study: a randomized study to evaluate the effects of cinacalcet plus low-dose vitamin D on vascular calcification in patients on hemodialysis, *Nephrol. Dial. Transplant. Off. Publ. Eur. Dial. Transpl. Assoc. - Eur. Ren. Assoc.* 26 (2011) 1327–1339. doi:10.1093/ndt/gfq725.
- [93] A. Levin, M. Tang, T. Perry, N. Zalunardo, M. Beaulieu, J.A. Dubland, K. Zerr, O. Djurdjev, Randomized Controlled Trial for the Effect of Vitamin D Supplementation on Vascular Stiffness in CKD, *Clin. J. Am. Soc. Nephrol. CJASN*. (2017). doi:10.2215/CJN.10791016.
- [94] M. Teng, M. Wolf, E. Lowrie, N. Ofsthun, J.M. Lazarus, R. Thadhani, Survival of patients undergoing hemodialysis with paricalcitol or calcitriol therapy, *N. Engl. J. Med.* 349 (2003) 446–456. doi:10.1056/NEJMoa022536.
- [95] J.G.E. Zelt, K.M. McCabe, B. Svajger, H. Barron, K. Laverty, R.M. Holden, M.A. Adams, Magnesium Modifies the Impact of Calcitriol Treatment on Vascular Calcification in Experimental Chronic Kidney Disease, *J. Pharmacol. Exp. Ther.* 355 (2015) 451–462. doi:10.1124/jpet.115.228106.
- [96] M. Mizobuchi, J.L. Finch, D.R. Martin, E. Slatopolsky, Differential effects of vitamin D receptor activators on vascular calcification in uremic rats, *Kidney Int.* 72 (2007) 709–715. doi:10.1038/sj.ki.5002406.
- [97] A. Cardús, S. Panizo, E. Parisi, E. Fernandez, J.M. Valdivielso, Differential effects of vitamin D analogs on vascular calcification, *J. Bone Miner. Res. Off. J. Am. Soc. Bone Miner. Res.* 22 (2007) 860–866. doi:10.1359/jbmr.070305.
- [98] S. Mathew, R.J. Lund, L.R. Chaudhary, T. Geurs, K.A. Hruska, Vitamin D Receptor Activators Can Protect against Vascular Calcification, *J. Am. Soc. Nephrol. JASN*. 19 (2008) 1509–1519. doi:10.1681/ASN.2007080902.
- [99] J.M. Martínez-Moreno, J.R. Muñoz-Castañeda, C. Herencia, A.M. de Oca, J.C. Estepa, R. Canalejo, M.E. Rodríguez-Ortiz, P. Perez-Martinez, E. Aguilera-Tejero, A. Canalejo, M. Rodríguez, Y. Almadén, In vascular smooth muscle cells paricalcitol prevents phosphate-induced Wnt/ $\beta$ -catenin activation, *Am. J. Physiol. Renal Physiol.* 303 (2012) F1136–1144. doi:10.1152/ajprenal.00684.2011.
- [100] A. Mary, L. Hénaut, C. Boudot, I. Six, M. Brazier, Z.A. Massy, T.B. Drüeke, S. Kamel, R. Mentaverri, Calcitriol prevents in vitro vascular smooth muscle cell mineralization by regulating calcium-sensing receptor expression, *Endocrinology*. 156 (2015) 1965–1974. doi:10.1210/en.2014-1744.
- [101] Y. Aoshima, M. Mizobuchi, H. Ogata, C. Kumata, A. Nakazawa, F. Kondo, N. Ono, F. Koiwa, E. Kinugasa, T. Akizawa, Vitamin D receptor activators inhibit vascular smooth muscle cell mineralization induced by phosphate and TNF- $\alpha$ , *Nephrol. Dial. Transplant. Off. Publ. Eur. Dial. Transpl. Assoc. - Eur. Ren. Assoc.* 27 (2012) 1800–1806. doi:10.1093/ndt/gfr758.
- [102] K.A. Lomashvili, X. Wang, W.C. O'Neill, Role of local versus systemic vitamin D receptors in vascular calcification, *Arterioscler. Thromb. Vasc. Biol.* 34 (2014) 146–151. doi:10.1161/ATVBAHA.113.302525.
- [103] S. Evrard, P. Delanaye, S. Kamel, J.-P. Cristol, E. Cavalier, SFBC/SN joined working group on vascular calcifications, Vascular calcification: from pathophysiology to biomarkers, *Clin. Chim. Acta Int. J. Clin. Chem.* 438 (2015) 401–414. doi:10.1016/j.cca.2014.08.034.
- [104] M. Kuro-o, Y. Matsumura, H. Aizawa, H. Kawaguchi, T. Suga, T. Utsugi, Y. Ohyama, M. Kurabayashi, T. Kaname, E. Kume, H. Iwasaki, A. Iida, T. Shiraki-Iida, S. Nishikawa, R. Nagai, Y.I. Nabeshima, Mutation of the mouse *klotho* gene leads to a syndrome resembling ageing, *Nature*. 390 (1997) 45–51. doi:10.1038/36285.

- [105] T. Shimada, M. Kakitani, Y. Yamazaki, H. Hasegawa, Y. Takeuchi, T. Fujita, S. Fukumoto, K. Tomizuka, T. Yamashita, Targeted ablation of Fgf23 demonstrates an essential physiological role of FGF23 in phosphate and vitamin D metabolism, *J. Clin. Invest.* 113 (2004) 561–568. doi:10.1172/JCI19081.
- [106] S. Yamada, C.M. Giachelli, Vascular calcification in CKD-MBD: Roles for phosphate, FGF23, and Klotho, *Bone*. 100 (2017) 87–93. doi:10.1016/j.bone.2016.11.012.
- [107] W.L. Lau, M. Linnes, E.Y. Chu, B.L. Foster, B.A. Bartley, M.J. Somerman, C.M. Giachelli, High phosphate feeding promotes mineral and bone abnormalities in mice with chronic kidney disease, *Nephrol. Dial. Transplant. Off. Publ. Eur. Dial. Transpl. Assoc. - Eur. Ren. Assoc.* 28 (2013) 62–69. doi:10.1093/ndt/gfs333.
- [108] M.M. El-Abbadi, A.S. Pai, E.M. Leaf, H.-Y. Yang, B.A. Bartley, K.K. Quan, C.M. Ingalls, H.W. Liao, C.M. Giachelli, Phosphate feeding induces arterial medial calcification in uremic mice: role of serum phosphorus, fibroblast growth factor-23, and osteopontin, *Kidney Int.* 75 (2009) 1297–1307. doi:10.1038/ki.2009.83.
- [109] M. Cozzolino, M.E. Staniforth, H. Liapis, J. Finch, S.K. Burke, A.S. Dusso, E. Slatopolsky, Sevelamer hydrochloride attenuates kidney and cardiovascular calcifications in long-term experimental uremia, *Kidney Int.* 64 (2003) 1653–1661. doi:10.1046/j.1523-1755.2003.00284.x.
- [110] A. Montes de Oca, J.A. Madueño, J.M. Martínez-Moreno, F. Guerrero, J. Muñoz-Castañeda, M.E. Rodríguez-Ortiz, F.J. Mendoza, Y. Almaden, I. Lopez, M. Rodríguez, E. Aguilera-Tejero, High-phosphate-induced calcification is related to SM22 $\alpha$  promoter methylation in vascular smooth muscle cells, *J. Bone Miner. Res. Off. J. Am. Soc. Bone Miner. Res.* 25 (2010) 1996–2005. doi:10.1002/jbmr.93.
- [111] N. Hosaka, M. Mizobuchi, H. Ogata, C. Kumata, F. Kondo, F. Koiwa, E. Kinugasa, T. Akizawa, Elastin degradation accelerates phosphate-induced mineralization of vascular smooth muscle cells, *Calcif. Tissue Int.* 85 (2009) 523–529. doi:10.1007/s00223-009-9297-8.
- [112] Y. BAI, J. ZHANG, J. XU, L. CUI, H. ZHANG, S. ZHANG, X. FENG, Magnesium prevents  $\beta$ -glycerophosphate-induced calcification in rat aortic vascular smooth muscle cells, *Biomed. Rep.* 3 (2015) 593–597. doi:10.3892/br.2015.473.
- [113] K.-M. Lee, H.-A. Kang, M. Park, H.-Y. Lee, H.-R. Choi, C.-H. Yun, J.-W. Oh, H.-S. Kang, Interleukin-24 attenuates  $\beta$ -glycerophosphate-induced calcification of vascular smooth muscle cells by inhibiting apoptosis, the expression of calcification and osteoblastic markers, and the Wnt/ $\beta$ -catenin pathway, *Biochem. Biophys. Res. Commun.* 428 (2012) 50–55. doi:10.1016/j.bbrc.2012.09.145.
- [114] T. Akiyoshi, H. Ota, K. Iijima, B.-K. Son, T. Kahyo, M. Setou, S. Ogawa, Y. Ouchi, M. Akishita, A novel organ culture model of aorta for vascular calcification, *Atherosclerosis*. 244 (2016) 51–58. doi:10.1016/j.atherosclerosis.2015.11.005.
- [115] S. Mune, M. Shibata, I. Hatamura, F. Saji, T. Okada, Y. Maeda, T. Sakaguchi, S. Negi, T. Shigematsu, Mechanism of phosphate-induced calcification in rat aortic tissue culture: possible involvement of Pit-1 and apoptosis, *Clin. Exp. Nephrol.* 13 (2009) 571–577. doi:10.1007/s10157-009-0208-0.
- [116] T. Sonou, M. Ohya, M. Yashiro, A. Masumoto, Y. Nakashima, T. Ito, T. Mima, S. Negi, H. Kimura-Suda, T. Shigematsu, Mineral Composition of Phosphate-Induced Calcification in a Rat Aortic Tissue Culture Model, *J. Atheroscler. Thromb.* 22 (2015) 1197–1206. doi:10.5551/jat.28647.
- [117] X. Li, H.-Y. Yang, C.M. Giachelli, Role of the sodium-dependent phosphate cotransporter, Pit-1, in vascular smooth muscle cell calcification, *Circ. Res.* 98 (2006) 905–912. doi:10.1161/01.RES.0000216409.20863.e7.
- [118] M.H. Crouthamel, W.L. Lau, E.M. Leaf, N.W. Chavkin, M.C. Wallingford, D.F. Peterson, X. Li, Y. Liu, M.T. Chin, M. Levi, C.M. Giachelli, Sodium-dependent phosphate cotransporters and phosphate-induced calcification of vascular smooth muscle cells: redundant roles for Pit-1 and Pit-2, *Arterioscler. Thromb. Vasc. Biol.* 33 (2013) 2625–2632. doi:10.1161/ATVBAHA.113.302249.

- [119] N.W. Chavkin, J.J. Chia, M.H. Crouthamel, C.M. Giachelli, Phosphate uptake-independent signaling functions of the type III sodium-dependent phosphate transporter, PiT-1, in vascular smooth muscle cells, *Exp. Cell Res.* 333 (2015) 39–48. doi:10.1016/j.yexcr.2015.02.002.
- [120] M.Y. Speer, H.-Y. Yang, T. Brabb, E. Leaf, A. Look, W.-L. Lin, A. Frutkin, D. Dichek, C.M. Giachelli, Smooth muscle cells give rise to osteochondrogenic precursors and chondrocytes in calcifying arteries, *Circ. Res.* 104 (2009) 733–741. doi:10.1161/CIRCRESAHA.108.183053.
- [121] T. Cai, D. Sun, Y. Duan, P. Wen, C. Dai, J. Yang, W. He, WNT/ $\beta$ -catenin signaling promotes VSMCs to osteogenic transdifferentiation and calcification through directly modulating Runx2 gene expression, *Exp. Cell Res.* 345 (2016) 206–217. doi:10.1016/j.yexcr.2016.06.007.
- [122] I. Alesutan, J. Voelkl, M. Feger, D.V. Kratschmar, T. Castor, S. Mia, M. Sacherer, R. Viereck, O. Borst, C. Leibrock, M. Gawaz, M. Kuro-O, S. Pilz, A. Tomaschitz, A. Odermatt, B. Pieske, C.A. Wagner, F. Lang, Involvement Of Vascular Aldosterone Synthase In Phosphate-Induced Osteogenic Transformation Of Vascular Smooth Muscle Cells, *Sci. Rep.* 7 (2017) 2059. doi:10.1038/s41598-017-01882-2.
- [123] K. Lee, H. Kim, D. Jeong, Protein kinase C regulates vascular calcification via cytoskeleton reorganization and osteogenic signaling, *Biochem. Biophys. Res. Commun.* 453 (2014) 793–797. doi:10.1016/j.bbrc.2014.10.026.
- [124] K. Lee, H. Kim, D. Jeong, Microtubule stabilization attenuates vascular calcification through the inhibition of osteogenic signaling and matrix vesicle release, *Biochem. Biophys. Res. Commun.* 451 (2014) 436–441. doi:10.1016/j.bbrc.2014.08.007.
- [125] T. Yoshida, M. Yamashita, M. Hayashi, Kruppel-like factor 4 contributes to high phosphate-induced phenotypic switching of vascular smooth muscle cells into osteogenic cells, *J. Biol. Chem.* 287 (2012) 25706–25714. doi:10.1074/jbc.M112.361360.
- [126] M.-M. Zhao, M.-J. Xu, Y. Cai, G. Zhao, Y. Guan, W. Kong, C. Tang, X. Wang, Mitochondrial reactive oxygen species promote p65 nuclear translocation mediating high-phosphate-induced vascular calcification in vitro and in vivo, *Kidney Int.* 79 (2011) 1071–1079. doi:10.1038/ki.2011.18.
- [127] A. Takemura, K. Iijima, H. Ota, B.-K. Son, Y. Ito, S. Ogawa, M. Eto, M. Akishita, Y. Ouchi, Sirtuin 1 retards hyperphosphatemia-induced calcification of vascular smooth muscle cells, *Arterioscler. Thromb. Vasc. Biol.* 31 (2011) 2054–2062. doi:10.1161/ATVBAHA.110.216739.
- [128] B.-K. Son, K. Kozaki, K. Iijima, M. Eto, T. Nakano, M. Akishita, Y. Ouchi, Gas6/Axl-PI3K/Akt pathway plays a central role in the effect of statins on inorganic phosphate-induced calcification of vascular smooth muscle cells, *Eur. J. Pharmacol.* 556 (2007) 1–8. doi:10.1016/j.ejphar.2006.09.070.
- [129] C.M. Shanahan, M.H. Crouthamel, A. Kapustin, C.M. Giachelli, Arterial calcification in chronic kidney disease: key roles for calcium and phosphate, *Circ. Res.* 109 (2011) 697–711. doi:10.1161/CIRCRESAHA.110.234914.
- [130] A.J. Felsenfeld, B.S. Levine, M. Rodriguez, Pathophysiology of Calcium, Phosphorus, and Magnesium Dysregulation in Chronic Kidney Disease, *Semin. Dial.* 28 (2015) 564–577. doi:10.1111/sdi.12411.
- [131] N.X. Chen, F. Kircelli, K.D. O’Neill, X. Chen, S.M. Moe, Verapamil inhibits calcification and matrix vesicle activity of bovine vascular smooth muscle cells, *Kidney Int.* 77 (2010) 436–442. doi:10.1038/ki.2009.481.
- [132] M. Tepel, M.V. der Giet, A. Park, W. Zidek, Association of calcium channel blockers and mortality in haemodialysis patients, *Clin. Sci. Lond. Engl.* 1979. 103 (2002) 511–515. doi:10.1042/.
- [133] G. Fleckenstein-Grün, F. Thimm, A. Czirfuz, S. Matyas, M. Frey, Experimental vasoprotection by calcium antagonists against calcium-mediated arteriosclerotic alterations, *J. Cardiovasc. Pharmacol.* 24 Suppl 2 (1994) S75-84.
- [134] M. Motro, J. Shemesh, E. Grossman, Coronary benefits of calcium antagonist therapy for patients with hypertension, *Curr. Opin. Cardiol.* 16 (2001) 349–355.
- [135] J.L. Reynolds, A.J. Joannides, J.N. Skepper, R. McNair, L.J. Schurgers, D. Proudfoot, W. Jahnen-Dechent, P.L. Weissberg, C.M. Shanahan, Human vascular smooth muscle cells undergo

- vesicle-mediated calcification in response to changes in extracellular calcium and phosphate concentrations: a potential mechanism for accelerated vascular calcification in ESRD, *J. Am. Soc. Nephrol. JASN.* 15 (2004) 2857–2867. doi:10.1097/01.ASN.0000141960.01035.28.
- [136] A. Masumoto, T. Sonou, M. Ohya, M. Yashiro, Y. Nakashima, K. Okuda, Y. Iwashita, T. Mima, S. Negi, T. Shigematsu, Calcium Overload Accelerates Phosphate-Induced Vascular Calcification Via Pit-1, but not the Calcium-Sensing Receptor, *J. Atheroscler. Thromb.* 24 (2017) 716–724. doi:10.5551/jat.36574.
- [137] H. Yang, G. Curinga, C.M. Giachelli, Elevated extracellular calcium levels induce smooth muscle cell matrix mineralization in vitro, *Kidney Int.* 66 (2004) 2293–2299. doi:10.1111/j.1523-1755.2004.66015.x.
- [138] R.C. Shroff, R. McNair, N. Figg, J.N. Skepper, L. Schurgers, A. Gupta, M. Hiorns, A.E. Donald, J. Deanfield, L. Rees, C.M. Shanahan, Dialysis accelerates medial vascular calcification in part by triggering smooth muscle cell apoptosis, *Circulation.* 118 (2008) 1748–1757. doi:10.1161/CIRCULATIONAHA.108.783738.
- [139] L.W. Hunter, J.E. Charlesworth, S. Yu, J.C. Lieske, V.M. Miller, Calcifying nanoparticles promote mineralization in vascular smooth muscle cells: implications for atherosclerosis, *Int. J. Nanomedicine.* 9 (2014) 2689–2698. doi:10.2147/IJN.S63189.
- [140] B.-K. Son, K. Kozaki, K. Iijima, M. Eto, T. Kojima, H. Ota, Y. Senda, K. Maemura, T. Nakano, M. Akishita, Y. Ouchi, Statins protect human aortic smooth muscle cells from inorganic phosphate-induced calcification by restoring Gas6-Axl survival pathway, *Circ. Res.* 98 (2006) 1024–1031. doi:10.1161/01.RES.0000218859.90970.8d.
- [141] Q. Zhu, R. Guo, C. Liu, D. Fu, F. Liu, J. Hu, H. Jiang, Endoplasmic Reticulum Stress-Mediated Apoptosis Contributing to High Glucose-Induced Vascular Smooth Muscle Cell Calcification, *J. Vasc. Res.* 52 (2015) 291–298. doi:10.1159/000442980.
- [142] A.E. Ewence, M. Bootman, H.L. Roderick, J.N. Skepper, G. McCarthy, M. Epple, M. Neumann, C.M. Shanahan, D. Proudfoot, Calcium phosphate crystals induce cell death in human vascular smooth muscle cells: a potential mechanism in atherosclerotic plaque destabilization, *Circ. Res.* 103 (2008) e28-34. doi:10.1161/CIRCRESAHA.108.181305.
- [143] L. Bessueille, D. Magne, Inflammation: a culprit for vascular calcification in atherosclerosis and diabetes, *Cell. Mol. Life Sci. CMLS.* 72 (2015) 2475–2489. doi:10.1007/s00018-015-1876-4.
- [144] O.M. Akchurin, F. Kaskel, Update on inflammation in chronic kidney disease, *Blood Purif.* 39 (2015) 84–92. doi:10.1159/000368940.
- [145] S. Yamada, M. Tokumoto, N. Tatsumoto, M. Taniguchi, H. Noguchi, T. Nakano, K. Masutani, H. Ooboshi, K. Tsuruya, T. Kitazono, Phosphate overload directly induces systemic inflammation and malnutrition as well as vascular calcification in uremia, *Am. J. Physiol. Renal Physiol.* 306 (2014) F1418-1428. doi:10.1152/ajprenal.00633.2013.
- [146] J. Takasu, R. Katz, D.M. Shavelle, K. O'Brien, S. Mao, J.J. Carr, M. Cushman, M.J. Budoff, Inflammation and descending thoracic aortic calcification as detected by computed tomography: the Multi-Ethnic Study of Atherosclerosis, *Atherosclerosis.* 199 (2008) 201–206. doi:10.1016/j.atherosclerosis.2007.11.005.
- [147] D. Raaz-Schrauder, L. Klinghammer, C. Baum, T. Frank, P. Lewczuk, S. Achenbach, I. Cicha, C. Stumpf, J. Wiltfang, J. Kornhuber, W.G. Daniel, C.D. Garlachs, Association of systemic inflammation markers with the presence and extent of coronary artery calcification, *Cytokine.* 57 (2012) 251–257. doi:10.1016/j.cyto.2011.11.015.
- [148] S. Patsalas, T. Eleftheriadis, S. Spaia, H. Theodoroglou, G. Antoniadi, V. Liakopoulos, P. Passadakis, G. Vayonas, V. Vargemesis, Thirty-month follow-up of coronary artery calcification in hemodialysis patients: different roles for inflammation and abnormal calcium-phosphorous metabolism?, *Ren. Fail.* 29 (2007) 623–629. doi:10.1080/08860220701395010.
- [149] L. Joly, W. Djaballah, G. Koehl, D. Mandry, G. Dolivet, P.-Y. Marie, A. Benetos, Aortic inflammation, as assessed by hybrid FDG-PET/CT imaging, is associated with enhanced aortic stiffness in addition to concurrent calcification, *Eur. J. Nucl. Med. Mol. Imaging.* 36 (2009) 979–985. doi:10.1007/s00259-008-1047-z.

- [150] H.-L. Lee, K.M. Woo, H.-M. Ryoo, J.-H. Baek, Tumor necrosis factor-alpha increases alkaline phosphatase expression in vascular smooth muscle cells via MSX2 induction, *Biochem. Biophys. Res. Commun.* 391 (2010) 1087–1092. doi:10.1016/j.bbrc.2009.12.027.
- [151] Y. Tintut, J. Patel, F. Parhami, L.L. Demer, Tumor necrosis factor-alpha promotes in vitro calcification of vascular cells via the cAMP pathway, *Circulation.* 102 (2000) 2636–2642.
- [152] K. Ikeda, Y. Souma, Y. Akakabe, Y. Kitamura, K. Matsuo, Y. Shimoda, T. Ueyama, S. Matoba, H. Yamada, M. Okigaki, H. Matsubara, Macrophages play a unique role in the plaque calcification by enhancing the osteogenic signals exerted by vascular smooth muscle cells, *Biochem. Biophys. Res. Commun.* 425 (2012) 39–44. doi:10.1016/j.bbrc.2012.07.045.
- [153] I. Karamouzis, P.A. Sarafidis, M. Karamouzis, S. Iliadis, A.-B. Haidich, A. Sioulis, A. Triantos, N. Vavatsi-Christaki, D.M. Grekas, Increase in oxidative stress but not in antioxidant capacity with advancing stages of chronic kidney disease, *Am. J. Nephrol.* 28 (2008) 397–404. doi:10.1159/000112413.
- [154] G. Xu, K. Luo, H. Liu, T. Huang, X. Fang, W. Tu, The progress of inflammation and oxidative stress in patients with chronic kidney disease, *Ren. Fail.* 37 (2015) 45–49. doi:10.3109/0886022X.2014.964141.
- [155] S. Yamada, M. Taniguchi, M. Tokumoto, J. Toyonaga, K. Fujisaki, T. Suehiro, H. Noguchi, M. Iida, K. Tsuruya, T. Kitazono, The antioxidant tempol ameliorates arterial medial calcification in uremic rats: important role of oxidative stress in the pathogenesis of vascular calcification in chronic kidney disease, *J. Bone Miner. Res. Off. J. Am. Soc. Bone Miner. Res.* 27 (2012) 474–485. doi:10.1002/jbmr.539.
- [156] L. Cui, Z. Li, X. Chang, G. Cong, L. Hao, Quercetin attenuates vascular calcification by inhibiting oxidative stress and mitochondrial fission, *Vascul. Pharmacol.* 88 (2017) 21–29. doi:10.1016/j.vph.2016.11.006.
- [157] C.H. Byon, A. Javed, Q. Dai, J.C. Kappes, T.L. Clemens, V.M. Darley-Usmar, J.M. McDonald, Y. Chen, Oxidative stress induces vascular calcification through modulation of the osteogenic transcription factor Runx2 by AKT signaling, *J. Biol. Chem.* 283 (2008) 15319–15327. doi:10.1074/jbc.M800021200.
- [158] E. Hecht, C. Freise, K.V. Websky, H. Nasser, N. Kretzschmar, P. Stawowy, B. Hoher, U. Querfeld, The matrix metalloproteinases 2 and 9 initiate uraemic vascular calcifications, *Nephrol. Dial. Transplant. Off. Publ. Eur. Dial. Transpl. Assoc. - Eur. Ren. Assoc.* 31 (2016) 789–797. doi:10.1093/ndt/gfv321.
- [159] A.W.Y. Chung, H.H.C. Yang, M.K. Sigrist, G. Brin, E. Chum, W.A. Gourlay, A. Levin, Matrix metalloproteinase-2 and -9 exacerbate arterial stiffening and angiogenesis in diabetes and chronic kidney disease, *Cardiovasc. Res.* 84 (2009) 494–504. doi:10.1093/cvr/cvp242.
- [160] A.W.Y. Chung, H.H.C. Yang, J.M. Kim, M.K. Sigrist, E. Chum, W.A. Gourlay, A. Levin, Upregulation of matrix metalloproteinase-2 in the arterial vasculature contributes to stiffening and vasomotor dysfunction in patients with chronic kidney disease, *Circulation.* 120 (2009) 792–801. doi:10.1161/CIRCULATIONAHA.109.862565.
- [161] A. Simionescu, K. Philips, N. Vyavahare, Elastin-derived peptides and TGF-beta1 induce osteogenic responses in smooth muscle cells, *Biochem. Biophys. Res. Commun.* 334 (2005) 524–532. doi:10.1016/j.bbrc.2005.06.119.
- [162] A. Simionescu, D.T. Simionescu, N.R. Vyavahare, Osteogenic responses in fibroblasts activated by elastin degradation products and transforming growth factor-beta1: role of myofibroblasts in vascular calcification, *Am. J. Pathol.* 171 (2007) 116–123.
- [163] J.A. Leopold, Vascular calcification: Mechanisms of vascular smooth muscle cell calcification, *Trends Cardiovasc. Med.* 25 (2015) 267–274. doi:10.1016/j.tcm.2014.10.021.
- [164] K.A. Lomashvili, S. Narisawa, J.L. Millán, W.C. O'Neill, Vascular calcification is dependent on plasma levels of pyrophosphate, *Kidney Int.* 85 (2014) 1351–1356. doi:10.1038/ki.2013.521.
- [165] R. Westenfeld, C. Schäfer, R. Smeets, V.M. Brandenburg, J. Floege, M. Ketteler, W. Jahnke-Dechent, Fetuin-A (AHSG) prevents extraosseous calcification induced by uraemia and phosphate challenge in mice, *Nephrol. Dial. Transplant. Off. Publ. Eur. Dial. Transpl. Assoc. - Eur. Ren. Assoc.* 22 (2007) 1537–1546. doi:10.1093/ndt/gfm094.

- [166] C. Schafer, A. Heiss, A. Schwarz, R. Westenfeld, M. Ketteler, J. Floege, W. Muller-Esterl, T. Schinke, W. Jahn-Dechent, The serum protein alpha 2-Heremans-Schmid glycoprotein/fetuin-A is a systemically acting inhibitor of ectopic calcification, *J. Clin. Invest.* 112 (2003) 357–366. doi:10.1172/JCI17202.
- [167] J.L. Reynolds, J.N. Skepper, R. McNair, T. Kasama, K. Gupta, P.L. Weissberg, W. Jahn-Dechent, C.M. Shanahan, Multifunctional roles for serum protein fetuin-a in inhibition of human vascular smooth muscle cell calcification, *J. Am. Soc. Nephrol. JASN.* 16 (2005) 2920–2930. doi:10.1681/ASN.2004100895.
- [168] L.J. Schurgers, H.M.H. Spronk, J.N. Skepper, T.M. Hackeng, C.M. Shanahan, C. Vermeer, P.L. Weissberg, D. Proudfoot, Post-translational modifications regulate matrix Gla protein function: importance for inhibition of vascular smooth muscle cell calcification, *J. Thromb. Haemost. JTH.* 5 (2007) 2503–2511. doi:10.1111/j.1538-7836.2007.02758.x.
- [169] M.Y. Speer, M.D. McKee, R.E. Guldberg, L. Liaw, H.-Y. Yang, E. Tung, G. Karsenty, C.M. Giachelli, Inactivation of the osteopontin gene enhances vascular calcification of matrix Gla protein-deficient mice: evidence for osteopontin as an inducible inhibitor of vascular calcification in vivo, *J. Exp. Med.* 196 (2002) 1047–1055.
- [170] P.A. Price, S.A. Faus, M.K. Williamson, Warfarin causes rapid calcification of the elastic lamellae in rat arteries and heart valves, *Arterioscler. Thromb. Vasc. Biol.* 18 (1998) 1400–1407.
- [171] C. Liu, J. Wan, Q. Yang, B. Qi, W. Peng, X. Chen, Effects of atorvastatin on warfarin-induced aortic medial calcification and systolic blood pressure in rats, *J. Huazhong Univ. Sci. Technol. Med. Sci. Hua Zhong Ke Ji Xue Xue Bao Yi Xue Ying Wen Ban Huazhong Keji Daxue Xuebao Yixue Yingdewen Ban.* 28 (2008) 535–538. doi:10.1007/s11596-008-0510-1.
- [172] A. Tanimura, D.H. McGregor, H.C. Anderson, Matrix vesicles in atherosclerotic calcification, *Proc. Soc. Exp. Biol. Med. Soc. Exp. Biol. Med. N. Y. N.* 172 (1983) 173–177.
- [173] H.H. Hsu, N.P. Camacho, Isolation of calcifiable vesicles from human atherosclerotic aortas, *Atherosclerosis.* 143 (1999) 353–362.
- [174] A.N. Kapustin, M.L.L. Chatrou, I. Drozdov, Y. Zheng, S.M. Davidson, D. Soong, M. Furmanik, P. Sanchis, R.T.M. De Rosales, D. Alvarez-Hernandez, R. Shroff, X. Yin, K. Muller, J.N. Skepper, M. Mayr, C.P. Reutelingsperger, A. Chester, S. Bertazzo, L.J. Schurgers, C.M. Shanahan, Vascular smooth muscle cell calcification is mediated by regulated exosome secretion, *Circ. Res.* 116 (2015) 1312–1323. doi:10.1161/CIRCRESAHA.116.305012.
- [175] L. Cui, D.A. Houston, C. Farquharson, V.E. MacRae, Characterisation of matrix vesicles in skeletal and soft tissue mineralisation, *Bone.* 87 (2016) 147–158. doi:10.1016/j.bone.2016.04.007.
- [176] Y.-A. Lee, S.-G. Kang, S.-W. Song, J.-S. Rho, E.-K. Kim, Association between metabolic syndrome, smoking status and coronary artery calcification, *PloS One.* 10 (2015) e0122430. doi:10.1371/journal.pone.0122430.
- [177] Y.-M. Eun, S.-G. Kang, S.-W. Song, Fasting plasma glucose levels and coronary artery calcification in subjects with impaired fasting glucose, *Ann. Saudi Med.* 36 (2016) 334–340. doi:10.5144/0256-4947.2016.334.
- [178] C.-H. Jung, E.-J. Rhee, K.-J. Kim, B.-Y. Kim, S.E. Park, Y. Chang, S. Ryu, C.-Y. Park, J.-O. Mok, K.-W. Oh, C.-H. Kim, S.-W. Park, S.-K. Kang, W.-Y. Lee, Relationship of glycated hemoglobin A1c, coronary artery calcification and insulin resistance in males without diabetes, *Arch. Med. Res.* 46 (2015) 71–77. doi:10.1016/j.arcmed.2014.11.011.
- [179] A. Avogaro, G.P. Fadini, Mechanisms of ectopic calcification: implications for diabetic vasculopathy, *Cardiovasc. Diagn. Ther.* 5 (2015) 343–352. doi:10.3978/j.issn.2223-3652.2015.06.05.
- [180] N.X. Chen, D. Duan, K.D. O’Neill, S.M. Moe, High glucose increases the expression of Cbfa1 and BMP-2 and enhances the calcification of vascular smooth muscle cells, *Nephrol. Dial. Transplant. Off. Publ. Eur. Dial. Transpl. Assoc. - Eur. Ren. Assoc.* 21 (2006) 3435–3442. doi:10.1093/ndt/gfl429.

- [181] L. Bessueille, M. Fakhry, E. Hamade, B. Badran, D. Magne, Glucose stimulates chondrocyte differentiation of vascular smooth muscle cells and calcification: A possible role for IL-1 $\beta$ , *FEBS Lett.* 589 (2015) 2797–2804. doi:10.1016/j.febslet.2015.07.045.
- [182] K.V. Ramana, R. Tammali, A.B.M. Reddy, A. Bhatnagar, S.K. Srivastava, Aldose reductase-regulated tumor necrosis factor-alpha production is essential for high glucose-induced vascular smooth muscle cell growth, *Endocrinology.* 148 (2007) 4371–4384. doi:10.1210/en.2007-0512.
- [183] Y. Tang, Q. Xu, H. Peng, Z. Liu, T. Yang, Z. Yu, G. Cheng, X. Li, G. Zhang, R. Shi, The role of vascular peroxidase 1 in ox-LDL-induced vascular smooth muscle cell calcification, *Atherosclerosis.* 243 (2015) 357–363. doi:10.1016/j.atherosclerosis.2015.08.047.
- [184] M.-S. Han, X. Che, G. Cho, H.-R. Park, K.-E. Lim, N.-R. Park, J.-S. Jin, Y.-K. Jung, J.-H. Jeong, I.-K. Lee, S. Kato, J.-Y. Choi, Functional cooperation between vitamin D receptor and Runx2 in vitamin D-induced vascular calcification, *PLoS One.* 8 (2013) e83584. doi:10.1371/journal.pone.0083584.
- [185] N.C.W. Mackenzie, D. Zhu, L. Longley, C.S. Patterson, S. Kommareddy, V.E. MacRae, MOVAS-1 cell line: a new in vitro model of vascular calcification, *Int. J. Mol. Med.* 27 (2011) 663–668. doi:10.3892/ijmm.2011.631.
- [186] M.-Y. Shin, I.-S. Kwun, Phosphate-induced rat vascular smooth muscle cell calcification and the implication of zinc deficiency in a7r5 cell viability, *Prev. Nutr. Food Sci.* 18 (2013) 92–97. doi:10.3746/pnf.2013.18.2.092.
- [187] N. Shobeiri, M.A. Adams, R.M. Holden, Vascular calcification in animal models of CKD: A review, *Am. J. Nephrol.* 31 (2010) 471–481. doi:10.1159/000299794.
- [188] N. Bucay, I. Sarosi, C.R. Dunstan, S. Morony, J. Tarpley, C. Capparelli, S. Scully, H.L. Tan, W. Xu, D.L. Lacey, W.J. Boyle, W.S. Simonet, osteoprotegerin-deficient mice develop early onset osteoporosis and arterial calcification, *Genes Dev.* 12 (1998) 1260–1268.
- [189] G. Luo, P. Ducy, M.D. McKee, G.J. Pinero, E. Loyer, R.R. Behringer, G. Karsenty, Spontaneous calcification of arteries and cartilage in mice lacking matrix GLA protein, *Nature.* 386 (1997) 78–81. doi:10.1038/386078a0.
- [190] Z. Al-Aly, J.-S. Shao, C.-F. Lai, E. Huang, J. Cai, A. Behrmann, S.-L. Cheng, D.A. Towler, Aortic Msx2-Wnt calcification cascade is regulated by TNF-alpha-dependent signals in diabetic Ldlr-/- mice, *Arterioscler. Thromb. Vasc. Biol.* 27 (2007) 2589–2596. doi:10.1161/ATVBAHA.107.153668.
- [191] M. Tölle, A. Reshetnik, M. Schuchardt, M. Höhne, M. van der Giet, Arteriosclerosis and vascular calcification: causes, clinical assessment and therapy, *Eur. J. Clin. Invest.* 45 (2015) 976–985. doi:10.1111/eci.12493.
- [192] P. Raggi, A. Bellasi, Clinical assessment of vascular calcification, *Adv. Chronic Kidney Dis.* 14 (2007) 37–43. doi:10.1053/j.ackd.2006.10.006.
- [193] P. Lanzer, M. Boehm, V. Sorribas, M. Thiriet, J. Janzen, T. Zeller, C. St Hilaire, C. Shanahan, Medial vascular calcification revisited: review and perspectives, *Eur. Heart J.* 35 (2014) 1515–1525. doi:10.1093/eurheartj/ehu163.
- [194] G.M. Chertow, S.K. Burke, P. Raggi, Treat to Goal Working Group, Sevelamer attenuates the progression of coronary and aortic calcification in hemodialysis patients, *Kidney Int.* 62 (2002) 245–252. doi:10.1046/j.1523-1755.2002.00434.x.
- [195] W. Qunibi, M. Moustafa, L.R. Muenz, D.Y. He, P.D. Kessler, J.A. Diaz-Buxo, M. Budoff, CARE-2 Investigators, A 1-year randomized trial of calcium acetate versus sevelamer on progression of coronary artery calcification in hemodialysis patients with comparable lipid control: the Calcium Acetate Renagel Evaluation-2 (CARE-2) study, *Am. J. Kidney Dis. Off. J. Natl. Kidney Found.* 51 (2008) 952–965. doi:10.1053/j.ajkd.2008.02.298.
- [196] D.V. Barreto, F. de C. Barreto, A.B. de Carvalho, L. Cuppari, S.A. Draibe, M.A. Dalboni, R.M.A. Moyses, K.R. Neves, V. Jorgetti, M. Miname, R.D. Santos, M.E.F. Canziani, Phosphate binder impact on bone remodeling and coronary calcification—results from the BRiC study, *Nephron Clin. Pract.* 110 (2008) c273–283. doi:10.1159/000170783.

- [197] C.D. Chue, J.N. Townend, W.E. Moody, D. Zehnder, N.A. Wall, L. Harper, N.C. Edwards, R.P. Steeds, C.J. Ferro, Cardiovascular effects of sevelamer in stage 3 CKD, *J. Am. Soc. Nephrol. JASN.* 24 (2013) 842–852. doi:10.1681/ASN.2012070719.
- [198] F.J. Mendoza, J. Martinez-Moreno, Y. Almaden, M.E. Rodriguez-Ortiz, I. Lopez, J.C. Estepa, C. Henley, M. Rodriguez, E. Aguilera-Tejero, Effect of calcium and the calcimimetic AMG 641 on matrix-Gla protein in vascular smooth muscle cells, *Calcif. Tissue Int.* 88 (2011) 169–178. doi:10.1007/s00223-010-9442-4.
- [199] N. Koleganova, G. Piecha, E. Ritz, C.P. Schmitt, M.-L. Gross, A calcimimetic (R-568), but not calcitriol, prevents vascular remodeling in uremia, *Kidney Int.* 75 (2009) 60–71. doi:10.1038/ki.2008.490.
- [200] N. Joki, I.G. Nikolov, A. Caudrillier, R. Mentaverri, Z.A. Massy, T.B. Drüeke, Effects of calcimimetic on vascular calcification and atherosclerosis in uremic mice, *Bone.* 45 Suppl 1 (2009) S30-34. doi:10.1016/j.bone.2009.03.653.
- [201] P. Raggi, G.M. Chertow, P.U. Torres, B. Csiky, A. Naso, K. Nossuli, M. Moustafa, W.G. Goodman, N. Lopez, G. Downey, B. Dehmel, J. Floege, ADVANCE Study Group, The ADVANCE study: a randomized study to evaluate the effects of cinacalcet plus low-dose vitamin D on vascular calcification in patients on hemodialysis, *Nephrol. Dial. Transplant. Off. Publ. Eur. Dial. Transpl. Assoc. - Eur. Ren. Assoc.* 26 (2011) 1327–1339. doi:10.1093/ndt/gfq725.
- [202] N.-C. Chen, C.-Y. Hsu, C.-L. Chen, The Strategy to Prevent and Regress the Vascular Calcification in Dialysis Patients, *BioMed Res. Int.* 2017 (2017) 9035193. doi:10.1155/2017/9035193.
- [203] T. Ariyoshi, K. Eishi, I. Sakamoto, S. Matsukuma, T. Odate, Effect of etidronic acid on arterial calcification in dialysis patients, *Clin. Drug Investig.* 26 (2006) 215–222.
- [204] K.A. Lomashvili, M.-C. Monier-Faugere, X. Wang, H.H. Malluche, W.C. O’Neill, Effect of bisphosphonates on vascular calcification and bone metabolism in experimental renal failure, *Kidney Int.* 75 (2009) 617–625. doi:10.1038/ki.2008.646.
- [205] L.B. Tankó, G. Qin, P. Alexandersen, Y.Z. Bagger, C. Christiansen, Effective doses of ibandronate do not influence the 3-year progression of aortic calcification in elderly osteoporotic women, *Osteoporos. Int. J. Establ. Result Coop. Eur. Found. Osteoporos. Natl. Osteoporos. Found. USA.* 16 (2005) 184–190. doi:10.1007/s00198-004-1662-x.
- [206] N.D. Toussaint, K.K. Lau, B.J. Strauss, K.R. Polkinghorne, P.G. Kerr, Effect of alendronate on vascular calcification in CKD stages 3 and 4: a pilot randomized controlled trial, *Am. J. Kidney Dis. Off. J. Natl. Kidney Found.* 56 (2010) 57–68. doi:10.1053/j.ajkd.2009.12.039.
- [207] S. Helas, C. Goettsch, M. Schoppet, U. Zeitz, U. Hempel, H. Morawietz, P.J. Kostenuik, R.G. Erben, L.C. Hofbauer, Inhibition of receptor activator of NF-kappaB ligand by denosumab attenuates vascular calcium deposition in mice, *Am. J. Pathol.* 175 (2009) 473–478. doi:10.2353/ajpath.2009.080957.
- [208] E.J. Samelson, P.D. Miller, C. Christiansen, N.S. Daizadeh, L. Grazette, M.S. Anthony, O. Egbuna, A. Wang, S.R. Siddhanti, A.M. Cheung, N. Franchimont, D.P. Kiel, RANKL inhibition with denosumab does not influence 3-year progression of aortic calcification or incidence of adverse cardiovascular events in postmenopausal women with osteoporosis and high cardiovascular risk, *J. Bone Miner. Res. Off. J. Am. Soc. Bone Miner. Res.* 29 (2014) 450–457. doi:10.1002/jbmr.2043.
- [209] E.A. Dennis, Introduction to Thematic Review Series: Phospholipases: Central Role in Lipid Signaling and Disease, *J. Lipid Res.* 56 (2015) 1245–1247. doi:10.1194/jlr.E061101.
- [210] G.M. Borrelli, D. Trono, Recombinant Lipases and Phospholipases and Their Use as Biocatalysts for Industrial Applications, *Int. J. Mol. Sci.* 16 (2015) 20774–20840. doi:10.3390/ijms160920774.
- [211] G.E. Lidgerwood, A. Pébay, Lysophosphatidic Acid and Sphingosine-1-Phosphate in Pluripotent Stem Cells, in: *Lipidomics Stem Cells*, Humana Press, Cham, 2017: pp. 1–9. doi:10.1007/978-3-319-49343-5\_1.
- [212] R.K. Nelson, M.A. Frohman, Physiological and pathophysiological roles for phospholipase D, *J. Lipid Res.* 56 (2015) 2229–2237. doi:10.1194/jlr.R059220.

- [213] M.A. Frohman, The phospholipase D superfamily as therapeutic targets, *Trends Pharmacol. Sci.* 36 (2015) 137–144. doi:10.1016/j.tips.2015.01.001.
- [214] J. Gomez-Cambronero, Phospholipase D in cell signaling: From a myriad of cell functions to cancer growth and metastasis, *J. Biol. Chem.* (2014) jbc.R114.574152. doi:10.1074/jbc.R114.574152.
- [215] R. Cazzolli, A.N. Shemon, M.Q. Fang, W.E. Hughes, Phospholipid signalling through phospholipase D and phosphatidic acid, *IUBMB Life.* 58 (2006) 457–461. doi:10.1080/15216540600871142.
- [216] K.P. Becker, Y.A. Hannun, Protein kinase C and phospholipase D: intimate interactions in intracellular signaling, *Cell. Mol. Life Sci. CMLS.* 62 (2005) 1448–1461. doi:10.1007/s00018-005-4531-7.
- [217] H.J. Mackay, C.J. Twelves, Targeting the protein kinase C family: are we there yet?, *Nat. Rev. Cancer.* 7 (2007) 554–562. doi:10.1038/nrc2168.
- [218] S.M. Hammond, J.M. Jenco, S. Nakashima, K. Cadwallader, Q. Gu, S. Cook, Y. Nozawa, G.D. Prestwich, M.A. Frohman, A.J. Morris, Characterization of two alternately spliced forms of phospholipase D1. Activation of the purified enzymes by phosphatidylinositol 4,5-bisphosphate, ADP-ribosylation factor, and Rho family monomeric GTP-binding proteins and protein kinase C-alpha, *J. Biol. Chem.* 272 (1997) 3860–3868.
- [219] T.G. Lee, J.B. Park, S.D. Lee, S. Hong, J.H. Kim, Y. Kim, K.S. Yi, S. Bae, Y.A. Hannun, L.M. Obeid, P.G. Suh, S.H. Ryu, Phorbol myristate acetate-dependent association of protein kinase C alpha with phospholipase D1 in intact cells, *Biochim. Biophys. Acta.* 1347 (1997) 199–204.
- [220] D.S. Min, S.K. Park, J.H. Exton, Characterization of a rat brain phospholipase D isozyme, *J. Biol. Chem.* 273 (1998) 7044–7051.
- [221] W.D. Singer, H.A. Brown, X. Jiang, P.C. Sternweis, Regulation of phospholipase D by protein kinase C is synergistic with ADP-ribosylation factor and independent of protein kinase activity, *J. Biol. Chem.* 271 (1996) 4504–4510.
- [222] T. Hu, J.H. Exton, Mechanisms of regulation of phospholipase D1 by protein kinase C alpha, *J. Biol. Chem.* 278 (2003) 2348–2355. doi:10.1074/jbc.M210093200.
- [223] Y.H. Lee, H.S. Kim, J.K. Pai, S.H. Ryu, P.G. Suh, Activation of phospholipase D induced by platelet-derived growth factor is dependent upon the level of phospholipase C-gamma 1, *J. Biol. Chem.* 269 (1994) 26842–26847.
- [224] K. Oishi, M. Takahashi, H. Mukai, Y. Banno, S. Nakashima, Y. Kanaho, Y. Nozawa, Y. Ono, PKC regulates phospholipase D1 through direct interaction, *J. Biol. Chem.* 276 (2001) 18096–18101. doi:10.1074/jbc.M010646200.
- [225] J.-S. Chen, J.H. Exton, Regulation of phospholipase D2 activity by protein kinase C alpha, *J. Biol. Chem.* 279 (2004) 22076–22083. doi:10.1074/jbc.M311033200.
- [226] Y.C. Chae, K.L. Kim, S.H. Ha, J. Kim, P.-G. Suh, S.H. Ryu, Protein kinase C delta-mediated phosphorylation of phospholipase D controls integrin-mediated cell spreading, *Mol. Cell. Biol.* 30 (2010) 5086–5098. doi:10.1128/MCB.00443-10.
- [227] Q. Zhang, D. Wang, V. Kundumani-Sridharan, L. Gadiparthi, D.A. Johnson, G.J. Tigyi, G.N. Rao, PLD1-dependent PKC gamma activation downstream to Src is essential for the development of pathologic retinal neovascularization, *Blood.* 116 (2010) 1377–1385. doi:10.1182/blood-2010-02-271478.
- [228] I. Gorshkova, D. He, E. Berdyshev, P. Usatuyk, M. Burns, S. Kalari, Y. Zhao, S. Pendyala, J.G.N. Garcia, N.J. Pyne, D.N. Brindley, V. Natarajan, Protein kinase C-epsilon regulates sphingosine 1-phosphate-mediated migration of human lung endothelial cells through activation of phospholipase D2, protein kinase C-zeta, and Rac1, *J. Biol. Chem.* 283 (2008) 11794–11806. doi:10.1074/jbc.M800250200.
- [229] P.E. Tenconi, N.M. Giusto, G.A. Salvador, M.V. Mateos, Phospholipase D1 modulates protein kinase C-epsilon in retinal pigment epithelium cells during inflammatory response, *Int. J. Biochem. Cell Biol.* 81 (2016) 67–75. doi:10.1016/j.biocel.2016.10.015.
- [230] Z. Yang, Small GTPases, *Plant Cell.* 14 (2002) s375–s388. doi:10.1105/tpc.001065.

- [231] I. Lopez, R.S. Arnold, J.D. Lambeth, Cloning and initial characterization of a human phospholipase D2 (hPLD2). ADP-ribosylation factor regulates hPLD2, *J. Biol. Chem.* 273 (1998) 12846–12852.
- [232] M. Hiroyama, J.H. Exton, Localization and regulation of phospholipase D2 by ARF6, *J. Cell. Biochem.* 95 (2005) 149–164. doi:10.1002/jcb.20351.
- [233] L.G. Henage, J.H. Exton, H.A. Brown, Kinetic analysis of a mammalian phospholipase D: allosteric modulation by monomeric GTPases, protein kinase C, and polyphosphoinositides, *J. Biol. Chem.* 281 (2006) 3408–3417. doi:10.1074/jbc.M508800200.
- [234] J.H. Kim, S.D. Lee, J.M. Han, T.G. Lee, Y. Kim, J.B. Park, J.D. Lambeth, P.G. Suh, S.H. Ryu, Activation of phospholipase D1 by direct interaction with ADP-ribosylation factor 1 and RalA, *FEBS Lett.* 430 (1998) 231–235.
- [235] M. Rankovic, L. Jacob, V. Rankovic, L.-O. Brandenburg, H. Schröder, V. Höllt, T. Koch, ADP-ribosylation factor 6 regulates mu-opioid receptor trafficking and signaling via activation of phospholipase D2, *Cell. Signal.* 21 (2009) 1784–1793. doi:10.1016/j.cellsig.2009.07.014.
- [236] N. Vitale, J. Mawet, J. Camonis, R. Regazzi, M.-F. Bader, S. Chasserot-Golaz, The Small GTPase RalA controls exocytosis of large dense core secretory granules by interacting with ARF6-dependent phospholipase D1, *J. Biol. Chem.* 280 (2005) 29921–29928. doi:10.1074/jbc.M413748200.
- [237] S.-W. Kim, M. Hayashi, J.-F. Lo, Y. Yang, J.-S. Yoo, J.-D. Lee, ADP-ribosylation factor 4 small GTPase mediates epidermal growth factor receptor-dependent phospholipase D2 activation, *J. Biol. Chem.* 278 (2003) 2661–2668. doi:10.1074/jbc.M205819200.
- [238] F. Momboisse, E. Lonchamp, V. Calco, M. Ceridono, N. Vitale, M.-F. Bader, S. Gasman, betaPIX-activated Rac1 stimulates the activation of phospholipase D, which is associated with exocytosis in neuroendocrine cells, *J. Cell Sci.* 122 (2009) 798–806. doi:10.1242/jcs.038109.
- [239] M.-S. Yoon, C.H. Cho, K.S. Lee, J.-S. Han, Binding of Cdc42 to phospholipase D1 is important in neurite outgrowth of neural stem cells, *Biochem. Biophys. Res. Commun.* 347 (2006) 594–600. doi:10.1016/j.bbrc.2006.06.111.
- [240] G. Du, Y.M. Altshuller, Y. Kim, J.M. Han, S.H. Ryu, A.J. Morris, M.A. Frohman, Dual requirement for rho and protein kinase C in direct activation of phospholipase D1 through G protein-coupled receptor signaling, *Mol. Biol. Cell.* 11 (2000) 4359–4368.
- [241] S.J. Walker, W.J. Wu, R.A. Cerione, H.A. Brown, Activation of phospholipase D1 by Cdc42 requires the Rho insert region, *J. Biol. Chem.* 275 (2000) 15665–15668. doi:10.1074/jbc.M000076200.
- [242] T. Maeda, S. Yuzawa, A. Suzuki, Y. Baba, Y. Nishimura, Y. Kato, RhoA mediates the expression of acidic extracellular pH-induced matrix metalloproteinase-9 mRNA through phospholipase D1 in mouse metastatic B16-BL6 melanoma cells, *Int. J. Oncol.* 48 (2016) 1251–1257. doi:10.3892/ijo.2016.3322.
- [243] H.-J. Peng, K.M. Henkels, M. Mahankali, M.C. Dinauer, J. Gomez-Cambronero, Evidence for two CRIB domains in phospholipase D2 (PLD2) that the enzyme uses to specifically bind to the small GTPase Rac2, *J. Biol. Chem.* 286 (2011) 16308–16320. doi:10.1074/jbc.M110.206672.
- [244] H.-J. Peng, K.M. Henkels, M. Mahankali, C. Marchal, P. Bubulya, M.C. Dinauer, J. Gomez-Cambronero, The dual effect of Rac2 on phospholipase D2 regulation that explains both the onset and termination of chemotaxis, *Mol. Cell. Biol.* 31 (2011) 2227–2240. doi:10.1128/MCB.01348-10.
- [245] M. Corrotte, A.P.T. Nyguyen, M.L. Harlay, N. Vitale, M.-F. Bader, N.J. Grant, Ral isoforms are implicated in Fc gamma R-mediated phagocytosis: activation of phospholipase D by RalA, *J. Immunol. Baltim. Md* 1950. 185 (2010) 2942–2950. doi:10.4049/jimmunol.0903138.
- [246] Y. Jiang, M.S. Sverdlov, P.T. Toth, L.S. Huang, G. Du, Y. Liu, V. Natarajan, R.D. Minshall, Phosphatidic Acid Produced by RalA-activated PLD2 Stimulates Caveolae-mediated Endocytosis and Trafficking in Endothelial Cells, *J. Biol. Chem.* 291 (2016) 20729–20738. doi:10.1074/jbc.M116.752485.

- [247] H. Jeon, D. Kwak, J. Noh, M.N. Lee, C.S. Lee, P.-G. Suh, S.H. Ryu, Phospholipase D2 induces stress fiber formation through mediating nucleotide exchange for RhoA, *Cell. Signal.* 23 (2011) 1320–1326. doi:10.1016/j.cellsig.2011.03.014.
- [248] M. Mahankali, H.-J. Peng, K.M. Henkels, M.C. Dinauer, J. Gomez-Cambronero, Phospholipase D2 (PLD2) is a guanine nucleotide exchange factor (GEF) for the GTPase Rac2, *Proc. Natl. Acad. Sci. U. S. A.* 108 (2011) 19617–19622. doi:10.1073/pnas.1114692108.
- [249] M. Mahankali, K.M. Henkels, J. Gomez-Cambronero, A GEF-to-phospholipase molecular switch caused by phosphatidic acid, Rac and JAK tyrosine kinase that explains leukocyte cell migration, *J. Cell Sci.* 126 (2013) 1416–1428. doi:10.1242/jcs.117960.
- [250] S. Pyne, D.R. Adams, N.J. Pyne, Sphingosine 1-phosphate and sphingosine kinases in health and disease: Recent advances, *Prog. Lipid Res.* 62 (2016) 93–106. doi:10.1016/j.plipres.2016.03.001.
- [251] A. Meshcheryakova, D. Mechtcheriakova, P. Pietschmann, Sphingosine 1-phosphate signaling in bone remodeling: multifaceted roles and therapeutic potential, *Expert Opin. Ther. Targets.* 21 (2017) 725–737. doi:10.1080/14728222.2017.1332180.
- [252] M. Maceyka, K.B. Harikumar, S. Milstien, S. Spiegel, Sphingosine-1-phosphate signaling and its role in disease, *Trends Cell Biol.* 22 (2012) 50–60. doi:10.1016/j.tcb.2011.09.003.
- [253] Y.A. Hannun, L.M. Obeid, Principles of bioactive lipid signalling: lessons from sphingolipids, *Nat. Rev. Mol. Cell Biol.* 9 (2008) 139–150. doi:10.1038/nrm2329.
- [254] R. Brunkhorst, R. Vutukuri, W. Pfeilschifter, Fingolimod for the treatment of neurological diseases-state of play and future perspectives, *Front. Cell. Neurosci.* 8 (2014) 283. doi:10.3389/fncel.2014.00283.
- [255] O. Cuvillier, G. Pirianov, B. Kleuser, P.G. Vanek, O.A. Coso, S. Gutkind, S. Spiegel, Suppression of ceramide-mediated programmed cell death by sphingosine-1-phosphate, *Nature.* 381 (1996) 800–803. doi:10.1038/381800a0.
- [256] M. Kawabori, R. Kacimi, J.S. Karliner, M.A. Yenari, Sphingolipids in cardiovascular and cerebrovascular systems: Pathological implications and potential therapeutic targets, *World J. Cardiol.* 5 (2013) 75–86. doi:10.4330/wjc.v5.i4.75.
- [257] N. Takasugi, T. Sasaki, K. Suzuki, S. Osawa, H. Isshiki, Y. Hori, N. Shimada, T. Higo, S. Yokoshima, T. Fukuyama, V.M.-Y. Lee, J.Q. Trojanowski, T. Tomita, T. Iwatsubo, BACE1 activity is modulated by cell-associated sphingosine-1-phosphate, *J. Neurosci. Off. J. Soc. Neurosci.* 31 (2011) 6850–6857. doi:10.1523/JNEUROSCI.6467-10.2011.
- [258] K.A. Parham, J.R. Zebol, K.L. Tooley, W.Y. Sun, L.M. Moldenhauer, M.P. Cockshell, B.L. Gliddon, P.A. Moretti, G. Tigyi, S.M. Pitson, C.S. Bonder, Sphingosine 1-phosphate is a ligand for peroxisome proliferator-activated receptor- $\gamma$  that regulates neoangiogenesis, *FASEB J. Off. Publ. Fed. Am. Soc. Exp. Biol.* 29 (2015) 3638–3653. doi:10.1096/fj.14-261289.
- [259] G.M. Strub, M. Paillard, J. Liang, L. Gomez, J.C. Allegood, N.C. Hait, M. Maceyka, M.M. Price, Q. Chen, D.C. Simpson, T. Kordula, S. Milstien, E.J. Lesnefsky, S. Spiegel, Sphingosine-1-phosphate produced by sphingosine kinase 2 in mitochondria interacts with prohibitin 2 to regulate complex IV assembly and respiration, *FASEB J. Off. Publ. Fed. Am. Soc. Exp. Biol.* 25 (2011) 600–612. doi:10.1096/fj.10-167502.
- [260] S. Panneer Selvam, R.M. De Palma, J.J. Oaks, N. Oleinik, Y.K. Peterson, R.V. Stahelin, E. Skordalakes, S. Ponnusamy, E. Garrett-Mayer, C.D. Smith, B. Ogretmen, Binding of the sphingolipid S1P to hTERT stabilizes telomerase at the nuclear periphery by allosterically mimicking protein phosphorylation, *Sci. Signal.* 8 (2015) ra58. doi:10.1126/scisignal.aaa4998.
- [261] N.C. Hait, J. Allegood, M. Maceyka, G.M. Strub, K.B. Harikumar, S.K. Singh, C. Luo, R. Marmorstein, T. Kordula, S. Milstien, S. Spiegel, Regulation of histone acetylation in the nucleus by sphingosine-1-phosphate, *Science.* 325 (2009) 1254–1257. doi:10.1126/science.1176709.
- [262] E. Meacci, V. Vasta, C. Donati, M. Farnararo, P. Bruni, Receptor-mediated activation of phospholipase D by sphingosine 1-phosphate in skeletal muscle C2C12 cells. A role for protein kinase C, *FEBS Lett.* 457 (1999) 184–188.

- [263] S. Orlati, A.M. Porcelli, S. Hrelia, J.R. Van Brocklyn, S. Spiegel, M. Rugolo, Sphingosine-1-phosphate activates phospholipase D in human airway epithelial cells via a G protein-coupled receptor, *Arch. Biochem. Biophys.* 375 (2000) 69–77. doi:10.1006/abbi.1999.1589.
- [264] A.M. Porcelli, A. Ghelli, S. Hrelia, M. Rugolo, Phospholipase D stimulation is required for sphingosine-1-phosphate activation of actin stress fibre assembly in human airway epithelial cells, *Cell. Signal.* 14 (2002) 75–81.
- [265] A. Ghelli, A.M. Porcelli, A. Facchini, S. Hrelia, F. Flamigni, M. Rugolo, Phospholipase D1 is threonine-phosphorylated in human-airway epithelial cells stimulated by sphingosine-1-phosphate by a mechanism involving Src tyrosine kinase and protein kinase Cdelta, *Biochem. J.* 366 (2002) 187–193. doi:10.1042/BJ20020264.
- [266] R.J. Cummings, N.L. Parinandi, A. Zaiman, L. Wang, P.V. Usatyuk, J.G.N. Garcia, V. Natarajan, Phospholipase D activation by sphingosine 1-phosphate regulates interleukin-8 secretion in human bronchial epithelial cells, *J. Biol. Chem.* 277 (2002) 30227–30235. doi:10.1074/jbc.M111078200.
- [267] L. Brizuela, M. Rábano, A. Peña, P. Gangoiti, J.M. Macarulla, M. Trueba, A. Gómez-Muñoz, Sphingosine 1-phosphate: a novel stimulator of aldosterone secretion, *J. Lipid Res.* 47 (2006) 1238–1249. doi:10.1194/jlr.M500510-JLR200.
- [268] E. Meacci, C. Donati, F. Cencetti, T. Oka, I. Komuro, M. Farnararo, P. Bruni, Dual regulation of sphingosine 1-phosphate-induced phospholipase D activity through RhoA and protein kinase C-alpha in C2C12 myoblasts, *Cell. Signal.* 13 (2001) 593–598.
- [269] Y. Banno, H. Fujita, Y. Ono, S. Nakashima, Y. Ito, N. Kuzumaki, Y. Nozawa, Differential phospholipase D activation by bradykinin and sphingosine 1-phosphate in NIH 3T3 fibroblasts overexpressing gelsolin, *J. Biol. Chem.* 274 (1999) 27385–27391.
- [270] E. Meacci, F. Nuti, S. Catarzi, V. Vasta, C. Donati, S. Bourgoïn, P. Bruni, J. Moss, M. Vaughan, Activation of phospholipase D by bradykinin and sphingosine 1-phosphate in A549 human lung adenocarcinoma cells via different GTP-binding proteins and protein kinase C delta signaling pathways, *Biochemistry (Mosc.)* 42 (2003) 284–292. doi:10.1021/bi026350a.
- [271] Y. Banno, H. Fujita, Y. Ono, S. Nakashima, Y. Ito, N. Kuzumaki, Y. Nozawa, Differential phospholipase D activation by bradykinin and sphingosine 1-phosphate in NIH 3T3 fibroblasts overexpressing gelsolin, *J. Biol. Chem.* 274 (1999) 27385–27391.
- [272] C. Delon, M. Manifava, E. Wood, D. Thompson, S. Krugmann, S. Pyne, N.T. Ktistakis, Sphingosine Kinase 1 Is an Intracellular Effector of Phosphatidic Acid, *J. Biol. Chem.* 279 (2004) 44763–44774. doi:10.1074/jbc.M405771200.
- [273] Z. Sartawi, E. Schipani, K.B. Ryan, C. Waeber, Sphingosine 1-phosphate (S1P) signalling: role in bone biology and potential therapeutic target for bone repair, *Pharmacol. Res.* (2017). doi:10.1016/j.phrs.2017.08.013.
- [274] R. Dziak, The role of sphingosine-1-phosphate (S1P) and lysophosphatidic acid (LPA) in regulation of osteoclastic and osteoblastic cells, *Immunol. Invest.* 42 (2013) 510–518. doi:10.3109/08820139.2013.823804.
- [275] Y. Hashimoto, M. Kobayashi, E. Matsuzaki, K. Higashi, F. Takahashi-Yanaga, A. Takano, M. Hirata, F. Nishimura, Sphingosine-1-phosphate-enhanced Wnt5a promotes osteogenic differentiation in C3H10T1/2 cells, *Cell Biol. Int.* 40 (2016) 1129–1136. doi:10.1002/cbin.10652.
- [276] Y. Hashimoto, E. Matsuzaki, K. Higashi, F. Takahashi-Yanaga, A. Takano, M. Hirata, F. Nishimura, Sphingosine-1-phosphate inhibits differentiation of C3H10T1/2 cells into adipocyte, *Mol. Cell. Biochem.* 401 (2015) 39–47. doi:10.1007/s11010-014-2290-1.
- [277] E. Matsuzaki, S. Hiratsuka, T. Hamachi, F. Takahashi-Yanaga, Y. Hashimoto, K. Higashi, M. Kobayashi, T. Hirofujii, M. Hirata, K. Maeda, Sphingosine-1-phosphate promotes the nuclear translocation of  $\beta$ -catenin and thereby induces osteoprotegerin gene expression in osteoblast-like cell lines, *Bone*. 55 (2013) 315–324. doi:10.1016/j.bone.2013.04.008.
- [278] K. Higashi, E. Matsuzaki, Y. Hashimoto, F. Takahashi-Yanaga, A. Takano, H. Anan, M. Hirata, F. Nishimura, Sphingosine-1-phosphate/S1PR2-mediated signaling triggers Smad1/5/8

- phosphorylation and thereby induces Runx2 expression in osteoblasts, *Bone*. 93 (2016) 1–11. doi:10.1016/j.bone.2016.09.003.
- [279] C. Bougault, A. El Jamal, A. Briolay, S. Mebarek, M.-A. Boutet, T. Garraud, B. Le Goff, F. Blanchard, D. Magne, L. Brizuela, Involvement of sphingosine kinase/sphingosine 1-phosphate metabolic pathway in spondyloarthritis, *Bone*. 103 (2017) 150–158. doi:10.1016/j.bone.2017.07.002.
- [280] L.-O. Brandenburg, T. Pufe, T. Koch, Role of phospholipase d in g-protein coupled receptor function, *Membranes*. 4 (2014) 302–318. doi:10.3390/membranes4030302.
- [281] R.C. Bruntz, C.W. Lindsley, H.A. Brown, Phospholipase D Signaling Pathways and Phosphatidic Acid as Therapeutic Targets in Cancer, *Pharmacol. Rev.* 66 (2014) 1033–1079. doi:10.1124/pr.114.009217.
- [282] S.G. Plonk, S.K. Park, J.H. Exton, The alpha-subunit of the heterotrimeric G protein G13 activates a phospholipase D isozyme by a pathway requiring Rho family GTPases, *J. Biol. Chem.* 273 (1998) 4823–4826.
- [283] A.M. Preininger, L.G. Henage, W.M. Oldham, E.J. Yoon, H.E. Hamm, H.A. Brown, Direct modulation of phospholipase D activity by Gbetagamma, *Mol. Pharmacol.* 70 (2006) 311–318. doi:10.1124/mol.105.021451.
- [284] T. Koch, L.-O. Brandenburg, S. Schulz, Y. Liang, J. Klein, V. Holtt, ADP-ribosylation factor-dependent phospholipase D2 activation is required for agonist-induced mu-opioid receptor endocytosis, *J. Biol. Chem.* 278 (2003) 9979–9985. doi:10.1074/jbc.M206709200.
- [285] H.A. Brown, P.G. Thomas, C.W. Lindsley, Targeting phospholipase D in cancer, infection and neurodegenerative disorders, *Nat. Rev. Drug Discov.* 16 (2017) 351–367. doi:10.1038/nrd.2016.252.
- [286] C. Zhao, G. Du, K. Skowronek, M.A. Frohman, D. Bar-Sagi, Phospholipase D2-generated phosphatidic acid couples EGFR stimulation to Ras activation by Sos, *Nat. Cell Biol.* 9 (2007) 706–712. doi:10.1038/ncb1594.
- [287] F.G. Buchanan, M. McReynolds, A. Couvillon, Y. Kam, V.R. Holla, R.N. DuBois, J.H. Exton, Requirement of phospholipase D1 activity in H-RasV12-induced transformation, *Proc. Natl. Acad. Sci. U. S. A.* 102 (2005) 1638–1642. doi:10.1073/pnas.0406698102.
- [288] F. Zhang, Z. Wang, M. Lu, Y. Yonekubo, X. Liang, Y. Zhang, P. Wu, Y. Zhou, S. Grinstein, J.F. Hancock, G. Du, Temporal production of the signaling lipid phosphatidic acid by phospholipase D2 determines the output of extracellular signal-regulated kinase signaling in cancer cells, *Mol. Cell. Biol.* 34 (2014) 84–95. doi:10.1128/MCB.00987-13.
- [289] R. Cipriano, B.L. Bryson, K.L.S. Miskimen, C.A. Bartel, W. Hernandez-Sanchez, R.C. Bruntz, S.A. Scott, C.W. Lindsley, H.A. Brown, M.W. Jackson, Hyperactivation of EGFR and downstream effector phospholipase D1 by oncogenic FAM83B, *Oncogene*. 33 (2014) 3298–3306. doi:10.1038/onc.2013.293.
- [290] Y. Kato, C.A. Lambert, A.C. Colige, P. Mineur, A. Noël, F. Frankenne, J.-M. Foidart, M. Baba, R.-I. Hata, K. Miyazaki, M. Tsukuda, Acidic extracellular pH induces matrix metalloproteinase-9 expression in mouse metastatic melanoma cells through the phospholipase D-mitogen-activated protein kinase signaling, *J. Biol. Chem.* 280 (2005) 10938–10944. doi:10.1074/jbc.M411313200.
- [291] R. Reich, M. Blumenthal, M. Liscovitch, Role of phospholipase D in laminin-induced production of gelatinase A (MMP-2) in metastatic cells, *Clin. Exp. Metastasis*. 13 (1995) 134–140.
- [292] Q. Chen, T. Hongu, T. Sato, Y. Zhang, W. Ali, J.-A. Cavallo, A. van der Velden, H. Tian, G. Di Paolo, B. Nieswandt, Y. Kanaho, M.A. Frohman, Key roles for the lipid signaling enzyme phospholipase d1 in the tumor microenvironment during tumor angiogenesis and metastasis, *Sci. Signal.* 5 (2012) ra79. doi:10.1126/scisignal.2003257.
- [293] Y. Zhang, M.A. Frohman, Cellular and physiological roles for phospholipase D1 in cancer, *J. Biol. Chem.* 289 (2014) 22567–22574. doi:10.1074/jbc.R114.576876.

- [294] J.N. Kanfer, I.N. Singh, J.W. Pettegrew, D.G. McCartney, G. Sorrentino, Phospholipid metabolism in Alzheimer's disease and in a human cholinergic cell, *J. Lipid Mediat. Cell Signal.* 14 (1996) 361–363. doi:10.1016/0929-7855(96)00545-7.
- [295] C. Ballard, S. Gauthier, A. Corbett, C. Brayne, D. Aarsland, E. Jones, Alzheimer's disease, *Lancet Lond. Engl.* 377 (2011) 1019–1031. doi:10.1016/S0140-6736(10)61349-9.
- [296] T.G. Oliveira, G. Di Paolo, Phospholipase D in brain function and Alzheimer's disease, *Biochim. Biophys. Acta.* 1801 (2010) 799–805. doi:10.1016/j.bbaliip.2010.04.004.
- [297] T.G. Oliveira, R.B. Chan, H. Tian, M. Laredo, G. Shui, A. Staniszewski, H. Zhang, L. Wang, T.-W. Kim, K.E. Duff, M.R. Wenk, O. Arancio, G. Di Paolo, Phospholipase d2 ablation ameliorates Alzheimer's disease-linked synaptic dysfunction and cognitive deficits, *J. Neurosci. Off. J. Soc. Neurosci.* 30 (2010) 16419–16428. doi:10.1523/JNEUROSCI.3317-10.2010.
- [298] A.T.K. Singh, A. Gilchrist, T. Voyno-Yasenetskaya, J.M. Radeff-Huang, P.H. Stern, G alpha12/G alpha13 subunits of heterotrimeric G proteins mediate parathyroid hormone activation of phospholipase D in UMR-106 osteoblastic cells, *Endocrinology.* 146 (2005) 2171–2175. doi:10.1210/en.2004-1283.
- [299] A.T.K. Singh, R.S. Bhattacharyya, J.M. Radeff, P.H. Stern, Regulation of parathyroid hormone-stimulated phospholipase D in UMR-106 cells by calcium, MAP kinase, and small G proteins, *J. Bone Miner. Res. Off. J. Am. Soc. Bone Miner. Res.* 18 (2003) 1453–1460. doi:10.1359/jbmr.2003.18.8.1453.
- [300] A.T.K. Singh, M.A. Frohman, P.H. Stern, Parathyroid hormone stimulates phosphatidylethanolamine hydrolysis by phospholipase D in osteoblastic cells, *Lipids.* 40 (2005) 1135–1140.
- [301] Y. Tian, Y. Xu, Q. Fu, M. He, Parathyroid hormone regulates osteoblast differentiation in a Wnt/ $\beta$ -catenin-dependent manner, *Mol. Cell. Biochem.* 355 (2011) 211–216. doi:10.1007/s11010-011-0856-8.
- [302] K. Suriyachand, A. Bunyaratvej, N. Bunyaratavej, M. Sila-Asna, Parathyroid hormone enhances osteoblast differentiation from human skin derived precursor cells in vitro, *J. Med. Assoc. Thai. Chotmaihet Thangphaet.* 94 Suppl 5 (2011) S1-6.
- [303] D.W. Kang, S.-H. Lee, J.W. Yoon, W.-S. Park, K.-Y. Choi, D.S. Min, Phospholipase D1 drives a positive feedback loop to reinforce the Wnt/ $\beta$ -catenin/TCF signaling axis, *Cancer Res.* 70 (2010) 4233–4242. doi:10.1158/0008-5472.CAN-09-3470.
- [304] D.W. Kang, C.Y. Choi, Y.-H. Cho, H. Tian, G. Di Paolo, K.-Y. Choi, D.S. Min, Targeting phospholipase D1 attenuates intestinal tumorigenesis by controlling  $\beta$ -catenin signaling in cancer-initiating cells, *J. Exp. Med.* 212 (2015) 1219–1237. doi:10.1084/jem.20141254.
- [305] H. Kaneki, J. Yokozawa, M. Fujieda, S. Mizuochi, C. Ishikawa, H. Ide, Phorbol ester-induced production of prostaglandin E2 from phosphatidylcholine through the activation of phospholipase D in UMR-106 cells, *Bone.* 23 (1998) 213–222.
- [306] O. Kozawa, A. Suzuki, J. Shinoda, N. Ozaki, Y. Oiso, T. Uematsu, Involvement of phospholipase D activation in endothelin-1-induced release of arachidonic acid in osteoblast-like cells, *J. Cell. Biochem.* 64 (1997) 376–381.
- [307] Y. Oiso, A. Suzuki, O. Kozawa, Effect of prostaglandin E2 on phospholipase D activity in osteoblast-like MC3T3-E1 cells, *J. Bone Miner. Res. Off. J. Am. Soc. Bone Miner. Res.* 10 (1995) 1185–1190. doi:10.1002/jbmr.5650100807.
- [308] S. Keila, A. Kelner, M. Weinreb, Systemic prostaglandin E2 increases cancellous bone formation and mass in aging rats and stimulates their bone marrow osteogenic capacity in vivo and in vitro, *J. Endocrinol.* 168 (2001) 131–139.
- [309] S. Choudhary, C. Alander, P. Zhan, Q. Gao, C. Pilbeam, L. Raisz, Effect of deletion of the prostaglandin EP2 receptor on the anabolic response to prostaglandin E2 and a selective EP2 receptor agonist, *Prostaglandins Other Lipid Mediat.* 86 (2008) 35–40. doi:10.1016/j.prostaglandins.2008.02.001.
- [310] C.B. Alander, L.G. Raisz, Effects of selective prostaglandins E2 receptor agonists on cultured calvarial murine osteoblastic cells, *Prostaglandins Other Lipid Mediat.* 81 (2006) 178–183. doi:10.1016/j.prostaglandins.2006.09.005.

- [311] K. Yoshida, H. Oida, T. Kobayashi, T. Maruyama, M. Tanaka, T. Katayama, K. Yamaguchi, E. Segi, T. Tsuboyama, M. Matsushita, K. Ito, Y. Ito, Y. Sugimoto, F. Ushikubi, S. Ohuchida, K. Kondo, T. Nakamura, S. Narumiya, Stimulation of bone formation and prevention of bone loss by prostaglandin E EP4 receptor activation, *Proc. Natl. Acad. Sci. U. S. A.* 99 (2002) 4580–4585. doi:10.1073/pnas.062053399.
- [312] D. Shamir, S. Keila, M. Weinreb, A selective EP4 receptor antagonist abrogates the stimulation of osteoblast recruitment from bone marrow stromal cells by prostaglandin E2 in vivo and in vitro, *Bone*. 34 (2004) 157–162.
- [313] X.-H. Liu, A. Kirschenbaum, B.M. Weinstein, M. Zaidi, S. Yao, A.C. Levine, Prostaglandin E2 modulates components of the Wnt signaling system in bone and prostate cancer cells, *Biochem. Biophys. Res. Commun.* 394 (2010) 715–720. doi:10.1016/j.bbrc.2010.03.057.
- [314] M. Feigenson, R.A. Eliseev, J.H. Jonason, B.N. Mills, R.J. O’Keefe, PGE2 Receptor Subtype 1 (EP1) Regulates Mesenchymal Stromal Cell Osteogenic Differentiation by Modulating Cellular Energy Metabolism, *J. Cell. Biochem.* (2017). doi:10.1002/jcb.26092.
- [315] A. Mirsaidi, A.N. Tiaden, P.J. Richards, Prostaglandin E2 inhibits matrix mineralization by human bone marrow stromal cell-derived osteoblasts via Epac-dependent cAMP signaling, *Sci. Rep.* 7 (2017). doi:10.1038/s41598-017-02650-y.
- [316] M.K. Shin, Y.H. Jang, H.J. Yoo, D.W. Kang, M.H. Park, M.K. Kim, J.H. Song, S.D. Kim, G. Min, H.K. You, K.-Y. Choi, Y.-S. Bae, D.S. Min, N-Formyl-Methionyl-Leucyl-Phenylalanine (fMLP) Promotes Osteoblast Differentiation via the N-Formyl Peptide Receptor 1-mediated Signaling Pathway in Human Mesenchymal Stem Cells from Bone Marrow, *J. Biol. Chem.* 286 (2011) 17133–17143. doi:10.1074/jbc.M110.197772.
- [317] M.-J. Kim, M.-U. Choi, C.-W. Kim, Activation of phospholipase D1 by surface roughness of titanium in MG63 osteoblast-like cell, *Biomaterials*. 27 (2006) 5502–5511. doi:10.1016/j.biomaterials.2006.06.023.
- [318] M. Fang, R. Olivares-Navarrete, M. Wieland, D.L. Cochran, B.D. Boyan, Z. Schwartz, The role of phospholipase D in osteoblast response to titanium surface microstructure, *J. Biomed. Mater. Res. A*. 93 (2010) 897–909. doi:10.1002/jbm.a.32596.
- [319] S. Helm, V.L. Sylvia, T. Harmon, D.D. Dean, B.D. Boyan, Z. Schwartz, 24,25-(OH)2D3 regulates protein kinase C through two distinct phospholipid-dependent mechanisms, *J. Cell. Physiol.* 169 (1996) 509–521. doi:10.1002/(SICI)1097-4652(199612)169:3<509::AID-JCP11>3.0.CO;2-0.
- [320] Z. Schwartz, D.D. Dean, J.K. Walton, B.P. Brooks, B.D. Boyan, Treatment of resting zone chondrocytes with 24,25-dihydroxyvitamin D3 [24,25-(OH)2D3] induces differentiation into a 1,25-(OH)2D3-responsive phenotype characteristic of growth zone chondrocytes, *Endocrinology*. 136 (1995) 402–411. doi:10.1210/endo.136.2.7530645.
- [321] V.L. Sylvia, Z. Schwartz, F. Del Toro, P. DeVeau, R. Whetstone, R.R. Hardin, D.D. Dean, B.D. Boyan, Regulation of phospholipase D (PLD) in growth plate chondrocytes by 24R,25-(OH)2D3 is dependent on cell maturation state (resting zone cells) and is specific to the PLD2 isoform, *Biochim. Biophys. Acta*. 1499 (2001) 209–221.
- [322] J. Kim, G. Min, Y.-S. Bae, D.S. Min, Phospholipase D is involved in oxidative stress-induced migration of vascular smooth muscle cells via tyrosine phosphorylation and protein kinase C, *Exp. Mol. Med.* 36 (2004) 103–109. doi:10.1038/emm.2004.15.
- [323] Y. Banno, S. Wang, Y. Ito, T. Izumi, S. Nakashima, T. Shimizu, Y. Nozawa, Involvement of ERK and p38 MAP kinase in oxidative stress-induced phospholipase D activation in PC12 cells, *Neuroreport*. 12 (2001) 2271–2275.
- [324] W. Feng, K. Zhang, Y. Liu, J. Chen, Q. Cai, Y. Zhang, M. Wang, J. Wang, H. Huang, Apocynin attenuates angiotensin II-induced vascular smooth muscle cells osteogenic switching via suppressing extracellular signal-regulated kinase 1/2, *Oncotarget*. 7 (2016) 83588–83600. doi:10.18632/oncotarget.13193.
- [325] G. Jia, R.M. Stormont, D.M. Gangahar, D.K. Agrawal, Role of matrix Gla protein in angiotensin II-induced exacerbation of vascular calcification, *Am. J. Physiol. Heart Circ. Physiol.* 303 (2012) H523-532. doi:10.1152/ajpheart.00826.2011.

- [326] C. Herencia, M.E. Rodríguez-Ortiz, J.R. Muñoz-Castañeda, J.M. Martínez-Moreno, R. Canalejo, A. Montes de Oca, J.M. Díaz-Tocados, E. Peralbo-Santaella, C. Marín, A. Canalejo, M. Rodríguez, Y. Almaden, Angiotensin II prevents calcification in vascular smooth muscle cells by enhancing magnesium influx, *Eur. J. Clin. Invest.* 45 (2015) 1129–1144. doi:10.1111/eci.12517.
- [327] Z.B. Armstrong, D.R. Boughner, M. Drangova, K.A. Rogers, Angiotensin II type 1 receptor blocker inhibits arterial calcification in a pre-clinical model, *Cardiovasc. Res.* 90 (2011) 165–170. doi:10.1093/cvr/cvq391.
- [328] E.J. Freeman, E.A. Tallant, Vascular smooth-muscle cells contain AT1 angiotensin receptors coupled to phospholipase D activation, *Biochem. J.* 304 ( Pt 2) (1994) 543–548.
- [329] R.M. Touyz, E.L. Schiffrin, Ang II-stimulated superoxide production is mediated via phospholipase D in human vascular smooth muscle cells, *Hypertens. Dallas Tex* 1979. 34 (1999) 976–982.
- [330] M. Ushio-Fukai, R.W. Alexander, M. Akers, P.R. Lyons, B. Lassègue, K.K. Griendling, Angiotensin II receptor coupling to phospholipase D is mediated by the betagamma subunits of heterotrimeric G proteins in vascular smooth muscle cells, *Mol. Pharmacol.* 55 (1999) 142–149.
- [331] K. Yasunari, K. Maeda, M. Nakamura, J. Yoshikawa, Pressure Promotes Angiotensin II–Mediated Migration of Human Coronary Smooth Muscle Cells Through Increase in Oxidative Stress, *Hypertension.* 39 (2002) 433–437. doi:10.1161/hy02t2.102991.
- [332] Y. Song, M. Hou, Z. Li, C. Luo, J.-S. Ou, H. Yu, J. Yan, L. Lu, TLR4/NF- $\kappa$ B/Ceramide signaling contributes to Ox-LDL-induced calcification of human vascular smooth muscle cells, *Eur. J. Pharmacol.* 794 (2017) 45–51. doi:10.1016/j.ejphar.2016.11.029.
- [333] L. Liao, Q. Zhou, Y. Song, W. Wu, H. Yu, S. Wang, Y. Chen, M. Ye, L. Lu, Ceramide Mediates Ox-LDL-Induced Human Vascular Smooth Muscle Cell Calcification via p38 Mitogen-Activated Protein Kinase Signaling, *PLOS ONE.* 8 (2013) e82379. doi:10.1371/journal.pone.0082379.
- [334] V. Natarajan, W.M. Scribner, C.M. Hart, S. Parthasarathy, Oxidized low density lipoprotein-mediated activation of phospholipase D in smooth muscle cells: a possible role in cell proliferation and atherogenesis, *J. Lipid Res.* 36 (1995) 2005–2016.
- [335] A. Gómez-Muñoz, J.S. Martens, U.P. Steinbrecher, Stimulation of phospholipase D activity by oxidized LDL in mouse peritoneal macrophages, *Arterioscler. Thromb. Vasc. Biol.* 20 (2000) 135–143.
- [336] M.-R. Ammar, Y. Humeau, A. Hanauer, B. Nieswandt, M.-F. Bader, N. Vitale, The Coffin-Lowry syndrome-associated protein RSK2 regulates neurite outgrowth through phosphorylation of phospholipase D1 (PLD1) and synthesis of phosphatidic acid, *J. Neurosci. Off. J. Soc. Neurosci.* 33 (2013) 19470–19479. doi:10.1523/JNEUROSCI.2283-13.2013.
- [337] M.R. Ammar, T. Thahouly, A. Hanauer, D. Stegner, B. Nieswandt, N. Vitale, PLD1 participates in BDNF-induced signalling in cortical neurons, *Sci. Rep.* 5 (2015) 14778. doi:10.1038/srep14778.
- [338] S.A. Scott, P.E. Selvy, J.R. Buck, H.P. Cho, T.L. Criswell, A.L. Thomas, M.D. Armstrong, C.L. Arteaga, C.W. Lindsley, H.A. Brown, Design of isoform-selective phospholipase D inhibitors that modulate cancer cell invasiveness, *Nat. Chem. Biol.* 5 (2009) 108–117. doi:10.1038/nchembio.140.
- [339] M. Hui, H.C. Tenenbaum, New face of an old enzyme: alkaline phosphatase may contribute to human tissue aging by inducing tissue hardening and calcification, *Anat. Rec.* 253 (1998) 91–94.
- [340] P.K. Smith, R.I. Krohn, G.T. Hermanson, A.K. Mallia, F.H. Gartner, M.D. Provenzano, E.K. Fujimoto, N.M. Goeke, B.J. Olson, D.C. Klenk, Measurement of protein using bicinchoninic acid, *Anal. Biochem.* 150 (1985) 76–85.
- [341] W.R. Moorehead, H.G. Biggs, 2-Amino-2-methyl-1-propanol as the alkalizing agent in an improved continuous-flow cresolphthalein complexone procedure for calcium in serum, *Clin. Chem.* 20 (1974) 1458–1460.

- [342] E.G. Bligh, W.J. Dyer, A rapid method of total lipid extraction and purification, *Can. J. Biochem. Physiol.* 37 (1959) 911–917. doi:10.1139/o59-099.
- [343] M. Balcerzak, S. Pikula, R. Buchet, Phosphorylation-dependent phospholipase D activity of matrix vesicles, *FEBS Lett.* 580 (2006) 5676–5680. doi:10.1016/j.febslet.2006.09.018.
- [344] H. Qiao, J. Bell, S. Juliao, L. Li, J.M. May, Ascorbic Acid Uptake and Regulation of Type I Collagen Synthesis in Cultured Vascular Smooth Muscle Cells, *J. Vasc. Res.* 46 (2009) 15–24. doi:10.1159/000135661.
- [345] S. Murad, D. Grove, K.A. Lindberg, G. Reynolds, A. Sivarajah, S.R. Pinnell, Regulation of collagen synthesis by ascorbic acid., *Proc. Natl. Acad. Sci. U. S. A.* 78 (1981) 2879–2882.
- [346] D. Darr, S. Combs, S. Pinnell, Ascorbic acid and collagen synthesis: rethinking a role for lipid peroxidation, *Arch. Biochem. Biophys.* 307 (1993) 331–335. doi:10.1006/abbi.1993.1596.
- [347] H. Orimo, T. Shimada, The role of tissue-nonspecific alkaline phosphatase in the phosphate-induced activation of alkaline phosphatase and mineralization in SaOS-2 human osteoblast-like cells, *Mol. Cell. Biochem.* 315 (2008) 51–60. doi:10.1007/s11010-008-9788-3.
- [348] L.C. Gerstenfeld, F.D. Shapiro, Expression of bone-specific genes by hypertrophic chondrocytes: implication of the complex functions of the hypertrophic chondrocyte during endochondral bone development, *J. Cell. Biochem.* 62 (1996) 1–9. doi:10.1002/(SICI)1097-4644(199607)62:1<1::AID-JCB1>3.0.CO;2-X.
- [349] V. Brinkmann, A. Billich, T. Baumruker, P. Heining, R. Schmouder, G. Francis, S. Aradhye, P. Burtin, Fingolimod (FTY720): discovery and development of an oral drug to treat multiple sclerosis, *Nat. Rev. Drug Discov.* 9 (2010) 883–897. doi:10.1038/nrd3248.
- [350] M.H. Gräler, E.J. Goetzl, The immunosuppressant FTY720 down-regulates sphingosine 1-phosphate G-protein-coupled receptors, *FASEB J. Off. Publ. Fed. Am. Soc. Exp. Biol.* 18 (2004) 551–553. doi:10.1096/fj.03-0910fje.
- [351] D. Pchejetski, T. Bohler, L. Brizuela, L. Sauer, N. Doumerc, M. Golzio, V. Salunkhe, J. Teissié, B. Malavaud, J. Waxman, O. Cuvillier, FTY720 (fingolimod) sensitizes prostate cancer cells to radiotherapy by inhibition of sphingosine kinase-1, *Cancer Res.* 70 (2010) 8651–8661. doi:10.1158/0008-5472.CAN-10-1388.
- [352] M. Maceyka, H. Sankala, N.C. Hait, H. Le Stunff, H. Liu, R. Toman, C. Collier, M. Zhang, L.S. Satin, A.H. Merrill, S. Milstien, S. Spiegel, SphK1 and SphK2, sphingosine kinase isoenzymes with opposing functions in sphingolipid metabolism, *J. Biol. Chem.* 280 (2005) 37118–37129. doi:10.1074/jbc.M502207200.
- [353] H.A. Neubauer, S.M. Pitson, Roles, regulation and inhibitors of sphingosine kinase 2, *FEBS J.* 280 (2013) 5317–5336. doi:10.1111/febs.12314.
- [354] M.A. Kraus, P.A. Kalra, J. Hunter, J. Menoyo, N. Stankus, The prevalence of vascular calcification in patients with end-stage renal disease on hemodialysis: a cross-sectional observational study, *Ther. Adv. Chronic Dis.* 6 (2015) 84–96. doi:10.1177/2040622315578654.
- [355] J.L. Górriz, P. Molina, M.J. Cerverón, R. Vila, J. Bover, J. Nieto, G. Barril, A. Martínez-Castelao, E. Fernández, V. Escudero, C. Piñera, T. Adragao, J.F. Navarro-Gonzalez, L.M. Molinero, C. Castro-Alonso, L.M. Pallardó, S.A. Jamal, Vascular calcification in patients with nondialysis CKD over 3 years, *Clin. J. Am. Soc. Nephrol. CJASN.* 10 (2015) 654–666. doi:10.2215/CJN.07450714.
- [356] Y. Tatami, Y. Yasuda, S. Suzuki, H. Ishii, A. Sawai, Y. Shibata, T. Ota, K. Shibata, M. Niwa, R. Morimoto, M. Hayashi, S. Kato, S. Maruyama, T. Murohara, Impact of abdominal aortic calcification on long-term cardiovascular outcomes in patients with chronic kidney disease, *Atherosclerosis.* 243 (2015) 349–355. doi:10.1016/j.atherosclerosis.2015.10.016.
- [357] V. Natarajan, W.M. Scribner, C.M. Hart, S. Parthasarathy, Oxidized low density lipoprotein-mediated activation of phospholipase D in smooth muscle cells: a possible role in cell proliferation and atherogenesis, *J. Lipid Res.* 36 (1995) 2005–2016.
- [358] T. Tani, H. Orimo, A. Shimizu, S. Tsuruoka, Development of a novel chronic kidney disease mouse model to evaluate the progression of hyperphosphatemia and associated mineral bone disease, *Sci. Rep.* 7 (2017) 2233. doi:10.1038/s41598-017-02351-6.

- [359] W.-K. Hua, Y.-H. Shiau, O.K. Lee, W.-J. Lin, Elevation of protein kinase  $\alpha$  stimulates osteogenic differentiation of mesenchymal stem cells through the TAT-mediated protein transduction system, *Biochem. Cell Biol. Biochim. Biol. Cell.* 91 (2013) 443–448. doi:10.1139/bcb-2013-0035.
- [360] A. Nakura, C. Higuchi, K. Yoshida, H. Yoshikawa, PKC $\alpha$  suppresses osteoblastic differentiation, *Bone*. 48 (2011) 476–484. doi:10.1016/j.bone.2010.09.238.
- [361] E. Matsuzaki, S. Hiratsuka, T. Hamachi, F. Takahashi-Yanaga, Y. Hashimoto, K. Higashi, M. Kobayashi, T. Hirofujii, M. Hirata, K. Maeda, Sphingosine-1-phosphate promotes the nuclear translocation of  $\beta$ -catenin and thereby induces osteoprotegerin gene expression in osteoblast-like cell lines, *Bone*. 55 (2013) 315–324. doi:10.1016/j.bone.2013.04.008.
- [362] S.W. Paugh, S.G. Payne, S.E. Barbour, S. Milstien, S. Spiegel, The immunosuppressant FTY720 is phosphorylated by sphingosine kinase type 2, *FEBS Lett.* 554 (2003) 189–193.
- [363] F. Tonelli, K.G. Lim, C. Loveridge, J. Long, S.M. Pitson, G. Tigyi, R. Bittman, S. Pyne, N.J. Pyne, FTY720 and (S)-FTY720 vinylphosphonate inhibit sphingosine kinase 1 and promote its proteasomal degradation in human pulmonary artery smooth muscle, breast cancer and androgen-independent prostate cancer cells, *Cell. Signal.* 22 (2010) 1536–1542. doi:10.1016/j.cellsig.2010.05.022.
- [364] O. Cuvillier, Les récepteurs de la sphingosine 1-phosphate - De la biologie à la physiopathologie, *médecine/sciences*. 28 (2012) 951–957. doi:10.1051/medsci/20122811013.
- [365] N.J. Pyne, S. Pyne, Selectivity and Specificity of Sphingosine 1-Phosphate Receptor Ligands: “Off-Targets” or Complex Pharmacology?, *Front. Pharmacol.* 2 (2011). doi:10.3389/fphar.2011.00026.
- [366] C.W. Lindsley, H.A. Brown, Phospholipase D as a Therapeutic Target in Brain Disorders, *Neuropsychopharmacology*. 37 (2012) 301–302. doi:10.1038/npp.2011.178.
- [367] R. Neale, S. Fallon, S. Gerhardt, J.M. Liebman, Acute dyskinesias in monkeys elicited by haloperamide, mezilamine and the “antidyskinetic” drugs, oxiperomide and tiapride, *Psychopharmacology (Berl.)*. 75 (1981) 254–257. doi:10.1007/BF00432434.
- [368] M.A. Frohman, The phospholipase D superfamily as therapeutic targets, *Trends Pharmacol. Sci.* 36 (2015) 137–144. doi:10.1016/j.tips.2015.01.001.
- [369] J.M. Joy, D.M. Gundermann, R.P. Lowery, R. Jäger, S.A. McCleary, M. Purpura, M.D. Roberts, S.M. Wilson, T.A. Hornberger, J.M. Wilson, Phosphatidic acid enhances mTOR signaling and resistance exercise induced hypertrophy, *Nutr. Metab.* 11 (2014) 29. doi:10.1186/1743-7075-11-29.
- [370] J.S. You, J.W. Frey, T.A. Hornberger, Mechanical Stimulation Induces mTOR Signaling via an ERK-Independent Mechanism: Implications for a Direct Activation of mTOR by Phosphatidic Acid, *PLoS ONE*. 7 (2012). doi:10.1371/journal.pone.0047258.
- [371] M.-S. Yoon, Y. Sun, E. Arauz, Y. Jiang, J. Chen, Phosphatidic Acid Activates Mammalian Target of Rapamycin Complex 1 (mTORC1) Kinase by Displacing FK506 Binding Protein 38 (FKBP38) and Exerting an Allosteric Effect, *J. Biol. Chem.* 286 (2011) 29568–29574. doi:10.1074/jbc.M111.262816.
- [372] C.H. Jung, S.-H. Ro, J. Cao, N.M. Otto, D.-H. Kim, mTOR regulation of autophagy, *FEBS Lett.* 584 (2010) 1287–1295. doi:10.1016/j.febslet.2010.01.017.
- [373] M. Nollet, S. Santucci-Darmanin, V. Breuil, R. Al-Sahlane, C. Cros, M. Topi, D. Momier, M. Samson, S. Pagnotta, L. Cailleteau, S. Battaglia, D. Farlay, R. Dacquin, N. Barois, P. Jurdic, G. Boivin, D. Heymann, F. Lafont, S.S. Lu, D.W. Dempster, G.F. Carle, V. Pierrefite-Carle, Autophagy in osteoblasts is involved in mineralization and bone homeostasis, *Autophagy*. 10 (2014) 1965–1977. doi:10.4161/auto.36182.
- [374] I.-R. Kim, S.-E. Kim, H.-S. Baek, B.-J. Kim, C.-H. Kim, I.-K. Chung, B.-S. Park, S.-H. Shin, The role of kaempferol-induced autophagy on differentiation and mineralization of osteoblastic MC3T3-E1 cells, *BMC Complement. Altern. Med.* 16 (2016) 333. doi:10.1186/s12906-016-1320-9.
- [375] A. Pantovic, A. Krstic, K. Janjetovic, J. Kocic, L. Harhaji-Trajkovic, D. Bugarski, V. Trajkovic, Coordinated time-dependent modulation of AMPK/Akt/mTOR signaling and autophagy

- controls osteogenic differentiation of human mesenchymal stem cells, *Bone*. 52 (2013) 524–531. doi:10.1016/j.bone.2012.10.024.
- [376] X.-Y. Dai, M.-M. Zhao, Y. Cai, Q.-C. Guan, Y. Zhao, Y. Guan, W. Kong, W.-G. Zhu, M.-J. Xu, X. Wang, Phosphate-induced autophagy counteracts vascular calcification by reducing matrix vesicle release, *Kidney Int.* 83 (2013) 1042–1051. doi:10.1038/ki.2012.482.
- [377] D. Liu, W. Cui, B. Liu, H. Hu, J. Liu, R. Xie, X. Yang, G. Gu, J. Zhang, H. Zheng, Atorvastatin protects vascular smooth muscle cells from TGF- $\beta$ 1-stimulated calcification by inducing autophagy via suppression of the  $\beta$ -catenin pathway, *Cell. Physiol. Biochem. Int. J. Exp. Cell. Physiol. Biochem. Pharmacol.* 33 (2014) 129–141. doi:10.1159/000356656.
- [378] R.N.A. Cecil, H. Clarke Anderson, Freeze-fracture studies of matrix vesicle calcification in epiphyseal growth plate, *Metab. Bone Dis. Relat. Res.* 1 (1978) 89–95. doi:10.1016/0221-8747(78)90043-7.
- [379] H.C. Anderson, R. Garimella, S.E. Tague, The role of matrix vesicles in growth plate development and biomineralization, *Front. Biosci. J. Virtual Libr.* 10 (2005) 822–837.
- [380] C. Thouverey, A. Strzelecka-Kiliszek, M. Balcerzak, R. Buchet, S. Pikula, Matrix vesicles originate from apical membrane microvilli of mineralizing osteoblast-like Saos-2 cells, *J. Cell. Biochem.* 106 (2009) 127–138. doi:10.1002/jcb.21992.
- [381] C. Thouverey, A. Malinowska, M. Balcerzak, A. Strzelecka-Kiliszek, R. Buchet, M. Dadlez, S. Pikula, Proteomic characterization of biogenesis and functions of matrix vesicles released from mineralizing human osteoblast-like cells, *J. Proteomics.* 74 (2011) 1123–1134. doi:10.1016/j.jprot.2011.04.005.
- [382] J.E. Hale, R.E. Wuthier, The mechanism of matrix vesicle formation. Studies on the composition of chondrocyte microvilli and on the effects of microfilament-perturbing agents on cellular vesiculation, *J. Biol. Chem.* 262 (1987) 1916–1925.
- [383] D. Abdallah, E. Hamade, R.A. Merhi, B. Bassam, R. Buchet, S. Mebarek, Fatty acid composition in matrix vesicles and in microvilli from femurs of chicken embryos revealed selective recruitment of fatty acids, *Biochem. Biophys. Res. Commun.* 446 (2014) 1161–1164. doi:10.1016/j.bbrc.2014.03.069.
- [384] W.H. Ali, Q. Chen, K.E. Delgiorno, W. Su, J.C. Hall, T. Hongu, H. Tian, Y. Kanaho, G.D. Paolo, H.C. Crawford, M.A. Frohman, Deficiencies of the Lipid-Signaling Enzymes Phospholipase D1 and D2 Alter Cytoskeletal Organization, Macrophage Phagocytosis, and Cytokine-Stimulated Neutrophil Recruitment, *PLOS ONE*. 8 (2013) e55325. doi:10.1371/journal.pone.0055325.
- [385] M.J. Cross, S. Roberts, A.J. Ridley, M.N. Hodgkin, A. Stewart, L. Claesson-Welsh, M.J. Wakelam, Stimulation of actin stress fibre formation mediated by activation of phospholipase D, *Curr. Biol. CB*. 6 (1996) 588–597.
- [386] Y. Kam, J.H. Exton, Phospholipase D Activity Is Required for Actin Stress Fiber Formation in Fibroblasts, *Mol. Cell. Biol.* 21 (2001) 4055–4066. doi:10.1128/MCB.21.12.4055-4066.2001.
- [387] A.N. Roach, Z. Wang, P. Wu, F. Zhang, R.B. Chan, Y. Yonekubo, G. Di Paolo, A.A. Gorfe, G. Du, Phosphatidic acid regulation of PIPKI is critical for actin cytoskeletal reorganization, *J. Lipid Res.* 53 (2012) 2598–2609. doi:10.1194/jlr.M028597.
- [388] S. Zouwail, T.R. Pettitt, S.K. Dove, M.V. Chibalina, D.J. Powner, L. Haynes, M.J.O. Wakelam, R.H. Insall, Phospholipase D activity is essential for actin localization and actin-based motility in *Dictyostelium*, *Biochem. J.* 389 (2005) 207–214. doi:10.1042/BJ20050085.
- [389] W. Jiang, Z. Zhang, H. Yang, Q. Lin, C. Han, X. Qin, The Involvement of miR-29b-3p in Arterial Calcification by Targeting Matrix Metalloproteinase-2, *BioMed Res. Int.* 2017 (2017). doi:10.1155/2017/6713606.
- [390] null Yasmin, C.M. McEniery, S. Wallace, Z. Dakham, P. Pulsalkar, P. Pusalkar, K. Maki-Petaja, M.J. Ashby, J.R. Cockcroft, I.B. Wilkinson, Matrix metalloproteinase-9 (MMP-9), MMP-2, and serum elastase activity are associated with systolic hypertension and arterial stiffness, *Arterioscler. Thromb. Vasc. Biol.* 25 (2005) 372. doi:10.1161/01.ATV.0000151373.33830.41.
- [391] M.H. Park, B.-H. Ahn, Y.-K. Hong, D.S. Min, Overexpression of phospholipase D enhances matrix metalloproteinase-2 expression and glioma cell invasion via protein kinase C and

- protein kinase A/NF-kappaB/Sp1-mediated signaling pathways, *Carcinogenesis*. 30 (2009) 356–365. doi:10.1093/carcin/bgn287.
- [392] B.T. Williger, W.T. Ho, J.H. Exton, Phospholipase D mediates matrix metalloproteinase-9 secretion in phorbol ester-stimulated human fibrosarcoma cells, *J. Biol. Chem.* 274 (1999) 735–738.
- [393] V.A. Blaho, T. Hla, An update on the biology of sphingosine 1-phosphate receptors, *J. Lipid Res.* 55 (2014) 1596–1608. doi:10.1194/jlr.R046300.
- [394] W.N. Suki, L.W. Moore, Phosphorus Regulation in Chronic Kidney Disease, *Methodist DeBakey Cardiovasc. J.* 12 (2016) 6–9. doi:10.14797/mdcj-12-4s1-6.
- [395] M. Schuchardt, M. Tölle, J. Prüfer, M. van der Giet, Pharmacological relevance and potential of sphingosine 1-phosphate in the vascular system, *Br. J. Pharmacol.* 163 (2011) 1140–1162. doi:10.1111/j.1476-5381.2011.01260.x.

## **Annex**

### **Article 1**

#### **Characterization and assessment of potential microRNAs involved in phosphate-induced aortic calcification**

Accepted article

Journal: Journal of Cellular Physiology

Date of acceptance: 01-Aug-2017

Reference: JCP-17-0234.R1

My position: Co-first author

My contribution to the work was done during the 9 months of the first year of my PhD thesis, in Lebanon: Laboratory of Cancer Biology and Molecular Immunology, Faculty of Sciences I, Lebanese University, Hadath, Beirut, Lebanon and Cardiovascular Physiology Lab, Department of Anatomy, Cell Biology and Physiology, Faculty of Medicine, American University of Beirut, Beirut, Lebanon.

Maya Fakhry<sup>1,2†</sup>, Najwa Skafi <sup>1,2†</sup>, Mohammad Fayyad-Kazan<sup>3</sup>, Firas Kobeissy<sup>4</sup>, Eva Hamade<sup>1\*</sup>, Saida Mebarek<sup>2</sup>, Aida Habib<sup>4,5</sup>, Nada Borghol<sup>2</sup>, Asad Zeidan<sup>6\*</sup>, David Magne<sup>2</sup>, Hussein Fayyad-Kazan <sup>1≈</sup> and Bassam Badran <sup>1≈</sup>

<sup>1</sup>Laboratory of Cancer Biology and Molecular Immunology, Faculty of Sciences I, Lebanese University, Hadath, Beirut, Lebanon, <sup>2</sup>Institute of Molecular and Supramolecular Chemistry and Biochemistry (ICBMS), UMR CNRS 5246, University of Lyon 1, Bâtiment Raulin, 43 Boulevard du 11 Novembre 1918, 69622 Villeurbanne Cedex, France, <sup>3</sup>Institut de Biologie et

de Médecine Moléculaires, Université Libre de Bruxelles, 6041 Gosselies, Belgium,

<sup>4</sup>Department of Biochemistry and Molecular Genetics, Faculty of Medicine, American University of Beirut, Beirut, Lebanon, <sup>5</sup>INSERM-U1149, CNRS-ERL8252, Centre de Recherche sur l'Inflammation, and the Sorbonne Paris Cité, Laboratoire d'Excellence Inflammex, Faculté de Médecine, Site Xavier Bichat, Université Paris Diderot, Paris, France.

<sup>6</sup>Cardiovascular Physiology Lab, Department of Anatomy, Cell Biology and Physiology, Faculty of Medicine, American University of Beirut, Beirut, Lebanon.

†, ≈These authors contributed equally to this work.

\* **Corresponding authors: Eva Hamade.** Laboratory of Cancer Biology and Molecular Immunology, Lebanese University, Faculty of Sciences I, Hadath, Beirut, Lebanon. Phone: +9613062719; Email: [eva.hamade@ul.edu.lb](mailto:eva.hamade@ul.edu.lb)

**Asad Zeidan.** Department of Anatomy, Cell Biology and Physiological Sciences, American University of Beirut, Faculty of Medicine. DTS, PO BOX 11-0236, Beirut 1107-2020. Phone: +961-1-350000 ext. office 4818; Email: [asad.zeidan@aub.edu.lb](mailto:asad.zeidan@aub.edu.lb)

**Running head:** Potential microRNAs in aortic calcification

**Key-words:** microRNAs; aorta; inorganic phosphate; calcification; trans-differentiation

**Total number of figures:** 6 figures

**Contract grant sponsor:** This study was supported by grants and scholarships from the Lebanese University and the Lebanese National Council for Scientific Research (CNRS-L, grant # 05-06 2014, E.H.).

## **Abstract (WORD # 250)**

Medial artery calcification, a hallmark of type 2 diabetes mellitus and chronic kidney disease (CKD), is known as an independent risk factor for cardiovascular mortality and morbidity. Hyperphosphatemia associated with CKD is a strong stimulator of vascular calcification but the molecular mechanisms regulating this process remain not fully understood. We showed that calcification was induced after exposing Sprague-Dawley rat aortic explants to high inorganic phosphate level ( $P_i$ , 6 mM) as examined by Alizarin red and Von Kossa staining. This calcification was associated with high Tissue-Nonspecific Alkaline Phosphatase (TNAP) activity, vascular smooth muscle cells de-differentiation, manifested by downregulation of smooth muscle 22 alpha ( $SM22\alpha$ ) protein expression which was assessed by immunoblot analysis, immunofluorescence, and trans-differentiation into osteochondrocyte-like cells revealed by upregulation of Runt related transcription factor 2 (Runx2), TNAP, osteocalcin, and osteopontin mRNA levels which were determined by quantitative real-time PCR. To unravel the possible mechanism(s) involved in this process, microRNA (miR) expression profile, which was assessed using TLDA technique and thereafter confirmed by individual qRT-PCR, revealed differential expression 10 miRs, five at day 3 and 5 at day 6 post  $P_i$  treatment versus control untreated aortas. At day 3, miR-200c, -155, 322 were upregulated and miR-708 and 331 were downregulated. After 6 days of treatment, miR-328, -546, -301a were upregulated whilst miR-409 and miR-542 were downregulated. Our results indicate that high  $P_i$  levels trigger aortic calcification and modulation of certain miRs. These observations suggest that mechanisms regulating aortic calcification might involve miRs, which warrant further investigations in future studies.

## 1. Introduction

Medial vascular calcification is a pathological process associated with chronic kidney disease (CKD) and type II diabetes mellitus (Sage et al., 2010; Zhu et al., 2012). Cardiovascular mortality in CKD dialysis patients is 10-20 times higher than in the general population, and accounts for more than half of all deaths in CKD patients (Foley et al., 1998a; Foley et al., 1998b; Gansevoort et al., 2011; Schlieper et al., 2008; Blacher et al., 2001; Sigrist et al., 2007). Virtually, all hemodialysis patients develop coronary artery calcification (Goodman et al., 2000) which is a strong predictor of coronary heart disease in patients with end-stage renal disease (ESRD, stage 5 CKD) (London et al., 2003). Clinically, the calcification of the medial layer mainly leads to an increase in arterial stiffness which can have an extremely detrimental effect, especially when considering large arteries, like the aorta (London et al., 2003). Normally, due to its elasticity, the aorta stores energy and blood during systole, and then releases it during diastole to the peripheral circulation as well as to the coronary artery thus providing a continuous blood flow and enabling left ventricular relaxation (Windkessel function of the aorta) (Belz, 1995). The loss of aortal elasticity and stiffness was reported to result in an increase in both systolic pressure and cardiac work which, in turn, can lead to heart failure, left ventricular hypertrophy along with diastolic dysfunction (Belz, 1995; Demer and Tintut, 2008).

Few therapeutical strategies have been proposed to attenuate vascular calcification in CKD patients, which includes phosphate binder, calcimimetic and vitamin K2 administration (Stenvinkel, 2010). Among those, none has provided satisfying cardio-therapeutic outcomes thus highlighting the urgent need for efficient therapies especially that CKD reached epidemic proportions of 10-13% in some countries (Stenvinkel, 2010).

Mechanistically, arterial calcification is known to be an active process mediated by VSMCs, the predominant cell type in the medial layer of the artery wall (Belz, 1995; Jono et al., 2000; Doherty et al., 2004). Under pathological conditions, these cells are able to trans-differentiate

into osteochondrocyte-like cells, with increased expression of osteoblast-chondrocytes markers including RUNX2, TNAP, osteocalcin and osteopontin (Doherty et al., 2004). In fact, CKD is associated with numerous metabolic and endocrine disturbances, including inflammation coupled to abnormalities in calcium and phosphate metabolism, that contribute to this event (Tintut et al., 2000; Nitschke and Rutsch, 2012; Lewis, 2012). Hyperphosphatemia is prevalent in this disease and is caused mainly by hormonal imbalances (de Oliveira et al., 2013). Elevation in phosphate levels was described to induce medial calcification and VSMC osteogenic differentiation in different *in-vitro*, *ex-vivo* and *in-vivo* models (Jono et al., 2000; Giachelli, 2009; Larsson et al., 2010; Chen et al., 2006). Phosphate has been shown to promote calcification of human aortic smooth muscle cells in culture (Jono et al., 2000). In addition, different reports indicated that high phosphate induces medial VSMC calcification using an *ex-vivo* rat aorta models (Giachelli, 2009; Larsson et al., 2010). Along the same line, high phosphate diet was shown to induce medial calcification and accelerate VSMC osteogenic differentiation in an uremic mouse model of CKD (Chen et al., 2006). Altogether, these studies highlight a critical role for elevated phosphate levels in promoting osteo/chondrogenic differentiation of VSMCs in the medial layer of artery wall. However, the specific mechanism(s) responsible for these changes remain to be fully characterized.

Recently, an important role for microRNAs (miRs) during vascular calcification has been reported (Leopold, 2014). MiRs are short noncoding RNAs that regulate gene expression, at post-transcriptional level, upon binding to the 3'/5'- untranslated region (UTR) of their target messenger RNA (mRNA) and triggering either mRNA degradation or inhibition of translation (Erson and Petty, 2008). MiRs have been identified as important regulators in diverse differentiation processes including chondrogenesis and osteogenesis (Fakhry et al., 2013; Hu et al., 2010). However, their contribution to these processes particularly in vascular calcification is not yet fully elucidated.

In this study, we first characterized a high phosphate model of vascular calcification after exposing rat aortic explants to high  $P_i$  concentration (6 mM). Those aortas showed calcified phenotype associated with elevated expression of trans-differentiation markers (Runx2, TNAP, osteocalcin, and osteopontin) compared to control untreated aortas. Next, we characterized the miR expression profile in high  $P_i$ -treated aorta versus control samples and showed a significant alteration of different miRs suggesting their potential importance in regulating the early inflammatory response and calcification and trans-differentiation events mediated by hyperphosphatemia.

## **2. Materials and Methods**

### **2.1 Animal study**

All procedures were in accordance with the National Institutes of Health Guide for the Care and Use of Laboratory Animals. The basic principles governing animal research were approved by the Animal Ethics Committee, American University of Beirut (IACUC # 12-08-235).

### **2.2 Aorta tissue harvest**

Male Sprague-Dawley rats (200-250 g) were euthanized by CO<sub>2</sub> inhalation. Under aseptic conditions, aorta was cut from its posterior till its anterior end, was cleaned, infused by phosphate-buffered saline (PBS) buffer (37°C) and adventitia layer was removed by gentle scraping of external part.

### **2.3 Aorta organ culture**

Tissues were cultured in Dulbecco's Modified Eagle's Medium (DMEM, Sigma), (4.5 g/L glucose) supplemented with 10% fetal bovine serum (FBS, Sigma), penicillin (100 U/mL), streptomycin (100 µg/mL), 20 mmol/L HEPES, and 2 mmol/L L-glutamine. Tissues were maintained at 37°C in a humidified atmosphere with 5% CO<sub>2</sub> in air. Treatment involved the addition of 5 mM inorganic phosphate (P<sub>i</sub>) into DMEM medium that contains initially 1 mM P<sub>i</sub> to reach a final concentration of 6 mM P<sub>i</sub>. For tissue sectioning, the collected aortas were snap-frozen in liquid nitrogen and stored at -80°C and processed according to standard procedures. Tissue sections (4 µm) were performed from the small part of the aortic arch

### **2.4 RNA extraction, reverse transcription and polymerase chain reaction (qRT-PCR)**

Total RNA was extracted using TriPure isolation reagent (Sigma-Aldrich, St Louis, MO, USA) according to the manufacturer's instructions. Integrity of RNA was checked by running a gel electrophoresis and 1 µg of each RNA sample was used for reverse transcription

performed using iScript reverse transcription kit (Bio-Rad, Hercules, CA, USA). The reaction was carried out at 25°C for 5 minutes, 42°C for 30 minutes and stopped with incubation at 85°C for 5 minutes. Quantitative PCR was performed using iQ SYBR Green Supermix (Bio-Rad) and a CFX96 PCR detection system (Bio-Rad). The cycling conditions began by 95.0°C for 10 min, 40 cycles of 95.0°C for 30 sec, 57.0°C for 30 sec, 72.0°C for 1 min, and a final extension at 72.0°C for 8 min. Relative quantification analysis was performed using the Livak method ( $2^{-\Delta\Delta Cq}$ ). GAPDH (glyceraldehyde-3-phosphate dehydrogenase) gene was used as a reference gene. The sequence of the primers is indicated in the table 1 of the supplement section and was synthesized by Sigma-Aldrich.

### **2.5 TNAP activity measurement**

Crushed aortas were lysed in 0.2% Nonidet-P40 followed by 30 seconds of sonication, centrifugation for 5 minutes at 4,000 g, and collection of the supernatants. TNAP activity was assessed using paranitrophenylphosphate (pNPP) (Lancaster Synthesis, Ward Hill, MA, USA) as substrate. Absorbance of yellow dephosphorylated product was measured with spectrophotometer at 405 nm after sample-reactive incubation at 37°C for 30 minutes. The activity was calculated and normalized to the protein concentration.

### **2.6 Alizarin red staining (AR-S)**

Intact aortas were fixed with ethanol 95% for 24 hours, stained with Alizarin red (Sigma-Aldrich) 0.003% in 1% potassium hydroxide (KOH) for 30 hours, and washed twice with 2% KOH. Images were captured with normal camera.

### **2.7 Von Kossa staining**

Intact aortas were fixed with 70% ethanol at room temperature and washed with autoclaved water. This was followed by incubation in 5% silver nitrate for 30 minutes and washes with autoclaved water. The tissues were thereafter incubated for 1 hour under UV light, washed

twice in 5% sodium thiosulfate and counter stained with 0.1% eosin dye. After washing and dryness, images were captured with a normal camera.

## **2.8 Immunoblot analysis**

Proteins were extracted from crushed aortas using Laemmli buffer with 5% protease inhibitor (Roche). After centrifugation at 8,000 g, supernatants were collected and heated at 95°C for 5 minutes. Protein concentration was determined by Lowry method (Bio-Rad). 5 %  $\beta$ -mercaptoethanol was added to the samples. 30  $\mu$ g of proteins were separated by 12% SDS-PAGE and transferred to nitrocellulose membranes which were next blocked by 5 % non-fat milk and further incubated with a rabbit polyclonal antibody anti-SM22 alpha (abcam, ab155272) (1:1,000). The immune complexes were detected using Clarity ECL Western blotting substrate (Bio-Rad) and were revealed with the high-resolution ChemiDoc MP system (Bio-Rad). Membranes were washed in 'stripping buffer' and further incubated with a mouse antibody anti-GAPDH (Cruz Biotechnology, Santa Cruz, CA, USA) (1:1,000). Band intensity was quantified using ImageJ software {Schneider, 2012 #27}.

## **2.9 SM22 $\alpha$ immunofluorescence**

Tissue sections on slides were washed twice with PBS buffer containing 1% Triton X-100, incubated in blocking solution for 1 hour at room temperature (normal goat serum 10%, bovine serum albumin 3%), washed twice with the same buffer, and incubated overnight at 4°C with the primary antibody rabbit anti-SM22 alpha antibody (cat # ab155272, 1/1000 dilution, Abcam,, Cambridge, UK). This was followed by 2 washes with the same buffer and then incubation with secondary anti-rabbit antibody conjugated to Alexa Fluor 488 (Abcam, cat # ab150077) (RRID: AB\_2630356) (1/1000) for 1 hour at room temperature. Three washes with the same buffer were performed prior to incubation with Hoechst solution for 10 minutes followed by 3 washes with the same buffer. Slides were mounted with Fluoromount Aqueous Mounting Medium (Sigma-Aldrich) mixed with Prolong Gold antifade reagent

(Thermo Fisher Scientific, Waltham, MA, USA). Pictures were taken using Zeiss Axio fluorescence microscope with ZEN software (<https://www.zeiss.com>, RRID: SCR\_013672) and fluorescence intensity was quantified using image J software (4 pictures per aorta/ 3 aortas).

## **2.10 TaqMan Low Density Array (TLDA)**

A two-step procedure was performed to profile the miRNAs. First, for cDNA synthesis from the miRNAs, 100 ng of total RNA from control and treated aortas was subjected to reverse transcription (RT) using a TaqMan® microRNA reverse transcription kit and Megaplex RT primers (Thermo Fisher Scientific) according to the manufacturer's protocol, allowing simultaneous reverse transcription of 380 mature rat miRNAs. RT was performed on a Mastercycler Eppgradient thermocycler (VWR International, Leuven, Belgium) with the following cycling conditions: 40 cycles of 16 °C for 2 min, 42 °C for 1 min, and 50 °C for 1 s, followed by a final step of 80 °C for 5 min to inactivate the reverse transcriptase.

After the amplification step, the products were diluted with RNase-free water, combined with TaqMan gene expression master mix, and then loaded into TaqMan rat MicroRNA array (Thermo Fisher Scientific), which is a 384-well formatted plate and real-time PCR-based microfluidic card with embedded TaqMan primers and probes in each well for the 380 different mature rat miRNAs; the U87 transcript was used as a normalization signal. Quantitative RT-PCR was performed according to the manufacturer's instructions. Real-time PCR was performed on an ABI PRISM 7900HT sequence detection system (Thermo Fisher Scientific) with the following cycling conditions: 50 °C for 2 min and 94.5 °C for 10 min followed by 40 cycles of 95 °C for 30 s and 59.7 °C for 1min. The cycle threshold (*C<sub>q</sub>*) was automatically given by SDS 2.3 software (Thermo Fisher Scientific) and is defined as the fractional cycle number at which the fluorescence passes the fixed threshold of 0.2. U87 embedded in the TaqMan rat microRNA arrays was used as an endogenous control. The

relative expression levels of miRNAs were calculated using the comparative  $\Delta\Delta Cq$  method. The -fold changes in miRNAs were calculated by the expression  $2^{-\Delta\Delta Cq}$ .

### **2.11 Taqman miRNA Assay for Individual miRNAs**

Gene-specific reverse transcription was performed for each miR using 10 ng of purified total RNA, 100 mM dNTPs, 50 units of MultiScribe reverse transcriptase, 20 units of RNase inhibitor, and 50 nM gene-specific RT primer samples using the TaqMan microRNA reverse transcription kit (Thermo Fisher Scientific). 15- $\mu$ l reactions were incubated for 30 min at 16 °C, 30 min at 42 °C, and 5 min at 85 °C to inactivate the reverse transcriptase. Real-time qRT-PCRs (5  $\mu$ l of RT product, 10  $\mu$ l of TaqMan 2 $\times$  universal PCR master mix (Thermo Fisher Scientific), and 1  $\mu$ l of TaqMan microRNA assay mix containing PCR primers and TaqMan probes) were carried out on an ABI Prism 7900HT sequence detection system (Thermo Fisher Scientific) at 95 °C for 10 min followed by 40 cycles at 95 °C for 15 s and 60 °C for 1 min. All quantitative qRT-PCRs were performed in triplicate. The expression levels ( $2^{-\Delta\Delta Cq}$ ) of miRNAs were calculated.

### **2.12 MicroRNAs-gene interaction analysis**

The identified miRs were analyzed using the Elsevier's Pathway Studio software package version 10.0 (Ariadne Genomics/Elsevier) (<http://www.elsevier.com/solutions/pathway-studio-biological-research>; RRID: SCR\_014979) to construct the downstream target genes using its proprietary molecular interaction database namely ResNet 9.0. We utilized direct interaction, downstream regulators as well as "Subnetwork Enrichment Analysis" (SNEA) algorithm to extract statistically significant altered biological processes pertaining to each identified set of regulated microRNAs. SNEA utilizes Fisher's statistical test to determine if there are non-randomized associations between two categorical variables organized by specific relationship.

### **2.13 Statistical analysis**

Experiments were performed in triplicates and repeated for three independent experiments. Results were expressed as mean  $\pm$  the standard error of the mean (SEM). For statistical analysis, a two-tailed unpaired student *t*-test was performed (Instat program, version 3.1, Graphpad, La Jolla, CA, USA) (Results were considered significant \* when  $P < 0.05$ , \*\* when  $P < 0.01$  and \*\*\* when  $p < 0.001$ ).

### **3. Results**

#### **3.1 High phosphate induces calcification of rat aortic explants**

In order to determine the effect of high phosphate on the calcification ability of aortic explants, calcium deposition was assessed by alizarin red and Von Kossa staining methods following incubation of the rat aortic explants with  $P_i$  (6 mM) for 6 days. Alizarin red staining revealed high calcification level, visualized as small alizarin red precipitates, in treated aortas compared to untreated controls (Figure 1A). Consistent with these results, Von Kossa staining revealed the presence of dark grey calcium deposits in high  $P_i$ -treated explants but not in control (Figure 1B).

#### **3.2 High phosphate induces TNAP activity**

Since VSMCs calcification largely relies on TNAP activity (Narisawa et al., 2007), we therefore examined the effect of  $P_i$  treatment. Figure 2 showed the TNAP activity in the explants the explants of 6 day treatment with high  $P_i$  concentration which exhibited a significant increase in TNAP specific activity compared to control untreated explants.

#### **3.3 High phosphate induces de-differentiation of aortic VSMCs**

To determine whether phosphate treatment induces de-differentiation of VSMCs in the aortic explants, we next investigated the expression level of the smooth muscle-specific protein SM22 $\alpha$  in high  $P_i$ -treated versus untreated aortic explants by immunoblot analysis (control). As shown by immunoblot (Figures 3A) and densitometric analysis of SM22 $\alpha$  (Figures 3B), explants incubated with high  $P_i$  for 6 day exhibited significant downregulation of SM22 $\alpha$  protein level. To further confirm this observation, we assessed SM22 $\alpha$  expression by immunofluorescence and showed that similar treatment of explants significantly attenuated the fluorescence intensity (Figures 3C and D). These data indicate that VSMCs de-differentiation is induced in response to high  $P_i$ .

### **3.4 High phosphate induces aortic VSMCs trans-differentiation into osteo-chondrocyte like cells**

To determine whether VSMCs in the rat aortic explants are capable to trans-differentiate into osteo-chondrocyte like cells in the presence of high Pi concentration (6 mM), the mRNA levels of different osteoblastic or chondrogenic differentiation markers were assessed using qRT-PCR.

Interestingly, phosphate treatment for 6 days induced a significant increase in the transcription level of Runx2, the transcription factor that is necessary for the differentiation of osteoblasts and hypertrophic chondrocytes (Figure 4A). In addition, the mRNA levels of other osteo-chondrocyte differentiation markers like *Tnap* and *Osteopontin (Opn)* were significantly elevated following P<sub>i</sub> treatment starting from 3 days treatment (Figures 4B and 4C) and 6 days for *Osteocalcin (Ocn)* (Figure 4D).

Finally, the mRNA expression level of collagen type II, indicative of an early stage in chondrocyte differentiation, was not altered after P<sub>i</sub> treatment for 6 days (data not shown). Altogether, these data indicate that phosphate triggers the trans-differentiation of VSMCs in the aortic explants into osteoblast/chondrocyte-like cells.

### **3.5 High phosphate induces an alteration in the microRNA expression profile of aortic explants**

To unravel the possible mechanism(s) by which calcification and trans-differentiation were mediated in response to high phosphate, we hypothesized that microRNAs might be involved in regulating this process. TLDA technique was applied to characterize the miR expression profile in high Pi- treated versus untreated aortas. TLDA analysis revealed 17 differentially expressed and statistically significant miRs after 3 days of P<sub>i</sub> treatment compared to untreated controls. These miRs include: miR-107, -133b, -135a, -223, -323, -331, -598, -708, -155, -186, -200c, -296, -322, -345, -375, -491, -582. Among those miRs, 5 were confirmed to have

a significant differential expression by individual qPCR assays. 3 miRs were upregulated (miR-155, -200c, -322) whereas 2 miRs were downregulated (miR -331, -708) in treated aortas (Figure 5). At day 6, TLDA analysis revealed 16 statistically significant differentially expressed miRs (miR-188-5p, -197, -215, -219, -291a, -335, -409, -499, -542, -672, -224, -301a, -31, -328, -546, -590) among which only five miRs (miR-328, -546, -301a, -409 and -542) were confirmed by individual qRT-PCR to be differentially expressed (Figure 5B). In fact, miR-328, -546, and -301a showed upregulated expression whereas miR-409 and -542 were downregulated in Pi-treated aortas compared (Figure 5). These data indicate a possible involvement of these miRs in regulating aortic calcification and the expression of the osteoblast-chondrocyte differentiation markers in response to phosphate treatment.

### **3.6 Potential genes found to be targeted by the differentially expressed microRNAs**

To further determine how these differentially expressed miRs can contribute to the process of aortic calcification, we have investigated their downstream regulated target genes using the Elsevier's Pathway Studio software package. Several genes were found to be targets for the differentially expressed miRs at day 6 (Figure 6). In the set of upregulated miRs, miR-328 was found to have 12 target genes including calcineurin whilst miR-301a showed 10 targets among which are inflammatory cytokines, Nuclear Factor kappa-light-chain-enhancer of activated B cells (NF- $\kappa$ B), and mitogen-activated protein kinase 3 (MAPK3). In the set of downregulated miRs, miR-409 was found to target matrix metalloproteinase2, 9 (MMP2, MMP9), fibrinogen, caspase 3 (CASP3) and UL16 binding protein 1 (ULBP1), whilst miR-542 was found to have matrix metalloproteinases, albumin (ALB), matrix metalloproteinase3 (MMP3), TNF receptor-associated factor 4 (TRAF4) and RNA-induced silencing complex (RISC) complex as targets. These results highlight several important networks of pathways and functions to be associated with the targeted genes, which in turn may contribute to the previously observed phenotypic changes of aortic explants in response to P<sub>i</sub>.

#### 4. Discussion

VSMCs trans-differentiation into osteoblast/chondrocyte-like cells plays a crucial role in promoting arterial calcification (Belz, 1995; Jono et al., 2000; Doherty et al., 2004). Among the multiple factors that might be involved, phosphate level is considered to be crucial (Jono et al., 2000; Giachelli, 2009; Larsson et al., 2010; Chen et al., 2006). Using a rodent *ex vivo* high phosphate model that mimics hyperphosphatemia-induced arterial calcification observed in CKD, we demonstrated that  $P_i$  treated aortic explants were capable to mineralize, in association with an increased TNAP activity. Although vascular calcification cause in CKD is multifactorial, it may rely largely on TNAP. In fact, TNAP hydrolyses the mineralization inhibitor, inorganic pyrophosphate ( $PP_i$ ) which is produced locally by VSMCs and is provided systematically by the liver (Jansen et al., 2014, p. 6).  $PP_i$  acts as a constitutive mineralization inhibitor whose mere removal is sufficient to induce calcification of the media of the artery wall (Rutsch et al., 2001; Sheen et al., 2015). Furthermore, aortas in culture release  $PP_i$  and their calcification in the presence of high phosphate and calcium concentrations proceeds only when  $PP_i$  is removed by TNAP (Lomashvili et al., 2004) which is known to have high activity in VSMCs of uremic animals' aortas (Lomashvili et al., 2008).

In fact, inflammation is likely one of the factors able to induce TNAP in VSMCs where tumor necrosis factor alpha (TNF- $\alpha$ ) for instance was shown to induce TNAP expression in VSMCs and trigger VSMC trans-differentiation into osteoblast/chondrocyte-like cells (Tintut et al., 2000; Masuda et al., 2013; Zhao et al., 2012; Bessueille and Magne, 2015). TNAP is tissue-nonspecific, and its expression is induced by TNF- $\alpha$  independently of osteoblast or chondrocyte differentiation (Lencel et al., 2011; Ding et al., 2009). Inflammation is known to play an important role in promoting vascular calcification, in particular in the context of diabetes (Bessueille, Cell Mol Life Sci 2015). In the context of chronic kidney disease, it is likely that the associated hyperphosphatemia is a more potent stimulator of calcification than

inflammation. Moreover, in the present study, we aimed at characterizing the miRNAs associated with trans-differentiation and calcification and treating aortas with inflammatory cytokines would probably have modulated the expression of many miRNAs involved in inflammation but not directly linked to calcification. In this study, we also showed that phosphate stimulated de-differentiation and osteo-chondrocyte-like trans-differentiation in aortic cells as evidenced by a lower expression of the VSMCs differentiation marker SM22 $\alpha$  and a higher expression of osteo-chondrocyte trans-differentiation markers including Runx2, TNAP, OCN and OPN in P<sub>i</sub> treated versus control untreated aortic cells. These results are expected and coherent with earlier reports demonstrating the calcification and trans-differentiation inductive roles of P<sub>i</sub> on VSMCs (Jono et al, 2000; Giachelli, 2009; Larsson et al., 2010; Chen et al., 2006). Indeed, this is particularly relevant in patients with CKD where it is generally observed that CKD VSMCs differentiate toward osteoblasts in the medial layer (Vattikuti and Towler, 2004). These observations might have been extended with primary culture of extracted VSMCs but in this study we only focused on organ culture which is more similar to physiological conditions. This work proves again medial artery calcification as an actively regulated process. However, the precise mechanism and the specific pathways by which phosphate mediates aortic calcification and trans-differentiation are not well understood.

Recently, microRNAs were importantly recognized as crucial regulators of many cellular functions including differentiation, proliferation, migration and apoptosis (Rana, 2007). These small noncoding RNA molecules often induce the mRNA degradation or the translational inhibition of several target genes (Guo et al., 2010; Huntzinger and Izaurralde, 2011). A series of these microRNAs were shown to regulate physiological osteoblast differentiation, a key step in bone formation and mineralization (Fakhry et al., 2013; Hu et al., 2010). In addition, several other microRNAs were also shown to likely modulate trans-differentiation of VSMCs and vascular calcification (Cui et al, 2012; Claudia Goettsch et al.,

2011; Gross et al., 2014; Panizo et al., 2015). In this study, we questioned whether a specific microRNA network is implicated in triggering rat artery calcification in response to  $P_i$  treatment.

In fact, our study pinpoints the possible involvement of microRNAs in regulating VSMC trans-differentiation and calcification in response to  $P_i$ , as we have speculated. This was revealed upon miR profiling which identified an altered miR expression level of five miRs (miR-155, -200c, -322, -331, -708) 3 days post  $P_i$  treatment and five miRs (miR-328, -546, -301a, -409, -542) 6 days post  $P_i$  treatment. This finding may suggest the presence of a network of targets regulated by these miRs leading to the onset of calcification. It is likely that miRs can regulate phenotype changes via distinctive microRNA programs with temporal and cell-specific signatures that initiate SMC calcification (Leopold, 2014). Importantly, we found different miR profiles between different days of culture. This is interesting because the process of vascular calcification involves many different steps starting with the initial trans-differentiation of smooth muscle cells under the effect of high phosphate the subsequent inflammation, oxidative stress and the increase in TNAP expression and activity, reaching the steps of osteoblasts or chondrocytes maturation before the steps of calcium deposition. At day 3, the cells were not showing a phenotype of mature osteo-chondrocytes when the osteocalcin expression was not changed, thus we were still in the steps of initial trans-differentiation. At day 6, we had a significant increase in osteocalcin gene expression, marking the presence of mature osteo-chondrocytes, which can directly calcify the extracellular matrix. These different processes in the two tested times are the bases of the change in the miR profile.

Among the miRs overexpressed in day 3, miR-155 and miR-200c have practical roles in inflammation in VSMCs. The overexpression of miR-155 in VSMCs isolated from rat thoracic aorta was shown to increase inflammation as seen by an NF- $\kappa$ B activation and oxidative stress as seen by p47<sup>phox</sup>. In this model the effects of miR-155 was mediated by ERK1/2 activation. Importantly, the overexpression of this miR also induced a decrease in

SM22 $\alpha$  expression, which was shown also to be downregulated in our model (yang et al. 2015). miR-200 family was also shown to induce inflammation in VSMCs isolated from mouse thoracic aorta through inducing the expression of COX2, and it was found to be overexpressed in VSMCs isolated from diabetic mice, which is also a risk factor for vascular calcification (Reddy et al. 2012). In contrast, in another study involving preosteoblasts and bone marrow mesenchymal stem cells, miR-200c was shown to decrease inflammation by targeting IL-6 and IL-8. However, in this study the overexpression of miR-200c enhanced the osteogenic differentiation as evidenced by increased osteocalcin expression, as seen in our model (Hong et al, 2016). Thus, in our model it may be helping the osteogenic differentiation, but its role in inflammation must be assessed. miR-322 was also upregulated in our model. Its overexpression in C2C12 myoblasts induces osteoblastic differentiation marked by an increase in the osteoblast transcription factors: Osterix and Runx2, and in osteocalcin. Also, it enhanced the osteogenesis induced by BMP in this cell type. Thus, in our model this miR also may be responsible of the later increase in *Ocn* and *Runx2* gene expression (Gámez et al, 2013). miR-331, which was downregulated in our model at day 3, was shown to be anti-inflammatory in human airway epithelial Beas-2B cells, where its overexpression inhibits the activation of NF- $\kappa$ B and the expression of IL-6 and IL-8 in response to particulate matter (song et al, 2017). Also, miR-708, which was also downregulated in our model, was proven to have anti-inflammatory roles in endothelial cells isolated from human aorta by inhibiting NF- $\kappa$ B signaling (chen et al, 2015).

The interaction analysis performed helped to unravel the molecular pathways that are most likely to be involved. Some of these pathways are probably linked to artery calcification which is known to be as a multifactorial induced process (Doherty et al., 2004). In fact, miR-301a which is up-regulated at 6 days was shown to regulate inflammatory cytokine expression in macrophages (Huang et al., 2013). In a complementary way, miR-301a was shown to downregulate NF- $\kappa$ B repressing factor (NKrf), leading to the increased activation of

NF- $\kappa$ B (Lu et al., 2011) thus increasing other NF- $\kappa$ B dependent factor expression such as interleukin-6 (IL-6)/TNF- $\alpha$  (Karin and Greten, 2005). TNF- $\alpha$  activated NF- $\kappa$ B was shown to promote inflammation-accelerated vascular calcification by inhibiting ankylosis protein homolog expression and consequent pyrophosphate secretion (Zhao et al., 2012). Moreover, MAPK3/ERK1 pathway might be also activated by miR-301a (Cao et al., 2010). In fact, phosphorylated ERK1/2 was shown to be involved in promoting calcification and osteochondrogenic differentiation. ERK1/2 activation decreases myocardin and SMC lineage markers to generate the osteochondrogenic precursor state (Speer et al., 2009) and has an essential role in expression of osteogenic genes including Runx2, osteopontin, osteocalcin, and bone sialoprotein (Xiao et al., 2000). Moreover, ERK1/2 pathway was found to be modulated by and it mediates the action of inorganic phosphate on bone-forming cells (Spina A et al, 2013; Khoshniat S et al, 2011). Thus, it seems that miR-301a is promoting an inflammatory state which is known to be involved in the calcification process in ESRD patients as evidenced by the strong link between inflammatory cytokines/proteins (e.g. IL-6 and C-reactive protein: CRP) and coronary artery, aortic and valvular calcification (Wang et al., 2008). Another upregulated miR at day 6 is miR-328, whose overexpression was shown to upregulate calcineurin and promote calcineurin-dependent 3 (NFATc3) translocation into the nucleus (Chen, 1988). NFAT signaling pathway was identified as a novel regulator of oxidized low-density lipoprotein (LDL)-induced trans-differentiation of human coronary artery SMCs towards an osteoblast-like phenotype (C. Goettsch et al., 2011). NFATc1 was identified in calcified aortic valves, indicating its involvement in the calcification process (Alexopoulos et al., 2010). Furthermore, the downregulation of miR-409 at day 6 may activate genes that are repressed by this miR like MMP2/9. MMP-2 is constitutively expressed in endothelial cells and VSMCs whereas MMP-9 expression is more common in monocytes and other bone marrow-derived cells (Bäck et al., 2010). Serum levels of MMP-9 and MMP-2 are elevated in hemodialysis patients with a history of cardiovascular disease

compared to those without disease and normal controls (Pawlak et al., 2007) and blockade of MMP activity can inhibit arterial calcification (Chen et al., 2011). Chung *et al.* also showed that diabetic arteries of a different set of patients with CKD demonstrated increased MMP-2 and MMP-9 activities by 42 and 116%, respectively, compared with non-diabetic arteries of patients with CKD. This enhanced MMP expression is highly correlated with arterial stiffness and pulse wave velocity (Chung et al., 2009). Recently, Peiskerova *et al.* reported that serum MMP-2 levels are higher in 80 patients with CKD stages 1 to 5 and 44 healthy control subjects (Peiskerová et al., 2009). The occurrence of calcification in tunica media of the radial artery of uremic patients was correlated with the expression of MMP-2 (Shan et al., 2013). It might be also involved in the development of medial layer vascular calcification in uremic rats (Kumata et al., 2011). Both gelatinases provide essential signals for phenotypic VSMC conversion, matrix remodeling and the initiation of vascular calcification (Hecht et al., 2015, p. 9). MMP-2 and 9 were also shown to promote vascular calcification by upregulating bone morphogenetic protein 2 (BMP-2) which induces expression of RUNX2 and msh-homeobox 2 (Msx-2), two proteins associated with phenotype transition of VSMCs in vascular calcification (Zhao et al., 2016).

Previous studies have addressed the implication of some microRNAs in vascular calcification. However, these miRNAs were not identified to be differentially regulated in our miRNA profiling. For example, miR-204, -205, -221, and -222 were found to be downregulated during the calcification of smooth muscle cells (Cui et al, 2012; Qiao et al, 2014; Mackenzie et al, 2014). Among these miR-204 and -205 inhibited calcification by targeting Runx2, whereas miR-221 and -222 were found to enhance calcification. Also, miR-223 was shown to be upregulated in Pi-treated human vascular smooth muscle cells (Rangrez et al, 2012). The discrepancies between our study and these studies may be due to one of two reasons. First, the time points tested in these studies may not correspond to the time point tested in our study. On the other hand, these studies were done on cells whereas our model

was done on tissues, containing smooth muscle cells with their extracellular matrix which can have important effects on the mechanism of calcification. In the aortic extracellular matrix, many factors may affect calcification; importantly, the elastin degradation products that are usually generated during vascular calcification can affect the expression of different genes in the smooth muscle cells by binding to the elastin laminin receptor (Simionescu et al, 2005).

In conclusion, in this study we report that microRNAs are pivotal mediators which may contribute to high phosphate-induced calcification of VSMCs and phenotypic switching into osteoblast/chondrocyte like cells in rat arteries. The exact roles of these miRs can be further validated through targeted downregulation by specific anti-miRs or overexpression by lentiviral transduction. From a clinical view, understanding the function of those miRs and their association with the molecular pathogenesis of vascular calcification will provide novel insights into the development of new therapeutic strategies.

### **Acknowledgments**

Authors are grateful to the Lebanese University (LU) and the Lebanese National Council for Scientific Research (CNRS-L) for providing PhD scholarships to Maya Fakhry and Najwa Skafi.

**Conflict of interest:** none declared.

### **Figure legends:**

**Figure 1: Calcification of aortic explants is induced by high phosphate.** (A) Alizarin red and (B) Von Kossa staining of intact aorta tissues. Calcium deposition was observed after 6 days of culture with high phosphate ( $P_i$ ) medium compared with culture with control medium.

**Figure 2: TNAP activity is induced by high phosphate.** TNAP activity was determined and normalized with specific protein concentration. A significant increase in TNAP specific activity was observed after 6 days of culture in high phosphate ( $P_i$ ) medium compared to control medium. Results represent the mean  $\pm$  SEM of three independent experiments, \*\* indicates p value $<0.01$ .

**Figure 3: De-differentiation of aortic cells is induced by high phosphate.** (A) Western blot analysis of SM22 $\alpha$  and GAPDH. (A) corresponds to the immunoblot. (B) represents the densitometric analysis of SM22 $\alpha$  corrected to GAPDH expression. Each value represents the mean  $\pm$  SEM of three independent experiments. \* indicates a statistical significance with p $<0.05$ . (C) shows the SM22 $\alpha$  examined by Immunofluorescence on tissue sections and (D) quantification analysis of the immunofluorescence of SM22 $\alpha$ . A significant downregulation of SM22 $\alpha$  protein level was observed after 6 days of culture in high phosphate ( $P_i$ ) medium compared to control medium. For the Immunofluorescence, the value represents the mean  $\pm$  SEM of four independent experiments. \*\* indicates a statistical significance with p $<0.01$ .

**Figure 4: Trans-differentiation of aortic cells into osteo-chondrocyte like cells is induced by high phosphate.** Aortic explants were cultured for 3 and 6 days under control or high phosphate ( $P_i$ ) and the mRNA level of different markers, *Runx2*, *Tnap*, *Ocn* and *Opn*, was assessed by qRT-PCR. Each value represents the mean  $\pm$  SEM of three independent experiments. \* indicates a statistical significance with p $<0.05$ .

**Figure 5: MicroRNAs differential expression profile in  $P_i$  treated aortas.** miRs were significantly differentially expressed between untreated control and high-phosphate treated aortas for 3 or 6 days from three independent experiments. Data obtained by qRT-PCR amplification of miRs were plotted. P-Values for each miRNA are shown.

**Figure 6: Dysregulated miRNAs target genes as determined from MicroRNA-Gene Regulatory Network.** Shown are the target genes for the dysregulated miRNAs.

Figure 1

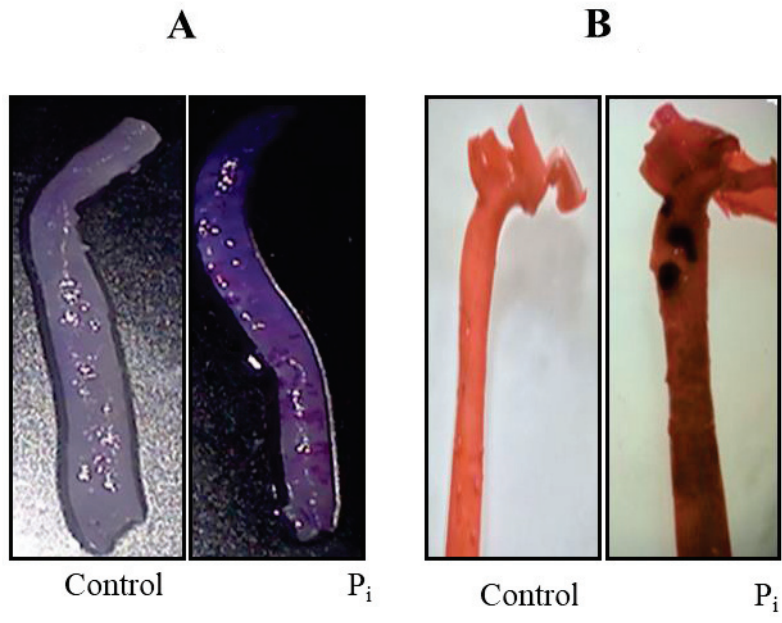


**Figure 2**

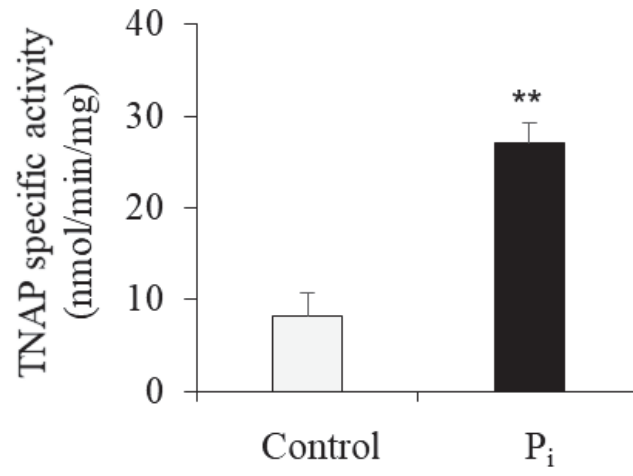


**Figure 3**

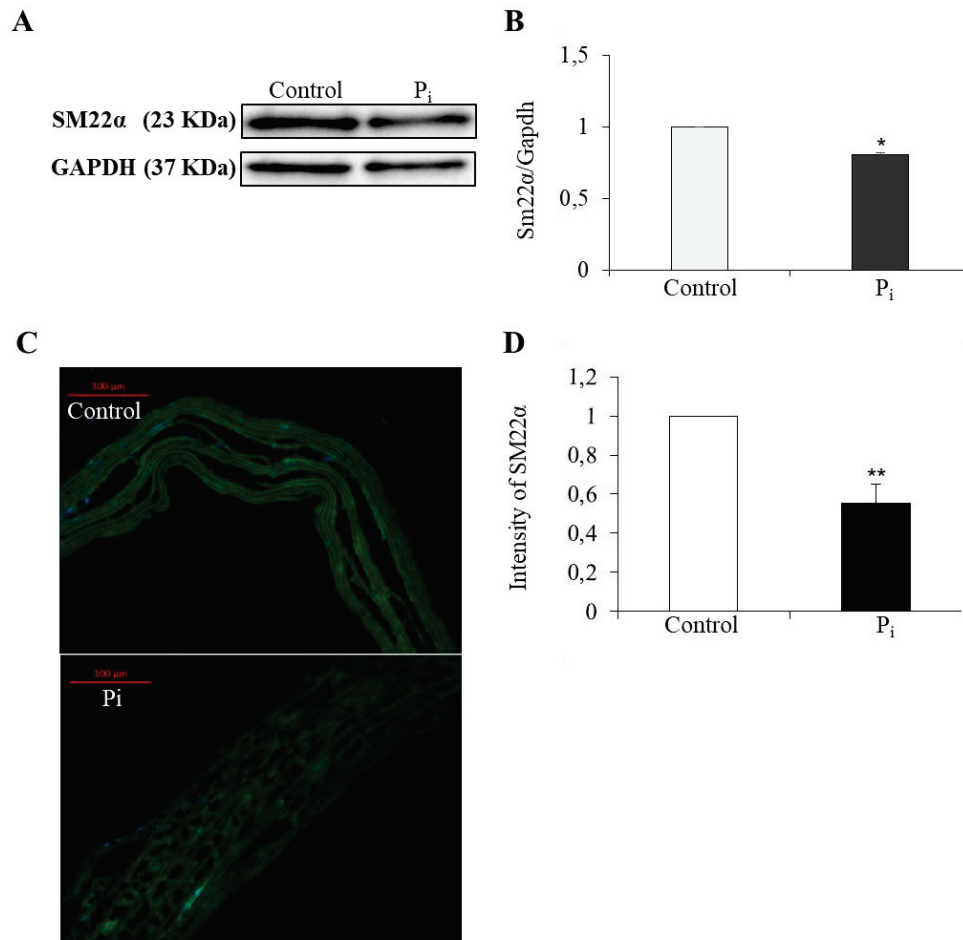


Figure 4

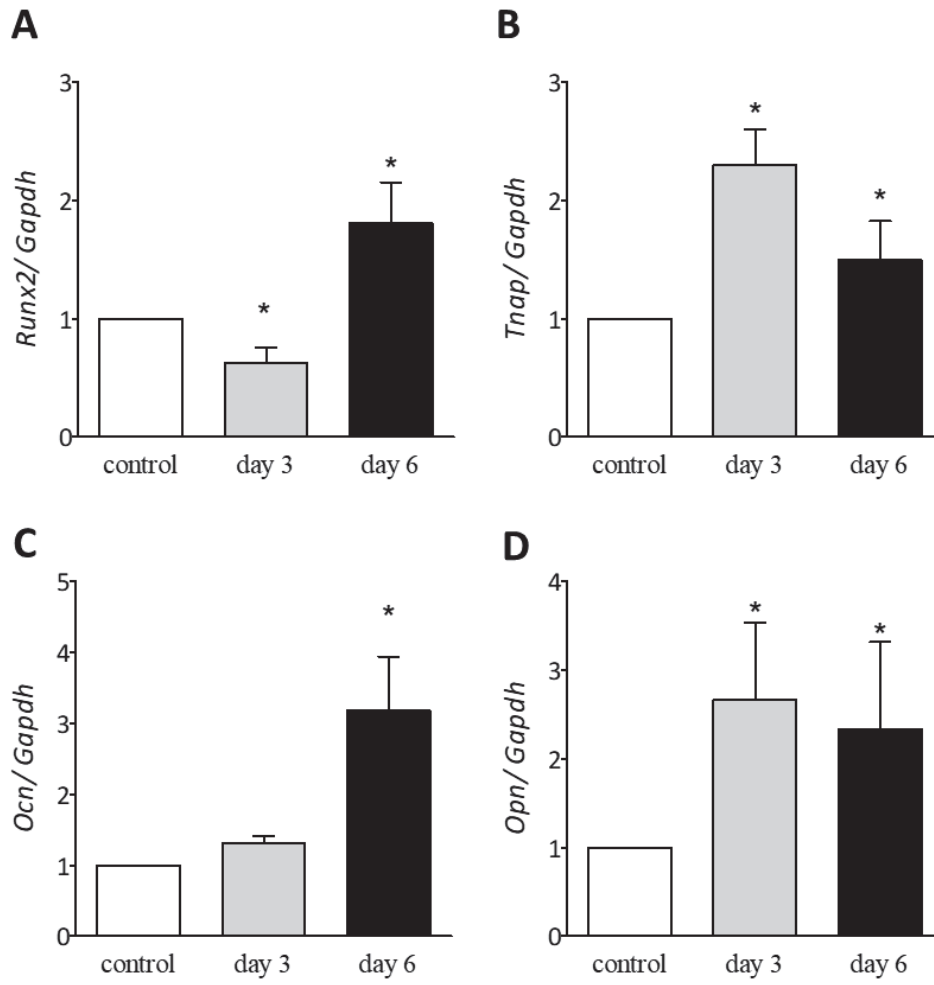


Figure 5

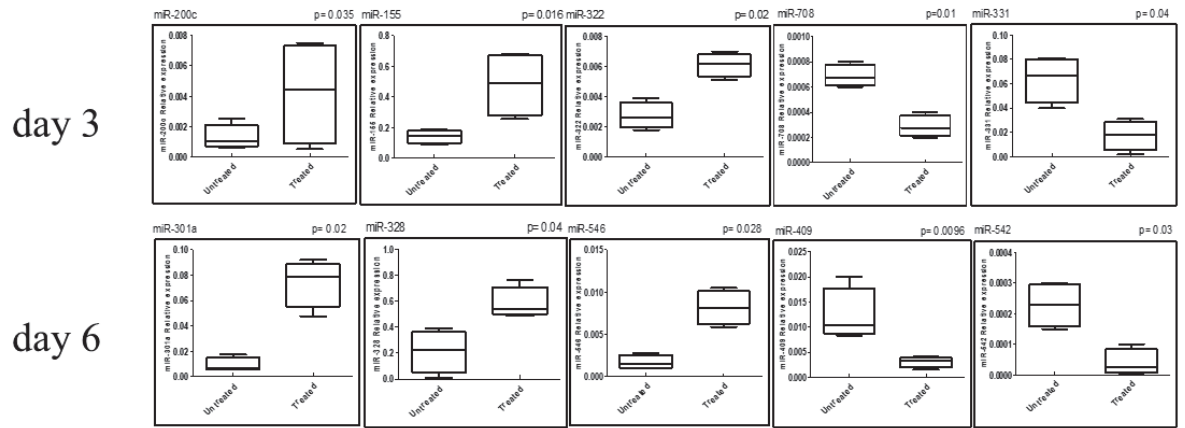
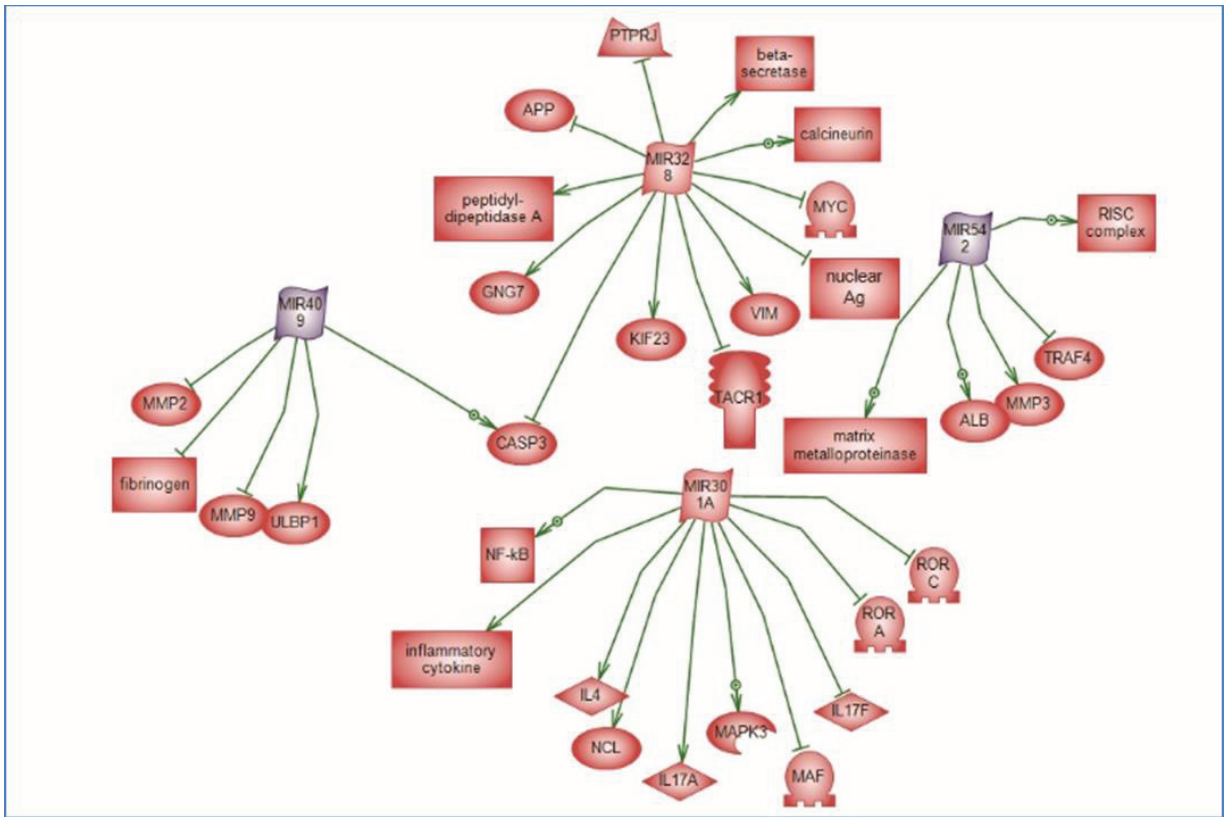


Figure 6



## References

- Alexopoulos, A., Bravou, V., Peroukides, S., Kaklamanis, L., Varakis, J., Alexopoulos, D., Papadaki, H., 2010. Bone regulatory factors NFATc1 and Osterix in human calcific aortic valves. *Int. J. Cardiol.* 139, 142–149.
- Bäck, M., Ketelhuth, D.F.J., Agewall, S., 2010. Matrix metalloproteinases in atherothrombosis. *Prog. Cardiovasc. Dis.* 52, 410–428.
- Belz, G.G., 1995. Elastic properties and Windkessel function of the human aorta. *Cardiovasc. Drugs Ther. Spons. Int. Soc. Cardiovasc. Pharmacother.* 9, 73–83.
- Bessueille, L., Magne, D., 2015. Inflammation: a culprit for vascular calcification in atherosclerosis and diabetes. *Cell. Mol. Life Sci. CMLS* 72, 2475–2489.
- Blacher, J., Guerin, A.P., Pannier, B., Marchais, S.J., London, G.M., 2001. Arterial calcifications, arterial stiffness, and cardiovascular risk in end-stage renal disease. *Hypertension* 38, 938–942.
- Cao, G., Huang, B., Liu, Z., Zhang, J., Xu, H., Xia, W., Li, J., Li, S., Chen, L., Ding, H., Zhao, Q., Fan, M., Shen, B., Shao, N., 2010. Intronic miR-301 feedback regulates its host gene, *ska2*, in A549 cells by targeting MEOX2 to affect ERK/CREB pathways. *Biochem. Biophys. Res. Commun.* 396, 978–982.
- Chen, L.-J., Chuang, L., Huang, Y.-H., Zhou, J., Lim, S.H., Lee, C.-I., Lin, W.-W., Lin, T.-E., Wang, W.-L., Chen, L., Chien, S., Chiu, J.-J., 2015. MicroRNA mediation of endothelial inflammatory response to smooth muscle cells and its inhibition by atheroprotective shear stress. *Circ. Res.* 116, 1157–1169.
- Chen, N.X., Duan, D., O'Neill, K.D., Wolisi, G.O., Koczman, J.J., Laclair, R., Moe, S.M., 2006. The mechanisms of uremic serum-induced expression of bone matrix proteins in bovine vascular smooth muscle cells. *Kidney Int.* 70, 1046–1053.
- Chen, N.X., O'Neill, K.D., Chen, X., Kiattisunthorn, K., Gattone, V.H., Moe, S.M., 2011. Activation of arterial matrix metalloproteinases leads to vascular calcification in chronic kidney disease. *Am. J. Nephrol.* 34, 211–219.
- Chen, R.H., 1988. [TLC identification of organochlorine (BHC, DDT) pesticide residues in crude drugs]. *Zhong Yao Tong Bao Beijing China* 13, 34–36, 63.
- Chung, A.W.Y., Yang, H.H.C., Sigrist, M.K., Brin, G., Chum, E., Gourlay, W.A., Levin, A., 2009. Matrix metalloproteinase-2 and -9 exacerbate arterial stiffening and angiogenesis in diabetes and chronic kidney disease. *Cardiovasc. Res.* 84, 494–504.
- Cui, R.-R., Li, S.-J., Liu, L.-J., Yi, L., Liang, Q.-H., Zhu, X., Liu, G.-Y., Liu, Y., Wu, S.-S., Liao, X.-B., Yuan, L.-Q., Mao, D.-A., Liao, E.-Y., 2012. MicroRNA-204 regulates vascular smooth muscle cell calcification in vitro and in vivo. *Cardiovasc. Res.* 96, 320–329.
- Demer, L.L., Tintut, Y., 2008. Vascular calcification: pathobiology of a multifaceted disease. *Circulation* 117, 2938–2948.
- De Oliveira, R.B., Okazaki, H., Stingen, A.E.M., Drüeke, T.B., Massy, Z.A., Jorgetti, V., 2013. Vascular calcification in chronic kidney disease: a review. *J. Bras. Nefrol. 'orgão Of. Soc. Bras. E Lat.-Am. Nefrol.* 35, 147–161.
- Ding, J., Ghali, O., Lencel, P., Broux, O., Chauveau, C., Devedjian, J.C., Hardouin, P., Magne, D., 2009. TNF-alpha and IL-1beta inhibit RUNX2 and collagen expression but increase alkaline phosphatase activity and mineralization in human mesenchymal stem cells. *Life Sci.* 84, 499–504.
- Doherty, T.M., Fitzpatrick, L.A., Inoue, D., Qiao, J.-H., Fishbein, M.C., Detrano, R.C., Shah, P.K., Rajavashisth, T.B., 2004. Molecular, endocrine, and genetic mechanisms of arterial calcification. *Endocr. Rev.* 25, 629–672.

- Erson, A.E., Petty, E.M., 2008. MicroRNAs in development and disease. *Clin. Genet.* 74, 296–306.
- Fakhry, M., Hamade, E., Badran, B., Buchet, R., Magne, D., 2013. Molecular mechanisms of mesenchymal stem cell differentiation towards osteoblasts. *World J. Stem Cells* 5, 136–148.
- Foley, R.N., Parfrey, P.S., Sarnak, M.J., 1998a. Clinical epidemiology of cardiovascular disease in chronic renal disease. *Am. J. Kidney Dis. Off. J. Natl. Kidney Found.* 32, S112–119.
- Foley, R.N., Parfrey, P.S., Sarnak, M.J., 1998b. Epidemiology of cardiovascular disease in chronic renal disease. *J. Am. Soc. Nephrol. JASN* 9, S16–23.
- Gámez, B., Rodríguez-Carballo, E., Bartrons, R., Rosa, J.L., Ventura, F., 2013. MicroRNA-322 (miR-322) and its target protein Tob2 modulate Osterix (Osx) mRNA stability. *J. Biol. Chem.* 288, 14264–14275.
- Gansevoort, R.T., Matsushita, K., van der Velde, M., Astor, B.C., Woodward, M., Levey, A.S., de Jong, P.E., Coresh, J., Chronic Kidney Disease Prognosis Consortium, 2011. Lower estimated GFR and higher albuminuria are associated with adverse kidney outcomes. A collaborative meta-analysis of general and high-risk population cohorts. *Kidney Int.* 80, 93–104.
- Giachelli, C.M., 2009. The emerging role of phosphate in vascular calcification. *Kidney Int.* 75, 890–897.
- Goettsch, C., Rauner, M., Hamann, C., Sinnigen, K., Hempel, U., Bornstein, S.R., Hofbauer, L.C., 2011. Nuclear factor of activated T cells mediates oxidised LDL-induced calcification of vascular smooth muscle cells. *Diabetologia* 54, 2690–2701.
- Goettsch, C., Rauner, M., Pacyna, N., Hempel, U., Bornstein, S.R., Hofbauer, L.C., 2011. miR-125b regulates calcification of vascular smooth muscle cells. *Am. J. Pathol.* 179, 1594–1600.
- Goodman, W.G., Goldin, J., Kuizon, B.D., Yoon, C., Gales, B., Sider, D., Wang, Y., Chung, J., Emerick, A., Greaser, L., Elashoff, R.M., Salusky, I.B., 2000. Coronary-artery calcification in young adults with end-stage renal disease who are undergoing dialysis. *N. Engl. J. Med.* 342, 1478–1483.
- Gross, P., Six, I., Kamel, S., Massy, Z.A., 2014. Vascular toxicity of phosphate in chronic kidney disease: beyond vascular calcification. *Circ. J. Off. J. Jpn. Circ. Soc.* 78, 2339–2346.
- Guo, H., Ingolia, N.T., Weissman, J.S., Bartel, D.P., 2010. Mammalian microRNAs predominantly act to decrease target mRNA levels. *Nature* 466, 835–840.
- Hecht, E., Freise, C., Websky, K.V., Nasser, H., Kretzschmar, N., Stawowy, P., Hocher, B., Querfeld, U., 2015. The matrix metalloproteinases 2 and 9 initiate uraemic vascular calcifications. *Nephrol. Dial. Transplant. Off. Publ. Eur. Dial. Transpl. Assoc. - Eur. Ren. Assoc.* 31:789–797.
- Hong, L., Sharp, T., Khorsand, B., Fischer, C., Eliason, S., Salem, A., Akkouch, A., Brogden, K., Amendt, B.A., 2016. MicroRNA-200c Represses IL-6, IL-8, and CCL-5 Expression and Enhances Osteogenic Differentiation. *PLoS One* 11, e0160915.
- Huang, L., Liu, Y., Wang, L., Chen, R., Ge, W., Lin, Z., Zhang, Y., Liu, S., Shan, Y., Lin, Q., Jiang, M., 2013. Down-regulation of miR-301a suppresses pro-inflammatory cytokines in Toll-like receptor-triggered macrophages. *Immunology* 140, 314–322.
- Huntzinger, E., Izaurralde, E., 2011. Gene silencing by microRNAs: contributions of translational repression and mRNA decay. *Nat. Rev. Genet.* 12, 99–110.
- Hu, R., Li, H., Liu, W., Yang, L., Tan, Y.-F., Luo, X.-H., 2010. Targeting miRNAs in osteoblast differentiation and bone formation. *Expert Opin. Ther. Targets* 14, 1109–1120.
- Jansen, R.S., Duijst, S., Mahakena, S., Sommer, D., Szeri, F., Váradi, A., Plomp, A., Bergen, A.A., Oude Elferink, R.P.J., Borst, P., van de Wetering, K., 2014. ABCC6-mediated ATP secretion by the liver is the main source of the mineralization inhibitor inorganic pyrophosphate in the systemic circulation—brief report. *Arterioscler. Thromb. Vasc. Biol.* 34, 1985–1989.

- Jono, S., McKee, M.D., Murry, C.E., Shioi, A., Nishizawa, Y., Mori, K., Morii, H., Giachelli, C.M., 2000. Phosphate regulation of vascular smooth muscle cell calcification. *Circ. Res.* 87, E10–17.
- Karin, M., Greten, F.R., 2005. NF- $\kappa$ B: linking inflammation and immunity to cancer development and progression. *Nat. Rev. Immunol.* 5, 749–759.
- Khoshniat, S., Bourguine, A., Julien, M., Petit, M., Pilet, P., Rouillon, T., Masson, M., Gatus, M., Weiss, P., Guicheux, J., Beck, L., 2011. Phosphate-dependent stimulation of MGP and OPN expression in osteoblasts via the ERK1/2 pathway is modulated by calcium. *Bone* 48, 894–902.
- Kumata, C., Mizobuchi, M., Ogata, H., Koiwa, F., Kondo, F., Kinugasa, E., Akizawa, T., 2011. Involvement of matrix metalloproteinase-2 in the development of medial layer vascular calcification in uremic rats. *Ther. Apher. Dial. Off. Peer-Rev. J. Int. Soc. Apher. Jpn. Soc. Apher. Jpn. Soc. Dial. Ther.* 15 Suppl 1, 18–22.
- Larsson, T.E., Olauson, H., Hagström, E., Ingelsson, E., Arnlöv, J., Lind, L., Sundström, J., 2010. Conjoint effects of serum calcium and phosphate on risk of total, cardiovascular, and noncardiovascular mortality in the community. *Arterioscler. Thromb. Vasc. Biol.* 30, 333–339.
- Lencel, P., Delplace, S., Pilet, P., Leterme, D., Miellot, F., Sourice, S., Caudrillier, A., Hardouin, P., Guicheux, J., Magne, D., 2011. Cell-specific effects of TNF- $\alpha$  and IL-1 $\beta$  on alkaline phosphatase: implication for syndesmophyte formation and vascular calcification. *Lab. Investig. J. Tech. Methods Pathol.* 91, 1434–1442.
- Leopold, J.A., 2014. MicroRNAs Regulate Vascular Medial Calcification. *Cells* 3, 963–980.
- Lewis, R., 2012. Mineral and bone disorders in chronic kidney disease: new insights into mechanism and management. *Ann. Clin. Biochem.* 49, 432–440.
- Lomashvili, K.A., Cobbs, S., Hennigar, R.A., Hardcastle, K.I., O'Neill, W.C., 2004. Phosphate-induced vascular calcification: role of pyrophosphate and osteopontin. *J. Am. Soc. Nephrol. JASN* 15, 1392–1401.
- Lomashvili, K.A., Garg, P., Narisawa, S., Millan, J.L., O'Neill, W.C., 2008. Upregulation of alkaline phosphatase and pyrophosphate hydrolysis: potential mechanism for uremic vascular calcification. *Kidney Int.* 73, 1024–1030.
- London, G.M., Guérin, A.P., Marchais, S.J., Métivier, F., Pannier, B., Adda, H., 2003. Arterial media calcification in end-stage renal disease: impact on all-cause and cardiovascular mortality. *Nephrol. Dial. Transplant. Off. Publ. Eur. Dial. Transpl. Assoc. - Eur. Ren. Assoc.* 18, 1731–1740.
- Lu, Z., Li, Y., Takwi, A., Li, B., Zhang, J., Conklin, D.J., Young, K.H., Martin, R., Li, Y., 2011. MiR-301a as an NF- $\kappa$ B activator in pancreatic cancer cells. *EMBO J.* 30, 57–67.
- Mackenzie, N.C.W., Staines, K.A., Zhu, D., Genever, P., Macrae, V.E., 2014. MiRNA-221 and miRNA-222 synergistically function to promote vascular calcification. *Cell Biochem. Funct.* 32, 209–216.
- Masuda, M., Miyazaki-Anzai, S., Levi, M., Ting, T.C., Miyazaki, M., 2013. PERK-eIF2 $\alpha$ -ATF4-CHOP signaling contributes to TNF $\alpha$ -induced vascular calcification. *J. Am. Heart Assoc.* 2, e000238.
- Narisawa, S., Harmey, D., Yadav, M.C., O'Neill, W.C., Hoylaerts, M.F., Millán, J.L., 2007. Novel inhibitors of alkaline phosphatase suppress vascular smooth muscle cell calcification. *J. Bone Miner. Res. Off. J. Am. Soc. Bone Miner. Res.* 22, 1700–1710.
- Nitschke, Y., Rutsch, F., 2012. Genetics in arterial calcification: lessons learned from rare diseases. *Trends Cardiovasc. Med.* 22, 145–149.
- Panizo, S., Naves-Díaz, M., Carrillo-López, N., Martínez-Arias, L., Fernández-Martín, J.L., Ruiz-Torres, M.P., Cannata-Andía, J.B., Rodríguez, I., 2015. MicroRNAs 29b, 133b, and 211 Regulate Vascular Smooth Muscle Calcification Mediated by High Phosphorus. *J. Am. Soc. Nephrol. JASN*.

- Pawlak, K., Pawlak, D., Mysliwiec, M., 2007. Serum matrix metalloproteinase-2 and increased oxidative stress are associated with carotid atherosclerosis in hemodialyzed patients. *Atherosclerosis* 190, 199–204.
- Peiskerová, M., Kalousová, M., Kratochvílová, M., Dusilová-Sulková, S., Uhrová, J., Bandúr, S., Malbohan, I.M., Zima, T., Tesar, V., 2009. Fibroblast growth factor 23 and matrix-metalloproteinases in patients with chronic kidney disease: are they associated with cardiovascular disease? *Kidney Blood Press. Res.* 32, 276–283.
- Qiao, W., Chen, L., Zhang, M., 2014. MicroRNA-205 regulates the calcification and osteoblastic differentiation of vascular smooth muscle cells. *Cell. Physiol. Biochem. Int. J. Exp. Cell. Physiol. Biochem. Pharmacol.* 33, 1945–1953.
- Rana, T.M., 2007. Illuminating the silence: understanding the structure and function of small RNAs. *Nat. Rev. Mol. Cell Biol.* 8, 23–36.
- Rangrez, A.Y., M'Baya-Moutoula, E., Metzinger-Le Meuth, V., Hénaut, L., Djelouat, M.S. el I., Benchitrit, J., Massy, Z.A., Metzinger, L., 2012. Inorganic phosphate accelerates the migration of vascular smooth muscle cells: evidence for the involvement of miR-223. *PloS One* 7, e47807.
- Reddy, M.A., Jin, W., Villeneuve, L., Wang, M., Lanting, L., Todorov, I., Kato, M., Natarajan, R., 2012. Pro-inflammatory role of microRNA-200 in vascular smooth muscle cells from diabetic mice. *Arterioscler. Thromb. Vasc. Biol.* 32, 721–729.
- Rutsch, F., Vaingankar, S., Johnson, K., Goldfine, I., Maddux, B., Schauerte, P., Kalhoff, H., Sano, K., Boisvert, W.A., Superti-Furga, A., Terkeltaub, R., 2001. PC-1 nucleoside triphosphate pyrophosphohydrolase deficiency in idiopathic infantile arterial calcification. *Am. J. Pathol.* 158, 543–554.
- Sage, A.P., Tintut, Y., Demer, L.L., 2010. Regulatory mechanisms in vascular calcification. *Nat. Rev. Cardiol.* 7, 528–536.
- Schlieper, G., Krüger, T., Djuric, Z., Damjanovic, T., Markovic, N., Schurgers, L.J., Brandenburg, V.M., Westenfeld, R., Dimkovic, S., Ketteler, M., Grootendorst, D.C., Dekker, F.W., Floege, J., Dimkovic, N., 2008. Vascular access calcification predicts mortality in hemodialysis patients. *Kidney Int.* 74, 1582–1587.
- Shan, A., Zhou, C., He, Y., Feng, W., Chen, G., Zhong, G., 2013. Expression of both matrix metalloproteinase-2 and its tissue inhibitor-2 in tunica media of radial artery in uremic patients. *Ren. Fail.* 35, 37–42.
- Sheen, C.R., Kuss, P., Narisawa, S., Yadav, M.C., Nigro, J., Wang, W., Chhea, T.N., Sergienko, E.A., Kapoor, K., Jackson, M.R., Hoylaerts, M.F., Pinkerton, A.B., O'Neill, W.C., Millán, J.L., 2015. Pathophysiological role of vascular smooth muscle alkaline phosphatase in medial artery calcification. *J. Bone Miner. Res. Off. J. Am. Soc. Bone Miner. Res.* 30, 824–836.
- Sigrist, M.K., Taal, M.W., Bungay, P., McIntyre, C.W., 2007. Progressive vascular calcification over 2 years is associated with arterial stiffening and increased mortality in patients with stages 4 and 5 chronic kidney disease. *Clin. J. Am. Soc. Nephrol. CJASN* 2, 1241–1248.
- Simionescu, A., Philips, K., Vyavahare, N., 2005. Elastin-derived peptides and TGF-beta1 induce osteogenic responses in smooth muscle cells. *Biochem. Biophys. Res. Commun.* 334, 524–532.
- Song, L., Li, D., Li, X., Ma, L., Bai, X., Wen, Z., Zhang, X., Chen, D., Peng, L., 2017. Exposure to PM2.5 induces aberrant activation of NF-κB in human airway epithelial cells by downregulating miR-331 expression. *Environ. Toxicol. Pharmacol.* 50, 192–199.
- Speer, M.Y., Yang, H.-Y., Brabb, T., Leaf, E., Look, A., Lin, W.-L., Frutkin, A., Dichek, D., Giachelli, C.M., 2009. Smooth muscle cells give rise to osteochondrogenic precursors and chondrocytes in calcifying arteries. *Circ. Res.* 104, 733–741.

- Spina, A., Sorvillo, L., Di Maiolo, F., Esposito, A., D'Auria, R., Di Gesto, D., Chiosi, E., Naviglio, S., 2013. Inorganic phosphate enhances sensitivity of human osteosarcoma U2OS cells to doxorubicin via a p53-dependent pathway. *J. Cell. Physiol.* 228, 198–206.
- Stenvinkel, P., 2010. Chronic kidney disease: a public health priority and harbinger of premature cardiovascular disease. *J. Intern. Med.* 268, 456–467.
- Tintut, Y., Patel, J., Parhami, F., Demer, L.L., 2000. Tumor necrosis factor- $\alpha$  promotes in vitro calcification of vascular cells via the cAMP pathway. *Circulation* 102, 2636–2642.
- Vattikuti, R., Towler, D.A., 2004. Osteogenic regulation of vascular calcification: an early perspective. *Am. J. Physiol. Endocrinol. Metab.* 286, E686–696.
- Wang, A.Y.-M., Lam, C.W.-K., Wang, M., Chan, I.H.-S., Yu, C.-M., Lui, S.-F., Sanderson, J.E., 2008. Increased circulating inflammatory proteins predict a worse prognosis with valvular calcification in end-stage renal disease: a prospective cohort study. *Am. J. Nephrol.* 28, 647–653.
- Xiao, G., Jiang, D., Thomas, P., Benson, M.D., Guan, K., Karsenty, G., Franceschi, R.T., 2000. MAPK pathways activate and phosphorylate the osteoblast-specific transcription factor, Cbfa1. *J. Biol. Chem.* 275, 4453–4459.
- Yang, Z., Zheng, B., Zhang, Y., He, M., Zhang, X., Ma, D., Zhang, R., Wu, X., Wen, J., 2015. MiR-155-dependent regulation of mammalian sterile 20-like kinase 2 (MST2) coordinates inflammation, oxidative stress and proliferation in vascular smooth muscle cells. *Biochim. Biophys. Acta* 1852, 1477–1489.
- Zhao, G., Xu, M.-J., Zhao, M.-M., Dai, X.-Y., Kong, W., Wilson, G.M., Guan, Y., Wang, C.-Y., Wang, X., 2012. Activation of nuclear factor- $\kappa$ B accelerates vascular calcification by inhibiting ankylosis protein homolog expression. *Kidney Int.* 82, 34–44.
- Zhao, Y.-G., Meng, F.-X., Li, B.-W., Sheng, Y.-M., Liu, M.-M., Wang, B., Li, H.-W., Xiu, R.-J., 2016. Gelatinases promote calcification of vascular smooth muscle cells by up-regulating bone morphogenetic protein-2. *Biochem. Biophys. Res. Commun.* 470, 287–293.
- Zhu, D., Mackenzie, N.C.W., Farquharson, C., Macrae, V.E., 2012. Mechanisms and clinical consequences of vascular calcification. *Front. Endocrinol.* 3, 95.

## Article 2

### **Phospholipase D is central to high phosphate-induced vascular calcification**

Submitted article

Journal: BBA - Molecular Basis of Disease

Date of submission: 03-Oct-2017

Ref: BBADIS-17-722

My position: First author

Work was done at Université Lyon, Université Claude Bernard Lyon 1, CNRS UMR 5246, ICBMS, F-69622, Lyon, France, during the following periods: May 2015-July 2015, Feb 2016-July 2016, Sept 2017-Dec 2017, Feb 2017-May 2017.

Najwa Skafi<sup>1</sup>, Dina Abdallah<sup>1</sup>, Christophe Soulage<sup>3</sup>, Sophie Reibel<sup>4</sup>, Nicolas Vitale<sup>5</sup>, Eva Hamade<sup>2</sup>, Wissam Faour<sup>2</sup>, Bassam Badran<sup>2</sup>, Nader Hussein<sup>2</sup>, Rene Buchet<sup>1</sup>, Leyre Brizuela<sup>1</sup> and Saida Mebarek<sup>1</sup>.

<sup>1</sup>Univ Lyon, Univ Claude Bernard Lyon 1, CNRS UMR 5246, ICBMS, F-69622, Lyon, France

<sup>2</sup>Genomic and Health Laboratory/PRASE-EDST Campus Rafic Hariri-Hadath-Beirut-Liban, Faculty of Sciences, Lebanese University, Beirut 999095, Lebanon.

<sup>3</sup> Univ. Lyon, CarMeN, INSERM U1060, INRA U1397, INSA de Lyon, Université Claude Bernard Lyon 1, F-69621 Villeurbanne, France

<sup>4</sup>Chronobiotron UMS 3415, 67084 Strasbourg, France

<sup>5</sup>Institut des Neurosciences Cellulaires et Intégratives (INCI), UPR-3212 CNRS and Université de Strasbourg, 5 Rue Blaise Pascal, 67084 Strasbourg, France.

To whom requests should be addressed:

Dr Saida Mebarek, CNRS UMR 5246 ICBMS, F-69622, Lyon, France

E-mail: [saida.youjil@univ-lyon1.fr](mailto:saida.youjil@univ-lyon1.fr)

Running title:

Phospholipase D and vascular calcification

Conflict of interest statement: no disclosures

## ABSTRACT

Vascular calcification (VC) is the pathological accumulation of calcium phosphate crystals in one of the layers of blood vessels, leading to loss of elasticity and causing severe calcification in vessels. Medial calcification is mostly seen in patients with chronic kidney disease (CKD) and diabetes. Identification of key enzymes and their actions during calcification, will contribute to understand the onset of pathological calcification. Phospholipase D (PLD1, PLD2) is active at the earlier steps of mineralization in osteoblasts and chondrocytes. In this work, we aimed to determine their effects during high-phosphate treatment in mouse vascular muscle cell line MOVAS, in *ex vivo* model of rat aorta and *in vivo* model of adenine-induced CKD. We observed an early increase in PLD1 gene and protein expression along with increase in PLD activity in MOVAS cells, during treatment with ascorbic acid and  $\beta$ -glycerophosphate. Moreover, inhibition of PLD1 by VU0155069, or the pan-PLD inhibitor, Halopemide, prevented calcification. The mechanism of PLD activation is PKC-independent since Bisindolylmaleimide X hydrochloride, a pan-PKC inhibitor, did not affect PLD activity. In agreement, we found an increase in *Pld1* gene expression and PLD activity in aortic explant cultures treated with high phosphate, whereas PLD inhibition by Halopemide decreased calcification. Finally, an increase in both *Pld1* and *Pld2* expression occurred simultaneously with the appearance of VC in a rat model of CKD. Thus, PLD, especially PLD1, plays a central role in VC in the context of CKD and could be an important target for preventing onset or progression of VC.

Keywords:

Vascular calcification, phospholipase D, chronic kidney disease, high phosphate, aorta

### *Highlights*

- PLD1 expression and PLD activity increased in MOVAS cells in osteogenic medium.
- PLD1 inhibitor, VU0155069, or PLD pan-inhibitor, Halopemide, abolished calcification.
- *Pld1* gene expression and PLD activity increased in mineralized aortic cultures.
- *Pld1* and *Pld2* expression increased with the onset of VC in CKD rat model.

### *Abbreviations*

AA: Ascorbic acid

BW : Body weight

CKD : Chronic kidney disease

DAG : Diacylglycerol

FGF23 : Klotho, a cofactor for the fibroblast growth factor

HRP : Horseradish peroxidase

LDL : Low density lipoprotein

LPA : Lysophosphatidic acid

MOVAS : Vascular muscle cell line

MGP : Matrix Gla protein

PA : Phosphatidic acid

PC : Phosphatidylcholine

PIP2 : Phosphatidylinositol 4,5-biphosphate

PLD: Phospholipase D

PLD1 : Isoform of phospholipase 1

PLD2 : Isoform of phospholipase 2

PTH : Parathyroid hormone

RT: Room temperature

RUNX2 : Runt-related transcription factor 2

TNAP : Tissue non-specific alkaline phosphatase

VC: Vascular calcification

VSMC: Vascular smooth muscle cells

$\beta$ -GP  $\beta$ -glycerophosphate

## **1. Introduction**

Vascular calcification (VC) is characterized by the accumulation of calcium-phosphate crystals in any layer of the blood vessels. It is a common characteristic associated with atherosclerosis, hypertension, diabetes, chronic kidney disease (CKD) and aging [1,2]. The location and the degree of calcification strongly depend on the disorder. The medial form is usually seen in patients with CKD or diabetes [1,2]. Cardiovascular complications are the leading cause of death in CKD patients, and arterial medial calcification was shown to be significantly associated with mortality in hemodialysis patients [3,4]. Medial calcification lowers vessels elasticity, an effect known to be detrimental when considering large arteries, such as the aorta [5]. Due to its Windkessel effect, the aorta acts as a reservoir that stores about half the blood ejected from heart during systole and releases it during diastole, thus providing a continuous blood flow. Therefore, the loss of aortic elasticity may lead to diastolic dysfunction, increased cardiac work, left ventricular hypertrophy and heart dysfunction [5,6]. The current treatments for VC are limited to those that attenuate hyperphosphatemia, like phosphate binders, or vitamin K [7]. There is an urgency to identify the molecular mechanisms underlying VC, in order to find novel efficient and specific treatments. VC was first thought to be a passive process in which phosphate and calcium co-precipitate when present in high concentrations, 2 mM and 2.4 mM, respectively [8]. However, it was later discovered to be a tightly regulated process involving different cellular and molecular events, many of which resemble the process of bone formation. Among the various hypothesis suggested, the most accepted one is the trans-differentiation of vascular smooth muscle cells (VSMC) into osteo-chondrocyte-like cells, which then induces

calcification in the vascular wall [8]. Like bone cells or chondrocytes, these cells express bone/cartilage specific transcription factors, such as *Runx2*, triggering the expression of bone/cartilage specific proteins, such as osteocalcin (encoded by *Bglap*) [9]. Moreover, these cells have increased tissue non-specific alkaline phosphatase (TNAP) activity, and can release matrix vesicles (MVs) that are able to accumulate calcium-phosphate crystals [9]. CKD is characterized by a gradual decrease in glomerular filtration rate. Different factors in CKD can induce calcification including inflammation, oxidative stress and hyperphosphatemia [1,10]. Phosphate homeostasis is perturbed in CKD due the dysregulation of different hormones, including the secondary parathyroidism and the loss of Klotho, a cofactor for the fibroblast growth factor (FGF23), all of which disrupt phosphate absorption and excretion [9]. It was shown that with high inorganic phosphate levels, VMSCs lose the expression of specific smooth muscle proteins, like smooth muscle 22 $\alpha$  (SM22 $\alpha$ ) and  $\alpha$ -smooth muscle actin ( $\alpha$ -SMA), and acquire an osteo-chondrogenic phenotype, characterized for example by upregulation of *Runx2* [11]. Moreover, due to high phosphate and calcium, VSMCs undergo apoptosis, releasing larger amounts of calcium and decreasing the production of matrix Gla protein (MGP), an inhibitor for calcification secreted by VSMC[9,12]. Thus, high phosphate is used as an inducer of calcification in different *in-vitro*, *ex-vivo* and *in-vivo* models.

Phospholipase D (PLD) is a family of ubiquitously expressed enzymes. In mammals, the two main isoforms, PLD1 and PLD2, catalyse the hydrolysis of phosphatidylcholine, the most abundant membrane phospholipid, into phosphatidic acid (PA) and choline. PLD1 exhibits low basal activity, and is activated by small GTP binding proteins (Rho, ARF...), protein kinase C (PKC) and phosphatidyl 4,5-biphosphate (PIP2). In contrast, PLD2 has a high basal activity, and it is less responsive to PLD1 activators [13]. PA can act as a second messenger, that can activate and/or recruit proteins to the membrane, or it can affect membrane curvature facilitating vesicle fusion and fission. Moreover, PA can be hydrolysed to other lipid second

messengers like diacylglycerol (DAG) by PA phosphohydrolases and lipid phosphate phosphatases and to lysophosphatidic acid (LPA) by phospholipase A2. As a consequence, PLDs have been suspected to be involved in many cellular events including vesicular trafficking, cytoskeletal organization, cell proliferation and migration [14]. On the other hand, PLDs were shown to be implicated in the pathogenesis of different diseases like cancer, vascular and neurological disorders [14,15].

PLD is potentially involved in bone formation and homeostasis. Its activity was detected in osteoblasts [16–19] and chondrocytes [20–22], and different factors involved in bone homeostasis like parathyroid hormone (PTH) [23,24], vitamin D [20,22] and EGF [21] stimulate its activity. Recently, we demonstrated that PLD1 contributed to cultured osteoblasts differentiation (Abdallah *et al*, under revision). Moreover, PLD activity was shown to be induced and needed in the differentiation of osteoblasts in response to surface roughness [16]. On the other hand, PLD was also activated by oxidative stress [25], angiotensin II [26,27] and oxidized LDLs [28,29], all of which are involved in vascular diseases and contribute to VC [1,10]. Thus, we aimed to determine the level of gene and protein expression of PLD and its effects in VC and during the trans-differentiation of VSMC into osteo-chondrocyte like cells. In this study, we used three VC models: an *in-vitro* model of murine smooth muscle cells (MOVAS cell line), an *ex-vivo* model of whole aortas from normal rats and from PLD knockout (KO) mice for PLD1 or PLD2 and an *in-vivo* model of high adenine-induced CKD rats. All models were first validated to assess calcification, and then the expression of PLD isoforms and PLD activity were evaluated along the course of calcification. Next, using specific pharmacological inhibition or genetic ablation, we studied the involvement of PLD in VC. Here we show for the first time that PLD1 is involved in the onset of VC.

## **2. Materials and Methods**

### **2.1 Chemicals and reagents**

Culture medium, serum, antibiotics, Alizarin red, *p*-nitrophenyl phosphate, Nonidet P-40, and cetylpyridinium chloride, were obtained from Sigma Aldrich (Lyon, FR). Bisindolylmaleimide X hydrochloride (Bisindolylmaleimide) was obtained from Enzo Life (Villeurbanne, FR). Pharmacological specific PLD inhibitors Halopemide (PLD paninhibitor), VU0155069 (PLD1 specific inhibitor) and CAY10594 (PLD2 specific inhibitor) were obtained from Cayman chemical (Montluçon, FR).

## 2.2 Cell culture

The mouse VSMC line MOVAS (ATCC® CRL-2797™) was cultured in high glucose (4.5 g/L) Dulbecco's modified Eagle's medium (DMEM) containing 10% (v/v) fetal bovine serum (FBS), 100 U/mL penicillin and 100 µg/mL streptomycin (all from Sigma Aldrich, Lyon, FR). This medium is identified as **control medium**. To stimulate calcification, cells were cultured with 50 µg/mL of L-ascorbic acid (L-AA) and 10 mM β-glycerophosphate (β-GP) for 28 days (**stimulation medium**). For calcification assessment and PLD activity analysis, cells were recuperated each week. **Non-treated cells** were cultured in control medium for one week. In the experiments involving PLD inhibition, cells were cultured in stimulation medium for 21 days with or without PLD inhibitors; Halopemide, a pan-inhibitor for PLD1 and PLD2 (used at 1 and 2 µM), a PLD1 specific inhibitor VU0155069 (used at 600 and 800 nM) and a PLD2 specific inhibitor CAY10594 (used at 200 and 300 nM). For experiments of PKC inhibition, cells were cultured in stimulation medium for 21 days with or without the PKC inhibitor: bisindolylmaleimide X hydrochloride at 1 and 5 µM. The same protocol was performed when analysing PLD activity but for 14 days instead of 21 days. The control described in these experiments is the cells cultured for 21 days in control medium. Cultures were maintained in a humidified atmosphere consisting of 95% air and 5% CO<sub>2</sub> at 37 °C.

## 2.3 Aortic explant culture

Whole aortas were isolated from male Sprague Dawley rats (Janvier-Labs, Le Genest-Saint-Isle, FR). They were cleaned with sterile Phosphate-buffered saline (PBS). The adventitia layer was removed by gentle scraping and the intima was removed by flushing in 37°C warmed PBS leaving only the medial layer for the *ex-vivo* culture. Then, aortas were cultured in high glucose (4.5 g/L) DMEM containing 10% (v/v) FBS, 100 U/mL penicillin and 100 µg/mL streptomycin (all from Sigma Aldrich, Lyon, FR) for 6 days (**control medium**). Calcification was stimulated by inorganic phosphate at 6 mM during 6 days (**stimulation medium** for aorta). Halopemide at 10 µM was used to inhibit PLD activity in these conditions. Aortas were further isolated from knock-out (KO) PLD1 and KO PLD2 mice using a similar protocol [30,31].

## 2.4 Animal experiments

All experiments were performed under the authorization n°69-266-0501 and were in agreement with the guidelines laid down by the French Ministry of Agriculture (n° 2013-118) and the European Union Council Directive for the protection of animals used for scientific purposes of September 22nd, 2010 (2010/63UE). The protocol was approved by the local ethical committee (Comité Ethique de l'INSA-Lyon - CETIL, CRNEEA n°102) under the reference APAFIS#4601-2016032110173355. Male Sprague Dawley (150-175 g) rats were purchased from Janvier-Labs and housed in an air-conditioned room with a controlled environment of 21 ± 0.5°C and 60-70 % humidity, under a 12h light/dark cycle (light on from 7 am to 7 pm) with free access to food and water. CKD was induced in rats using an adenine rich-diet. Rats were randomized to either a CKD or a control group. The animals assigned to the CKD group were fed rat chow-containing 0.75% (w/w) adenine on A04 basis (SAFE, Augy, FR) for 4 weeks. The control animals were fed regular rat chow (A04, 13.4 kJ/g) throughout the observation period.

To induce VC, the animals were further fed for 5 or 7 weeks with a custom diet containing 0.9% (w/w) calcium and 0.9% (w/w) phosphorus on A04 basis. They were injected

threetimes weekly with 80 ng/kg of calcitriol (Rocaltrol, Roche, FR) diluted in propylene glycol.

The control animals were fed with the standard diet (A04, Safe, Augy, FR) containing 0.71% (w/w) calcium and 0.55% (w/w) phosphorus.

Animals were sacrificed after 5 or 7 weeks of phosphorus/calcium (P/Ca) rich diet. Rats were deeply anesthetized with sodium pentobarbital (200 mg/kg ip). The body weight (BW) and body length were measured and Lee index (i.e. adiposity index) calculated as the cubic root of BW divided by naso-anal length. Blood (~10 ml) was collected through cardiac puncture in heparinized syringe, centrifuged two minutes at 2000 g to separate plasma, snap-frozen in liquid nitrogen and stored at -80°C until analysis. Liver, heart, kidneys, gastrocnemius muscle, thoracic aorta, femur and several deposits of white adipose tissue (eWAT: epididymal WAT, rWAT: retroperitoneal and inguinal, scWAT: subcutaneous WAT) were dissected out according to anatomical landmarks, weighed to the nearest milligram and snapfrozen in liquid nitrogen and stored at -80°C. One kidney was stored in formalin for histological study.

The plasma concentration of urea was determined using UREA-kit S180 (Sobioda, Montbonnot, FR). The plasma glucose was determined using a glucometer (Accu-check Performa, Roche, Meylan, FR). The plasma concentration of total cholesterol and triacylglycerols was determined enzymatically, using cholesterol RTU and triacylglycerols PAP assay kit (bioMérieux, Marcy l'Etoile, FR) according to the manufacturer's recommendations.

## **2.5 Alkaline phosphatase (AP) activity assay**

For determination of AP activity [32], cells were harvested in 0.2% (v/v) Nonidet P-40 and disrupted by sonication. For aortas, tissues were smashed using liquid nitrogen and then added to 0.2% Nonidet P-40 and disrupted by sonication. The homogenate was centrifuged at 1500 g for 5 min. In the supernatant, AP activity was determined using p-nitrophenyl

phosphate (pNPP) as substrate at pH=10.4. The absorbance was measured at 405 nm (using an  $\epsilon$  of 18.8 mM<sup>-1</sup> cm<sup>-1</sup>). In the same lysates, the protein content was determined by bicinchoninic acid [33] (BCA, Sigma-Aldrich, Lyon, FR). Results were expressed as nmol of paranitrophenol (pNP) produced/min/mg protein and were normalized relative to their respective controls.

## **2.6 Calcium assay**

For aortic explants and MOVAS cells, deposited calcium was extracted from the extracellular matrix using HCl 0.6 M, and kept overnight at room temperature (RT). The calcium content of HCl supernatants was dosed by a colorimetric assay using o-cresolphthaline complexone method (Sigma Aldrich, Lyon, FR) [34] . The absorbance was measured at 570 nm. Calcium deposition was normalized to the weight of aortas or to the amount of proteins in cells. For the cells, proteins were harvested in NaOH 0.1 M / SDS 0.1 % and centrifuged at 700 g, 5 min at 4°C. In the supernatant, the protein content was determined by bicinchoninic acid.

## **2.7 Total RNA extraction, reverse transcription and quantitative real-time polymerase chain reaction (qPCR) analysis**

RNA was extracted from cells using the NucleoSpin RNA isolation kit by Macherey-Nagel (Villeurbanne, FR) according to the manufacturer's instructions. For aortas, tissues were smashed in liquid nitrogen and then transferred to tubes containing TRI Reagent (Sigma Aldrich, Lyon, FR), and then RNA was extracted according to the manufacturer's instructions. Total RNA was quantified by a spectrophotometer at 260 nm, and its purity was determined by the A<sub>260</sub>/A<sub>280</sub> and A<sub>260</sub>/A<sub>230</sub> (A: Absorbance). 1 µg of the resulting RNA was used for reverse transcription, using Superscript II reverse transcriptase (Invitrogen, Villebon-sur-Yvette, FR) and random hexamers (Invitrogen, Villebon-sur-Yvette, FR) in a 20-µl final volume. The reaction was done at 42°C for 30 min and stopped by incubation at 99°C for 5 min. 1 µl of cDNA template was used in subsequent qPCRs. qPCR was done using a Light Cycler system (Roche Diagnostics, Meylan, FR). The reactions were performed

in a 10- $\mu$ l final volume with 0.3  $\mu$ M primers, 2 mM MgCl<sub>2</sub> and 2  $\mu$ L of Light Cycler Fast Start DNA Master SYBR Green I mix (Roche, Meylan, FR). The sequences of primers used in qPCR is shown in Table 1. The protocol started by an activation step (10 min at 95°C) followed by 40 cycles consisting of a denaturation step (95°C) for 10 s, an annealing step (Ta) for 10 s and an elongation step at 72°C for 25 s. primer sequences and the annealing temperature (Ta) for each gene are listed in table 1. Relative quantification was done according to Livak's method using *GAPDH* as a reference gene.

<b>Gene name</b>	<b>Species</b>	<b>Forward primer (5'-3')</b>	<b>Reverse primer (5'-3')</b>	<b>Ta (°C)</b>
<i>Pld1</i>	Rat	CAACTCGGACAGCAT TAGCA	TCCCATGCCAAAACC TAGTC	62
<i>Pld2</i>	Rat	CCCTTTCTGGCCATC TATGA	ATCCGCTGGTGTATC TTTCG	62
<i>Opn</i>	Rat	TGAGACTGGCAGTGG TTTGC	CCACTTTCACCGGGA GACA	60
<i>Runx2</i>	Rat	GCCGGGAATGATGA GAACTA	TTGGGGAGGATTTGT GAAGA	60
<i>Bglap</i>	Rat	GTGCAGACCTAGCAG ACACCA	GTAGCGCCGGAGTCT ATTCA	60
<i>Gapdh</i>	Rat	GCAAGTTCAACGGCA CAG	GCCAGTAGACTCCAC GACA	60
<i>Pld1</i>	Mouse	AAGTGCAGTTGCTCC GATCT	TTCTCTGGGCGATAG CATCT	56
<i>Pld2</i>	Mouse	GGGCACCGAAAGAT ACACCA	CTCAGAACCTCCTCG GGGTA	56
<i>Gapdh</i>	Mouse	GGCATTGCTCTCAAT GACAA	TGTGAGGGAGATGCT CAGTG	62

Table 1: The sequences of the primers used in qPCR with their respective annealing temperatures (Ta).

## 2.8 Western blot

Cells were homogenized in 20 mM Tris / HCl pH 7.6 buffer containing 100 mM NaCl, 1% Triton X-100, and 1% of a protease inhibitor cocktail from Sigma Aldrich. Cell lysates were mixed with Laemmli buffer (BioRad, Californie, US), boiled for precisely 1 min, and separated on 8% SDS polyacrylamide gel containing 4 M urea. The western blots were probed with anti-PLD1- and anti-PLD2-specific polyclonal antibodies kindly provided by Dr S. Bourgoin (Laval University, CA), used at dilutions of 1/10000 and 1/5000, respectively. Immunoblots were revealed with the enhanced chemiluminescence (ECL) detection system (GE Healthcare, Limonest, FR) and X-ray film autoradiography. Membranes were incubated with an anti  $\beta$ -actin monoclonal antibody (clone AC-74) from Sigma Aldrich for normalization. Bands were then quantified by Image J software (<https://imagej.nih.gov/ij/>).

## 2.9 PLD activity assay

For cells:

PLD activity was determined by measuring the production of  $^{14}\text{C}$  -phosphatidylbutanol, which is the product of its transphosphatidylation activity. Briefly, cells were incubated for 16 h with 0.5  $\mu\text{Ci}$   $^{14}\text{C}$ -palmitate/ml to label phosphatidylcholine. The radioactive medium was then removed, and cells were washed 3 times with nonradioactive DMEM containing 0.2% BSA. 1-butanol, at a final concentration of 0.8%, was added and the cells were incubated further for 30 min, the optimal time to recover the maximal formation of phosphatidylbutanol (PtdButOH). Lipids were next extracted as described by Bligh and Dyer [35], except that 2 M KCl in 0.2 M HCl were added to the extraction mixture instead of water for the separation of the aqueous and organic phases. Chloroform phases were then evaporated overnight and resuspended in 50  $\mu\text{l}$  of chloroform. Lipids were separated by thin layer chromatography (TLC) using Silica Gel 60 plates. The TLC plates were developed with the superior phase containing mixture of ethylacetate/isooctane/acetic acid/water

(55/25/10/50). The positions of lipids were identified after staining with iodine vapour by comparison with authentic standards. The silica gel containing radioactive lipids were quantitated by liquid scintillation counting after scraping the spots off the plates.

For aortas:

Amplex Red PLD Kit (Molecular Probes, Eugene, OR, US) was used to measure the rate of choline production from PC hydrolysis by PLD, according to the manufacturer's instructions with slight modifications [36].

Tissues were smashed in liquid nitrogen and added to Tris 50 mM buffer pH=8.0. They were then lysed by three freeze/thaw cycles. Samples were incubated with 0.5 mM PC (Avanti Polar Lipids, Alabaster, AL, US) and 2 mM levamisol for 30 min at 37 °C. Then, 100 µL aliquots were collected. Extracts were mixed with 100 µL of reaction buffer containing 100 µM Amplex Red reagent, 2 U/mL horseradish peroxidase (HRP) (Molecular Probes, Eugene, OR, US), 0.2 U/mL choline oxidase from *Alcaligenes* sp. (MP Biomedicals, Illkirch-Graffenstaden, FR). 2 mM of levamisol (Sigma Aldrich, Lyon, FR) was added in the reaction buffer, to prevent dephosphorylation of phosphocholine produced by phospholipase C. PLD activity was estimated by measuring the fluorescence of resorufin after 30 min incubation at 37°C using a micro-titre plate reader (NanoQuant Infinite M200, Tecan, Salzburg, AU) at 590 nm after sample excitation at 530 nm. A standard curve was done using choline. PLD activity was normalized to the total protein amount (BCA, Sigma-Aldrich, Lyon, FR).

### **2.10 Statistical analysis**

For each analysis, at least three independent experiments were performed. Groups were compared using two-sided unpaired t-test. Results were expressed as mean ± standard error of the mean (SEM). Results were considered significant when  $p < 0.05$  (\*), highly significant when  $p < 0.01$  (\*\*), and extremely significant when  $p < 0.001$  (\*\*\*)

## **3. Results**

### **3.1 PLD expression and activity are increased during the onset of calcification induced by trans-differentiation of MOVAS cells**

The capacity of MOVAS to calcify was evaluated by measuring specific AP activity and calcium deposition during 28 days of culture in the presence of 50 µg/mL L-AA and 10 mM β-GP (stimulation medium). AP activity increased gradually and significantly starting from day 14 (Figure 1A), with an increase in calcium deposition that was significant starting from day 21 (Figure 1B). We next determined the patterns of PLD expression and activity during the trans-differentiation of MOVAS into osteo-chondrocyte-like cells. *Pld1* gene expression showed a small but significant increase at day 7 (Figure 1C) with a subsequent increase in its protein expression starting at day 7 and reaching its maximum at day 14 (Figure 1D, E). In contrast, PLD2 protein expression did not show any significant change. Of note, during late steps of MOVAS cell calcification, both *Pld1* and *Pld2* gene expression decreased gradually (Figure 1C). The increase in PLD1 expression was accompanied by a significant increase in total PLD activity starting from day 7, reaching maximum level at day 14 and then decreasing to reach the basal level at day 28 (Figure 1F).

### **3.2 PLD inhibition affects the calcification induced in MOVAS cells**

The increase in PLD activity observed in our cell model suggests a role for PLD in MOVAS trans-differentiation and associated calcification. To validate this hypothesis, PLD activity was inhibited during 21 days of MOVAS culture in stimulation medium. The use of Halopemide, which can inhibit the activities of both PLD1 and PLD2, at 1 µM or 2 µM maintained both the specific AP activity and calcium deposition significantly to the basal level seen in the non-treated cells (cells cultured in control medium) (Figure 2A and B). Furthermore, the specific inhibition of PLD1 by VU0155069 (used at 600 and 800 nM) kept the specific AP activity and the calcium deposition to the basal level (Figure 2A and B). However, the specific inhibition of PLD2 by CAY10594 (at 200 and 300 nM) failed to prevent calcification (Figure 2A and B). Of note, Halopemide treatment inhibited 80% of

total PLD activity under these conditions, while the highest concentrations of VU0155069 and CAY10594 tested, inhibited PLD activity by 60% and 40% respectively. Lower concentrations of VU0155069 and CAY10594 did not inhibit PLD activity significantly (data not shown).

### **3.3 PKC inhibition disturbs calcification but not PLD activity in MOVAS cells**

We next aimed to check whether the activation of PLD seen during calcification involves PKC. The pan-PKC inhibitor Bisindolylmaleimide X hydrochloride (bisindolylmaleimide), at 1 or 5  $\mu$ M significantly inhibited AP activity in a dose-dependent manner (Figure 3A). With respect to calcium deposition, PKC inhibition had a partial effect at 5  $\mu$ M where the calcium content decreased significantly but not to basal level (Figure 3B). To assess whether PKC effect on calcification is mediated by PLD activation, the effect of PKC inhibition on PLD activity was tested after 14 days of culture (the time at which PLD activity reached its maximum, Figure 1F). PKC inhibition did not induce any change in PLD activity (Figure 3C). These results show that PKC affected MOVAS trans-differentiation into calcifying cells in a mechanism that did not involve PLD and that PLD is activated during MOVAS calcification in a PKC-independent manner.

### **3.4 PLD expression and activity are increased during calcification in aorta *ex-vivo* model**

Calcification was induced in rat aortas by culturing them in 6 mM phosphate medium for 6 days. The calcification was confirmed by the significant increase in AP specific activity (Figure 4A) and in calcium deposition (Figure 4B). Moreover, the gene expression of two osteo-chondrocyte markers, *Runx2* and *Bglap*, increased significantly at day 6 (Figure 4C), evidencing the trans-differentiation of the aortic cells into calcifying cells. Simultaneously, gene expression of *Opn*, a calcification inhibitor, was significantly decreased in aorta *ex-vivo* model (Figure 4C). Accompanying calcification, there was an increment in the *Pld1* gene

expression, but not that of *Pld2*, along with a significant rise in the total PLD activity (figure 4D, E), arguing for an involvement of PLD1 activity during rat aortas calcification.

### **3.5 PLD inhibition diminishes calcification in aorta *ex-vivo* model**

To ratify the implication of PLD in calcification in aorta *ex-vivo* model, PLD activity was blocked during 6 days using Halopemide at 10  $\mu$ M. PLD inhibition maintained AP activity to its normal level (Figure 5A), and significantly reduced calcium deposition (Figure 5B). Importantly, PLD inhibition also abolished the trans-differentiation of aortic cells as evidenced by the expression of *Runx2* and *Bglap* that did not differ from the non-treated aortas (Figure 5C and D). Furthermore, the use of Halopemide pan-PLD inhibitor increased significantly *Opn* gene expression (Figure 5E). In order to determine precisely the role of each PLD isoform, aortas were taken from wild-type (WT), PLD1 or PLD2 KO mice, and cultured in 6 mM phosphate for 6 days. At the end of culture time, the ability of aortas to calcify was measured by the amount of calcium deposited. PLD1 KO aortas were significantly less able to calcify than WT or PLD2 KO aortas, as evidenced by a lower amount of calcium deposited (Figure 5F), strongly arguing for a positive role of PLD1 in aorta calcification.

### **3.6 PLD expression in calcified rat aortas in a rat model of chronic kidney disease**

CKD was induced by feeding rats with an adenine-enriched diet (0.75% w/w) for four weeks (Figure 6A). The plasma urea level was then measured, and found to be strikingly increased in rats given adenine diet compared to control rats, unambiguously evidencing the kidney failure (Figure 6B). Then, the adenine diet was replaced with high P/Ca diet (0.9%, 0.9% w/w, respectively) and injections of calcitriol (active vitamin D, 80 ng/kg, 3 times per week) for 5 (VC1) or 7 (VC2) weeks in order to induce vascular calcification (Figure 6A). The plasma urea level measured 4 weeks after the end of adenine diet was significantly increased in CKD rats compared to control animals (Figure 6B) evidencing that kidney failure induced by adenine was not reversible.

The main characteristics of control and CKD rats are shown in Table 2. CKD rats exhibited a significant decrease in body weight (-16% compared to control,  $p < 0.05$ ) (Table 2, Figure 6B) that was further lowered by the treatment with P/Ca and calcitriol (-27%,  $p < 0.005$ ) (Table 2, Figure 6B). CKD rats exhibited an increased kidney weight (2 fold,  $p < 0.01$ ) and kidney exhibited macroscopic changes (Figure 6A). At the time of sacrifice, the plasma urea concentration was 2.6 fold higher in CKD rats compared to controls ( $p < 0.001$ ) unambiguously evidencing the kidney failure. Remarkably, in CKD rats, plasma cholesterol and glucose levels were increased compared to controls, while, decrease was observed for plasma triglycerides. Treatment with only P/Ca and calcitriol neither significantly altered the kidney weight nor the plasma biochemical parameters.

Rats were divided into five groups: “Control” group was kept on normal diet during the whole experimental time, “CKD” group which was given high adenine diet for 4 weeks and then kept on normal diet, “Control + P/Ca + calcitriol” group which was kept on normal diet for four weeks and then was given the high P/Ca diet with calcitriol, “VC1” and “VC2” that were given the high adenine diet for four weeks and the second type of diet for five and seven weeks, respectively. The aortas from these rats were isolated and the accumulated calcium was assayed. The amounts of calcium in the first three groups were similar with a clear increase in VC1 group and a further increase in VC2 group (Figure 7A). Moreover, the gene expression of *Runx2* also increased significantly in VC1 and in VC2 compared to the first three groups (Figure 7B). The expression of *Pld1* and *Pld2* genes was significantly increased in VC1 group, before dropping to control levels in VC2 group (Figure 7C).

#### 4. Discussion

VC is a life threatening disease, especially for patients with CKD and diabetes, due to its detrimental effects of the cardiac system. PLD is an important enzyme involved in many cellular events and it is implicated in the pathogenesis of different diseases like cancer and neurodegenerative diseases [14,15]. PLD activity was detected in bone forming cells and it

was found to be induced by different factors promoting bone formation [16–24]. Given the similarities between bone formation and VC, including the acquirement of a phenotype for vascular cells that resemble that of osteoblasts and/or chondrocytes, we decided to decipher whether PLD activity is involved in the onset and/or progression of VC. Our hypothesis was strongly supported by the fact that PLD was shown to be activated by hydrogen peroxide [25] and angiotensin II [27, 36], factors known to be associated with vascular diseases and VC. The common features of VC with physiological bone formation process make it more difficult to find a treatment that could target it without any adverse effects on skeletal structures. Thus, it is pivotal to understand the detailed mechanism of its onset and progression, in order to be able to provide specific, effective and preventive treatments. Three models of VC were used: i) an *in-vitro* model of murine smooth muscle cells (MOVAS) trans-differentiating into osteochondrocyte-like cells and cultured in presence of  $\beta$ -GP (an organic source of phosphate) and AA (a cofactor needed in collagen synthesis), ii) an *ex-vivo* model of rat or KO PLD mice aortas cultured in a high phosphate medium and iii) an *in vivo* rat model of adenine-induced CKD in which VC was provoked by high phosphorus and calcium diet with active vitamin D treatment. In these three models, which have been already validated by other research groups [37, 38], calcification was confirmed via the analysis of calcium deposition, AP activity, and the expression of bone marker genes. We found an increase in the expression of *Pld1* in all three models and an increase in *Pld2* gene expression in the *in-vivo* model only. Importantly, the increase in *Pld1* expression was seen only in the first 7 days of MOVAS calcification, but it was associated with a significant increase in PLD1 expression between days 7 and 14, along with a matching increase in PLD activity that reached its maximum at day 14 before a return to background levels. All these changes were occurring just before and during the initial increase in AP activity, and just before the start of calcium deposition. This timing may give PLD a specific role in the initial steps of trans-differentiation of VSMC and calcification. Interestingly, the increase in *Pld1* and *Pld2*

expression in the *in-vivo* model was also temporarily and restricted to the initial phase of the calcification process, which means that the mechanism of PLD activation may be similar in both models. The increase in PLD activity was also evident in the aortic explant, but this *ex-vivo* model did not allow us to reach a point for which *pld1* expression or PLD activity decreased again. This difference may reflect the shorter time of culture (6 days) or modifications in the mechanism of calcification between cultured cells and isolated tissues. In MOVAS, the inhibition of PLD1 activity, either specifically by VU0155069 or by the panPLD inhibitor Halopemide, abolished significantly the calcification observed after 21 days of culture. Concurrently, PLD inhibition by Halopemide in aortas strongly decreased AP activity and prevented the expression of bone markers. Calcium deposition also decreased significantly upon PLD inhibition, but only partially, suggesting that PLD has only a limited regulatory action in the process or the occurrence of passive calcium-phosphate deposits. In contrast, the specific inhibition of PLD2 in MOVAS did not prevent calcification. In accordance with pharmacological inhibition, genetic ablation of PLD1, but not that of PLD2, suppressed the ability of mouse aortas to calcify. Altogether these results suggest crucial role of PLD, specifically PLD1, in the onset of vascular calcification.

Then, we aimed to identify the mechanism by which PLD is activated during calcification process. PKC is an important activator of PLD, especially PLD1 [40]. Moreover, PKC is activated by different growth factors and is important for osteogenic differentiation [40–43]. PKC inhibition decreased calcification in our cell model; however, it did not affect PLD activity. This indicates that PKC is involved in VC, but not through activating PLD, and that PLD activation in this process is PKC-independent. BIBLIO PKC VC PLD and the lipid messengers generated by its enzymatic activity may be implicated in VC in many different ways. For instance, PA produced by PLD can favour calcification by inhibiting autophagy via the binding and activation on mTOR [43, 44]. Indeed autophagy was seen to play a protective role against VC [45, 46]. Another way by which PLD may be acting is by facilitating the

release of MVs, the structures that form the initial site at which calciumphosphate crystals accumulate. In normal condition, the release of these vesicles takes place after the acquirement of osteoblastic or chondrocytic phenotype, and just before the deposition of calcium. Intriguingly, this is the same timing as the increase in PLD activity and PLD1-generated PA has been involved in vesicle exocytosis in different cell models through its ability to change membrane topology [49]. Furthermore PLD, and its product PA, have important roles in actin cytoskeletal reorganization, which is a determinant step in the formation and release of MVs [49–51]. On the other hand, PLD is also known to induce the expression and activity of matrix metalloproteases MMP2 and MMP9 in cancer cells [53,54]. These two MMPs are very important in elastin degradation [55], which is an important step in the progression of VC, because the resultant elastin fragments can act as sites for calcium deposition and can bind to receptors on smooth muscle cells favouring the transdifferentiation [55, 56]. These are just some examples of how PLD may be acting but other mechanisms cannot be excluded.

## **5. Concluding remarks and perspectives**

Our results suggest that PLD can be a valuable target for treatments against VC. PLD1/2 double KO mice are phenotypically normal, with no important adverse health effects [58]. However, these mice are partially protected against cancer and brain disorders than wild type mice [59]. Probably under physiological conditions PLD functions and/or production of PA are adequately compensated by other mechanisms and other enzymes that can keep the level of PA constant [58]. In contrast, under pathological conditions, where lack of enzymes or their overexpression may occur, such compensation mechanisms are not adequately regulated. Moreover, Halopemide, the pan-PLD inhibitor, was already used to treat neurological disorders as a dopamine antagonist, and it did not have any negative effects [59,60], and PLD isoform specific inhibitors are currently in clinical trial. Thus, it will be

interesting to try inhibiting the onset and the progression of VC by giving patients these drugs.

In conclusion, our work suggests a central role for PLD, specifically PLD1, in VC, especially in the onset of the process. During this pathological process, PLD is activated in a PKC-independent manner. Blocking the progression of VC by the use of PLD inhibitors may be an interesting new strategy to decrease cardiovascular complications in patients with CKD.

## **6. ACKNOWLEDGMENTS**

This work was supported by the Centre National de la Recherche Scientifique (CNRS) and the Université Claude Bernard Lyon 1. Authors are grateful to the Lebanese University (LU) and the Lebanese National Council for Scientific Research (CNRS-L) for providing PhD scholarships to Dina Abdallah and Najwa Skafi.

## **AUTHOR CONTRIBUTIONS**

NS and LBM planned the experimental design, conducted experiments, and wrote the manuscript. DA conducted the *in vitro* and *ex vivo* experiments. CS, NS, LBM and SM realized the *in vivo* experiments. SR and NV entertained and furnished the KO mice. EH, BB, NH, NV, and RB proofread the manuscript. SM conceived the project, planned the experimental design, conducted experiments, interpreted the data and wrote the manuscript.

## FIGURE LEGENDS

**Figure 1: PLD expression and activity during calcification induced by MOVAS cells.** MOVAS cells were incubated with 10 mM  $\beta$ -GP 10 mM and 50  $\mu$ g/ml AA during 28 days (D28). (A) Relative specific AP activity was calculated by a colorimetric assay using p-nitrophenyl phosphate (pNPP) as substrate. (B) Relative calcium deposition was quantified using o-cresolphthaline complexone in a colorimetric assay. (C) *Pld1* and *Pld2* gene expression was relatively quantified by qPCR according to Livak's method and using *Gapdh* as a reference gene. (D) Protein expression of PLD1 and PLD2 was examined by western blot with  $\beta$ -actin being used as a loading control. (E) PLD1 and PLD2 bands obtained by western blot were quantified by image J and normalized to the expression of  $\beta$ -actin. (F) Relative PLD activity in MOVAS cells was measured as amount of PtdButOH produced relative to total phospholipids. All results are represented relative to non-treated cells (NT) which was incubated with control medium for 7 days. At least 3 independent experiments were performed for each assay and statistical significance compared to NT cells was estimated by student t test. \* Indicated  $p < 0.05$ , \*\* indicated  $p < 0.01$  and \*\*\* indicated  $p < 0.001$ .

**Figure 2: The effects of PLD inhibition on calcification induced by MOVAS cells.**

MOVAS cells were incubated with 10mM  $\beta$ -GP 10 mM and 50  $\mu$ g/ml AA during 21 days (D21) with or without PLD inhibitors: Halopemide, a pan-inhibitor for PLD1 and PLD2 (used at 1 and 2  $\mu$ M), a PLD1-specific inhibitor VU0155069 (used at 600 and 800 nM) and a PLD2-specific inhibitor CAY10594 (used at 200 and 300 nM). NT are non-treated cells incubated in control medium for 3 weeks. (A) Relative specific AP activity was calculated by a colorimetric assay using p-nitrophenyl phosphate (pNPP) as substrate. (B) Relative calcium deposition was quantified using o-cresolphthaline complexone in a colorimetric assay. All results are represented relative to cells stimulated for calcification for 3 weeks without treatment with any inhibitor (D21). At least 3 independent experiments were performed for

each assay and statistical significance compared to D21 was estimated by student t test. \* Indicated  $p < 0.05$ , \*\* indicated  $p < 0.01$  and \*\*\* indicated  $p < 0.001$ .

**Figure 3: The effects of PKC inhibition on calcification induced by MOVAS cells and PLD activity.** MOVAS cells were incubated with 10mM  $\beta$ -GP 10 mM and 50  $\mu$ g/ml AA during 21 days (D21) with or without the PKC inhibitor: Bisindolylmaleimide X hydrochloride at 1 or 5  $\mu$ M. NT are non-treated cells incubated in control medium for 3 weeks. (A) Relative specific AP activity was calculated by a colorimetric assay using p-nitrophenyl phosphate (pNPP) as substrate. (B) Relative calcium deposition was quantified using o-cresolphthaline complexone in a colorimetric assay. (C) PLD activity in MOVAS cells was measured as amount of PtdButOH produced relative to total phospholipids. All results are represented relative to cells stimulated for calcification for 3 weeks without treatment with any inhibitor (D21). At least 3 independent experiments were performed for each assay and statistical significance compared to D21 was estimated by student t test. \* Indicated  $p < 0.05$ , \*\* indicated  $p < 0.01$  and \*\*\* indicated  $p < 0.001$ .

**Figure 4: PLD expression and activity during rat aorta calcification.** Rat aortas were incubated in 6 mM inorganic phosphate (Pi) for 6 days (D6) and were compared to nontreated aortas that were incubated in control medium for 6 days also (NT). (A) Relative specific AP activity was calculated by a colorimetric assay using p-nitrophenyl phosphate (pNPP) as substrate after smashing of the tissue. (B) Relative calcium deposition was quantified using o-cresolphthaline complexone in a colorimetric assay. (C) The gene expression of the osteochondrogenic markers, *Runx2* and *Bglap*, and the calcification inhibitor *Opn*, was relatively quantified by qPCR using *Gapdh* as a reference gene. (D) The gene expression of *Pld1* and *Pld2* was also relatively calculated using qPCR. (E) Relative PLD activity was estimated by measuring choline production and normalization to total

protein amount. All results are represented relative to non-treated aortas (NT). At least 3 independent experiments were performed for each assay and statistical significance compared to NT aortas was estimated by student t test. \* Indicated  $p < 0.05$ , \*\* indicated  $p < 0.01$  and \*\*\* indicated  $p < 0.001$ .

**Figure 5: The effects of PLD inhibition on rat aorta calcification.** Rat aortas were incubated in 6 mM inorganic phosphate (Pi) for 6 days (D6) with or without Halopemide 10  $\mu$ M. (A) relative specific AP activity was calculated by a colorimetric assay using p-nitrophenyl phosphate (pNPP) as substrate after smashing of the tissue. (B) Relative calcium deposition was quantified using o-cresolphthaline complexone in a colorimetric assay. The gene expression of the osteochondrogenic markers, *Runx2* (C) and *Bglap* (D), and the calcification inhibitor *Opn* (E), was relatively quantified by qPCR using *Gapdh* as a reference gene. (F) Relative calcium accumulation was quantified in mouse aortas taken from WT, KO PLD1 and PLD2 mice cultured in 6 mM of high-phosphate medium for 6 days. All results are represented relative to D6 or WT aortas. At least 3 independent experiments were performed for each assay and statistical significance compared to D6 or WT aortas was estimated by student t test. \* Indicated  $p < 0.05$ , \*\* indicated  $p < 0.01$  and \*\*\* indicated  $p < 0.001$ .

**Figure 6: Induction of vascular calcification (VC) in an adenine-induced model of chronic kidney disease (CKD) in rat.** (A) Detailed schematic representation of the in vivo protocol for induction of renal failure and VC in rats. Rats were fed with adenine diet (CKD group, N=12) or with control diet (Control group, N=12). 2 independent experiments were performed. For more details, see the Material and methods section. (B) Evolution of rat body weight during the in vivo experiment, along with plasma urea measured at the end of the adenine diet and at the end of VC induction by Ca/P + calcitriol diet. Graphics represent the results from the 2 independent experiments that were performed.

**Figure 7: *Pld* expression in aorta during VC induced in-vivo by high phosphore and calcium diet in CKD rats.** CKD was induced in rats by high adenine diet as described in Material and methods. In CKD rats, VC was induced by additional high calcium and phosphorus diet with active vitamin D administration for 5 (VC1) of 7 weeks (VC2). Rat aortas were isolated and used for subsequent analysis (A) relative calcium deposition was quantified using o-cresolphthaline complexone in a colorimetric assay. Relative gene expression was calculated by qPCR for *Runx2* (B), *Pld1* and *Pld2* (C), using *Gapdh* as a reference gene. All results are represented relative to control. Statistical significance was estimated by student t test. \* Indicated  $p < 0.05$ , \*\* indicated  $p < 0.01$  and \*\*\* indicated  $p < 0.001$ , all with respect to control. # indicated  $p > 0.05$ , ## indicated  $p < 0.01$  and ### indicated  $p < 0.001$ , all with respect to CKD group. \$ indicated  $p < 0.05$ , \$\$ indicated  $p < 0.01$  and \$\$\$ indicated  $p < 0.001$ , all with respect to control+ P/Ca+ calcitriol group.

Figure 1

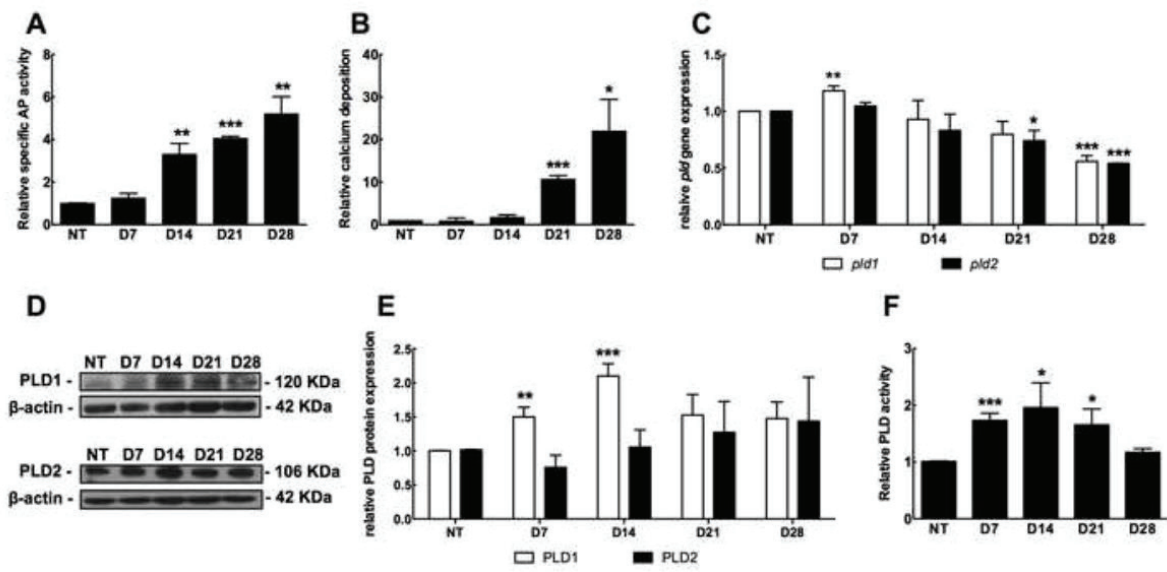


Figure 2

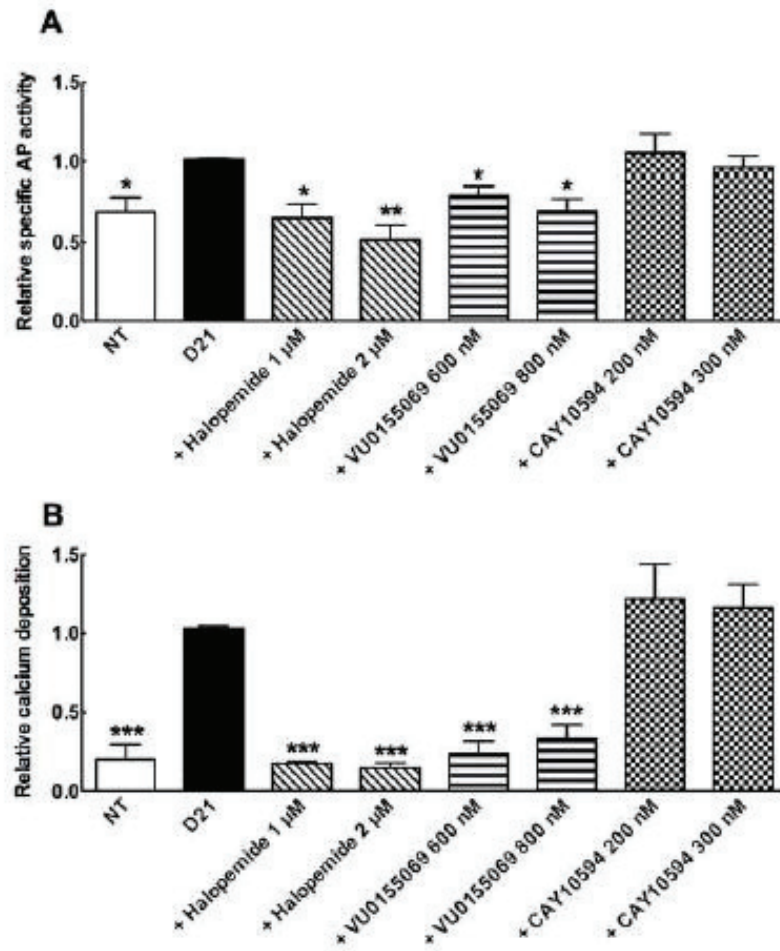


Figure 3

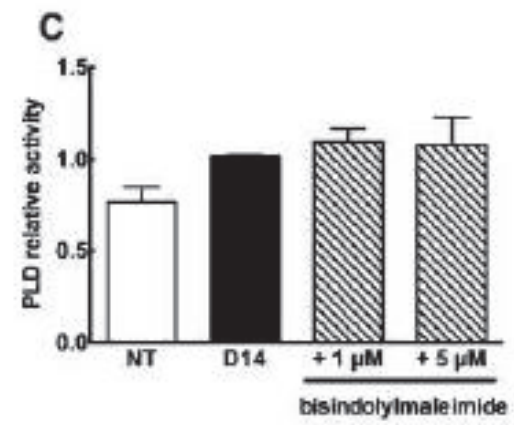
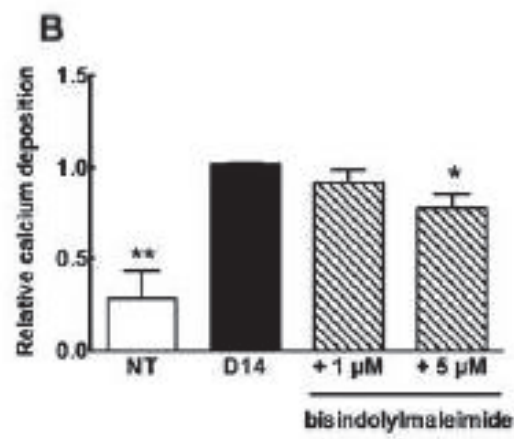
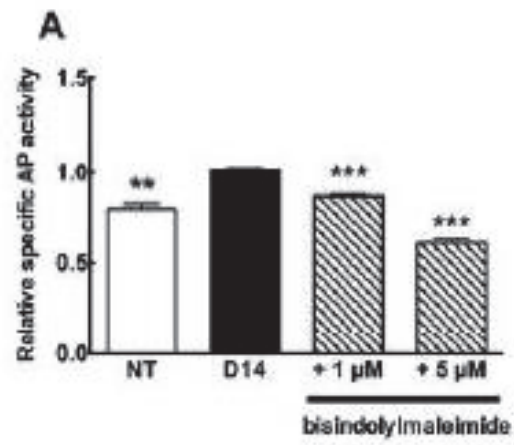


Figure 4

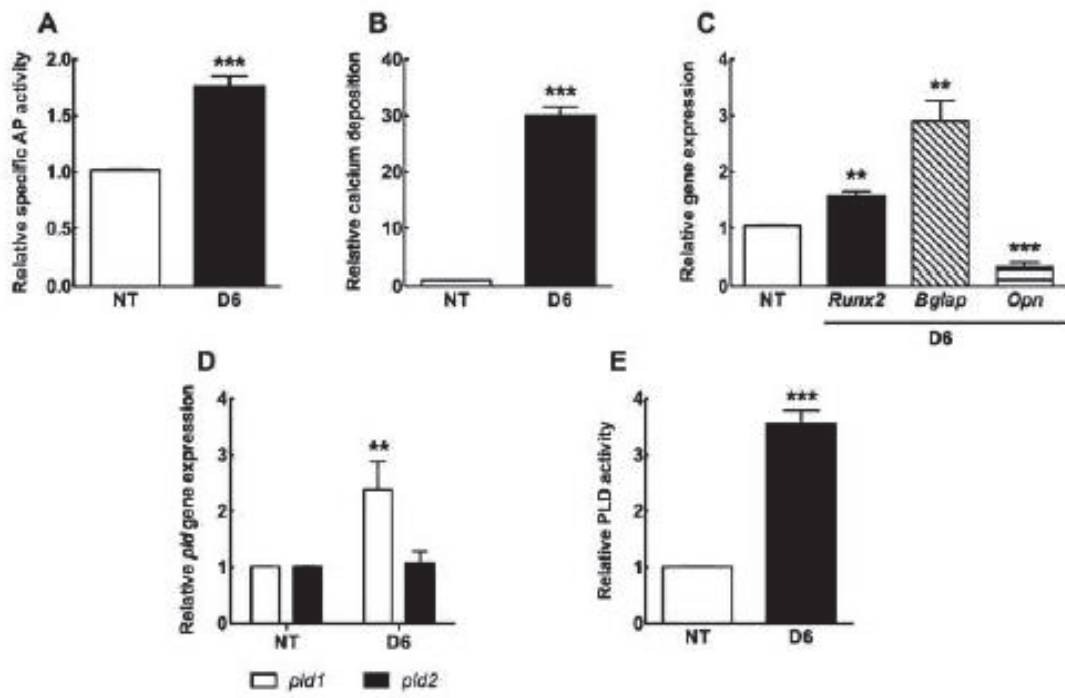


Figure 5

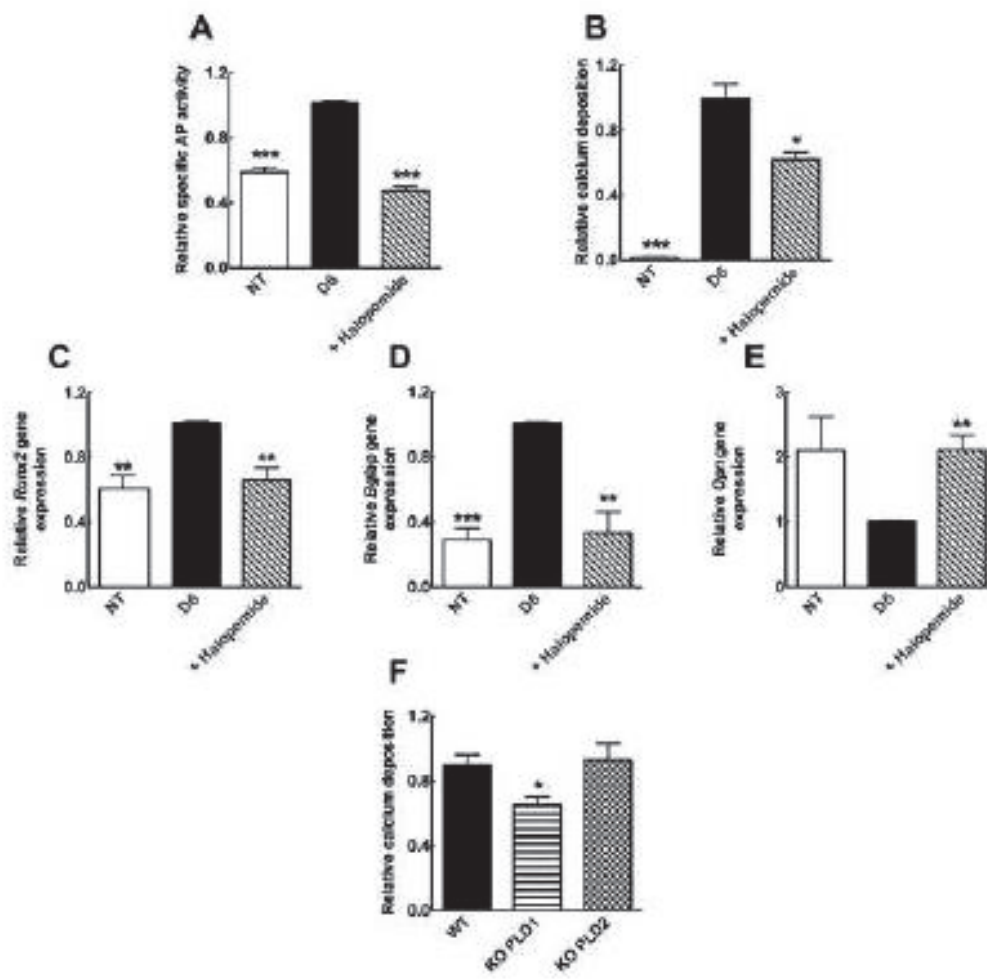


Figure 6

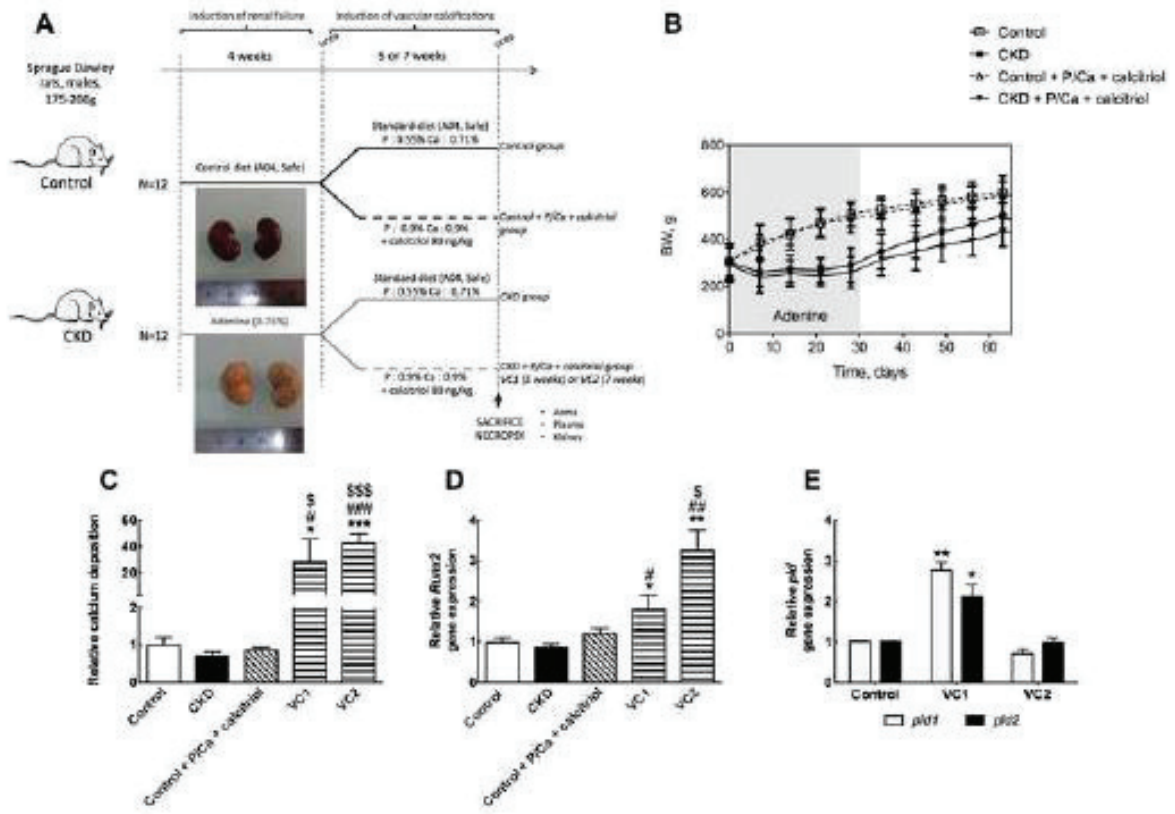


Figure 7

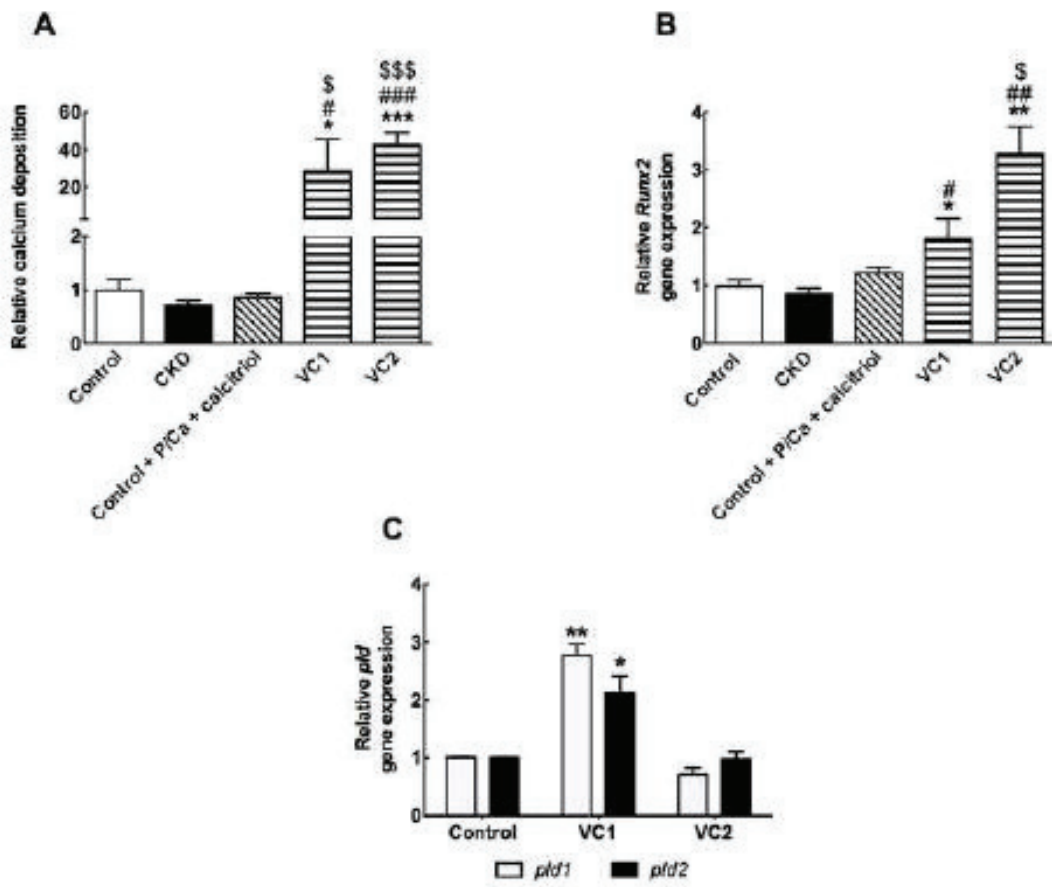


Table 2

General characteristics of control and CKD rats

Renal function	Control		CKD		ANOVA-2		
	Standard diet	P/Ca + caloric diet	Standard diet	P/Ca + caloric diet	Renal status	Treatment	Interaction
Treatment							
N	9	9	9	11			
<b>Biometry</b>							
RR, g	607 ± 15a	580 ± 28a	509 ± 16b	461 ± 18c	<b>0.002</b>	<b>0.021</b>	0.726
Body length, cm	27.6 ± 0.2a	27.4 ± 0.3a	25.9 ± 0.2b	25.2 ± 0.4b	<b>0.016</b>	0.117	0.321
Lee index	307 ± 2a	304 ± 1a	307 ± 1a	301 ± 2a	0.34	<b>0.008</b>	0.724
<b>Organ weight</b>							
Liver, g/100 g BW	2.89 ± 0.07	2.97 ± 0.1	2.85 ± 0.05	2.86 ± 0.07	0.109	0.916	0.334
Heart, g/100 g BW	0.26 ± 0.01	0.28 ± 0.02	0.28 ± 0.01	0.30 ± 0.02	0.608	0.320	0.086
Kidneys, g/100 g BW	0.53 ± 0.03a	0.54 ± 0.02a	0.93 ± 0.08b	1.04 ± 0.06b	<b>&lt;0.001</b>	0.665	0.614
<b>Plasma biochemistry</b>							
Urea, mmol/L	6.99 ± 0.69a	5.85 ± 0.20a	17.94 ± 2.14b	17.03 ± 2.64b	<b>&lt;0.001</b>	0.633	0.056
Glucose, mmol/L	5 ± 0.2a	6.4 ± 0.2a	7.3 ± 0.2b	7.1 ± 0.1b	<b>&lt;0.001</b>	0.173	0.389
Triglycerides, mmol/L	2.21 ± 0.22a	2.06 ± 0.20a	0.91 ± 0.10b	1.06 ± 0.11b	<b>&lt;0.001</b>	0.985	0.386
Total cholesterol, mmol/L	2.46 ± 0.18a	1.83 ± 0.13a	3.26 ± 0.27b	4.11 ± 0.49b	<b>&lt;0.001</b>	0.7343	0.023

Data are mean ± SEM. Data were compared using Student t test, and when appropriate, Welch correction for variance heterogeneity. Lee adiposity index was calculated as the cube root of the BW divided by nasal anal length. Differences were considered significant at the P<0.05 level. Abbreviation: BW, body weight; CKD, chronic kidney disease. Different letters indicate a significant difference between group at the p<0.05 level.

## REFERENCES

- [1] A.P. Sage, Y. Tintut, L.L. Demer, Regulatory mechanisms in vascular calcification, *Nat. Rev. Cardiol.* 7 (2010) 528–536. doi:10.1038/nrcardio.2010.115.
- [2] D. Zhu, N.C.W. Mackenzie, C. Farquharson, V.E. Macrae, Mechanisms and clinical consequences of vascular calcification, *Front. Endocrinol.* 3 (2012) 95. doi:10.3389/fendo.2012.00095.
- [3] G.M. London, A.P. Guérin, S.J. Marchais, F. Métivier, B. Pannier, H. Adda, Arterial media calcification in end-stage renal disease: impact on all-cause and cardiovascular mortality, *Nephrol. Dial. Transplant. Off. Publ. Eur. Dial. Transpl. Assoc. - Eur. Ren. Assoc.* 18 (2003) 1731–1740.
- [4] R.N. Foley, P.S. Parfrey, M.J. Sarnak, Clinical epidemiology of cardiovascular disease in chronic renal disease, *Am. J. Kidney Dis. Off. J. Natl. Kidney Found.* 32 (1998) S112–119.
- [5] L.L. Demer, Y. Tintut, Vascular calcification: pathobiology of a multifaceted disease, *Circulation.* 117 (2008) 2938–2948. doi:10.1161/CIRCULATIONAHA.107.743161.
- [6] G.G. Belz, Elastic properties and Windkessel function of the human aorta, *Cardiovasc. Drugs Ther. Spons. Int. Soc. Cardiovasc. Pharmacother.* 9 (1995) 73–83.
- [7] W.C. O'Neill, K.A. Lomashvili, Recent progress in the treatment of vascular calcification, *Kidney Int.* 78 (2010) 1232–1239. doi:10.1038/ki.2010.334.
- [8] M. Liberman, A.E.P. Pesaro, L.S. Carmo, C.V. Serrano Jr, Vascular calcification: pathophysiology and clinical implications, *Einstein São Paulo Braz.* 11 (2013) 376–382.
- [9] R. Shroff, D.A. Long, C. Shanahan, Mechanistic insights into vascular calcification in CKD, *J. Am. Soc. Nephrol. JASN.* 24 (2013) 179–189. doi:10.1681/ASN.2011121191.
- [10] C.H. Byon, A. Javed, Q. Dai, J.C. Kappes, T.L. Clemens, V.M. Darley-Usmar, J.M. McDonald, Y. Chen, Oxidative stress induces vascular calcification through modulation of the osteogenic transcription factor Runx2 by AKT signaling, *J. Biol. Chem.* 283 (2008) 15319–15327. doi:10.1074/jbc.M800021200.
- [11] S. Jono, M.D. McKee, C.E. Murray, A. Shioi, Y. Nishizawa, K. Mori, H. Morii, C.M. Giachelli, Phosphate regulation of vascular smooth muscle cell calcification, *Circ. Res.* 87 (2000) E10–17.
- [12] H. Rahabi-Layachi, R. Ourouda, A. Boullier, Z.A. Massy, C. Amant, Distinct Effects of Inorganic Phosphate on Cell Cycle and Apoptosis in Human Vascular Smooth Muscle Cells, *J. Cell. Physiol.* 230 (2015) 347–355. doi:10.1002/jcp.24715.
- [13] M.N. Hodgkin, M.R. Masson, D. Powner, K.M. Saqib, C.P. Ponting, M.J. Wakelam, Phospholipase D regulation and localisation is dependent upon a phosphatidylinositol 4,5-bisphosphate-specific PH domain, *Curr. Biol. CB.* 10 (2000) 43–46.
- [14] J. Gomez-Cambronero, Phospholipase D in cell signaling: From a myriad of cell functions to cancer growth and metastasis, *J. Biol. Chem.* (2014) jbc.R114.574152. doi:10.1074/jbc.R114.574152.
- [15] H.A. Brown, P.G. Thomas, C.W. Lindsley, Targeting phospholipase D in cancer, infection and neurodegenerative disorders, *Nat. Rev. Drug Discov.* 16 (2017) 351–367. doi:10.1038/nrd.2016.252.
- [16] M.-J. Kim, M.-U. Choi, C.-W. Kim, Activation of phospholipase D1 by surface roughness of titanium in MG63 osteoblast-like cell, *Biomaterials.* 27 (2006) 5502–5511. doi:10.1016/j.biomaterials.2006.06.023.
- [17] J. Shinoda, A. Suzuki, Y. Oiso, O. Kozawa, Thromboxane A<sub>2</sub>-stimulated phospholipase D in osteoblast-like cells: possible involvement of PKC, *Am. J. Physiol.* 269 (1995) E524–529.
- [18] A. Suzuki, Y. Oiso, O. Kozawa, Effect of endothelin-1 on phospholipase D activity in osteoblastlike cells, *Mol. Cell. Endocrinol.* 105 (1994) 193–196.
- [19] A. Suzuki, J. Shinoda, Y. Oiso, O. Kozawa, Mechanism of phospholipase D activation induced by extracellular ATP in osteoblast-like cells, *J. Endocrinol.* 145 (1995) 81–86.
- [20] V.L. Sylvia, Z. Schwartz, F. Del Toro, P. DeVeau, R. Whetstone, R.R. Hardin, D.D. Dean, B.D. Boyan, Regulation of phospholipase D (PLD) in growth plate chondrocytes by 24R,25-(OH)<sub>2</sub>D<sub>3</sub> is dependent on cell maturation state (resting zone cells) and is specific to the PLD2 isoform, *Biochim. Biophys. Acta.* 1499 (2001) 209–221.
- [21] J.A. Conquer, S.A. Jones, T.F. Cruz, Effect of interleukin 1, lipopolysaccharide and phorbol esters on phospholipase D activity in chondrocytes, *Osteoarthr. Cartil. OARS Osteoarthr. Res. Soc.* 2 (1994) 269–273.
- [22] Z. Schwartz, V.L. Sylvia, M.H. Luna, P. DeVeau, R. Whetstone, D.D. Dean, B.D. Boyan, The effect of 24R,25-(OH)<sub>2</sub>D<sub>3</sub> on protein kinase C activity in chondrocytes is mediated by phospholipase D whereas the effect of 1 $\alpha$ ,25-(OH)<sub>2</sub>D<sub>3</sub> is mediated by phospholipase C, *Steroids.* 66 (2001) 683–694.

- [23] A.T.K. Singh, A. Gilchrist, T. Voyno-Yasenetskaya, J.M. Radeff-Huang, P.H. Stern, G $\alpha$ 12/G $\alpha$ 13 subunits of heterotrimeric G proteins mediate parathyroid hormone activation of phospholipase D in UMR-106 osteoblastic cells, *Endocrinology*. 146 (2005) 2171–2175. doi:10.1210/en.2004-1283.
- [24] A.T.K. Singh, M.A. Frohman, P.H. Stern, Parathyroid hormone stimulates phosphatidylethanolamine hydrolysis by phospholipase D in osteoblastic cells, *Lipids*. 40 (2005) 1135–1140.
- [25] J. Kim, G. Min, Y.-S. Bae, D.S. Min, Phospholipase D is involved in oxidative stress-induced migration of vascular smooth muscle cells via tyrosine phosphorylation and protein kinase C, *Exp. Mol. Med.* 36 (2004) 103–109. doi:10.1038/emm.2004.15.
- [26] J.-H. Parmentier, Z. Pavicevic, K.U. Malik, ANG II stimulates phospholipase D through PKC $\zeta$  activation in VSMC: implications in adhesion, spreading, and hypertrophy, *Am. J. Physiol. Heart Circ. Physiol.* 290 (2006) H46-54. doi:10.1152/ajpheart.00769.2005.
- [27] K. Yasunari, K. Maeda, M. Nakamura, J. Yoshikawa, Pressure Promotes Angiotensin II-Mediated Migration of Human Coronary Smooth Muscle Cells Through Increase in Oxidative Stress, *Hypertension*. 39 (2002) 433–437. doi:10.1161/hy02t2.102991.
- [28] A. Gómez-Muñoz, J.S. Martens, U.P. Steinbrecher, Stimulation of phospholipase D activity by oxidized LDL in mouse peritoneal macrophages, *Arterioscler. Thromb. Vasc. Biol.* 20 (2000) 135–143.
- [29] V. Natarajan, W.M. Scribner, C.M. Hart, S. Parthasarathy, Oxidized low density lipoprotein-mediated activation of phospholipase D in smooth muscle cells: a possible role in cell proliferation and atherogenesis, *J. Lipid Res.* 36 (1995) 2005–2016.
- [30] M.-R. Ammar, Y. Humeau, A. Hanauer, B. Nieswandt, M.-F. Bader, N. Vitale, The Coffin-Lowry syndrome-associated protein RSK2 regulates neurite outgrowth through phosphorylation of phospholipase D1 (PLD1) and synthesis of phosphatidic acid, *J. Neurosci. Off. J. Soc. Neurosci.* 33 (2013) 19470–19479. doi:10.1523/JNEUROSCI.2283-13.2013.
- [31] M.R. Ammar, T. Thahouly, A. Hanauer, D. Stegner, B. Nieswandt, N. Vitale, PLD1 participates in BDNF-induced signalling in cortical neurons, *Sci. Rep.* 5 (2015) 14778. doi:10.1038/srep14778.
- [32] M. Hui, H.C. Tenenbaum, New face of an old enzyme: alkaline phosphatase may contribute to human tissue aging by inducing tissue hardening and calcification, *Anat. Rec.* 253 (1998) 91–94.
- [33] P.K. Smith, R.I. Krohn, G.T. Hermanson, A.K. Mallia, F.H. Gartner, M.D. Provenzano, E.K. Fujimoto, N.M. Goeke, B.J. Olson, D.C. Klenk, Measurement of protein using bicinchoninic acid, *Anal. Biochem.* 150 (1985) 76–85.
- [34] W.R. Moorehead, H.G. Biggs, 2-Amino-2-methyl-1-propanol as the alkalizing agent in an improved continuous-flow cresolphthalein complexone procedure for calcium in serum, *Clin. Chem.* 20 (1974) 1458–1460.
- [35] E.G. Bligh, W.J. Dyer, A rapid method of total lipid extraction and purification, *Can. J. Biochem. Physiol.* 37 (1959) 911–917. doi:10.1139/o59-099.
- [36] M. Balcerzak, S. Pikula, R. Buchet, Phosphorylation-dependent phospholipase D activity of matrix vesicles, *FEBS Lett.* 580 (2006) 5676–5680. doi:10.1016/j.febslet.2006.09.018.
- [37] ANG II stimulates phospholipase D through PKC $\zeta$  activation in VSMC: implications in adhesion, spreading, and hypertrophy | *Heart and Circulatory Physiology*, (n.d.). <http://ajpheart.physiology.org/content/290/1/H46> (accessed June 6, 2017).
- [38] N.C.W. Mackenzie, D. Zhu, L. Longley, C.S. Patterson, S. Kommareddy, V.E. MacRae, MOVAS-1 cell line: a new in vitro model of vascular calcification, *Int. J. Mol. Med.* 27 (2011) 663–668. doi:10.3892/ijmm.2011.631.
- [39] L. Bessueille, M. Fakhry, E. Hamade, B. Badran, D. Magne, Glucose stimulates chondrocyte differentiation of vascular smooth muscle cells and calcification: A possible role for IL-1 $\beta$ , *FEBS Lett.* 589 (2015) 2797–2804. doi:10.1016/j.febslet.2015.07.045.
- [40] M.N. Hodgkin, J.M. Clark, S. Rose, K. Saqib, M.J. Wakelam, Characterization of the regulation of phospholipase D activity in the detergent-insoluble fraction of HL60 cells by protein kinase C and small G-proteins, *Biochem. J.* 339 ( Pt 1) (1999) 87–93.
- [41] G. Boguslawski, L.V. Hale, X.P. Yu, R.R. Miles, J.E. Onyia, R.F. Santerre, S. Chandrasekhar, Activation of osteocalcin transcription involves interaction of protein kinase A- and protein kinase C-dependent pathways, *J. Biol. Chem.* 275 (2000) 999–1006.

- [42] J.L. Sanders, P.H. Stern, Expression and phorbol ester-induced down-regulation of protein kinase C isozymes in osteoblasts, *J. Bone Miner. Res. Off. J. Am. Soc. Bone Miner. Res.* 11 (1996) 1862–1872. doi:10.1002/jbmr.5650111206.
- [43] J.T. Swarthout, T.A. Doggett, J.L. Lemker, N.C. Partridge, Stimulation of extracellular signal-regulated kinases and proliferation in rat osteoblastic cells by parathyroid hormone is protein kinase C-dependent, *J. Biol. Chem.* 276 (2001) 7586–7592. doi:10.1074/jbc.M007400200.
- [44] F. Zhu, M.T. Sweetwyne, K.D. Hankenson, PKC $\delta$  is required for Jagged-1 induction of human mesenchymal stem cell osteogenic differentiation, *Stem Cells Dayt. Ohio.* 31 (2013) 1181–1192. doi:10.1002/stem.1353.
- [45] M.-S. Yoon, Y. Sun, E. Arauz, Y. Jiang, J. Chen, Phosphatidic Acid Activates Mammalian Target of Rapamycin Complex 1 (mTORC1) Kinase by Displacing FK506 Binding Protein 38 (FKBP38) and Exerting an Allosteric Effect, *J. Biol. Chem.* 286 (2011) 29568–29574. doi:10.1074/jbc.M111.262816.
- [46] C.H. Jung, S.-H. Ro, J. Cao, N.M. Otto, D.-H. Kim, mTOR regulation of autophagy, *FEBS Lett.* 584 (2010) 1287–1295. doi:10.1016/j.febslet.2010.01.017.
- [47] X.-Y. Dai, M.-M. Zhao, Y. Cai, Q.-C. Guan, Y. Zhao, Y. Guan, W. Kong, W.-G. Zhu, M.-J. Xu, X. Wang, Phosphate-induced autophagy counteracts vascular calcification by reducing matrix vesicle release, *Kidney Int.* 83 (2013) 1042–1051. doi:10.1038/ki.2012.482.
- [48] D. Liu, W. Cui, B. Liu, H. Hu, J. Liu, R. Xie, X. Yang, G. Gu, J. Zhang, H. Zheng, Atorvastatin protects vascular smooth muscle cells from TGF- $\beta$ 1-stimulated calcification by inducing autophagy via suppression of the  $\beta$ -catenin pathway, *Cell. Physiol. Biochem. Int. J. Exp. Cell. Physiol. Biochem. Pharmacol.* 33 (2014) 129–141. doi:10.1159/000356656.
- [49] M.R. Ammar, N. Kassas, S. Chasserot-Golaz, M.-F. Bader, N. Vitale, Lipids in Regulated Exocytosis: What are They Doing?, *Front. Endocrinol.* 4 (2013). doi:10.3389/fendo.2013.00125.
- [50] C. Thouverey, A. Strzelecka-Kiliszek, M. Balcerzak, R. Buchet, S. Pikula, Matrix vesicles originate from apical membrane microvilli of mineralizing osteoblast-like Saos-2 cells, *J. Cell. Biochem.* 106 (2009) 127–138. doi:10.1002/jcb.21992.
- [51] M.J. Cross, S. Roberts, A.J. Ridley, M.N. Hodgkin, A. Stewart, L. Claesson-Welsh, M.J. Wakelam, Stimulation of actin stress fibre formation mediated by activation of phospholipase D, *Curr. Biol. CB.* 6 (1996) 588–597.
- [52] K.S. Ha, E.J. Yeo, J.H. Exton, Lysophosphatidic acid activation of phosphatidylcholinehydrolysing phospholipase D and actin polymerization by a pertussis toxin-sensitive mechanism. *Biochem. J.* 303 (1994) 55–59.
- [53] Y. Kato, C.A. Lambert, A.C. Colige, P. Mineur, A. Noël, F. Frankenne, J.-M. Foidart, M. Baba, R.-I. Hata, K. Miyazaki, M. Tsukuda, Acidic extracellular pH induces matrix metalloproteinase-9 expression in mouse metastatic melanoma cells through the phospholipase D-mitogenactivated protein kinase signaling, *J. Biol. Chem.* 280 (2005) 10938–10944. doi:10.1074/jbc.M411313200.
- [54] M.H. Park, B.-H. Ahn, Y.-K. Hong, D.S. Min, Overexpression of phospholipase D enhances matrix metalloproteinase-2 expression and glioma cell invasion via protein kinase C and protein kinase A/NF-kappaB/Sp1-mediated signaling pathways, *Carcinogenesis.* 30 (2009) 356–365. doi:10.1093/carcin/bgn287.
- [55] N.J. Paloian, C.M. Giachelli, A current understanding of vascular calcification in CKD, *Am. J. Physiol. Renal Physiol.* 307 (2014) F891-900. doi:10.1152/ajprenal.00163.2014.
- [56] A. Simionescu, K. Philips, N. Vyavahare, Elastin-derived peptides and TGF-beta1 induce osteogenic responses in smooth muscle cells, *Biochem. Biophys. Res. Commun.* 334 (2005) 524–532. doi:10.1016/j.bbrc.2005.06.119.
- [57] N. Hosaka, M. Mizobuchi, H. Ogata, C. Kumata, F. Kondo, F. Koiwa, E. Kinugasa, T. Akizawa, Elastin degradation accelerates phosphate-induced mineralization of vascular smooth muscle cells, *Calcif. Tissue Int.* 85 (2009) 523–529. doi:10.1007/s00223-009-9297-8.
- [58] M.A. Frohman, The phospholipase D superfamily as therapeutic targets, *Trends Pharmacol. Sci.* 36 (2015) 137–144. doi:10.1016/j.tips.2015.01.001.
- [59] C.W. Lindsley, H.A. Brown, Phospholipase D as a Therapeutic Target in Brain Disorders, *Neuropsychopharmacology.* 37 (2012) 301–302. doi:10.1038/npp.2011.178.
- [60] R. Neale, S. Fallon, S. Gerhardt, J.M. Liebman, Acute dyskinesias in monkeys elicited by halopemide, mezilamine and the “antidyskinetic” drugs, oxiperomide and tiapride, *Psychopharmacology (Berl.).* 75 (1981) 254–257. doi:10.1007/BF00432434.



## **Article 3 (in preparation)**

### **Involvement of phospholipase D in the mineralization process in cultured osteoblasts**

My position: co-first author

My contribution to this work was done at Université Lyon, Université Claude Bernard Lyon 1, CNRS UMR 5246, ICBMS, F-69622, Lyon, France, during the following periods: May 2015-July 2015, Feb 2016-July 2016, Sept 2017-Dec 2017, Feb 2017-May 2017.

Dina Abdallah<sup>1\*</sup>, Najwa Skafi<sup>1\*</sup>, Eva Hamade<sup>2</sup>, Sophie Reibel<sup>3</sup>, Nicolas Vitale<sup>4</sup>, Alaeddine El Jamal<sup>1</sup>, Carole Bougault<sup>1</sup>, Bassam Badran<sup>2</sup>, Nader Hussein<sup>2</sup>, Rene Buchet<sup>1</sup>, Leyre Brizuela<sup>1</sup> and Saida Mebarek<sup>1</sup>.

<sup>1</sup>Univ Lyon, Univ Claude Bernard Lyon 1, CNRS UMR 5246, ICBMS, F-69622, Lyon, France

<sup>2</sup>Genomic and Health Laboratory/PRASE-EDST Campus Rafic Hariri-Hadath-Beirut-Liban, Faculty of Sciences, Lebanese University, Beirut 999095, Lebanon.

<sup>3</sup>Chronobiotron UMS 3415, 67084 Strasbourg, France

<sup>4</sup>Institut des Neurosciences Cellulaires et Intégratives (INCI), UPR-3212 CNRS and Université de Strasbourg, 5 Rue Blaise Pascal, 67084 Strasbourg, France.

\* These authors contributed equally to the work

To whom requests should be addressed:

Dr Saida Mebarek, CNRS UMR 5246 ICBMS, F-69622, Lyon, France

E-mail: [saida.youjil@univ-lyon1.fr](mailto:saida.youjil@univ-lyon1.fr)

Running title:

Phospholipase D and mineralization

Conflict of interest statement: no disclosures

## ABSTRACT

The mammalian phospholipase D (PLD) hydrolyzes phospholipids (mostly phosphatidylcholine) producing phosphatidic acid and the corresponding head group (choline). PLD has two main isoforms, PLD1 and PLD2. PLD activity was detected in different osteoblastic cell models, and different growth factors involved in bone homeostasis were reported to further increase its activity. We aimed to determine the role of both PLD isoforms during maturation of osteoblasts by assessing mineralization and the expression of osteogenic markers. Saos-2 osteoblast-like cell line and primary osteoblasts isolated from wild-type (WT), KO PLD1 and KO PLD2 mouse calvaria served as cell models. PLD1 genetic and protein expressions, along with total PLD activity, increased during differentiation of Saos-2 cells and primary WT osteoblasts, and it reached maximum once the mineralization was optimum. Then, both PLD1 expression and total activity decreased, indicating that PLD1 function is regulated during maturation. In contrast, PLD2 genetic and protein expression were not significantly affected during differentiation of osteoblasts. The inhibition of PLD1, by the pan-PLD inhibitor halopemide or by the PLD1-specific inhibitor VU0155069, led to a decrease in mineralization in both cell types as detected by alkaline phosphatase (AP) activity and calcium deposition. The selective inhibition of PLD2 by CAY10594 didn't affect the mineralization process. Similarly, the primary osteoblasts isolated from PLD1 KO mice were less efficient in mineralization as compared to those isolated from WT or KO PLD2 mice. Moreover, overexpression of PLD1 in Saos-2 cells increased their mineralization potential as detected by AP activity and calcium deposition. The increase in PLD activity and the mineralization were inhibited in both cell types by PKC inhibitors; bisindolylmaleimide X hydrochloride and sphingosine. Taken together, our finding suggests that PKC-activated PLD1 fine tune the earlier process of osteoblast maturation and mineralization.

**Keywords:**

phospholipase D, mineralization, osteoblast, protein kinase C, alkaline phosphatase

## INTRODUCTION

Phospholipases are suspected to participate in bone remodelling and formation, as evidenced by their expression and activity in bone-forming osteoblasts, chondrocytes and in bone-resorbing osteoclasts. Among phospholipases, we focused on phospholipases D (PLDs), which are activated and regulated by a number of hormones, growth factors, neurotransmitters and cytokines. PLD activity modulates important cell functions such as mitogenesis, vesicular trafficking, cytoskeletal reorganization and apoptosis [1-3]. Mammalian PLDs catalyze generally the hydrolysis of the principal membrane phospholipid, phosphatidylcholine (PC), producing phosphatidic acid (PA) and choline. PA is an important signaling lipid and it can be metabolized to diacylglycerol or to lysophosphatidic acid and trigger additional lipid signalling pathways [4, 5]. The PLD/PA metabolic pathway can directly activate regulatory proteins, such as PI-4-phosphate 5-kinase, PKC, PLC $\gamma$ , Raf-1 kinase and MAP kinases [6-8], all of which can induce osteoblast proliferation and differentiation [9].

The presence of PLDs in chondrocytes [10-12] and in osteoblasts [13-17] has already been described, suggesting that they may regulate their differentiation, maturation and function. It has been reported that a glycosphosphatidylinositol-specific PLD is expressed during the process of bone formation during mouse embryogenesis [18]. The earliest experimental evidence of PLD activity in osteoblasts and its regulation was described in the murine osteoblast-like MC3T3-E1 cell line [19]. Since then, a controlled regulation of PLD activity has been observed in other bone cells. Parathyroid hormone (PTH), a major regulator of bone remodelling and a therapeutically effective bone anabolic agent, stimulates PLD activity in UMR-106 rat osteoblastic cells [20, 21]. Furthermore, MG63 human osteosarcoma cells

exhibit increased PLD activity during differentiation on titanium biomaterial [22]. Moreover, epidermal growth factor (EGF) was shown to activate PLD signalling cascade in rat osteoblast primary cells [23].

There are two main mammalian isoforms of PLD: PLD1 and PLD2, each having several splice variants. These isoforms share 50% homology, but they are regulated and localized differently in the cell [4]. It is generally accepted that, under basal conditions, PLD1 is localized to perinuclear membranes, including early endosomes and Golgi [8]. Upon stimulation, PLD1 translocates to the plasma membrane or late endosomes [8]. PLD2 is usually located in the plasma membrane under basal conditions, and it translocates to recycling vesicles after stimulation. *In vitro*, PLD2 has a higher basal activity than PLD1. PLD1 can be activated by different isoforms of PKC, such as PKC $\alpha$ , and GTPases such as RhoA, Rac1, Cdc42, and ADP ribosylation factor (ARF), whereas PLD2 is not, or substantially less, responsive to PLD1 activators [8]. Numerous studies on the activation of PLDs are available. However, the current literature provides little information regarding the expression patterns of PLDs, their regulation and their role in bone-forming osteoblasts. In this report, we investigated the role of PLDs during osteoblastic differentiation by using murine primary osteoblasts and Saos-2 osteoblast-like cell line. We followed the changes in PLD isoforms expression accompanying cell differentiation and matrix mineralization. Using pharmacological inhibition, ectopic PLD overexpression or genetic knockout (KO), we studied the influence of alterations in PLD activity on the mineralization process of osteoblastic cells. Our findings indicated that PLD1 activity plays a role in osteoblast maturation, and is decisive for adequate mineralization.

## **MATERIALS AND METHODS**

## **Chemicals and reagents**

Culture medium, serum, antibiotics, Alizarin red, *p*-nitrophenyl phosphate, Nonidet P-40, and cetylpyridinium chloride, were obtained from Sigma Aldrich (Lyon, FR). Bisindolylmaleimide X hydrochloride and sphingosine were obtained from Enzo. Pharmacological specific PLD inhibitors (halopemide, VU0155069 and CAY10594) were obtained from Cayman chemical (Montluçon, FR).

## **Ethic statements**

Animal experiments were performed under the authorization n°69-266-0501 (INSA-Lyon, DDPP-SV, Direction Départementale de la Protection des Populations—Services Vétérinaires du Rhône), according to the guidelines laid down by the French Ministère de l'Agriculture (n° 87–848) and the E.U. Council Directive for the Care and Use of Laboratory Animals of November 24th, 1986 (86/609/EEC). MLC (n°692661241), AG (n°69266332) and COS (n°69266257) hold special licenses to experiment on living vertebrates issued by the French Ministry of Agriculture and Veterinary Service Department.

## **Cell cultures**

Primary osteoblasts were enzymatically isolated from calvaria of new-born SWISS mice (4-7 days), PLD1- or PLD2- Knock-Out (KO) mice [24]. Briefly, calvaria were dissected aseptically, and cells were isolated by sequential digestion at 37 °C with 0.05% trypsin/EDTA for 20 min and then with liberase (Sigma Aldrich, Lyon, FR) 0.8 U/mL for 20 min. The first two digestions were discarded, and the cells obtained after the two other digestions (each time incubated with 0.8 U/mL liberase for 45 min) were collected, pooled and then

filtered through a 100 µm-diameter-pore cell strainer. The cells were plated at a density of 25,000 cells/cm<sup>2</sup> in 12-well plates (Corning Inc, Boulogne-Billancourt, FR) in Dulbecco's modified Eagle's medium (DMEM) containing 15% (v:v) fetal bovine serum (FBS), 100 U/mL penicillin and 100 µg/mL streptomycin ( both from Sigma Aldrich, Lyon, FR). 72 h later, cells were switched to DMEM containing 10% FBS (v:v) supplemented with 50 µg/mL of L-ascorbic acid (AA) for 7 days. Then, cells were switched to DMEM containing 10% FBS (v:v) supplemented with 50 µg/mL of L-AA and 10 mM β-glycerophosphate (β-GP) during 10 more days. AA and β-GP are two osteogenic factors commonly used to stimulate osteoblastic differentiation and mineralization [25-27]. Cultures were maintained in a humidified atmosphere consisting of 95% air and 5% CO<sub>2</sub> at 37 °C.

Human Saos-2 osteoblast-like cell line (ATCC HTB-85) was cultured in DMEM supplemented with 100 U/ml penicillin, 100 µg/ml streptomycin, and 10% FBS (v:v) at 37°C in an atmosphere of 5 % CO<sub>2</sub> and 95 % air. Cells were plated at a density of 25,000 cells/cm<sup>2</sup>. Cells were grown confluent in medium supplemented with 50 µg/ml AA and 10 mM β-GP during 10 days to induce mineralization.

Cells were then used for the mineralization assessment, gene expression and activity assays.

### **Transient transfections**

The hPLD1b- and hPLD2-carrying pCDNA3 plasmids were kindly provided by Dr. M. Record (Institut National de la Santé et de la Recherche Médicale Unit 563, Toulouse, France). The green fluorescent protein (GFP-PLD) constructs were prepared by inserting the hPLD1b and hPLD2 coding sequences at EcoRI and Sall sites, respectively, of the pEGFP-C1 vector polylinker (BD Biosciences Clontech, Palo Alto, CA). Plasmid DNA (1 µg for pEGFP-C1 constructs) was mixed with diluted lipofectamine (Invitrogen, Cergy-Pontoise, FR) and left in contact for 5 min. The mix was then added dropwise to Saos-2 cells in 1 ml of

15% FBS-medium. Cells were then cultured for 24 h in the same medium and visualized under fluorescence microscope to monitor transfection efficiency and then treated with osteogenic medium for 5 days.

### **Calcium nodule detection**

Cell cultures were washed with Phosphate-buffered saline (PBS) and stained with 0.5% (w:v) Alizarin Red-S (AR-S) in PBS (pH 5.0) for 30 min at room temperature. Then, they were washed four times with PBS to remove free calcium ions. Cell cultures were destained with 3.6% (w:v) cetylpyridinium chloride in PBS pH=7.0 for 2 hours at room temperature [27]. AR-S concentration was estimated by measuring the absorbance at 562 nm. Results were normalized relatively to their respective controls.

### **Alkaline Phosphatase (AP) activity**

For determination of AP activity [28], cells were harvested in 0.2% Nonidet P-40 and disrupted by sonication. The homogenate was centrifuged at 1500 g for 5 min. In the supernatant, AP activity was determined by using *p*-nitrophenyl phosphate (pNPP) as substrate at pH 10.4. The optical density was measured at 405 nm ( $\epsilon$  is equal  $18.8 \text{ mM}^{-1} \text{ cm}^{-1}$ ). In the same lysates, the protein content was determined by bicinchoninic acid [29] (BCA, Sigma-Aldrich, Lyon, FR). Results were calculated as nmol of paranitrophenol (pNP) produced/min/mg protein, they were normalized relatively to their respective controls.

### **PLD activity assay**

Amplex Red PLD Kit (Molecular Probes, Eugene, OR, USA) was used to measure the rate of choline production during PC hydrolysis by PLD, according to the manufacturer's instructions with slight modifications [30].

Briefly, cells were washed twice with PBS and scraped in ice-cold Tris 50 mM buffer at pH=8.0. Cells were then lysed by three freeze/thaw cycles. Samples were incubated with 0.5 mM PC (Avanti Polar Lipids, Alabaster, AL) and 2 mM levamisol for 30 min at 37 °C. Then, 100 µL aliquots of sample were collected. Extracts were mixed with 100 µL of reaction buffer containing 100 µM Amplex Red reagent, 2 U/mL horseradish peroxidase (HRP) (Molecular Probes, Eugene, OR), 0.2 U/mL choline oxidase from *Alcaligenes sp.* (MP Biomedicals, Ilkirch-Graffenstaden, FR). 2 mM of levamisol (Sigma Aldrich, Lyon, FR) was added in the reaction buffer, in order to prevent dephosphorylation of phosphocholine produced by phospholipase C. The PLD activity was estimated by measuring the fluorescence of resorufin after 30 min incubation at 37 °C using a micro-titre plate reader (NanoQuant Infinite M200, Tecan, Salzburg, AUS) at 590 nm after sample excitation at 530 nm. A standard curve was done using choline. PLD activity was normalized to the total protein amount (BCA, Sigma-Aldrich, Lyon, FR).

### **Western blot assay**

Cells were homogenized in 20 mM Tris/HCl pH=7.6 buffer containing 100 mM NaCl, 1% Triton X-100, and 1% of a protease inhibitor cocktail from Sigma Aldrich (Lyon, FR). Cell lysates were mixed with Laemmli buffer (BioRad, Californie, USA), boiled for precisely 1 min, and separated on 8% SDS polyacrylamide gel containing 4 M urea. The western blots were probed with anti-PLD1- and anti-PLD2-specific polyclonal antibodies kindly provided by Dr S. Bourgoïn (Laval University, Canada). Immunoblots were revealed with the enhanced chemiluminescence (ECL) detection system (GE Healthcare, Limonest, France)

and X-ray film autoradiography. Membranes were incubated with an anti  $\beta$ -actin monoclonal antibody (clone AC-74) from Sigma Aldrich (Lyon, FR) for normalization. Bands were then quantified by Image J software.

### **RNA Extraction, Reverse Transcription and real-time PCR**

Total RNA was extracted using Extract-All reagent according to the manufacturer's instructions (Macherey-Nagel, Hoerd, FR). Total RNA was quantified by spectrophotometer at 260 nm. The integrity of RNA was controlled by the 28S/18S rRNA ratio after agarose gel electrophoresis. Contaminating DNA was removed from the RNA samples in a 30 min digestion at 37°C with DNase I. In all, 1  $\mu$ g of each RNA sample was then used for reverse transcription performed under standard conditions with Superscript II reverse transcriptase (Invitrogen, Villebon-sur-Yvette, France) and random hexamers primers (Invitrogen, Villebon-sur-Yvette, France) in a 20- $\mu$ l final volume. The reaction was carried out at 42°C for 30 min and stopped with incubation at 99°C for 5 min. In all, 1  $\mu$ l of cDNA template was used in subsequent PCRs.

Gene name	Forward primer (5'-3')	Reverse primer (5'-3')	Ta (°C)
<i>Human PLD1</i>	TGTCGTGATACCACT TCTGCCA	AGCATTTTCGAGCTGC TGTTGAA	60
<i>Human PLD2</i>	CATCCAGGCCATTCT GCAC	GTGCTTCCGCAGACT CAAGG	60
<i>Human GAPDH</i>	GTTCCAATATGATTC CACCC	AGGGATGATGTTCTG GAGAG	55
<i>Mouse Pld1</i>	AAGTGCAGTTGCTCC GATCT	TTCTCTGGGCGATAG CATCT	56
<i>Mouse Pld2</i>	GGGCACCGAAAGAT ACACCA	CTCAGAACCTCCTCG GGGTA	56
<i>Mouse Gapdh</i>	GGCATTGCTCTCAAT GACAA	TGTGAGGGAGATGCT CAGTG	62
<i>Mouse Runx2</i>	GCCGGGAATGATGA GAACTA	GGACCGTCCACTGTC ACTTT	60
<i>Mouse Bglap</i>	AAGCAGGAGGGCAA TAAGGT	CGTTTGTAGGCGGTC TTCA	60

Table 1. The sequences of the primers used in qPCR, with their respective annealing temperatures.

Real-time PCR was performed using a LightCycler system (Roche Diagnostics, Meylan, FR). The reactions were performed in a 10- $\mu$ l final volume with 0.3  $\mu$ M primers, 2 mM MgCl<sub>2</sub> and 2  $\mu$ L of LightCycler-FastStart DNA Master SYBR Green I mix (Roche Diagnostic, Meylan, FR). The protocol consisted of an activation step (10 min at 95°C) followed by 40 cycles consisting of a 10 s denaturation step (95°C), a 10 s annealing step (Ta) and an elongation step at 72°C for 25 s. The primer sequences and Ta for each gene are listed in table 1. Relative quantification analysis were performed by RelQuant 1.01 Software (Roche Diagnostics, Meylan, FR) according to Livak's method, using GAPDH as reference gene.

### Statistical analysis

For each analysis, at least three independent experiments were performed (except for the Knock-Out model). Two-sided unpaired T-test was used to analyze the data. Results were expressed as mean  $\pm$  standard error (SEM). Results were considered significant when  $p <$

0.05 (\*), highly significant when  $p < 0.01$  (\*\*), and extremely significant when  $p < 0.001$  (\*\*\*).

## **RESULTS**

### **The evolution of AP activity and calcium deposition over time of culture**

In both culture models, mouse primary cells from calvaria and Saos-2 cell line, osteoblastic differentiation was confirmed by an increase in AP activity (Figure 1A, 1D) and in calcium deposition seen by AR-S (Figure 1B, 1E), following the treatment with AA 50  $\mu\text{g}/\text{mL}$  and  $\beta\text{-GP}$  10 mM. For primary osteoblasts, cells were cultured over 21 days and mineralization drastically increased between day 9 and day 16. For Saos-2 cells, cells were cultured for 10 days, and the rise in mineralized nodules was observed between days 5 and 8.

### **PLD expression and activity during mineralization process**

To investigate whether PLDs are involved in the maturation of primary osteoblasts and Saos-2 cells, the changes in PLD activity was monitored in these cells during mineralization. For primary osteoblasts, PLD activity was significantly increased between days 9 and 16, peaking at day 13 (Figure 1C). A 9-fold increase was also observed at day 5 for Saos-2 cells, as compared to non-differentiated cells (Figure 1F). Interestingly, PLD activity returned back to control level once mineralization was well under process. Compared to the evolution of AP activity and calcium deposition over time, we observed that PLD activity increased only during early stages of matrix mineralization in our models, especially when mineralization rate is the most drastic. Therefore, PLD activity could be involved in the initial steps of osteoblast mineralization.

Also, the expression of different of PLD isoforms was determined during the maturation of both cell types. In osteoblasts, there was a significant increase in *Pld1* gene expression from day 10, peaking at day 17 (Figure 2A). The upregulation in PLD1 expression was also manifested at protein level, with a 2.5-fold increase at day 17 (Figure 2C). A progressive increase in *Pld2* mRNA was noticeable until day 21 (Figures 2B), but it was not confirmed significantly at protein level (Figures 2D). In Saos-2 cells, *PLD1* expression increased starting from day 5 and peaking at day 8 (Figure 2E), but *PLD2* expression did not change significantly during mineralization process (Figure 2F). Thus, both *Pld1* and *Pld2* isoforms were detected in our osteoblastic models. However, during the mineralization process, *Pld1* expression was upregulated with the same pattern in the two cell types, whereas *Pld2* expression did not seem to change.

### **The effect of pharmacological inhibition of PLD activity on mineralization in osteoblastic cells**

To assess whether the PLD activity affects the mineralization process, we analyzed AP activity and calcium nodules formation in primary osteoblasts and Saos-2 cells in presence of small-molecule PLD inhibitors. Hence, cells were treated with different pharmacological inhibitors: Halopemide, a pan-inhibitor for PLD1 and PLD2 (used at 600 and 800 nM), a PLD1 specific inhibitor VU0155069 (used at 600 and 800 nM) and a PLD2 specific inhibitor CAY10594 (used at 200 and 300 nM).

We first checked their efficiency by measuring PLD activity after inhibitor treatment at different concentrations. At 800 nM, halopemide and VU0155069 caused a highly significant reduction of PLD activity (of  $67\% \pm \text{SD}$  and  $37\% \pm \text{SD}$ , respectively) in primary osteoblasts. Conversely, CAY10594, at 300 nM, reduced PLD activity by at least 50% (data not shown).

The PLD inhibitors affected PLD activity in Saos-2 cells in a similar manner (data not shown).

Primary osteoblasts and Saos-2 cells were then treated with the PLD inhibitors during 10 and 5 days in the presence of AA and  $\beta$ -GP, respectively. Mineralization was assessed at day 21 and 10, respectively. Treatment with halopemide or PLD1 specific inhibitor diminished AP activity in both cell models at the two concentrations tested (Figure 3A, 3C). Moreover, at 800 nM, these inhibitors significantly decreased calcium deposition (Figure 3B, 3D). Interestingly, the PLD2 specific inhibitor did not reduce AP activity or calcium deposition in the two cell types (Figure 3). Therefore, these data suggests that PLD activity, mainly that of PLD1, favors the mineralization process of primary osteoblasts and Saos-2 osteoblast-like cell line.

#### **The effect of PLD overexpression on mineralization in Saos-2 cell line**

To further support the hypothesis that PLD activity affects mineralization, Saos-2 cells were transiently transfected with GFP-tagged PLD1 and PLD2 isoforms. AP activity and the deposition of calcium nodules were measured after 5 days of mineralization (Figure 4). pEGFP served as a control, and transfection efficiency was monitored by GFP expression. After 3 days of culture of culture the transfection efficiency was estimated to range from 30 to 50% (data not shown). Saos-2 cells transfected with GFP-tagged PLD1 or PLD2 isoforms showed at least 2-fold increase in PLD activity (data not shown), suggesting that the ectopically expressed PLDs retained the enzymetic activity.

Saos-2 cells overexpressing PLD1 and PLD2 exhibited a higher AP activity than cells transfected with the empty vector (Figure 4A). Additionally, overexpression of PLD1 stimulated the formation of calcium nodules, stained by AR-S, but the overexpression of PLD2 had no significant effect on this parameter (Figure 4B). All together, these findings

confirmed that PLD activity, especially that of the PLD1 isoform, may play an important role in the mineralization process in Saos-2 osteoblast-like cells.

### **Regulation of PLD by a PKC-dependent mechanism**

We next analyzed the possible regulation of PLD activity by PKC during the mineralization process. We used two pan-inhibitors of PKCs, bisindolylmaleimide and sphingosine, at 1  $\mu$ M. Cells were treated with these inhibitors in osteogenic conditions during 10 days for primary osteoblasts and 5 days for Saos-2 cells as described before. These treatments induced a decrease in PLD activity (by more than 50%) for primary osteoblasts (Figure 5A) and Saos-2 cells (Figure 5D). The mineralization was estimated at day 21 and at day 10 for osteoblasts and Saos-2 cells, respectively. The addition of PKC inhibitors significantly decreased AP activity (Figure 5B and 5E) and mineralized nodules (Figure 5C and 5F), induced by AA and  $\beta$ -GP in primary osteoblasts and Saos-2 osteoblast-like cells. This result suggests that, in osteoblastic cells, PLD activation during the mineralization process might be, to some extent, PKC-dependent.

### **Effect of the *in-vivo* genetic ablation of PLD1 or PLD2 on the mineralization of murine primary osteoblasts.**

To validate the function of PLD1 and PLD2 during the mineralization induced by osteoblasts, we used recently developed mouse models that are deficient in PLD1 or PLD2. We determined the effect of PLD deficiency on mineralization by monitoring AP activity, calcium deposition and bone markers gene expression in cultures of primary osteoblasts (Figure 6).

The genetic ablation of PLD1 affected AP activity of murine primary osteoblasts (Figure 6A) and matrix mineralization (Figure 6B) as compared with the wild-type counterparts. Moreover, PLD2 deficiency tended to inhibit AP activity but did not alter calcium deposition (data not shown). The gene expression patterns of two key bone markers, *Runx2* and *Bglap*, were also altered, indicating that the absence of PLD1 resulted in a decrease in the osteogenic potential (Figure 6C, 6D). Finally, PLD2 deletion did not affect the gene expression of both bone markers as compared with the osteoblasts from wild-type mice (data not shown). In conclusion, these results obtained with the genetic KO mouse models corroborated the data obtained by pharmacological inhibition of PLD activity.

## **Discussion**

PLD activity has been demonstrated to increase after stimulation with platelet-derived growth factor [31], extracellular ATP [16] or prostaglandin in a murine osteoblast-like MC3T3 cell line [32, 33] and epidermal growth factor in rat osteoblastic cells [23]. However, the role of PLD during osteoblast mineralization is not yet known. In this report, we demonstrated that PLD1 is positively involved in the mineralization process induced by osteoblastic cells.

First, we characterized our cell culture models. As expected, AP activity and calcium deposits progressively increased in murine primary osteoblasts and Saos-2 osteoblast-like cells during the 20 and 10 days of osteogenic medium treatment, respectively (Figure 1). Then, we demonstrated that PLD activity was significantly increased during mineralization process, peaking at day 13 for murine primary osteoblasts and at day 5 for Saos-2 cells (Figure 1). The maximum of PLD activity correspond to the middle of the process, when the increase in calcium deposition is the most drastic. In addition, the gene and protein expression of PLD1, but not PLD2, was increased during differentiation and maturation of primary osteoblasts and

Saos-2 cells (Figure 2). Taken together, our results indicate that PLD1 upregulation and PLD activation are synchronized with mineralization process in both murine primary osteoblasts and Saos-2 osteoblast-like cells.

To analyze the function of PLD in these cells, three approaches were adopted: inhibition of PLD activity by selective pharmacological methods in both cell models, overexpression of PLD1 or PLD2 in Saos-2 cells and studying primary osteoblasts isolated from PLD1 or PLD2 KO mice. The inhibition of both PLD isoforms by halopemide or the specific inhibition of PLD1 partially blocked mineralization process by diminishing AP activity and calcium deposition in our two cell models. Furthermore, transient overexpression of PLD1 in Saos-2 osteoblast-like cells significantly increased AP activity and calcium deposits in extracellular matrix. Finally, AP activity, calcium deposits and bone markers seemed to diminish in primary osteoblasts from KO PLD1 mice compared to WT counter-parts after 21 days of differentiation (Figure 6). On the contrary, PLD2 specific inhibition, overexpression or deletion seems to have very little effects. These results suggest that PLD1 activity, among other factors, participates in the maturation of osteoblastic cells and in the mineralization induced by them.

We observed that the pharmacological specific inhibition of PLD1 in WT osteoblasts had a more profound effect than genetic deletion. This may be due to the fact that chronic loss of PLD activity leads to compensation through the activation of other enzymes that produce PA (diacylglycerol kinases or lysophosphatidyl-acetyl transferase), or to the inactivation of enzymes that degrade it, allowing the maintenance of PA levels near to normal values. On the contrary, pharmacological inhibition allows shutting down PLD1 activity for short time, so that compensatory mechanisms may not be established in cultured cells. Therefore, drug-induced inhibition of PLD1 may lead to a neat decrease in the amount of its products and thus to more noticeable effects [4].

The observation that the manipulation of PLD2 level and activity didn't have significant effects on the mineralization process is in agreement with the finding that PLD1 is the main isoform involved in other physiological processes of differentiation. For instance, myogenesis was potentiated by PLD1b isoform overexpression but not by PLD2 overexpression [1, 34]. Both PLD1 and PLD2 catalyze the hydrolysis of phospholipids forming PA and a head group with similar specificities. However, the two isoforms are differentially localised and regulated [2, 35]. In particular, PLD1 is more responsive to activation by PKC, and other activators, than PLD2 [36]. Interestingly, PKC, which can be stimulated by various growth factors, has important roles in osteogenic differentiation [37-40]. We thus investigated whether PLD1 role in mineralization was linked to PKC pathway. Indeed, the PKC competitive pan-inhibitors, bisindolylmaleimide X and sphingosine, inhibited osteoblasts maturation and mineralization in our models, along with inhibition of PLD activity. Thus, our results suggest that PKC activity is positively involved in the mineralization process through PLD activation.

The mechanism by which PLD participates in the mineralization process deserves further investigations. The PLD-dependent remodelling of actin cytoskeleton could participate in promoting matrix vesicle (MV) release. MVs are extracellular small vesicles in which the accumulation of calcium-phosphate crystals is initiated. In fact, actin depolymerization was involved in the formation of mineralization-competent MV [41], and PLD has a functional link with actin fibers [42]. Interestingly, PLD activity was increased only in early stages of matrix mineralization in our models, especially when the MVs are known to have role in the mineralization process. Therefore, it is tempting to propose PLD-mediated release of MVs as PLD mechanism of action in mineralization. However, PLD may also act by affecting other pathways, such as PI-4-phosphate 5-kinase, PLC $\gamma$ , Raf-1 kinase and MAP kinases [6], leading to changes in osteoblastic genes expression.

## **Conclusion**

Taken together, our results indicate that PLD activity, mainly through that of the PLD1 isoform, strongly participates in the mechanism leading maturation of osteoblasts and mineralization. They validate the hypothesis that PLD activity and mineralization process are thoroughly linked.

### **Acknowledgements**

We acknowledge S. Bourgoïn for the gift of PLD-specific antibodies, and M. Nemoz for sharing plasmids carrying PLD. Authors are grateful to the Lebanese University (LU) and the Lebanese National Council for Scientific Research (CNRS-L) for providing PhD scholarships to Dina Abdallah and Najwa Skafi.

## LEGENDS TO FIGURES

**Figure 1. Characterization of the models and PLD activity.** The Alkaline Phosphatase (AP) specific activity is shown relative to the control in primary osteoblasts (A) and Saos-2 cell line (D) during differentiation induced by 10 mM  $\beta$ -GP and 50  $\mu$ g/ mL AA. The calcium deposition quantified from AR-S is shown relative to the control in primary osteoblasts (B) and in Saos-2 cell line (E). PLD specific activity was calculated by measuring choline production and normalization to total protein amount. It is shown relative to the control in primary osteoblasts (C) and Saos-2 cell line (F). In all, the statistical analysis was done on at least 3 independent experiments using student t test; \*:  $p < 0.05$ , \*\*:  $p < 0.01$ , \*\*\*:  $p < 0.001$ .

**Figure 2. Gene and protein expression of PLD during osteoblast maturation.** The gene expression of *pld* was assessed by qPCR using Livak's method to obtain the fold change relative to control. GAPDH was used as reference gene. The relative gene expression of *pld1* (A) and *pld2* (B) in primary osteoblasts are shown during the differentiation. Also, the relative gene expression of *PLD1* (E) and *PLD2* (F) are shown in Saos-2 cell line. Protein expression of PLD1 (C) and PLD2 (D) was estimated by doing western blots and quantifying the bands using ImageJ software. B-actin was used as a loading control. In all, the statistical analysis was done on at least 3 independent experiments using student t test; \*:  $p < 0.05$ , \*\*:  $p < 0.01$ , \*\*\*:  $p < 0.001$ .

**Figure 3. Effect of PLD inhibition on the mineralization.** Primary osteoblasts and Saos-2 cells were treated with PLD inhibitors during 10 and 5 days in the presence of AA and  $\beta$ -GP, respectively. Mineralization was assessed at day 21 and 10, respectively. Cells were treated with different pharmacological inhibitors: Halopemide, a pan-inhibitor for PLD1 and PLD2 (used at 600 and 800 nM), a PLD1 specific inhibitor, VU0155069 (used at 600 and 800 nM) and a PLD2 specific inhibitor, CAY10594 (used at 200 and 300 nM). Specific AP activity is

shown relative to mineralization-stimulated cells in primary osteoblasts (A) and Saos-2 cells (C). Calcium deposition quantified from AR-S was shown also relative to mineralization-stimulated cells in primary osteoblasts (B) and Saos-2 cells (D). In all, the statistical analysis was done on at least 3 independent experiments using student t test; \*:  $p < 0.05$ , \*\*:  $p < 0.01$ , \*\*\*:  $p < 0.001$ .

**Figure 4. Effect of PLD overexpression on the mineralization.** Saos-2 cells were transiently transfected with GFP-tagged PLD1 and PLD2 isoforms. Relative specific AP activity (A) and the deposition of calcium nodules by AR-S (B) were measured after 5 days of mineralization (Figure 4). pEGFP served as a control, and transfection efficiency was monitored by GFP expression (data not shown). In all, the statistical analysis was done on at least 3 independent experiments using student t test; \*:  $p < 0.05$ , \*\*:  $p < 0.01$ , \*\*\*:  $p < 0.001$ .

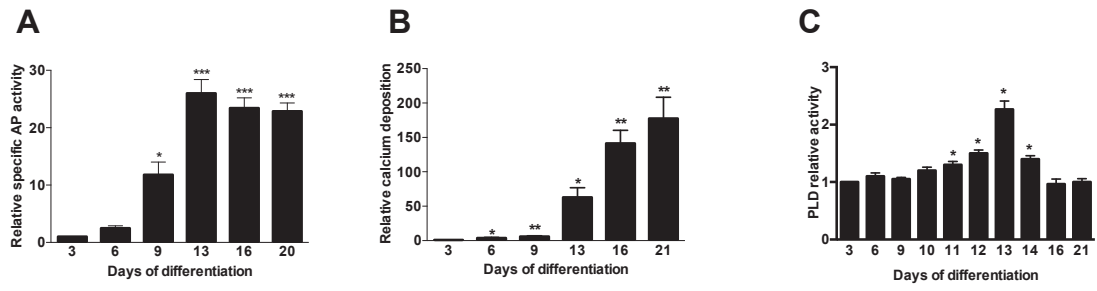
**Figure 5. Effect of protein kinase C inhibitors on PLD activity and the mineralization.** Two pan-inhibitors of PKCs were used, bisindolylmaleimide X and sphingosine, at 1  $\mu\text{M}$ . Cells were treated with these inhibitors in osteogenic conditions during 10 days for primary osteoblasts and 5 days for Saos-2 cells. The PLD activity and mineralization were assessed at day 21 and at day 10 for osteoblasts and Saos-2 cells, respectively. The PLD specific activity (A, D), AP specific activity (B, E) and calcium accumulation as quantified from AR-S (C, F) are all presented relative to mineralization-stimulated cells. In all, the statistical analysis was done on at least 3 independent experiments using student t test; \*:  $p < 0.05$ , \*\*:  $p < 0.01$ , \*\*\*:  $p < 0.001$ .

**Figure 6. Effect of PLD genetic ablation on the mineralization of primary osteoblasts.** Wild-type or PLD1 knock-out primary osteoblasts were isolated from the calvaria of WT or PLD1 KO new-born mice. Differentiation was induced by 10 mM  $\beta$ -GP and 50  $\mu\text{g}/\text{mL}$  AA

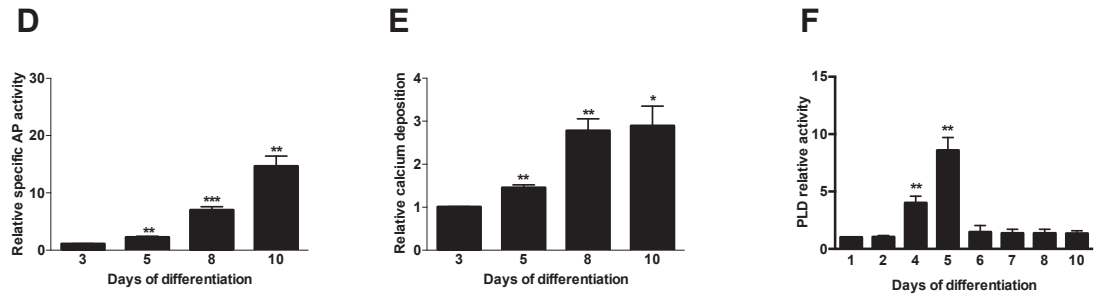
for 21 days. Mineralization was estimated by relative AP specific activity (A) and calcium deposition as quantified from AR-S (B). Also, the fold changes of *Runx2* (C) and *Bglap* (D) gene expression with respect to control were obtained by RT-qPCR using GAPDH as a reference gene. In all, the statistical analysis was done on at least 3 independent experiments using student t test; \*:  $p < 0.05$ , \*\*:  $p < 0.01$ , \*\*\*:  $p < 0.001$ .

Figure 1

Primary osteoblasts



Saos-2 cells



**Figure 2 Primary osteoblasts**

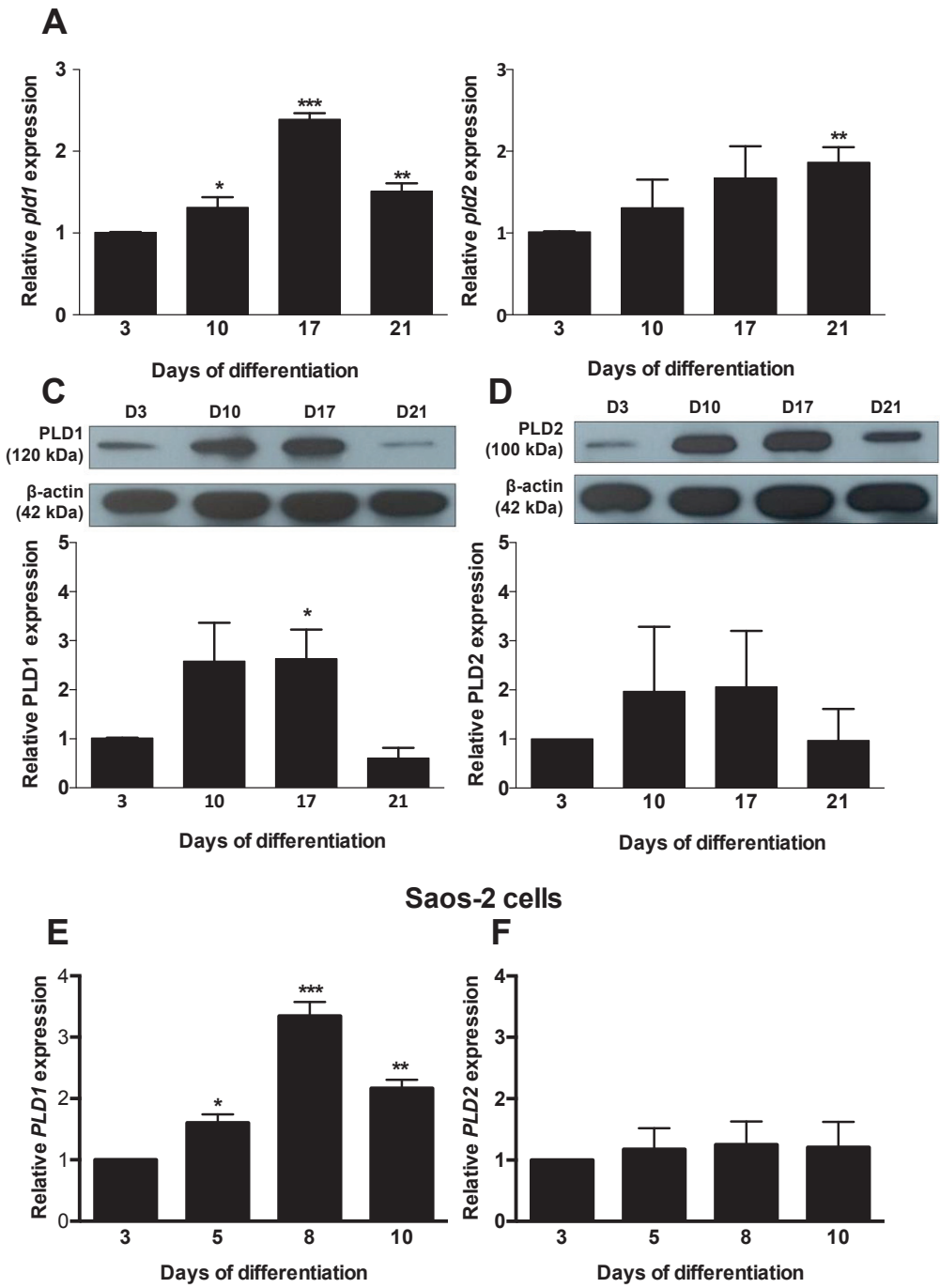


Figure 3

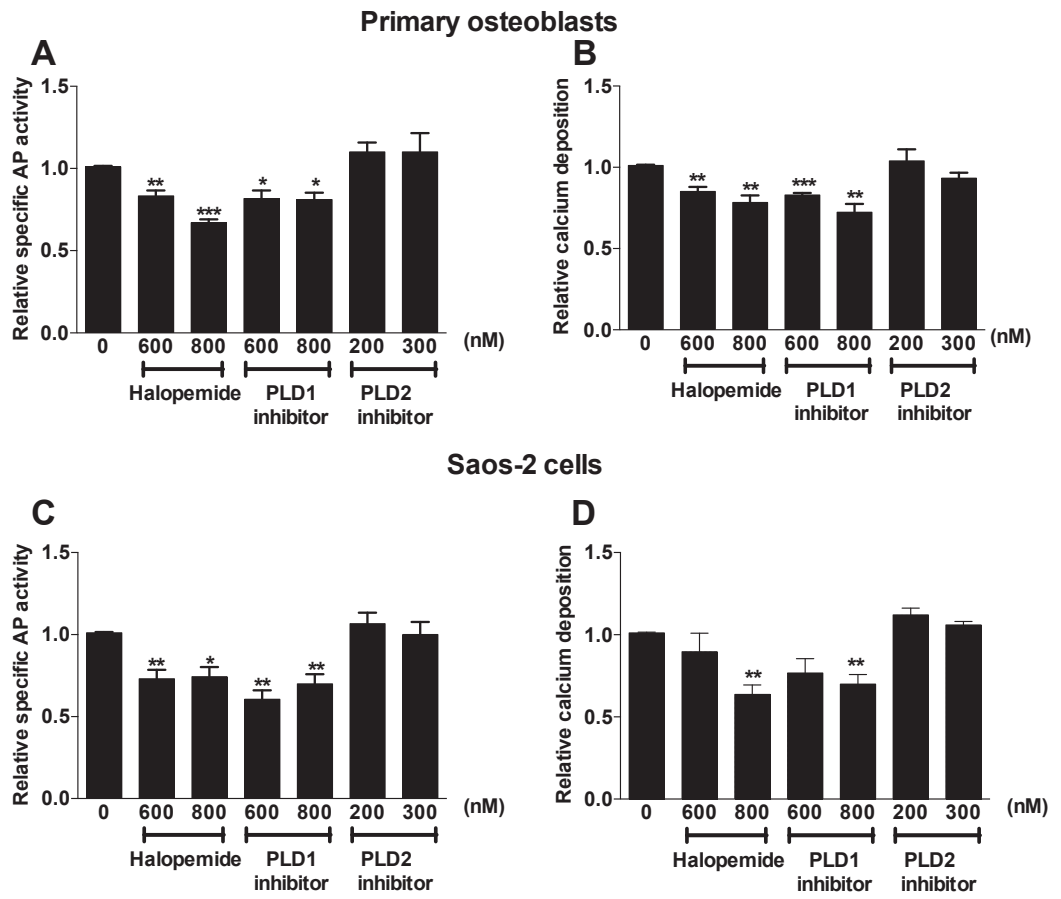


Figure 4

Saos-2 cells

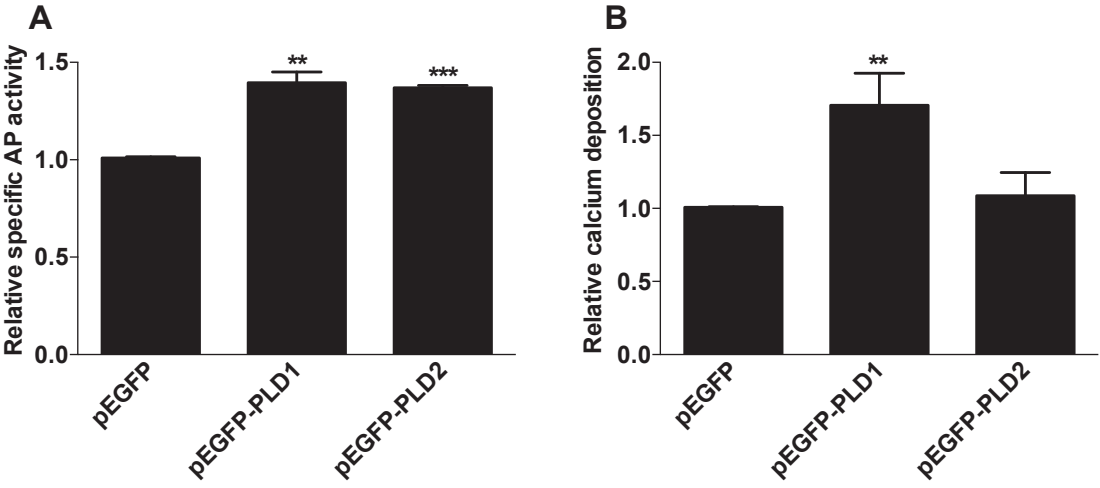


Figure 5

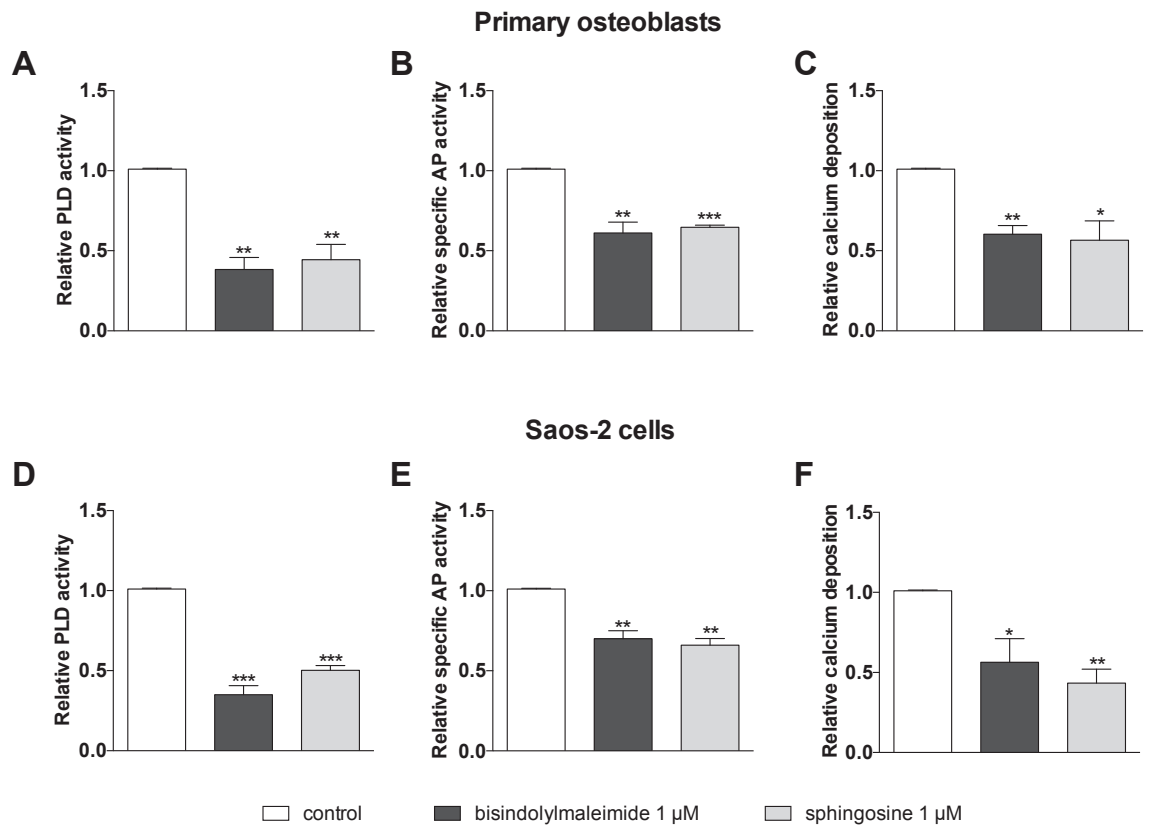
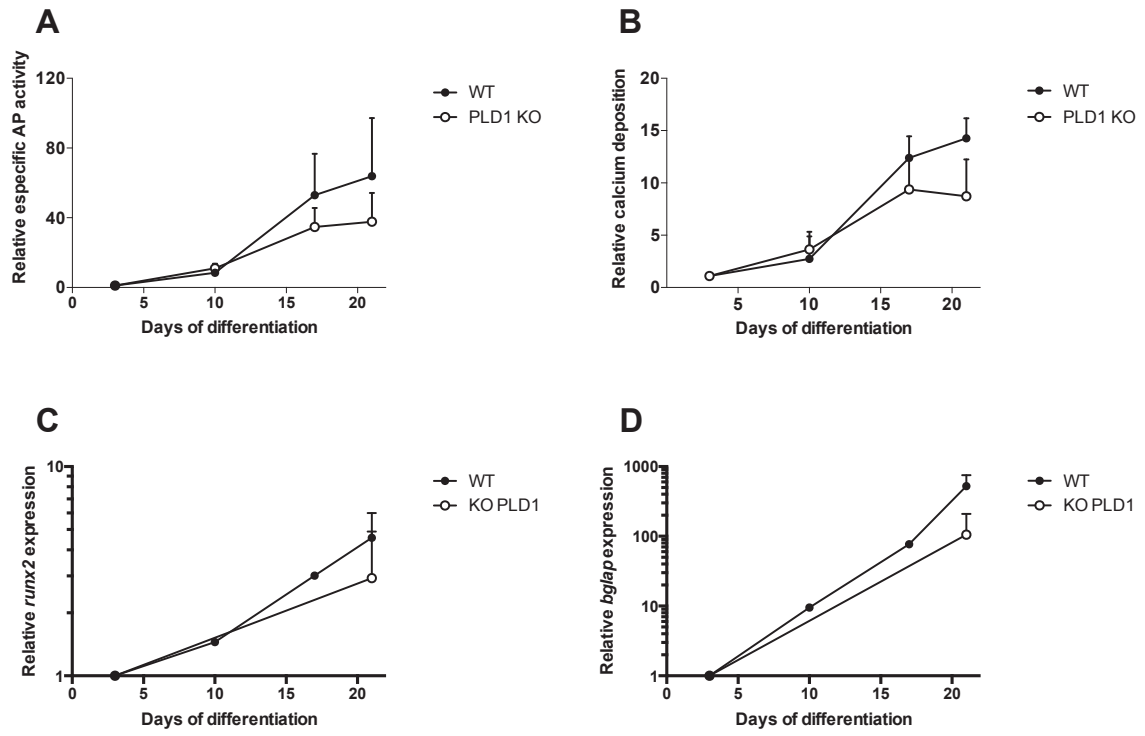


Figure 6

Primary osteoblasts



## REFERENCES

- [1] H. Komati, F. Naro, S. Mebarek, V. De Arcangelis, S. Adamo, M. Lagarde, A.F. Prigent, G. Némoy, Phospholipase D is involved in myogenic differentiation through remodeling of actin cytoskeleton, *Mol Biol Cell* 16(3) (2005) 1232-44.
- [2] O. Diaz, S. Mébarek-Azzam, A. Benzaria, M. Dubois, M. Lagarde, G. Némoy, A.F. Prigent, Disruption of lipid rafts stimulates phospholipase d activity in human lymphocytes: implication in the regulation of immune function, *J Immunol* 175(12) (2005) 8077-86.
- [3] X. Peng, M.A. Frohman, Mammalian phospholipase D physiological and pathological roles, *Acta Physiol (Oxf)* 204(2) (2012) 219-26.
- [4] M.A. Frohman, The phospholipase D superfamily as therapeutic targets, *Trends Pharmacol Sci* (2015).
- [5] H.A. Brown, L.G. Henage, A.M. Preininger, Y. Xiang, J.H. Exton, Biochemical analysis of phospholipase D., *Methods Enzymol* 434 (2007) 49-87.
- [6] M. Rizzo, G. Romero, Pharmacological importance of phospholipase D and phosphatidic acid in the regulation of the mitogen-activated protein kinase cascade, *Pharmacol Ther* 94(1-2) (2002) 35-50.
- [7] P.E. Selvy, R.R. Lavieri, C.W. Lindsley, H.A. Brown, Phospholipase D: enzymology, functionality, and chemical modulation, *Chem Rev* 111(10) (2011) 6064-119.
- [8] M.N. Hodgkin, M.R. Masson, D. Powner, K.M. Saqib, C.P. Ponting, M.J. Wakelam, Phospholipase D regulation and localisation is dependent upon a phosphatidylinositol 4,5-bisphosphate-specific PH domain, *Curr Biol* 10(1) (2000) 43-6.
- [9] M.K. Park, Y.M. Her, M.L. Cho, H.J. Oh, E.M. Park, S.K. Kwok, J.H. Ju, K.S. Park, D.S. Min, H.Y. Kim, S.H. Park, IL-15 promotes osteoclastogenesis via the PLD pathway in rheumatoid arthritis, *Immunol Lett* 139(1-2) (2011) 42-51.
- [10] V.L. Sylvia, Z. Schwartz, F. Del Toro, P. DeVeau, R. Whetstone, R.R. Hardin, D.D. Dean, B.D. Boyan, Regulation of phospholipase D (PLD) in growth plate chondrocytes by 24R,25-(OH)2D3 is dependent on cell maturation state (resting zone cells) and is specific to the PLD2 isoform, *Biochim Biophys Acta* 1499(3) (2001) 209-21.
- [11] J.A. Conquer, S.A. Jones, T.F. Cruz, Effect of interleukin 1, lipopolysaccharide and phorbol esters on phospholipase D activity in chondrocytes, *Osteoarthritis Cartilage* 2(4) (1994) 269-73.
- [12] Z. Schwartz, V.L. Sylvia, M.H. Luna, P. DeVeau, R. Whetstone, D.D. Dean, B.D. Boyan, The effect of 24R,25-(OH)(2)D(3) on protein kinase C activity in chondrocytes is mediated by phospholipase D whereas the effect of 1alpha,25-(OH)(2)D(3) is mediated by phospholipase C, *Steroids* 66(9) (2001) 683-94.
- [13] M.J. Kim, M.U. Choi, C.W. Kim, Activation of phospholipase D1 by surface roughness of titanium in MG63 osteoblast-like cell, *Biomaterials* 27(32) (2006) 5502-11.
- [14] J. Shinoda, A. Suzuki, Y. Oiso, O. Kozawa, Thromboxane A2-stimulated phospholipase D in osteoblast-like cells: possible involvement of PKC, *Am J Physiol* 269(3 Pt 1) (1995) E524-9.
- [15] A. Suzuki, Y. Oiso, O. Kozawa, Effect of endothelin-1 on phospholipase D activity in osteoblast-like cells, *Mol Cell Endocrinol* 105(2) (1994) 193-6.
- [16] A. Suzuki, J. Shinoda, Y. Oiso, O. Kozawa, Mechanism of phospholipase D activation induced by extracellular ATP in osteoblast-like cells, *J Endocrinol* 145(1) (1995) 81-6.
- [17] Y. Watanabe-Tomita, A. Suzuki, J. Shinoda, Y. Oiso, O. Kozawa, Arachidonic acid release induced by extracellular ATP in osteoblasts: role of phospholipase D, *Prostaglandins Leukot Essent Fatty Acids* 57(3) (1997) 335-9.
- [18] P. Gregory, E. Kraemer, G. Zürcher, R. Gentinetta, V. Rohrbach, U. Brodbeck, A.C. Andres, A. Ziemiecki, P. Bütikofer, GPI-specific phospholipase D (GPI-PLD) is expressed during mouse development and is localized to the extracellular matrix of the developing mouse skeleton, *Bone* 37(2) (2005) 139-47.
- [19] H. Tokuda, A. Suzuki, Y. Watanabe-Tomita, J. Shinoda, Y. Imamura, Y. Oiso, A. Igata, O. Kozawa, Function of Ca<sup>2+</sup> in phosphatidylcholine-hydrolyzing phospholipase D activation in osteoblast-like cells, *Bone* 19(4) (1996) 347-52.
- [20] A.T. Singh, A. Gilchrist, T. Voyno-Yasenetskaya, J.M. Radeff-Huang, P.H. Stern, G alpha12/G alpha13 subunits of heterotrimeric G proteins mediate parathyroid hormone activation of phospholipase D in UMR-106 osteoblastic cells, *Endocrinology* 146(5) (2005) 2171-5.

- [21] A.T. Singh, M.A. Frohman, P.H. Stern, Parathyroid hormone stimulates phosphatidylethanolamine hydrolysis by phospholipase D in osteoblastic cells, *Lipids* 40(11) (2005) 1135-40.
- [22] M. Fang, R. Olivares-Navarrete, M. Wieland, D.L. Cochran, B.D. Boyan, Z. Schwartz, The role of phospholipase D in osteoblast response to titanium surface microstructure, *J Biomed Mater Res A* 93(3) (2010) 897-909.
- [23] L.C. Carpio, R. Dziak, Activation of phospholipase D signaling pathway by epidermal growth factor in osteoblastic cells, *J Bone Miner Res* 13(11) (1998) 1707-13.
- [24] M. Zeniou-Meyer, A. Béglé, M.F. Bader, N. Vitale, The Coffin-Lowry syndrome-associated protein RSK2 controls neuroendocrine secretion through the regulation of phospholipase D1 at the exocytotic sites, *Ann N Y Acad Sci* 1152 (2009) 201-8.
- [25] J.M. Gillette, S.M. Nielsen-Preiss, The role of annexin 2 in osteoblastic mineralization, *J Cell Sci* 117(Pt 3) (2004) 441-9.
- [26] S.M. Vaingankar, T.A. Fitzpatrick, K. Johnson, J.W. Goding, M. Maurice, R. Terkeltaub, Subcellular targeting and function of osteoblast nucleotide pyrophosphatase phosphodiesterase 1, *Am J Physiol Cell Physiol* 286(5) (2004) C1177-87.
- [27] C.M. Stanford, P.A. Jacobson, E.D. Eanes, L.A. Lembke, R.J. Midura, Rapidly forming apatitic mineral in an osteoblastic cell line (UMR 106-01 BSP), *J Biol Chem* 270(16) (1995) 9420-8.
- [28] M. Hui, H.C. Tenenbaum, New face of an old enzyme: alkaline phosphatase may contribute to human tissue aging by inducing tissue hardening and calcification, *Anat Rec* 253(3) (1998) 91-4.
- [29] P.K. Smith, R.I. Krohn, G.T. Hermanson, A.K. Mallia, F.H. Gartner, M.D. Provenzano, E.K. Fujimoto, N.M. Goeke, B.J. Olson, D.C. Klenk, Measurement of protein using bicinchoninic acid, *Anal Biochem* 150(1) (1985) 76-85.
- [30] M. Balcerzak, S. Pikula, R. Buchet, Phosphorylation-dependent phospholipase D activity of matrix vesicles, *FEBS Lett* 580(24) (2006) 5676-80.
- [31] O. Kozawa, A. Suzuki, Y. Watanabe, J. Shinoda, Y. Oiso, Effect of platelet-derived growth factor on phosphatidylcholine-hydrolyzing phospholipase D in osteoblast-like cells, *Endocrinology* 136(10) (1995) 4473-8.
- [32] Y. Oiso, A. Suzuki, O. Kozawa, Effect of prostaglandin E2 on phospholipase D activity in osteoblast-like MC3T3-E1 cells, *J Bone Miner Res* 10(8) (1995) 1185-90.
- [33] T. Sugiyama, T. Sakai, Y. Nozawa, N. Oka, Prostaglandin F2 alpha-stimulated phospholipase D activation in osteoblast-like MC3T3-E1 cells: involvement in sustained 1,2-diacylglycerol production, *Biochem J* 298 ( Pt 2) (1994) 479-84.
- [34] S. Mebarek, H. Komati, F. Naro, C. Zeiller, M. Alvisi, M. Lagarde, A.F. Prigent, G. Némoy, Inhibition of de novo ceramide synthesis upregulates phospholipase D and enhances myogenic differentiation, *J Cell Sci* 120(Pt 3) (2007) 407-16.
- [35] M. Liscovitch, M. Czarny, G. Fiucci, Y. Lavie, X. Tang, Localization and possible functions of phospholipase D isozymes, *Biochim Biophys Acta* 1439(2) (1999) 245-63.
- [36] S. Kook, J.H. Exton, Identification of interaction sites of protein kinase Calpha on phospholipase D1, *Cell Signal* 17(11) (2005) 1423-32.
- [37] G. Boguslawski, L.V. Hale, X.P. Yu, R.R. Miles, J.E. Onyia, R.F. Santerre, S. Chandrasekhar, Activation of osteocalcin transcription involves interaction of protein kinase A- and protein kinase C-dependent pathways, *J Biol Chem* 275(2) (2000) 999-1006.
- [38] J.L. Sanders, P.H. Stern, Expression and phorbol ester-induced down-regulation of protein kinase C isozymes in osteoblasts, *J Bone Miner Res* 11(12) (1996) 1862-72.
- [39] J.T. Swarthout, T.A. Doggett, J.L. Lemker, N.C. Partridge, Stimulation of extracellular signal-regulated kinases and proliferation in rat osteoblastic cells by parathyroid hormone is protein kinase C-dependent, *J Biol Chem* 276(10) (2001) 7586-92.
- [40] F. Zhu, M.T. Sweetwyne, K.D. Hankenson, PKC $\delta$  is required for Jagged-1 induction of human mesenchymal stem cell osteogenic differentiation, *Stem Cells* 31(6) (2013) 1181-92.
- [41] C. Thouverey, A. Strzelecka-Kiliszek, M. Balcerzak, R. Buchet, S. Pikula, Matrix vesicles originate from apical membrane microvilli of mineralizing osteoblast-like Saos-2 cells, *J Cell Biochem* 106(1) (2009) 127-38.
- [42] W.C. Colley, T.C. Sung, R. Roll, J. Jenco, S.M. Hammond, Y. Altshuller, D. Bar-Sagi, A.J. Morris, M.A. Frohman, Phospholipase D2, a distinct phospholipase D isoform with novel regulatory properties that provokes cytoskeletal reorganization., *Curr Biol* 7(3) (1997) 191-201.

